



UNIVERSITY OF
LIVERPOOL

**From medicinal chemistry optimisation of antimalarial
2-aryl quinolones to synthesis and application of
endoperoxide activity-based protein profiling probes**

Thesis submitted in accordance with the requirements of the University of Liverpool
for the degree of Doctor in Philosophy (Chemistry)

Written by Sitthivut Charoensutthivarakul

Department of Chemistry, University of Liverpool

October 2014

Declaration

This thesis is the result of my own work. The material contained in the thesis has not been presented, nor is currently being presented, either wholly or in part for any other degree or other qualification.

Sitthivut Charoensutthivarakul

This thesis was carried out in the Department of Chemistry, University of Liverpool

Table of contents

	page
Acknowledgment	iv
Abstract	v
Publications	vi
List of abbreviations	vii
Chapter I: Malaria overview	1
Chapter II: Antimalarial quinolone targeting <i>Pf</i> electron transport chain	29
Chapter III: Lead optimisation of antimalarial 2-aryl quinolones	52
Chapter IV: Alternative synthetic route towards PG227	140
Chapter V: Design, synthesis and <i>in vitro</i> evaluation of activity-based protein profiling probes in <i>Plasmodium falciparum</i>	165

Acknowledgment

I am using this opportunity to express my gratitude to everyone who supported me throughout the course of my PhD. I would like to express my special thanks to Professor Paul M. O'Neill, who has been a fantastic and tremendous mentor to me. I would like to thank you for your encouragement and support allowing me to grow as a research chemist. Your advice on both research, as well as on my career have been invaluable. I would also like to pass my gratitude to Dr. Neil Berry for his supportive and helpful comments. I thank Professor Rui Moreira, the external examiner, and Dr. Andrew Carnell for their useful and constructive discussion. I would like to express my deep gratitude to Mahidol University whom I am indebted to for a prestigious scholarship allowing me to pursue my dream at Liverpool. I also thank the late Professor Stang Mongkolsuk, the founding dean of science at Mahidol, who is always my role model in scientific career.

I would especially like to thank all the past and current post-doc members of PON group including Dr. W. David Hong, Dr. Paul Stocks, Dr. Suet C. Leung, Dr. Richard Amewu, Dr. Peter Gibbons, Dr. Andrew Stachulski, Dr. Chadrakala Pidathala, Dr. Neil Kershaw, Dr. Sunil Sabbani, Dr. Raman Sharma, Dr. Alexandre Lawrenson, Dr. James Chadwick, Dr. Ian Hale, Dr. Francesc Marti, Dr. Olivier Berger and Dr. Louise La Pensée. I also thank all of my PhD student friends and colleagues namely Matthew Pye, Mike Wong, Emma Shore, Christopher Riley, Lee Taylor, Rudi Oliveira, Natalie Roberts, Paul McGillan, Adam Rolt, Kathryn Price, and Emma Yang. All of you have been parts of my life here at the University of Liverpool. I am also indebted to staffs member of the Department of Chemistry, University of Liverpool especially the analytical service members including Dr. Konstantin Luzyanin, Moya McCarron, Jean and Tony Ellis for their useful help and advice. I would like to thank the Liverpool School of Tropical Medicine and its staff members especially Professor Stephen A. Ward, Professor Giancarlo Biagini, Dr. Gemma Nixon, Dr. Alison Shone, Dr. Paul Bedingfield and Matthew Phanchana for their works on antimalarial and biological assessment and useful discussion. I thank the University of Liverpool ChemSoc and the Liverpool Thai Society for many fantastic activities and night outs.

A special thanks to my family. Words cannot describe how grateful I am for all the sacrifices you have made on my behalf. I especially thank my mum who is always on the other side of the phone cheering me up during my time at Liverpool. Distance never keeps us apart. At the end, I would also like to express my appreciation to my beloved boyfriend, James Guthrie, who supported me in writing and motivated me to achieve my goal. You were always my support when there is no one to answer my queries.

Abstract

Malaria is one of the most prevalent and deadliest parasitic diseases affecting various systems of the body and leading to death. Resistance against antimalarial treatment is a major threat in controlling and eliminating malaria. New drugs are urgently needed especially when artemisinin resistance has emerged. The mitochondrial electron transport chain of *Plasmodium falciparum* is an attractive target for chemotherapy. Two enzymes in the pathway - *Pfbc₁* and *PfNDH2* - are druggable target enzymes. The dual inhibition of both enzymes can be seen in 2-aryl quinolone pharmacophore giving added therapeutic benefit. The development from this series leads to the potent lead compounds including SL-2-25 and PG227.

In Chapter III, following the hit-to-lead optimisation of SL-2-25, a 5-7 step synthesis of a library of 2-aryl quinolones has been described. *In vitro* antimalarial assessment of these quinolones revealed the advantages of the 7-methoxy moiety. The potency increases 3-8 folds when the 7-OMe group is attached. Further lead modification led to a more flexible quinolone **61i** retaining high potency against the 3D7 strain of *P. falciparum*. This structure also possesses no cross resistance, greater aqueous solubility and low potential for cardiotoxicity. Following a similar study on related quinolones, 3,4-dichlorophenyl analogues were briefly investigated. This led to the discovery of **61o** possessing an outstanding potency against 3D7 strain of *P. falciparum* of 18 nM. It also shows low cardiotoxicity when compare to other quinolones. **61u** featuring 6-Cl and 7-OMe substitution was identified with an *in vitro* IC₅₀ potency of 9 nM against *Plasmodium*. *In silico* molecular modelling based on the yeast *bc₁* protein complex shows that all quinolones bind tightly to the target protein with essential interactions in place.

PG227 (**69**) exhibits outstanding pharmacological properties amongst the series of quinolones. Its original synthesis suffers from reproducibility and low overall yields. **69** can be made in a multi-gram scale using an alternative method for cyclisation. The 5-step synthesis of PG227 can be achieved from commercially available starting materials involving the synthesis of β -keto ester intermediate, the Conrad-Limpach cyclisation and chlorination using NCS. The overall yield was 7%.

Artemisinin combination therapy (ACT) is used as the first line treatment in most of the malarial endemic areas. The emerged artemisinin resistance requires greater understanding of drug action. In Chapter V, activity-based protein profiling (ABPP) was employed to identify the molecular target of artemisinin for the first time. The novel "tag-free" ABPP proteomic technique is introduced based on the click chemistry between a chemical probe and a reporter tag. The synthesis of the artemisinin-based ABPP chemical probes was achieved. The peroxide-containing probes show an excellent *in vitro* potency against the 3D7 malaria parasite. The preliminary result reveals that active probe **99** can perform well in protein pull down resulting in 45 different proteins being identified.

Publications

1. Biagini, G.A., Fisher, N., Shone, A.E., Mubarakia, M.A., Srivastava, A. Hill, A., Antoine, T., Warman, A.J., Davies, J., Pidathala, C., Amewu, R.K., Leung, S.C., Sharma, R., Gibbons, P., Hong, D.W., Pacorel, B., Lawrenson, A.S., **Charoensutthivarakul, S.**, Taylor, L., Berger, O., Mbekeani, A., Stocks, P.A., Nixon, G.L., Chadwick, J., Hemingway, J., Delves, M.J., Sinden, R.E., Zeeman, A-M. Kocken, C.H.M., Berry, N.G., O'Neill, P.M., Ward, S.A. (2012) Generation of quinolone antimalarials targeting the Plasmodium falciparum mitochondrial respiratory chain for the treatment and prophylaxis of malaria. *Proceedings of the National Academy of Science (USA)*, 109, 8298-8303

2. S. C. Leung, P. Gibbons, R. Amewu, G. L. Nixon, C. Pidathala, W. D. Hong, B. Pacorel, N. G. Berry, R. Sharma, P. A. Stocks, A. Srivastava, A. E. Shone, **S. Charoensutthivarakul**, L. Taylor, O. Berger, A. Mbekeani, A. Hill, N. E. Fisher, A. J. Warman, G. A. Biagini, S. A. Ward and P. M. O'Neill (2012) Identification, Design and Biological Evaluation of Heterocyclic Quinolones Targeting Plasmodium falciparum Type II NADH:Quinone Oxidoreductase (PfNDH2). *Journal of Medicinal Chemistry*, 55(5), 1844-1857.

3. C. Pidathala, R. Amewu, B. Pacorel, G. L. Nixon, P. Gibbons, W. D. Hong, S. C. Leung, N. G. Berry, R. Sharma, P. A. Stocks, A. Srivastava, A. E. Shone, **S. Charoensutthivarakul**, L. Taylor, O. Berger, A. Mbekeani, A. Hill, N. E. Fisher, A. J. Warman, G. A. Biagini, S. A. Ward and P. M. O'Neill (2012) Identification, Design and Biological Evaluation of Bisaryl Quinolones Targeting Plasmodium falciparum Type II NADH:Quinone Oxidoreductase (PfNDH2). *Journal of Medicinal Chemistry*, 55(5), 1831-1843.

List of abbreviation

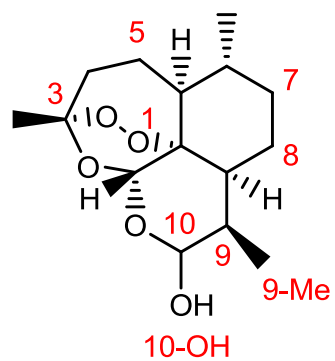
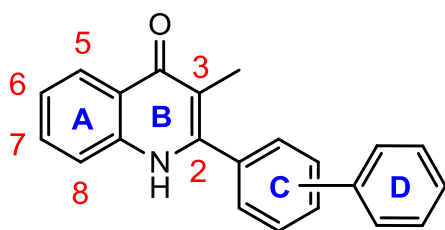
Abbreviations	Full name
\$	US dollars
%F	bioavailability
ABPP	activity-based protein profiling
Ac	acetyl
ACN	acetonitrile
ACT	artemisinin-based combination therapy
ADMET	absorption, distribution, metabolism, excretion and toxicity
AHA	anhydroartemisinin
AL	artemether and lumefantrine
Å	angstrom(s)
AQ	amodiaquine
aq	aqueous
Ar	aryl
ART	artemisinin
ATP	adenosine triphosphate
ATQ	atovaquone
Bu	butyl
°C	degree Celsius
cat.	catalytic
CC	column chromatography
CI	chemical ionisation
ClogP	partition-coefficient
CNS	central nervous system
conc.	concentrated
CQ	chloroquine
CYP450	cytochrome P450 oxidases
d	doublet
DCE	dichloroethane
DCM	dichloromethane
dd	double of doublet
ddd	double of double of doublet
DDT	dichlorodiphenyltrichloroethane

δ	chemical shift
DFO	desferrioxamine
DHA	dihydroartemisinin
DHFR	dihydrofolate reductase
DHODH	dihydroorotate dehydrogenase
DMAP	4-dimethylaminopyridine
DMF	<i>N,N</i> -dimethylformamide
DMP	Dess-Martin periodinane
DMPK	drug metabolism and pharmacokinetics
DMSO	dimethylsulphoxide
DNA	deoxyribonucleic acid
D-PBS	Dulbecco's phosphate buffered saline
dt	double of triplet
EC _{xx}	concentration at which the drug achieves the desired effect in xx % of the cells targeted
ED _{xx}	dose of drug which produces xx % of its maximum response
EDCI	1-ethyl-3-(3-dimethylaminopropyl)carbodiimide
EMA	European Medicines Agency
eq.	molar equivalent(s)
ESI	electrospray ionisation
Et	ethyl
ETC	electron transport chain
g	gram(s)
G6PD	glucose-6-phosphate dehydrogenase
GI	gastrointestinal
GSK	GlaxoSmithKline
h	hour(s)
HDQ	hydroxyl-2-dodecyl-4-(1H)-quinolone
HPLC	high-performance liquid chromatography
HRMS	high resolution mass spectrometry
Hz	Hertz
IC _{xx}	inhibitory concentration of drug at xx % inhibition in vitro
IRS	indoor residual spray
ISP	Iron-sulfur protein
ITN	Insecticide-treated nets

<i>J</i>	coupling constant
kDa	kiloDalton
kg	kilogram(s)
LC	liquid chromatography
LDA	lithium diisopropylamide
M	molar
m	multiplet
<i>m-</i>	<i>meta</i>
m/z	mass over charge ratio
Me	methyl
MF	mefloquine
mg	milligram(s)
MHz	megahertz
min	minute(s)
mL	millilitre(s)
mm	millimetre(s)
MMV	Medicines for Malaria Venture
mp	melting point
mRNA	messenger RNA
MS	mass spectrometry
N	normality
<i>n-</i>	normal
NAD ⁺	an oxidised form of nicotinamide adenine dinucleotide
NADH	a reduced form of nicotinamide adenine dinucleotide
NCS	<i>N</i> -chlorosuccinimide
ND	not determined
NDH2	type II NADH:ubiquinone oxidoreductase
nM	nanomolar
nm	nanometre(s)
NMR	nuclear magnetic resonance spectroscopy
<i>o-</i>	<i>ortho</i>
<i>p-</i>	<i>para</i>
<i>P.</i>	<i>Plasmodium</i>
PAGE	polyacrylamide gel electrophoresis
PCC	pyridinium chlorochromate

PDB	Protein Data Bank
<i>Pf</i>	<i>Plasmodium falciparum</i>
<i>Pf</i> ATP4	<i>P. falciparum</i> sodium transporter ATPase4
<i>Pf</i> CRT	<i>Plasmodium falciparum</i> chloroquine resistance transporter
Ph	phenyl
pH	a logarithmic measure of the acidity
PK	pharmacokinetics
pKa	a logarithmic measure of the acid dissociation constant
ppm	part per million
PYR	pyrimethamine
q	quartet
RMSD	root-mean-square deviation
rt	room temperature
s	singlet
S/P	sulphadoxine and pyrimethamine
SAR	structure-activity relationship
SD	standard deviation
SDH	succinate dehydrogenase
SDS	sodium dodecyl sulphate
SERCA	sarco/endoplasmic reticulum membrane calcium ATPase
t	triplet
<i>t</i> -or <i>tert</i> -	tertiary
TF	tafenoquine
THF	tetrahydrofuran
TLC	thin layer chromatography
TMS	tetramethylsilane
μL	microlitre(s)
μM	micromolar
WHO	World Health Organization

Numbering schemes used throughout this thesis



Chapter I : Malaria Overview

Chapter I : Malaria Overview

	page
1.1 Malaria: Biology and Pathology	3
1.2 Malaria: the prevention and treatment	5
1.3 Drug resistant Malaria	6
1.4 Antimalarial Chemotherapies	8
1.4.1 Antimalarials interfering the heme polymerisation	11
1.4.2 Inhibitors of <i>Plasmodium</i> DHFR	14
1.4.3 Inhibitors of <i>Plasmodium</i> DHODH	15
1.4.4 Antimalarials targeting mitochondrial respiration	16
1.4.5 Endoperoxides	18
1.4.6 Antimalarials targeting exoerythrocytic stage <i>Plasmodium</i>	19
1.4.7 Novel antimalarials from whole-cell screens	21
1.5 Conclusion	22
1.6 References	23

Malaria Overview

1.1 Malaria: Biology and Pathology

Malaria remains a massive global health challenge and is still one of the most prevalent and deadliest parasitic diseases. It is caused by the eukaryotic parasite *Plasmodium* (Phylum Apicomplexa) widespread in tropical and subtropical regions of the world. Malaria is transmitted from person to person through the bite of female parasite-carrying mosquito vector *Anopheles* which requires human blood to cultivate her eggs. In 2012 the World Health Organization (WHO) estimates around 200 million malarial infection cases and almost 627,000 deaths. Although nearly half the world's populations are exposed to malaria, it was estimated that 90% of deaths due to malaria occur in sub-Saharan Africa and 77% of deaths occur in children less than five years old¹. An independent study estimated that malaria costs Africa \$12 billion/year in term of economic burden². The rest of the malaria endemic areas include central and southern America, south and Southeast Asia and the western Pacific. This makes malaria a disease of poor and developing countries.

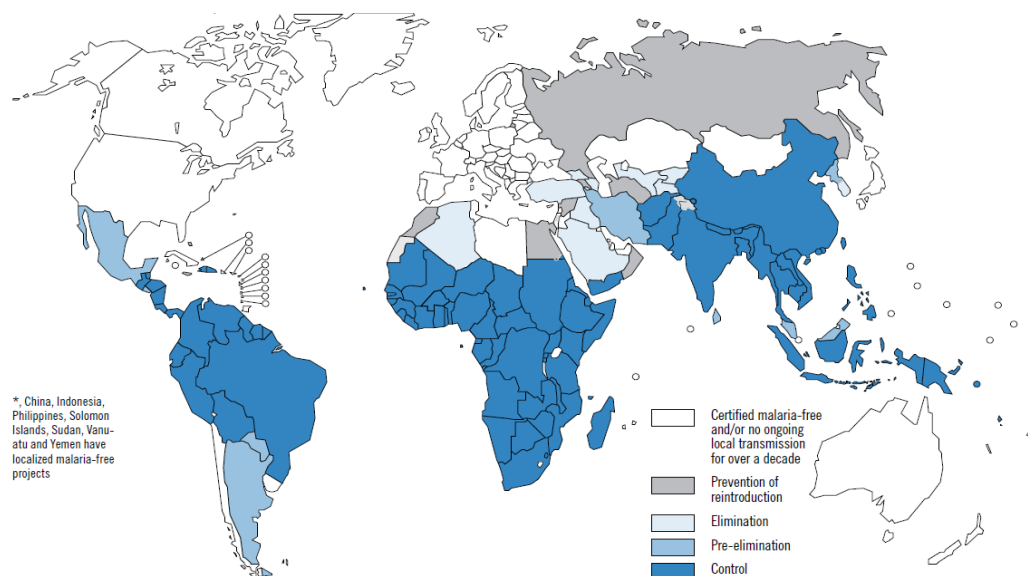


Figure 1.1 World's Malaria distribution and control¹.

Malaria is a complex disease affecting various systems of the body. Symptoms of malaria infection in humans are caused by the activities of asexual

blood stage of the parasites. In humans, these general and uncomplicated symptoms include fever, headache, myalgia, coughing, shaking chills, and paroxysm of fever while severe infection shows in nausea, vomiting, and diarrhoea. Mortality can be attributed to coma, anaemia, respiratory distress, acidosis, hypoglycaemia or renal failure³. The symptoms can be different between children and adults.

Several species of *Plasmodium* are responsible for malaria in human including *Plasmodium falciparum*, *Plasmodium vivax*, *Plasmodium malariae*, *Plasmodium ovale* and the recently reported simian *Plasmodium knowlesi* which has been found in Southeast Asia forest regions⁴. Although *P. falciparum* causes almost all severe malaria including cerebral malaria, leading to coma and eventually death⁵, *P. vivax* is responsible for almost 80 million cases each year⁶. Both of them are becoming difficult to treat and control due to the emergence of drug resistance during the past three decades. However, there is an increased number of evidence reported that the lethality of *P. vivax* is underestimated⁷.

The malaria parasite itself has a complex life cycle and in order to eradicate the disease, each stage should be well considered for treatment. Its life cycle is composed of 3 main stages.

1. Liver stage. Once an infected female mosquito feeds and transfers the parasite (sporozoites) into the host's blood stream, the plasmodial parasites then migrate to the liver within half an hour via blood circulation. The asexual parasites, liver schizonts, rapidly multiply and form thousands of merozoites.

2. Blood stage (sometimes called erythrocytic stage). After 5 -10 days, infected red blood cells burst and release merozoites which then readily invade other red blood cells where they rapidly grow and proliferate causing the illness symptoms. This is referred as an asexual blood stage. During this development phase, the merozoites go through various stages – rings, trophozoites, schizonts – to produce around 20 daughter merozoites which are then released to the blood stream and infect other red blood cells. Most drugs target parasites at this blood stage.

After several propagation cycles, some merozoites differentiate into male and female gametocytes which are then ingested by the mosquito when it bites and takes infected blood.

3. Mosquito stage. In the mosquito gut, after ingestion, the gametocytes develop into gametes which then fuse and form a zygote. The zygote transforms into an ookinete and becomes an oocyst in the mosquito stomach. The oocyst divides to produce sporozoites, which move to the salivary gland and ready for the next human host.

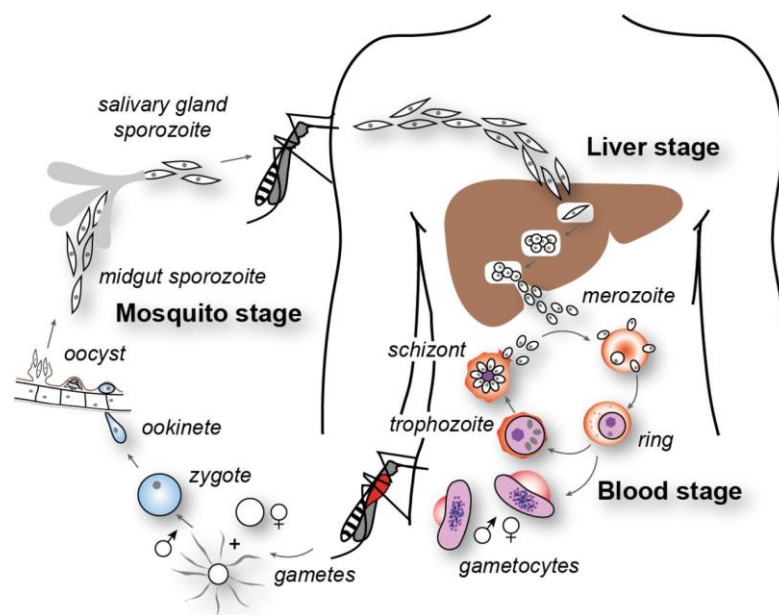


Figure 1.2 *Plasmodium* life cycle⁸

1.2 Malaria: the prevention and treatment

As with other infectious diseases, the fight against malaria is challenging and several attempts to control the malaria endemic have been used. These include vector control, vaccine, and chemotherapy. Vector control is based on two main activities: indoor residual spray (IRS) and insecticide-treated nets (ITN). Although the use of insecticidal dichlorodiphenyltrichloroethane (DDT) (1) introduced in 1950s as the first IRS had successfully reduced malaria in many parts of the world, its undesirable environmental effects and human health risk led to the end of its era around 1970s due to public concern. Other IRS alternatives, such as pyrethroid (2), have been introduced even they are more expensive than DDT. Several trials to

control the mosquito vector including the use of ITNs have shown positive results in decreasing child mortality in many African countries⁹. Currently, both IRS and ITN are mainly dependent on pyrethroid class due to its low toxicity to humans. New insecticides are consequently needed to retain the effectiveness of the malaria control programmes¹⁰.

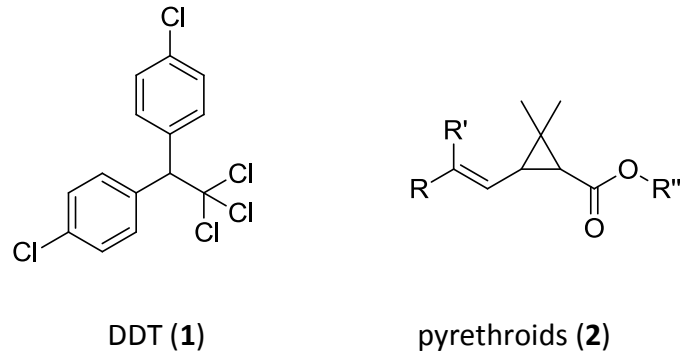


Figure 1.3 Chemical structures of DDT and pyrethroid insecticides

Although tremendous efforts are currently invested in vaccine development, malaria vaccines are still not yet in the market. Unfortunately, due to the *Plasmodium* complicated life cycle, it may take another 5- 10 years before it will be introduced and widely used. The most advanced of vaccine candidate – RTS,S/AS01 – is currently in phase III¹¹ and the preliminary experiment conducted in sub-Saharan Africa showed promising efficacy and a reduction in malaria by 55%¹². While malaria vaccines complete their development, it is clear that the fight against malaria will involve chemotherapy as a vital tool. Unfortunately, clinical resistance has emerged for most established therapeutic treatments.

1.3 Drug resistant Malaria

Parasite resistance against antimalarial treatment is a major threat in controlling and eliminating malaria. This is continuing to reduce the efficiency of available chemotherapies¹³. Resistance spreads when parasites are exposed to sub-lethal drug concentrations through poor antimalarial drug management. Drug resistant plasmodia are transformed into gametocytes and picked up when uninfected mosquitoes bite leading to transmission of resistance. The problem of emerged drug resistance means that new drugs are required.

The best example of drug resistance problem can be depicted by one of the well-known antimalarial drugs called chloroquine (CQ) (3) which is proven to be an effective and successful drug against malaria. CQ has an outstanding efficacy combined with a low price and this makes CQ affordable in poor developing countries where malaria is a massive economic and health burden. Unfortunately, resistance to CQ has emerged after decades of introduction, and today it is widespread throughout the malaria-endemic countries leading to its reduced efficacy and clinical failure¹⁴. Mefloquine (MF) (4) emerged as a successor of CQ in the 1980s; however, cases of resistance appeared within a few years¹⁵.

Combining drugs can limit the emergence of resistance but this technique is still fallible. A once effective combination of antifolates pyrimethamine (5) and sulphadoxine (7) (S/P) is another example. S/P was a widely used treatment, and it has been a relatively cheap and highly effective drug combination. Unluckily, resistance owing to point mutations in target enzymes rapidly emerged after its introduction resulting in ineffective treatment.

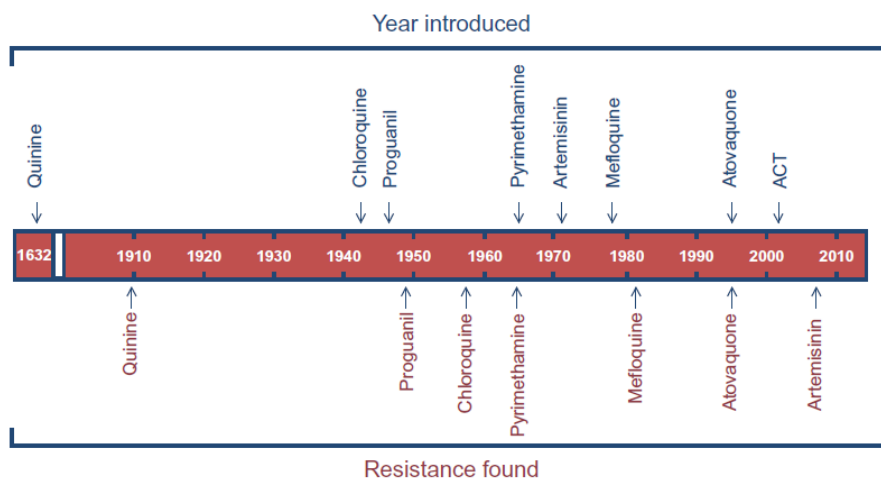


Figure 1.4 Comparative year of introduction of new antimalarial therapies versus the emergence of clinical resistance¹⁵

In the scenario described above, artemisinin-combination therapies (ACTs) stand as the last frontline treatment against the increase in drug resistant malaria. They are widely used as national policies for the first-line treatment in most endemic countries. Artemether-lumefantrine (AL) is the first fixed-dose and most

widely used ACT recommended and pre-qualified by WHO. It has been shown to be effective in sub-Saharan Africa and in Southeast Asia where the multi-drug resistant *P.falciparum* is endemic. Following the success of AL, artesunate-amodiaquine was launched in 2007, even though other combinations are also clinically explored¹⁶.

While ACTs remain clinically effective and there are no absolute cases of treatment failure, it is evident that the resistance to the artemisinin component has emerged¹⁷. In Pailin, the western province of Cambodia, where the WHO malaria centre is located, clinical recrudescence occurs in almost 30% of the patients when treated with artesunate monotherapy and only 5% when a combination of artesunate-mefloquine is used¹⁸.

Consequently, due to resistance, the discovery of novel drug candidates remains a top priority to provide new medicine to back up current ACT therapies. There are several ongoing drug discovery projects focusing on antimalarials. Some are structurally distinct from available drugs and possibly possess a novel mechanism of action that exhibit excellent efficacy against drug resistant parasites. Not only showing no cross resistance, but the new drugs should be (i) fast acting, (ii) safe to children and pregnant women, and (iii) ideally used as a single dose.

1.4 Antimalarial Chemotherapy

As stated earlier, antimalarial chemotherapy is still the most effective way to treat and control malaria. New drugs are urgently needed especially since artemisinin resistant parasites have emerged. Over the last decade, there has been an increased investment in antimalarial research and development through the Medicines for Malaria Venture (MMV) and their partners¹⁹. New molecules with novel modes of action are entering into preclinical development; some are in early clinical trial stages. In this chapter, some highlights of the MMV portfolio are briefly summarised and categorised according to their modes of action to demonstrate how these molecules were discovered and developed. However, antibiotics will not be discussed since this class were discovered following repurposing against malaria parasites.

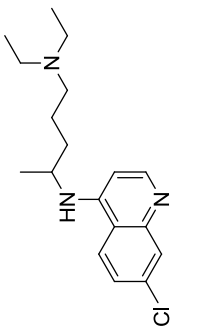
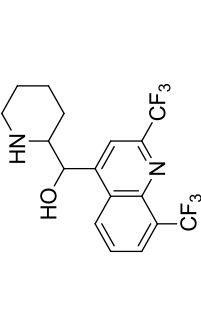
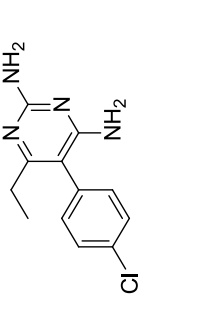
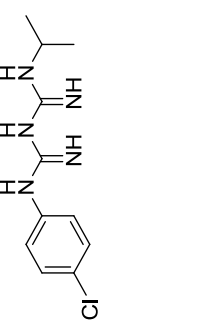
Name	Structure	Chemical class	Other Drugs from the family	Mode of action
Chloroquine (3)		4-Aminoquinoline	Amodiaquine (12)	Interference with heme polymerisation
Mefloquine (4)		Quinolinalcohol	Quinine (11), halofantrine, lumefantrine	Interference with heme polymerisation
Pyrimethamine (5)		Diamino pyrimidine	Cycloguanil (diamino dihydrotriazine)	DHFR inhibitors (show synergism with sulphadoxine)
Proguanil (6)		Bi-guanidine	None	Metabolised <i>in vitro</i> to cycloguanil, a DHFR inhibitor (shows synergism with atovaquone)

Table 1.1 Representative antimalarials from the different structural classes.

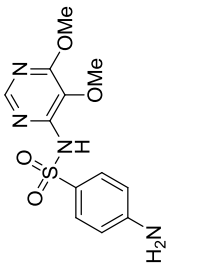
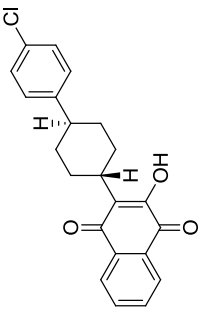
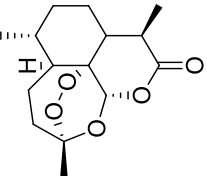
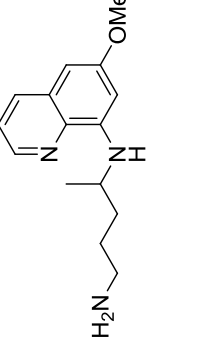
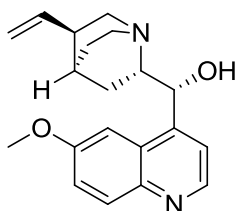
Name	Structure	Chemical class	Other Drugs from the family	Mode of action
Sulphadoxine (7)		aminosulphonamide	Dapsone (aminosulphone)	DHPS inhibitors (show synergism with pyrimethamine)
Atovaquone (8)		Naphthoquinone	None	Mitochondrial cytochrome <i>bc</i> ₁ complex inhibitor
Artemisinins (9)		Endoperoxide	Artesunate (86), artemether (84), arteether (85), dihydroartemisinin (83)	Unknown
Primaquine (10)		8-Aminoquinoline	Pamaquine, bulaquine	Unknown (only class that active against liver hypnozoites)

Table 1.1 Representative antimalarials from the different structural classes (cont.)

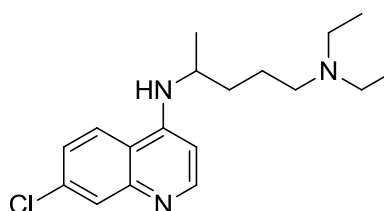
1.4.1 Antimalarials interfering the heme polymerisation

Quinine (**11**), a major chemical component in the bark of cinchona (quina-quina) tree, is the first described antimalarial treatment and has retained its efficacy for almost 400 years after it was first reported²⁰. Quinine was the main malaria treatment until the 1920s when more effective antimalarial quinoline became available. The synthetic 4-aminoquinoline, chloroquine (CQ) (**3**), was the most important developed²¹, and, doubtlessly, it has been widely used since World War II due to its outstanding efficacy and low cost of production.

The antimalarial mode of action of both CQ and quinine relies on disruption of the formation of hemozoin within the parasite's digestive vacuole²². During the asexual blood stage, the malaria parasite digests haemoglobin leading to the production of "free heme". As heme is toxic to the parasite, heme is detoxified by forming a non-toxic dimer β -hematin which crystallises to produce hemozoin crystals (also known as malaria pigment). CQ is thought to form a complex with toxic heme preventing its crystallisation, which leads to disruption of the detoxification process.



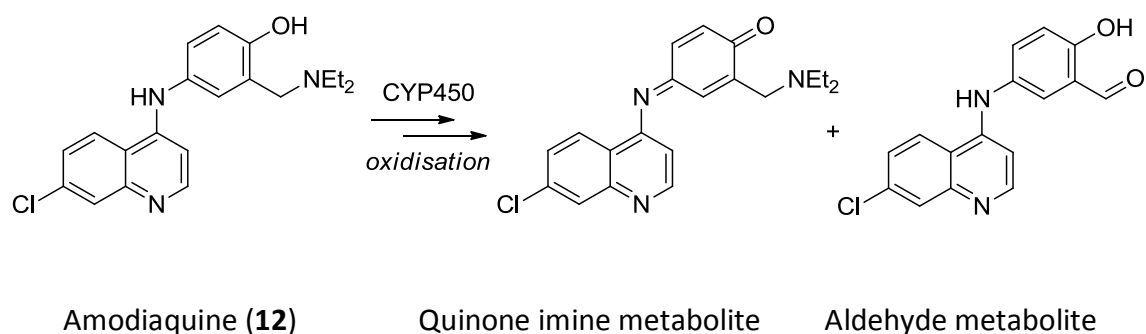
Quinine (**11**)



Chloroquine (**3**)

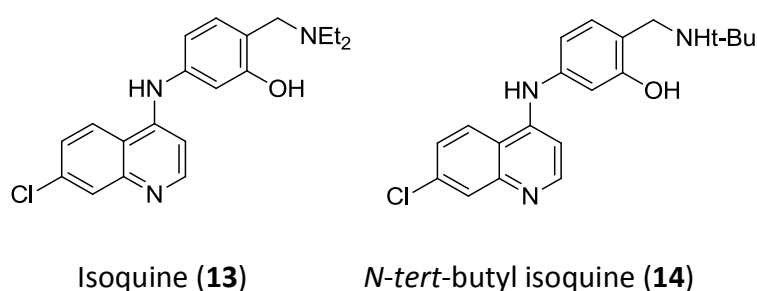
It took decades for resistance to CQ to emerge, but now it is widespread¹⁴. The most widely accepted explanation of the CQ resistance mechanism has been derived from the investigation of *P. falciparum* chloroquine resistance transporter (*PfCRT*). This gene encodes a protein which is believed to connect the digestive vacuolar lumen to the parasite's cytoplasm. Mutations in this transporter protein facilitate protonated CQ leaving the vacuole back to the cytoplasm, and even away from the cellular compartment where the lethal β -hematin binding effect takes place²³.

The introduction of aromatic group into the amine side chain of CQ has led to the discovery of new derivatives which have overcome the resistance problem. The incorporation of 4-hydroxyaniline, for instance, into the amine linker formed amodiaquine (AQ) (**12**) which is active against most CQ-resistant strains; however, its oxidised metabolites are found to cause hepatotoxicity and agranulocytosis which restrict its use²⁴. Nonetheless, AQ is used as a part of ACTs especially in a fixed combination with artesunate and more than 10 million doses were used in 2010¹.

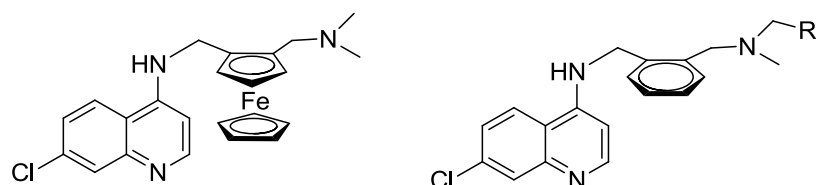


Scheme 1.1 Chemical structures of amodiaquine and its metabolite.

To avoid the formation of reactive toxic metabolites, Isoquine (**13**) was discovered by swapping the regiochemistry of hydroxyl and diethylaminomethylene groups²⁵. Isoquine contains the aminomethylene moiety at *para* position. By replacing the metabolically susceptible *N*-ethyl with *N*-*t*-butyl, *N*-*tert*-butyl isoquine (GSK369796) (**14**) was discovered by O'Neill *et al*²⁶. *N*-*tert*-butyl isoquine is potent *in vitro* against K1 (EC₅₀ = 13 nM) and eventually entered Phase I studies. It also shows relatively good *in vivo* efficacy (ED₅₀ = 3.8 mg/kg/day) following oral administration in mouse model. Despite its excellent activity, its development was discontinued due to the inability to demonstrate an improved safety window over AQ and CQ and lower than expected human exposure²⁷.

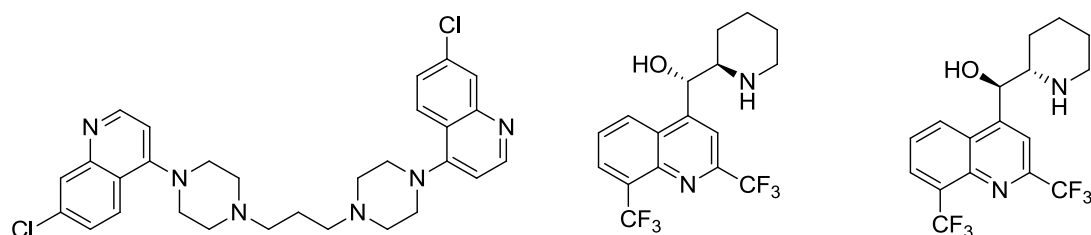


Unlike CQ, ferroquine (**15**) was found to be highly active *in vivo* against CQ-resistant strains, and after preclinical development entered clinical trials. Ferroquine in a combination with OZ439 (**29**) is now in Phase II studies (MMV portfolio). By replacing the unusual ferrocene with a simple phenyl ring, **15a** and **15b** retains activity against CQ-resistant strains K1 and W2²⁸.



Ferroquine (**15**) **15a**; R = H : EC₅₀ = 6.9 nM (K1)
 EC₅₀ = 6.6 ± 0.9 nM (W2) **15b**; R = Ph : EC₅₀ = 23 ± 2 nM (W2)

The preparation of compounds linking two quinoline cores with an aliphatic or aromatic ring led to the discovery of piperaquine (**16**). Piperaquine has an outstanding *in vivo* efficacy and has been widely used clinically in China²⁹; however, resistance has developed in the areas where piperaquine used. A combination of piperaquine and dihydroartemisinin (**83**) has shown high efficacy in clinical trials and has been approved relatively recently by the European Medicines Agency (EMA) despite being widely used for over 10 years³⁰.



Piperaquine (**16**) (+)-(11*S*,12*R*)-mefloquine (**4**) (-)-mefloquine

Quinolinealcohols are another class of antimalarials that interfere with haemoglobin metabolism. Research started in 1970s when CQ began to fail due to the resistance resulted in the quinine-like molecule, mefloquine (MF) (**4**)³¹. Both share the same aryl aminoalcohol core. Due to the urgency, MF is sold as a racemate. Even though both enantiomers are active³², (-)-mefloquine is believed to

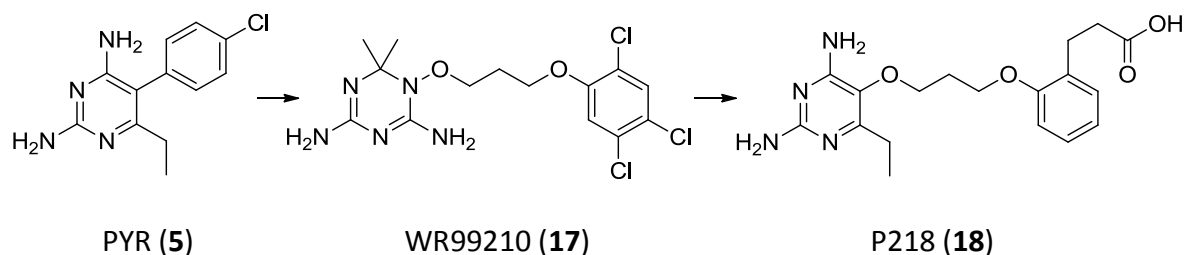
associate with adverse effects in CNS and GI tract³³. It has been widely used in a combination with artesunate due to its long half-life (2-4 weeks in human).

1.4.2 Inhibitors of *Plasmodium* DHFR

Classical dihydrofolate reductase (DHFR) inhibitors such as pyrimethamine (PYR)(**5**) and cycloguanil have been widely used as antimalarials. PYR was one of the most subscribed antimalarial, typically in a fixed-dose combination with sulphadoxine (**7**) (S/P). It is well known that malaria parasites require *de novo* synthesis of folate cofactors to survive and DHFR is the key enzyme in the folate biosynthetic pathway³⁴. DHFR converts dihydrofolate to tetrahydrofolate, a cofactor that is essential for one-carbon transfer reaction and in the biosynthesis of nucleic acid. Inhibiting DHFR consequently leads to the collapse of DNA replication³⁵. Antifolates are extremely safe drugs even for children and pregnant women thanks to the structural difference between human and plasmodial DHFR³⁶. However, PYR and sulphadoxine both have long half-lives: this means parasites are undoubtedly exposed to drugs at sub-inhibitory concentrations. Under pressure from S/P, resistance is widespread due to mutations of the enzyme.

In DHFR mutants, it is well studied that a single S108 mutation is sufficient to reduce the sensitivity to PYR around 10-fold due to a repulsive interaction caused by the mutated amino acid residues and PYR. Yuthavong *et al.* showed that by moving *p*-Cl atom present in PYR to the *meta* position, the steric clash can be avoided and the modified PYR retains good activity³⁷.

Importantly WR99210 (**17**) discovered at the Walter-Reed Institute with a flexible dioxypolyene linker are described as being active against the mutant parasites; however, it shows low bioavailability in animal models¹⁵. Due to the potential of this feature in resolving the DHFR resistance problem, using structure-based drug design strategies combining with the X-ray structure of *Pf*DHFR, Yuthavong *et al.* have identified P218 (**18**) which is active against all clinical-related DHFR mutants³⁸.



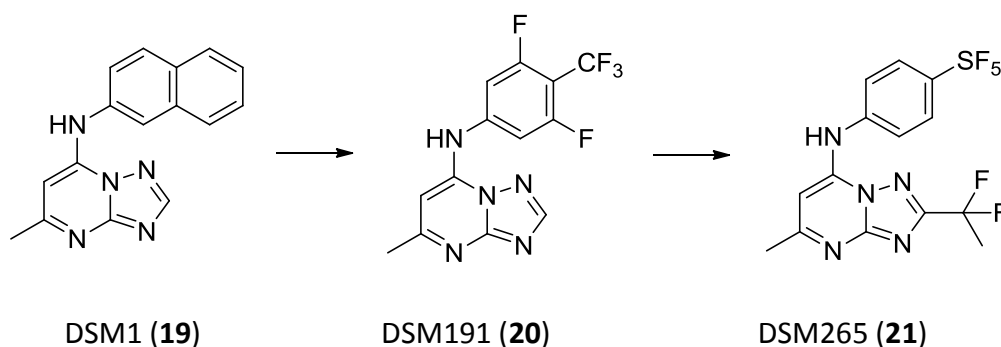
Scheme 1.2 The discovery of P218

P218 brings back potency at both wild-type TM4 strain and quadruple mutant V1/S with IC_{50} values of 4.6 and 56 nM, respectively, and it also shows a good pharmacokinetics profile and a good safety margin³⁹. P218 is being progressed further as a clinical candidate and has a potential to become a new generation inhibitor targeting the folate pathway³⁸.

1.4.3 Inhibitors of *Plasmodium* DHODH

Unlike its human host, *Plasmodia* are unable to salvage pyrimidines and therefore rely on their *de novo* biosynthesis⁴⁰. Dihydroorotate dehydrogenase (DHODH) is a flavoenzyme which catalyses the rate-determining oxidation of L-dihydroorotate to orotate⁴¹. DHODH activity also links to the parasite's electron transport chain as it uses mitochondrial ubiquinone as the electron acceptor. *Plasmodium* DHODH has not been clinically validated as an antimalarial target, although X-ray structure shows significant differences in the binding regions between human and *Pf*DHODH.

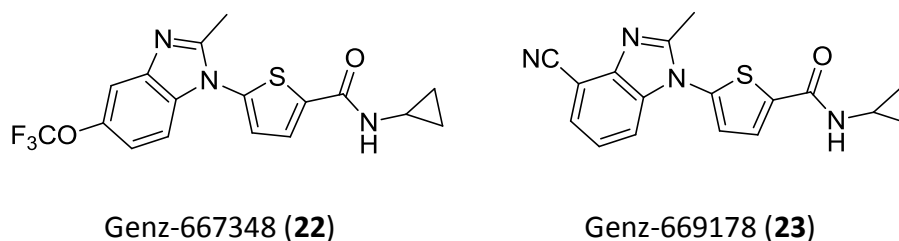
To identify parasite DHODH inhibitors, two independent high-throughput enzyme screens were performed. A team led by Phillips screened over 200,000 compounds and the most promising candidate DSM1 (**19**) was identified. Triazolopyrimidine-based DSM1 had potency in the whole cell assay ($PfIC_{50} = 0.079$ μ M); however, it later was inactive *in vivo* due to its poor pharmacokinetics profile⁴².



Scheme 1.3 DSM265 development

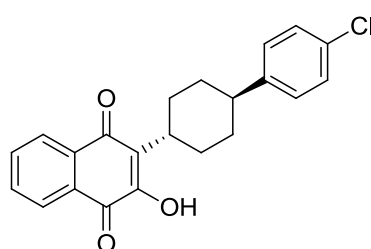
A systematic SAR and X-ray structure demonstrated that, by substitution of naphthalene with electron-withdrawing phenyl ring, analogues with improved potency and better stability were found. This successfully led to the identification of DSM265 (**21**) which has a good potency and safety profile from preclinical studies⁴³. This makes it a promising candidate for human use. If successful, DSM265 would be the first antimalarial chemotherapy to target DHODH³⁸. The compound entered Phase I clinical trials in 2013 and the team is preparing a Phase IIa (so called proof-of-concept) clinical trial in Peru to begin in late 2014 (MMV portfolio).

Clardy *et al.* from Harvard also reported the most attractive benzimidazole hit as a potential drug candidate from their screens within the Genzyme collection⁴⁴. Following a further optimisation, Genz-667348 (**22**) and Genz-669178 (**23**) were identified. The latter was selected as the lead from this programme as it showed moderate bioavailability in both rat and dog (%F = 49 and 19, respectively), and good activity *in vivo* ($PfED_{90} = 27$ mg/kg/day)⁴⁵.

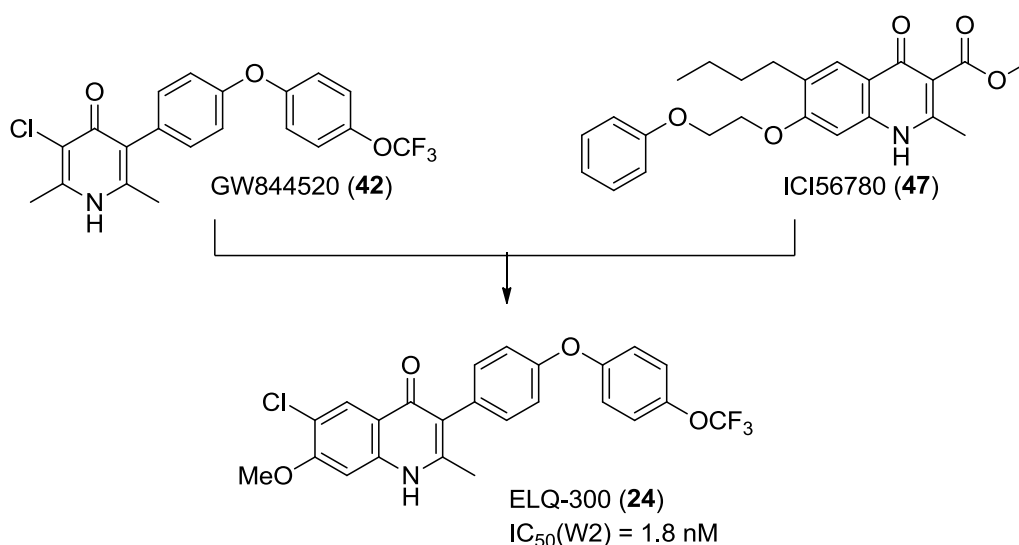


1.4.4 Antimalarials targeting mitochondrial respiration

As part of the cytochrome bc_1 complex, cytochrome b is an essential component of the mitochondrial electron transport chain (ETC). Interrupting the parasite ETC through inhibition of cytochrome bc_1 enzyme has been clinically validated through the use of atovaquone (ATQ). ATQ (**8**) is currently used in a combination with proguanil (**6**) as Malarone. However, cases of clinical resistance to Malarone have been reported. Currently a number of new compounds targeting ETC are at preclinical development stage. The most advanced is ELQ-300 (**24**) which is a quinolone with an ether linkage side chain⁴⁶. The discovery of ELQ-300 is based on a quinolone central scaffold that resembles the structural characteristic in the side-chain present in related pyridone GW844520 (**42**). ELQ-300 is now in preclinical studies progressing to phase I studies and it retains potency against atovaquone-resistant parasites with a high metabolic stability⁴⁷. The detail will be discussed extensively in the next chapter since it is the main target being focused in this thesis.

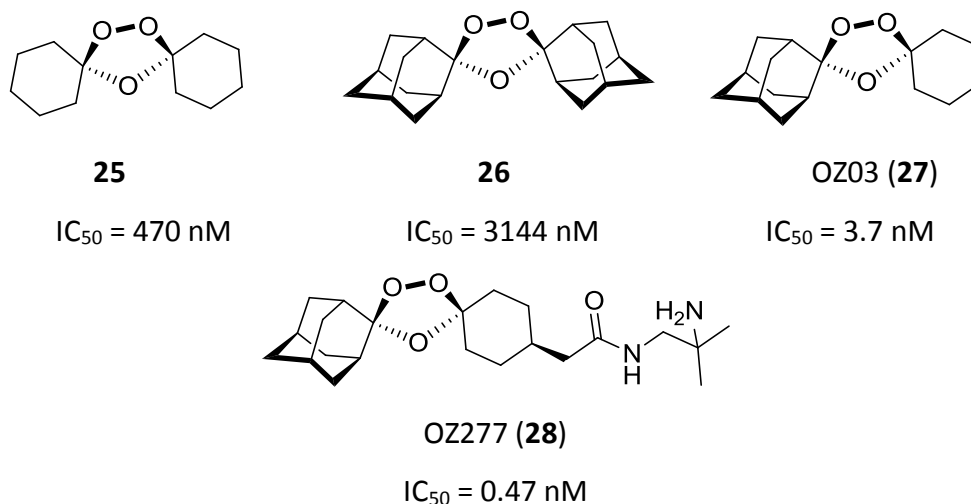


Atovaquone (**8**)



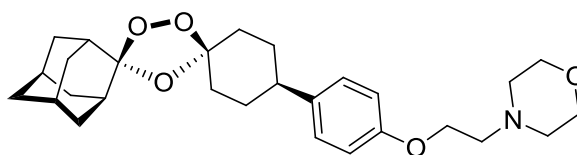
1.4.5 Endoperoxides

Artemisinin (ART) (**9**), a sesquiterpene lactone from Chinese herb *Artemisia annua*, has long been used as antimalarials. The main drawback of ART and its first generation derivative is the short half-life of the active metabolite dihydroartemisinin (**83**) thus efforts have been made to identify a new stable chemotype. The most notable development of second generation inhibitors has been the discovery of ozonide (1,2,4-trioxolane) as potent antimalarial agents⁴⁸. As a starting point, Vennerstrom *et al.* developed a synthetic trioxolane substituted with two cyclohexyl groups (**25**) which was potent but lacked stability. The diadamantyl derivative (**26**) had improved stability due to the fact that O-O bond is protected by bulky adamantyl groups; however its efficacy dropped. A hybrid analogue (**27**) has been made and it exhibited good potency and stability. The addition of acetamide group improved physicochemical property and delivered the desired ADMET profile⁴⁹. OZ277 (Arterolane) (**28**) went into Phase II clinical trials and has been considered as a combination therapy with piperazine phosphate⁵⁰. This combination was approved in India in 2012 as a 3-day treatment and it had widely been used for a short period. Unfortunately, it showed lower exposure in patients than expected due to its unstable interaction with ferrous ion³⁸.

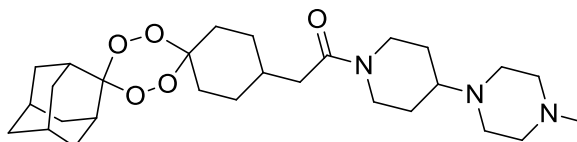


Following the discovery of OZ277, the Vennerstrom group then focused on replacing the amide with a stable phenyl ring and an ether linkage. OZ439 (**29**)

which possesses a longer half-life has also progressed through Phase I clinical trials and show a good safety profile⁵¹. The clinical half-life of OZ439 is 25-30 h (1 h for OZ277) and it also shows a potential to deliver a 20mg/kg single-dose cure in mice⁵². OZ439 is now in Phase II studies and its combination with ferroquine is also being explored (MMV portfolio).

OZ439 (**29**)

Another way of stabilising O-O bond is to form tetraoxanes, O'Neill *et al.* have discovered RKA182 (**30**) based on a similar strategy used in OZ439 development. RKA182 displays good potency against both CQ-sensitive and -resistant strains. It inhibits parasite growth with an ED₅₀ of 1.8mg/kg/day with a good bioavailability in rodents⁵³. Unfortunately, RKA182 is not curative as a single dose. Further work is underway to enhance the half-life of tetraoxane analogues.

RKA182 (**30**)

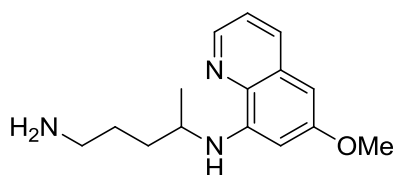
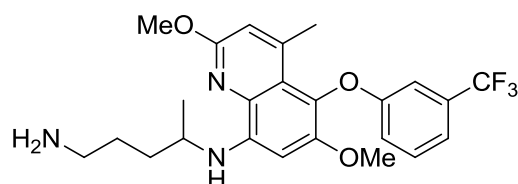
1.4.6 Antimalarials targeting exoerythrocytic stage *Plasmodium*

Currently, most antimalarial agents target only the blood stage of the parasite life cycle. Two exceptions are the combination of atovaquone/proguanil and primaquine⁵⁴. Primaquine (**10**) can cure not only liver schizonts but also hypnozoites, the dormant liver-stage parasites found in *P.vivax* and *P.ovale* infection⁵⁵. The search for liver stage drugs is difficult due to the lack of culture technique.

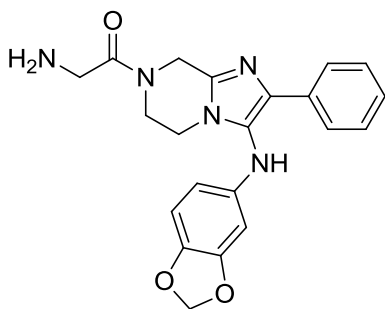
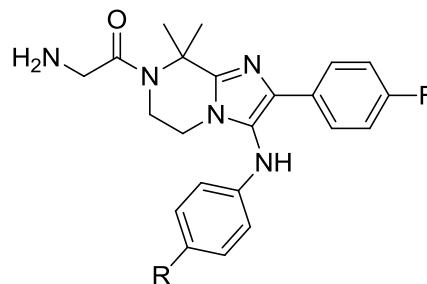
Primaquine, an 8-aminoquinoline, is a slow-acting drug⁵⁶ and is consequently given in a combination with other drugs like chloroquine. Even its mechanism of action is unclear; its main drawback is the adverse side effect

including haemolytic anaemia found in patient deficient glucose-6-phosphate dehydrogenase (G6PD) which occurs in approximately 10% of the population⁵⁷. This has driven the search for alternative agents that can prevent relapsing *P.vivax* malaria.

Tafenoquine (TF) (**31**), in development with GSK, is the lead compound towards the treatment and radical cure of *P.vivax* malaria. TF is generally well tolerated, has a long pharmacokinetic half-life and has completed Phase II studies⁵⁸. These studies recruited more than 300 patients with confirmed *P.vivax* malaria from seven centres in Brazil, Peru, India and Thailand – some of the countries severely affected by relapsing malaria. TF has the same G6PD patient problem with primaquine, but has the advantage of being a single-dose cure. The studies suggested a 300-mg dose of TF as the optimal dose to take forward, as this dose was found to have an acceptable overall safety profile. Plans are now underway to start Phase III studies in 2014 (MMV portfolio).

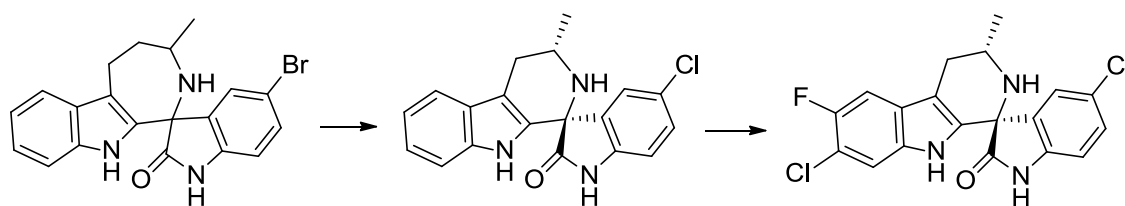
Primaquine (**10**)Tafenoquine (**31**)

To provide novel non-8-aminoquinoline drugs⁵⁹, a Novartis-led research consortium has identified the imidazolopiperazines hit as a new class of antimalarial drugs by whole-cell screening techniques. The lead GNF-Pf-5069 (**32**) was then optimised to provide GNF179 (**33**) and GNF 156 (**34**). The latter, also known as KAF156, exhibits *in vitro* and *in vivo* potency against blood and liver stages of *Plasmodium* with an ED₉₉ in the *P.berghei* mouse of 1.1mg/kg⁶⁰. GNF156 is well tolerated in Phase I safety studies and is currently in Phase IIa clinical trials (MMV portfolio). It is noteworthy that GNF156 not only inhibits the liver stage parasite but also transmission⁶¹.

GNF-Pf-5069 (**32**); $EC_{50}(3D7) = 460 \text{ nM}$ GNF179 (**33**) (R = Cl); $EC_{50}(3D7) = 6 \text{ nM}$ GNF156 (**34**) (R = F); $EC_{50}(3D7) = 6 \text{ nM}$, %F > 40

1.4.7 Novel antimalarials from whole-cell screens

During the past few decades, target-based screening has been the major route towards the discovery of novel antimalarials, but this approach has not proven successful as it is shown in the low number of new chemical entities currently under development¹⁵. Recently three different teams from St. Jude Hospital⁶², GSK,⁶³ and Novartis⁶⁴ have extensively reported their hits from whole-cell screens. The most advanced development belongs to the Novartis where spiroindolones (**35**) was reported as a novel hit with moderate potency against both the sensitive NF54 and the CQ-resistant K1 *P.falciparum* strain⁶⁵. Replacing the 7-membered ring with a 6-membered piperidyl led to the increase in potency. However, its metabolic stability is not optimal, and this was improved by the introduction of halogens onto the tetrahydro- β -carboline core. The resulting compound NITD609 (**37**), also known as KAE609, has demonstrated even greater potency, excellent pharmacokinetics, and safety profile in humans. Its mode of action is believed to be the sodium transporter ATPase4 (*Pf*ATP4) inhibitor⁶⁵, and this causes an increase in the concentration of sodium ions in the parasite, which is toxic to the cell.



35; EC₅₀ 90 nM

36; EC₅₀ 9.2 nM

NITD609 (**37**); EC₅₀ 0.7 nM

Just under 5 years after the initial screen, NITD609 was the first molecule with a novel mechanism of action to successfully complete Phase IIa studies for malaria in the last 20 years (MMV portfolio).

1.5 Conclusion

Malaria is still one of the most prevalent and deadliest parasitic diseases affecting various systems of the body and leading to death. Resistance against antimalarial treatment is a major threat in controlling and eliminating malaria. New drugs are urgently needed especially when artemisinin resistant parasites has emerged. Over the last decade, there has been an increased investment in antimalarial research. As a result of this work, an unprecedented amount of new chemicals are entering into preclinical development; some are structurally distinct and in early clinical trials.

1.6 References

1. WHO World Malaria Report 2013. http://www.who.int/malaria/publications/world_malaria_report_2013/en/ (accessed 27 March 2014).
2. Sachs, J.; Malaney, P., The economic and social burden of malaria. *Nature* **2002**, *415* (6872), 680-5.
3. Weatherall, D. J.; Miller, L. H.; Baruch, D. I.; Marsh, K.; Doumbo, O. K.; Casals-Pascual, C.; Roberts, D. J., Malaria and the red cell. *Hematology / the Education Program of the American Society of Hematology. American Society of Hematology. Education Program* **2002**, 35-57.
4. (a) Oddoux, O.; Debourgogne, A.; Kantele, A.; Kocken, C. H.; Jokiranta, T. S.; Vedy, S.; Puyhardy, J. M.; Machouart, M., Identification of the five human Plasmodium species including *P. knowlesi* by real-time polymerase chain reaction. *European journal of clinical microbiology & infectious diseases : official publication of the European Society of Clinical Microbiology* **2011**, *30* (4), 597-601; (b) Kantele, A.; Jokiranta, T. S., Review of cases with the emerging fifth human malaria parasite, Plasmodium knowlesi. *Clinical infectious diseases : an official publication of the Infectious Diseases Society of America* **2011**, *52* (11), 1356-62.
5. Gething, P. W.; Patil, A. P.; Smith, D. L.; Guerra, C. A.; Elyazar, I. R.; Johnston, G. L.; Tatem, A. J.; Hay, S. I., A new world malaria map: Plasmodium falciparum endemicity in 2010. *Malaria journal* **2011**, *10*, 378.
6. Ridley, R. G., Chemotherapeutic hope on the horizon for Plasmodium vivax malaria? *Proceedings of the National Academy of Sciences of the United States of America* **2002**, *99* (21), 13362-4.
7. Battle, K. E.; Gething, P. W.; Elyazar, I. R.; Moyes, C. L.; Sinka, M. E.; Howes, R. E.; Guerra, C. A.; Price, R. N.; Baird, K. J.; Hay, S. I., The global public health significance of Plasmodium vivax. *Advances in parasitology* **2012**, *80*, 1-111.
8. Cowman, A. F.; Berry, D.; Baum, J., The cellular and molecular basis for malaria parasite invasion of the human red blood cell. *The Journal of cell biology* **2012**, *198* (6), 961-71.
9. Greenwood, B. M.; Bojang, K.; Whitty, C. J.; Targett, G. A., Malaria. *Lancet* **2005**, *365* (9469), 1487-98.
10. (a) Ranson, H.; N'Guessan, R.; Lines, J.; Moiroux, N.; Nkuni, Z.; Corbel, V., Pyrethroid resistance in African anopheline mosquitoes: what are the implications for malaria control? *Trends in parasitology* **2011**, *27* (2), 91-8; (b) van den Berg, H.; Zaim, M.; Yadav, R. S.; Soares, A.; Ameneshewa, B.; Mnzava, A.; Hii, J.; Dash, A. P.; Ejov, M., Global trends in the use of insecticides to control vector-borne diseases. *Environmental health perspectives* **2012**, *120* (4), 577-82.
11. (a) Cohen, J.; Bennis, S.; Vekemans, J.; Leach, A., [The malaria vaccine candidate RTS,S/AS is in phase III clinical trials]. *Annales pharmaceutiques francaises* **2010**, *68* (6), 370-9; (b) Cohen, J.; Nussenzweig, V.; Nussenzweig, R.; Vekemans, J.; Leach, A., From the circumsporozoite protein to the RTS, S/AS candidate vaccine. *Human vaccines* **2010**, *6* (1), 90-6.
12. Agnandji, S. T.; Lell, B.; Soulanoudjingar, S. S.; Fernandes, J. F.; Abossolo, B. P.; Conzelmann, C.; Methogo, B. G.; Doucka, Y.; Flamen, A.; Mordmuller, B.; Issifou, S.; Kremsner, P. G.; Sacarlal, J.; Aide, P.; Lanaspá, M.; Aponte, J. J.; Nhamuave, A.; Quelhas, D.; Bassat, Q.; Mandjate, S.; Macete, E.; Alonso, P.; Abdulla, S.; Salim, N.; Juma, O.; Shomari, M.; Shubis, K.; Machera, F.; Hamad, A. S.; Minja, R.; Mtoro, A.; Sykes, A.; Ahmed, S.; Urassa, A. M.; Ali, A. M.; Mwangoka, G.; Tanner, M.; Tinto, H.; D'Alessandro, U.; Sorgho, H.; Valea, I.; Tahita, M. C.; Kabore, W.; Ouedraogo, S.; Sandrine, Y.; Guiguemde, R. T.; Ouedraogo, J. B.; Hamel, M. J.; Kariuki, S.; Odero, C.; Onoko, M.; Otieno, K.; Awino, N.; Omoto, J.;

- Williamson, J.; Muturi-Kioi, V.; Laserson, K. F.; Slutsker, L.; Otieno, W.; Otieno, L.; Nekoye, O.; Gondi, S.; Otieno, A.; Ogutu, B.; Wasuna, R.; Owira, V.; Jones, D.; Onyango, A. A.; Njuguna, P.; Chilengi, R.; Akoo, P.; Kerubo, C.; Gitaka, J.; Maingi, C.; Lang, T.; Olotu, A.; Tsofa, B.; Bejon, P.; Peshu, N.; Marsh, K.; Owusu-Agyei, S.; Asante, K. P.; Osei-Kwakye, K.; Boahen, O.; Ayamba, S.; Kayan, K.; Owusu-Ofori, R.; Dosoo, D.; Asante, I.; Adjei, G.; Adjei, G.; Chandramohan, D.; Greenwood, B.; Lusingu, J.; Gesase, S.; Malabeja, A.; Abdul, O.; Kilavo, H.; Mahende, C.; Liheluka, E.; Lemnge, M.; Theander, T.; Drakeley, C.; Ansong, D.; Agbenyega, T.; Adjei, S.; Boateng, H. O.; Rettig, T.; Bawa, J.; Sylverken, J.; Sambian, D.; Agyekum, A.; Owusu, L.; Martinson, F.; Hoffman, I.; Mvalo, T.; Kamthunzi, P.; Nkomo, R.; Msika, A.; Jumbe, A.; Chome, N.; Nyakuipa, D.; Chintedza, J.; Ballou, W. R.; Bruls, M.; Cohen, J.; Guerra, Y.; Jongert, E.; Lapierre, D.; Leach, A.; Lievens, M.; Ofori-Anyinam, O.; Vekemans, J.; Carter, T.; Leboulleux, D.; Loucq, C.; Radford, A.; Savarese, B.; Schellenberg, D.; Sillman, M.; Vansadia, P.; Rts, S. C. T. P., First results of phase 3 trial of RTS,S/AS01 malaria vaccine in African children. *The New England journal of medicine* **2011**, *365* (20), 1863-75.
13. Petersen, I.; Eastman, R.; Lanzer, M., Drug-resistant malaria: molecular mechanisms and implications for public health. *FEBS letters* **2011**, *585* (11), 1551-62.
14. Fidock, D. A.; Eastman, R. T.; Ward, S. A.; Meshnick, S. R., Recent highlights in antimalarial drug resistance and chemotherapy research. *Trends in parasitology* **2008**, *24* (12), 537-44.
15. Calderon, F.; Wilson, D. M.; Gamo, F. J., Antimalarial drug discovery: recent progress and future directions. *Progress in medicinal chemistry* **2013**, *52*, 97-151.
16. Consortium, M. Artemisinin-based Combination Therapy. <http://www.malariaconsortium.org/pages/112.htm> (accessed 27/03/14).
17. (a) Mok, S.; Imwong, M.; Mackinnon, M. J.; Sim, J.; Ramadoss, R.; Yi, P.; Mayxay, M.; Chotivanich, K.; Liong, K. Y.; Russell, B.; Socheat, D.; Newton, P. N.; Day, N. P.; White, N. J.; Preiser, P. R.; Nosten, F.; Dondorp, A. M.; Bozdech, Z., Artemisinin resistance in *Plasmodium falciparum* is associated with an altered temporal pattern of transcription. *BMC genomics* **2011**, *12*, 391; (b) Saralamba, S.; Pan-Ngum, W.; Maude, R. J.; Lee, S. J.; Tarning, J.; Lindegardh, N.; Chotivanich, K.; Nosten, F.; Day, N. P.; Socheat, D.; White, N. J.; Dondorp, A. M.; White, L. J., Intrahost modeling of artemisinin resistance in *Plasmodium falciparum*. *Proceedings of the National Academy of Sciences of the United States of America* **2011**, *108* (1), 397-402.
18. Dondorp, A. M.; Nosten, F.; Yi, P.; Das, D.; Phyto, A. P.; Tarning, J.; Lwin, K. M.; Ariey, F.; Hanpithakpong, W.; Lee, S. J.; Ringwald, P.; Silamut, K.; Imwong, M.; Chotivanich, K.; Lim, P.; Herdman, T.; An, S. S.; Yeung, S.; Singhasivanon, P.; Day, N. P.; Lindegardh, N.; Socheat, D.; White, N. J., Artemisinin resistance in *Plasmodium falciparum* malaria. *The New England journal of medicine* **2009**, *361* (5), 455-67.
19. MMV website. <http://www.mmv.org/> (accessed 27 March 2014).
20. Achan, J.; Talisuna, A. O.; Erhart, A.; Yeka, A.; Tibenderana, J. K.; Baliraine, F. N.; Rosenthal, P. J.; D'Alessandro, U., Quinine, an old anti-malarial drug in a modern world: role in the treatment of malaria. *Malaria journal* **2011**, *10*, 144.
21. Krafts, K.; Hempelmann, E.; Skorska-Stania, A., From methylene blue to chloroquine: a brief review of the development of an antimalarial therapy. *Parasitology research* **2012**, *111* (1), 1-6.
22. Schlitzer, M., Malaria chemotherapeutics part I: History of antimalarial drug development, currently used therapeutics, and drugs in clinical development. *ChemMedChem* **2007**, *2* (7), 944-86.
23. Bray, P. G.; Mungthin, M.; Hastings, I. M.; Biagini, G. A.; Saidu, D. K.; Lakshmanan, V.; Johnson, D. J.; Hughes, R. H.; Stocks, P. A.; O'Neill, P. M.; Fidock, D. A.; Warhurst, D. C.; Ward, S. A., PfCRT and the trans-vacuolar proton electrochemical gradient: regulating the

- access of chloroquine to ferriprotoporphyrin IX. *Molecular microbiology* **2006**, *62* (1), 238-51.
24. (a) Neftel, K. A.; Woodtly, W.; Schmid, M.; Frick, P. G.; Fehr, J., Amodiaquine induced agranulocytosis and liver damage. *British medical journal* **1986**, *292* (6522), 721-3; (b) O'Neill, P. M.; Bray, P. G.; Hawley, S. R.; Ward, S. A.; Park, B. K., 4-Aminoquinolines--past, present, and future: a chemical perspective. *Pharmacology & therapeutics* **1998**, *77* (1), 29-58.
25. O'Neill, P. M.; Mukhtar, A.; Stocks, P. A.; Randle, L. E.; Hindley, S.; Ward, S. A.; Storr, R. C.; Bickley, J. F.; O'Neil, I. A.; Maggs, J. L.; Hughes, R. H.; Winstanley, P. A.; Bray, P. G.; Park, B. K., Isoquine and related amodiaquine analogues: a new generation of improved 4-aminoquinoline antimalarials. *Journal of medicinal chemistry* **2003**, *46* (23), 4933-45.
26. (a) O'Neill, P. M.; Shone, A. E.; Stanford, D.; Nixon, G.; Asadollahy, E.; Park, B. K.; Maggs, J. L.; Roberts, P.; Stocks, P. A.; Biagini, G.; Bray, P. G.; Davies, J.; Berry, N.; Hall, C.; Rimmer, K.; Winstanley, P. A.; Hindley, S.; Bambal, R. B.; Davis, C. B.; Bates, M.; Gresham, S. L.; Brigandi, R. A.; Gomez-de-Las-Heras, F. M.; Gargallo, D. V.; Parapini, S.; Vivas, L.; Lander, H.; Taramelli, D.; Ward, S. A., Synthesis, antimalarial activity, and preclinical pharmacology of a novel series of 4'-fluoro and 4'-chloro analogues of amodiaquine. Identification of a suitable "back-up" compound for N-tert-butyl isoquine. *Journal of medicinal chemistry* **2009**, *52* (7), 1828-44; (b) O'Neill, P. M.; Park, B. K.; Shone, A. E.; Maggs, J. L.; Roberts, P.; Stocks, P. A.; Biagini, G. A.; Bray, P. G.; Gibbons, P.; Berry, N.; Winstanley, P. A.; Mukhtar, A.; Bonar-Law, R.; Hindley, S.; Bambal, R. B.; Davis, C. B.; Bates, M.; Hart, T. K.; Gresham, S. L.; Lawrence, R. M.; Brigandi, R. A.; Gomez-delas-Heras, F. M.; Gargallo, D. V.; Ward, S. A., Candidate selection and preclinical evaluation of N-tert-butyl isoquine (GSK369796), an affordable and effective 4-aminoquinoline antimalarial for the 21st century. *Journal of medicinal chemistry* **2009**, *52* (5), 1408-15.
27. Staines, H. M.; Krishna, S., *Treatment and prevention of malaria : antimalarial drug chemistry, action, and use*. Springer: Basel, 2012; p x , 315 p.
28. (a) Domarle, O.; Blampain, G.; Agnani, H.; Nzadiyabi, T.; Lebibi, J.; Brocard, J.; Maciejewski, L.; Biot, C.; Georges, A. J.; Millet, P., In vitro antimalarial activity of a new organometallic analog, ferrocene-chloroquine. *Antimicrobial agents and chemotherapy* **1998**, *42* (3), 540-4; (b) Supan, C.; Mombo-Ngoma, G.; Dal-Bianco, M. P.; Ospina Salazar, C. L.; Issifou, S.; Mazuir, F.; Filali-Ansary, A.; Biot, C.; Ter-Minassian, D.; Ramharther, M.; Kremsner, P. G.; Lell, B., Pharmacokinetics of ferroquine, a novel 4-aminoquinoline, in asymptomatic carriers of Plasmodium falciparum infections. *Antimicrobial agents and chemotherapy* **2012**, *56* (6), 3165-73.
29. Davis, T. M.; Hung, T. Y.; Sim, I. K.; Karunajeewa, H. A.; Ilett, K. F., Piperavaquine: a resurgent antimalarial drug. *Drugs* **2005**, *65* (1), 75-87.
30. Keating, G. M., Dihydroartemisinin/Piperavaquine: a review of its use in the treatment of uncomplicated Plasmodium falciparum malaria. *Drugs* **2012**, *72* (7), 937-61.
31. Trenholme, C. M.; Williams, R. L.; Desjardins, R. E.; Frischer, H.; Carson, P. E.; Rieckmann, K. H.; Canfield, C. J., Mefloquine (WR 142,490) in the treatment of human malaria. *Science* **1975**, *190* (4216), 792-4.
32. Tansley, R.; Lotharius, J.; Priestley, A.; Bull, F.; Duparc, S.; Mohrle, J., A randomized, double-blind, placebo-controlled study to investigate the safety, tolerability, and pharmacokinetics of single enantiomer (+)-mefloquine compared with racemic mefloquine in healthy persons. *The American journal of tropical medicine and hygiene* **2010**, *83* (6), 1195-201.
33. Schmidt, M.; Sun, H.; Rogne, P.; Scriba, G. K.; Griesinger, C.; Kuhn, L. T.; Reinscheid, U. M., Determining the absolute configuration of (+)-mefloquine HCl, the side-effect-reducing enantiomer of the antimalaria drug Lariam. *Journal of the American Chemical Society* **2012**, *134* (6), 3080-3.

34. Hyde, J. E., Exploring the folate pathway in Plasmodium falciparum. *Acta tropica* **2005**, *94* (3), 191-206.
35. Huang, H.; Lu, W.; Li, X.; Cong, X.; Ma, H.; Liu, X.; Zhang, Y.; Che, P.; Ma, R.; Li, H.; Shen, X.; Jiang, H.; Huang, J.; Zhu, J., Design and synthesis of small molecular dual inhibitor of falcipain-2 and dihydrofolate reductase as antimalarial agent. *Bioorganic & medicinal chemistry letters* **2012**, *22* (2), 958-62.
36. Zhang, K.; Rathod, P. K., Divergent regulation of dihydrofolate reductase between malaria parasite and human host. *Science* **2002**, *296* (5567), 545-7.
37. Kamchonwongpaisan, S.; Quarrell, R.; Charoensetakul, N.; Ponsinet, R.; Vilaivan, T.; Vanichtanankul, J.; Tarnchompoo, B.; Sirawaraporn, W.; Lowe, G.; Yuthavong, Y., Inhibitors of multiple mutants of Plasmodium falciparum dihydrofolate reductase and their antimalarial activities. *Journal of medicinal chemistry* **2004**, *47* (3), 673-80.
38. Burrows, J. N.; Burlot, E.; Campo, B.; Cherbuin, S.; Jeanneret, S.; Leroy, D.; Spangenberg, T.; Waterson, D.; Wells, T. N.; Willis, P., Antimalarial drug discovery - the path towards eradication. *Parasitology* **2014**, *141* (1), 128-39.
39. Yuthavong, Y.; Tarnchompoo, B.; Vilaivan, T.; Chitnumsub, P.; Kamchonwongpaisan, S.; Charman, S. A.; McLennan, D. N.; White, K. L.; Vivas, L.; Bongard, E.; Thongphanchang, C.; Taweechai, S.; Vanichtanankul, J.; Rattanajak, R.; Arwon, U.; Fantauzzi, P.; Yuvaniyama, J.; Charman, W. N.; Matthews, D., Malarial dihydrofolate reductase as a paradigm for drug development against a resistance-compromised target. *Proceedings of the National Academy of Sciences of the United States of America* **2012**, *109* (42), 16823-8.
40. Hyde, J. E., Targeting purine and pyrimidine metabolism in human apicomplexan parasites. *Current drug targets* **2007**, *8* (1), 31-47.
41. Krungkrai, J., Purification, characterization and localization of mitochondrial dihydroorotate dehydrogenase in Plasmodium falciparum, human malaria parasite. *Biochimica et biophysica acta* **1995**, *1243* (3), 351-60.
42. Gujjar, R.; Marwaha, A.; El Mazouni, F.; White, J.; White, K. L.; Creason, S.; Shackelford, D. M.; Baldwin, J.; Charman, W. N.; Buckner, F. S.; Charman, S.; Rathod, P. K.; Phillips, M. A., Identification of a metabolically stable triazolopyrimidine-based dihydroorotate dehydrogenase inhibitor with antimalarial activity in mice. *Journal of medicinal chemistry* **2009**, *52* (7), 1864-72.
43. Coteron, J. M.; Marco, M.; Esquivias, J.; Deng, X.; White, K. L.; White, J.; Koltun, M.; El Mazouni, F.; Kokkonda, S.; Katneni, K.; Bhamidipati, R.; Shackelford, D. M.; Angulo-Barturen, I.; Ferrer, S. B.; Jimenez-Diaz, M. B.; Gamo, F. J.; Goldsmith, E. J.; Charman, W. N.; Bathurst, I.; Floyd, D.; Matthews, D.; Burrows, J. N.; Rathod, P. K.; Charman, S. A.; Phillips, M. A., Structure-guided lead optimization of triazolopyrimidine-ring substituents identifies potent Plasmodium falciparum dihydroorotate dehydrogenase inhibitors with clinical candidate potential. *Journal of medicinal chemistry* **2011**, *54* (15), 5540-61.
44. Booker, M. L.; Bastos, C. M.; Kramer, M. L.; Barker, R. H., Jr.; Skerlj, R.; Sidhu, A. B.; Deng, X.; Celatka, C.; Cortese, J. F.; Guerrero Bravo, J. E.; Crespo Llado, K. N.; Serrano, A. E.; Angulo-Barturen, I.; Jimenez-Diaz, M. B.; Viera, S.; Garuti, H.; Wittlin, S.; Papastogiannidis, P.; Lin, J. W.; Janse, C. J.; Khan, S. M.; Duraisingh, M.; Coleman, B.; Goldsmith, E. J.; Phillips, M. A.; Munoz, B.; Wirth, D. F.; Klinger, J. D.; Wiegand, R.; Sybertz, E., Novel inhibitors of Plasmodium falciparum dihydroorotate dehydrogenase with anti-malarial activity in the mouse model. *The Journal of biological chemistry* **2010**, *285* (43), 33054-64.
45. Skerlj, R. T.; Bastos, C. M.; Booker, M. L.; Kramer, M. L.; Barker, R. H.; Celatka, C. A.; O'Shea, T. J.; Munoz, B.; Sidhu, A. B.; Cortese, J. F.; Wittlin, S.; Papastogiannidis, P.; Angulo-Barturen, I.; Jimenez-Diaz, M. B.; Sybertz, E., Optimization of Potent Inhibitors of P. falciparum Dihydroorotate Dehydrogenase for the Treatment of Malaria. *Acs Med Chem Lett* **2011**, *2* (9), 708-713.

46. Winter, R.; Kelly, J. X.; Smilkstein, M. J.; Hinrichs, D.; Koop, D. R.; Riscoe, M. K., Optimization of endochin-like quinolones for antimalarial activity. *Experimental parasitology* **2011**, *127* (2), 545-51.
47. Nilsen, A.; LaCrue, A. N.; White, K. L.; Forquer, I. P.; Cross, R. M.; Marfurt, J.; Mather, M. W.; Delves, M. J.; Shackelford, D. M.; Saenz, F. E.; Morrissey, J. M.; Steuten, J.; Mutka, T.; Li, Y.; Wirjanata, G.; Ryan, E.; Duffy, S.; Kelly, J. X.; Sebayang, B. F.; Zeeman, A. M.; Noviyanti, R.; Sinden, R. E.; Kocken, C. H.; Price, R. N.; Avery, V. M.; Angulo-Barturen, I.; Jimenez-Diaz, M. B.; Ferrer, S.; Herreros, E.; Sanz, L. M.; Gamo, F. J.; Bathurst, I.; Burrows, J. N.; Siegl, P.; Guy, R. K.; Winter, R. W.; Vaidya, A. B.; Charman, S. A.; Kyle, D. E.; Manetsch, R.; Riscoe, M. K., Quinolone-3-diarylethers: a new class of antimalarial drug. *Science translational medicine* **2013**, *5* (177), 177ra37.
48. (a) Wang, X.; Creek, D. J.; Schiaffo, C. E.; Dong, Y.; Chollet, J.; Scheurer, C.; Wittlin, S.; Charman, S. A.; Dussault, P. H.; Wood, J. K.; Vennerstrom, J. L., Spiroadamantyl 1,2,4-trioxolane, 1,2,4-trioxane, and 1,2,4-trioxepane pairs: relationship between peroxide bond iron(II) reactivity, heme alkylation efficiency, and antimalarial activity. *Bioorganic & medicinal chemistry letters* **2009**, *19* (16), 4542-5; (b) Park, B. K.; O'Neill, P. M.; Maggs, J. L.; Pirmohamed, M., Safety assessment of peroxide antimalarials: clinical and chemical perspectives. *British journal of clinical pharmacology* **1998**, *46* (6), 521-9.
49. Dong, Y.; Wittlin, S.; Sriraghavan, K.; Chollet, J.; Charman, S. A.; Charman, W. N.; Scheurer, C.; Urwyler, H.; Santo Tomas, J.; Snyder, C.; Creek, D. J.; Morizzi, J.; Koltun, M.; Matile, H.; Wang, X.; Padmanilayam, M.; Tang, Y.; Dorn, A.; Brun, R.; Vennerstrom, J. L., The structure-activity relationship of the antimalarial ozonide arterolane (OZ277). *Journal of medicinal chemistry* **2010**, *53* (1), 481-91.
50. (a) Valecha, N.; Looareesuwan, S.; Martensson, A.; Abdulla, S. M.; Krudsood, S.; Tangpukdee, N.; Mohanty, S.; Mishra, S. K.; Tyagi, P. K.; Sharma, S. K.; Moehrl, J.; Gautam, A.; Roy, A.; Paliwal, J. K.; Kothari, M.; Saha, N.; Dash, A. P.; Bjorkman, A., Arterolane, a new synthetic trioxolane for treatment of uncomplicated Plasmodium falciparum malaria: a phase II, multicenter, randomized, dose-finding clinical trial. *Clinical infectious diseases : an official publication of the Infectious Diseases Society of America* **2010**, *51* (6), 684-91; (b) Valecha, N.; Krudsood, S.; Tangpukdee, N.; Mohanty, S.; Sharma, S. K.; Tyagi, P. K.; Anvikar, A.; Mohanty, R.; Rao, B. S.; Jha, A. C.; Shahi, B.; Singh, J. P.; Roy, A.; Kaur, P.; Kothari, M.; Mehta, S.; Gautam, A.; Paliwal, J. K.; Arora, S.; Saha, N., Arterolane maleate plus piperazine phosphate for treatment of uncomplicated Plasmodium falciparum malaria: a comparative, multicenter, randomized clinical trial. *Clinical infectious diseases : an official publication of the Infectious Diseases Society of America* **2012**, *55* (5), 663-71.
51. Wang, X.; Dong, Y.; Wittlin, S.; Charman, S. A.; Chiu, F. C.; Chollet, J.; Katneni, K.; Mannila, J.; Morizzi, J.; Ryan, E.; Scheurer, C.; Steuten, J.; Santo Tomas, J.; Snyder, C.; Vennerstrom, J. L., Comparative antimalarial activities and ADME profiles of ozonides (1,2,4-trioxolanes) OZ277, OZ439, and their 1,2-dioxolane, 1,2,4-trioxane, and 1,2,4,5-tetraoxane isosteres. *Journal of medicinal chemistry* **2013**, *56* (6), 2547-55.
52. Charman, S. A.; Arbe-Barnes, S.; Bathurst, I. C.; Brun, R.; Campbell, M.; Charman, W. N.; Chiu, F. C.; Chollet, J.; Craft, J. C.; Creek, D. J.; Dong, Y.; Matile, H.; Maurer, M.; Morizzi, J.; Nguyen, T.; Papastogiannidis, P.; Scheurer, C.; Shackelford, D. M.; Sriraghavan, K.; Stingelin, L.; Tang, Y.; Urwyler, H.; Wang, X.; White, K. L.; Wittlin, S.; Zhou, L.; Vennerstrom, J. L., Synthetic ozonide drug candidate OZ439 offers new hope for a single-dose cure of uncomplicated malaria. *Proceedings of the National Academy of Sciences of the United States of America* **2011**, *108* (11), 4400-5.
53. O'Neill, P. M.; Amewu, R. K.; Nixon, G. L.; Bousejra ElGarah, F.; Mungthin, M.; Chadwick, J.; Shone, A. E.; Vivas, L.; Lander, H.; Barton, V.; Muangnoicharoen, S.; Bray, P. G.; Davies, J.; Park, B. K.; Wittlin, S.; Brun, R.; Preschel, M.; Zhang, K.; Ward, S. A., Identification of a 1,2,4,5-tetraoxane antimalarial drug-development candidate (RKA 182) with superior properties to the semisynthetic artemisinins. *Angewandte Chemie* **2010**, *49* (33), 5693-7.

54. Fernando, D.; Rodrigo, C.; Rajapakse, S., Primaquine in vivax malaria: an update and review on management issues. *Malaria journal* **2011**, *10*, 351.
55. Vale, N.; Nogueira, F.; do Rosario, V. E.; Gomes, P.; Moreira, R., Primaquine dipeptide derivatives bearing an imidazolidin-4-one moiety at the N-terminus as potential antimalarial prodrugs. *European journal of medicinal chemistry* **2009**, *44* (6), 2506-16.
56. Dow, G. S.; Gettayacamin, M.; Hansukjariya, P.; Imerbsin, R.; Komcharoen, S.; Sattabongkot, J.; Kyle, D.; Milhous, W.; Cozens, S.; Kenworthy, D.; Miller, A.; Veazey, J.; Ohrt, C., Radical curative efficacy of tafenoquine combination regimens in Plasmodium cynomolgi-infected Rhesus monkeys (Macaca mulatta). *Malaria journal* **2011**, *10*, 212.
57. Cappellini, M. D.; Fiorelli, G., Glucose-6-phosphate dehydrogenase deficiency. *Lancet* **2008**, *371* (9606), 64-74.
58. Llanos-Cuentas, A.; Lacerda, M. V.; Rueangweerayut, R.; Krudsood, S.; Gupta, S. K.; Kochar, S. K.; Arthur, P.; Chuenchom, N.; Mohrle, J. J.; Duparc, S.; Ugwuegbulam, C.; Kleim, J. P.; Carter, N.; Green, J. A.; Kellam, L., Tafenoquine plus chloroquine for the treatment and relapse prevention of Plasmodium vivax malaria (DETECTIVE): a multicentre, double-blind, randomised, phase 2b dose-selection study. *Lancet* **2014**, *383* (9922), 1049-58.
59. Wells, T. N.; Burrows, J. N.; Baird, J. K., Targeting the hypnozoite reservoir of Plasmodium vivax: the hidden obstacle to malaria elimination. *Trends in parasitology* **2010**, *26* (3), 145-51.
60. Nagle, A.; Wu, T.; Kuhen, K.; Gagaring, K.; Borboa, R.; Francek, C.; Chen, Z.; Plouffe, D.; Lin, X.; Caldwell, C.; Ek, J.; Skolnik, S.; Liu, F.; Wang, J.; Chang, J.; Li, C.; Liu, B.; Hollenbeck, T.; Tuntland, T.; Isbell, J.; Chuan, T.; Alper, P. B.; Fischli, C.; Brun, R.; Lakshminarayana, S. B.; Rottmann, M.; Diagana, T. T.; Winzeler, E. A.; Glynne, R.; Tully, D. C.; Chatterjee, A. K., Imidazolopiperazines: lead optimization of the second-generation antimalarial agents. *Journal of medicinal chemistry* **2012**, *55* (9), 4244-73.
61. Biamonte, M. A.; Wanner, J.; Le Roch, K. G., Recent advances in malaria drug discovery. *Bioorganic & medicinal chemistry letters* **2013**, *23* (10), 2829-43.
62. Guiguemde, W. A.; Shelat, A. A.; Bouck, D.; Duffy, S.; Crowther, G. J.; Davis, P. H.; Smithson, D. C.; Connelly, M.; Clark, J.; Zhu, F.; Jimenez-Diaz, M. B.; Martinez, M. S.; Wilson, E. B.; Tripathi, A. K.; Gut, J.; Sharlow, E. R.; Bathurst, I.; El Mazouni, F.; Fowble, J. W.; Forquer, I.; McGinley, P. L.; Castro, S.; Angulo-Barturen, I.; Ferrer, S.; Rosenthal, P. J.; Derisi, J. L.; Sullivan, D. J.; Lazo, J. S.; Roos, D. S.; Riscoe, M. K.; Phillips, M. A.; Rathod, P. K.; Van Voorhis, W. C.; Avery, V. M.; Guy, R. K., Chemical genetics of Plasmodium falciparum. *Nature* **2010**, *465* (7296), 311-5.
63. Gamo, F. J.; Sanz, L. M.; Vidal, J.; de Cozar, C.; Alvarez, E.; Lavandera, J. L.; Vanderwall, D. E.; Green, D. V.; Kumar, V.; Hasan, S.; Brown, J. R.; Peishoff, C. E.; Cardon, L. R.; Garcia-Bustos, J. F., Thousands of chemical starting points for antimalarial lead identification. *Nature* **2010**, *465* (7296), 305-10.
64. Plouffe, D.; Brinker, A.; McNamara, C.; Henson, K.; Kato, N.; Kuhen, K.; Nagle, A.; Adrian, F.; Matzen, J. T.; Anderson, P.; Nam, T. G.; Gray, N. S.; Chatterjee, A.; Janes, J.; Yan, S. F.; Trager, R.; Caldwell, J. S.; Schultz, P. G.; Zhou, Y.; Winzeler, E. A., In silico activity profiling reveals the mechanism of action of antimalarials discovered in a high-throughput screen. *Proceedings of the National Academy of Sciences of the United States of America* **2008**, *105* (26), 9059-64.
65. Rottmann, M.; McNamara, C.; Yeung, B. K.; Lee, M. C.; Zou, B.; Russell, B.; Seitz, P.; Plouffe, D. M.; Dharia, N. V.; Tan, J.; Cohen, S. B.; Spencer, K. R.; Gonzalez-Paez, G. E.; Lakshminarayana, S. B.; Goh, A.; Suwanarusk, R.; Jegla, T.; Schmitt, E. K.; Beck, H. P.; Brun, R.; Nosten, F.; Renia, L.; Dartois, V.; Keller, T. H.; Fidock, D. A.; Winzeler, E. A.; Diagana, T. T., Spiroindolones, a potent compound class for the treatment of malaria. *Science* **2010**, *329* (5996), 1175-80.

Chapter II : Antimalarial quinolone targeting *Pf*
electron transport chain

Chapter II : Antimalarial quinolone targeting *Pf* electron transport chain

	page
2.1 <i>Plasmodium</i> Electron transport chain	31
2.2 <i>Plasmodium falciparum</i> cytochrome <i>bc</i> ₁ complex	32
2.2.1 The mechanism of cytochrome <i>bc</i> ₁	32
2.2.2 The inhibitors of <i>Pf</i> cytochrome <i>bc</i> ₁	33
2.3 <i>Plasmodium falciparum</i> type II NADH:ubiquinone oxidoreductase	38
2.3.1 The introduction to <i>Pf</i> NDH2	38
2.3.2 The discovery and development of <i>Pf</i> NDH2 inhibitors	38
2.4 2-Aryl quinolones targeting both <i>Pf</i> NDH2 and <i>Pfbc</i> ₁ : the dual inhibition	40
2.5 Chemistry of 4-quinolones	41
2.5.1 Cyclisation of bond <i>a</i>	42
2.5.2 Cyclisation of bond <i>b</i>	42
2.5.3 Cyclisation of bond <i>c</i>	44
2.5.4 Cyclisation of bond <i>d</i>	45
2.5.5 Cyclisation of bond <i>e</i>	46
2.6 Conclusion	46
2.7 Reference	47

Antimalarial quinolone targeting *Pf* electron transport chain

2.1 *Plasmodium* Electron transport chain

Mitochondrion is generally known as a power plant of any cell. Like humans, the plasmodial mitochondria play a critical and essential role in its life cycle. The mitochondrial electron transport chain of *Plasmodium falciparum* (*Pf*ETC) is an attractive target for chemotherapy due to several molecular and functional differences between the parasite's and human's mitochondria¹. For instance, in contrast to eukaryotic cell, *Plasmodiums* harvest most energy they need from glycolysis rather than their mitochondrial oxidative phosphorylation. Rather, the parasites mitochondria act as an electron sink for the electrons produced in other processes such as *de novo* pyrimidine biosynthesis².

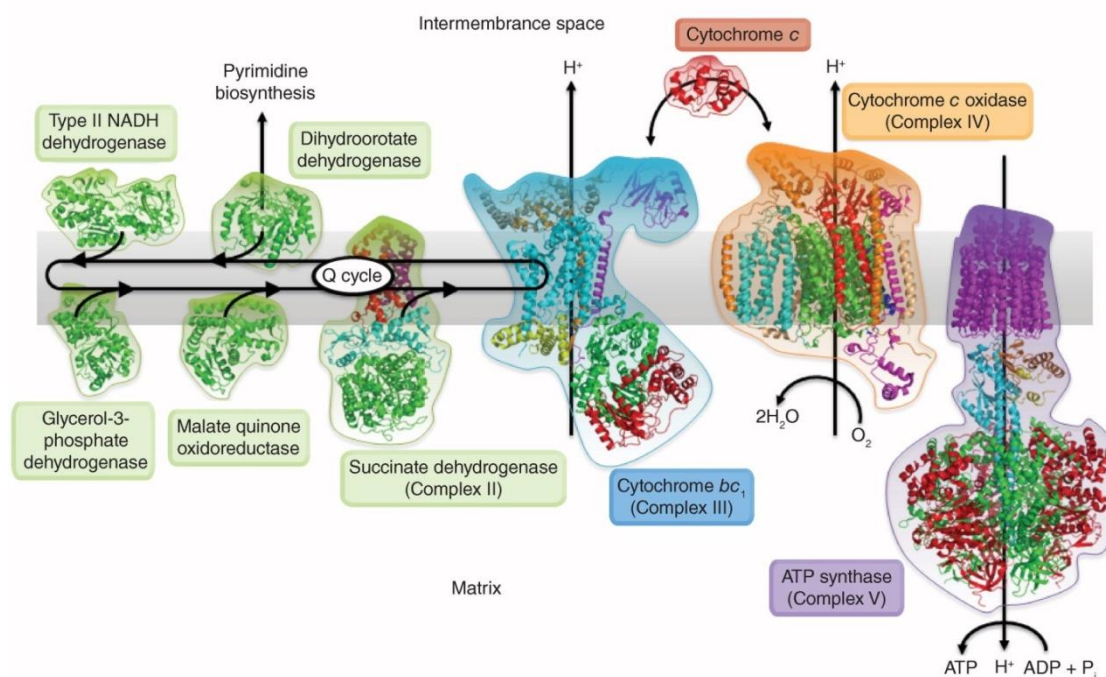


Figure 2.1 Mitochondrial *Plasmodium* Electron transport chain³

The *Pf*ETC of blood stage parasites is believed to contain five dehydrogenases, namely glycerol-3-phosphate dehydrogenase, malate quinone oxidoreductase, type II NADH:ubiquinone oxidoreductase (*Pf*NDH2), dihydroorotate dehydrogenase (DHODH), and succinate dehydrogenase (complex II or SDH), respectively. Although the functions of these enzymes are not completely

understood, one of their activities is to provide electrons to the downstream complexes such as cytochrome bc_1 (complex III) and cytochrome c oxidase (complex IV) with ubiquinone (CoQ) and cytochrome c acting as electron carriers between the complexes⁴. It is noteworthy that the *Pf* ATP synthase (complex V) is not reported to generate any ATP, unlike its mammalian counterpart⁵. Only complex III has been clinically validated as an antimalarial drug target through the use of atovaquone (**8**). As previously described, DSM265 (**21**) is now under Phase IIa studies and if successful, it would be the first compound targeting DHODH.

2.2 *Plasmodium falciparum* cytochrome bc_1 complex

2.2.1 The mechanism of cytochrome bc_1

The cytochrome bc_1 complex is a key enzyme catalysing the transfer of electron from ubiquinol to cytochrome c ⁶. The catalytic core is composed of three main subunits; cytochrome b (43 kDa), cytochrome c_1 (27 kDa), and the Reiske iron-sulfur protein ([2Fe2S] ISP, 21 kDa) with these subunits participating directly in electron transfer pathway. The function of the remaining residues is not well understood, but they seem to contribute to complex stability and the assembly process⁷.

The protonmotive mechanism of bc_1 complex was reviewed elsewhere^{6b, 8} but initially described by Mitchell's Q-cycle hypothesis⁹. In summary, the bc_1 complex contains two distinct quinone-binding sites namely the quinone oxidation site Q_o and the quinone reduction site Q_i . They are located on the opposite sides of the mitochondrial membrane and linked by a transmembrane electron-transfer pathway containing two hemes with different redox potentials (low potential b_l and high potential b_h). Quinol antagonists such as naturally occurring stigmatellin (**38**) can bind to oxidation site (Q_o) and are oxidised to release two protons and two electrons into the intermembrane space. One electron reduces the ISP whilst the other reduces heme b_l . The electron from b_l is then transfer to b_h and to a quinone bound at the reduction site (Q_i) converting quinone back to quinol. Meanwhile, the reduced ISP undergoes a conformational change enabling the close contact and an electron transfer between ISP and cytochrome c_1 . Electron carrying cytochrome c_1 is

oxidised by a soluble cytochrome *c*, an electron donor to cytochrome *c* oxidase (complex IV). Overall, two protons are translocated per one quinol bound at Q_o from the negative (n, matrix) to the positive side (p, intermembrane space) of mitochondrial membrane¹⁰.

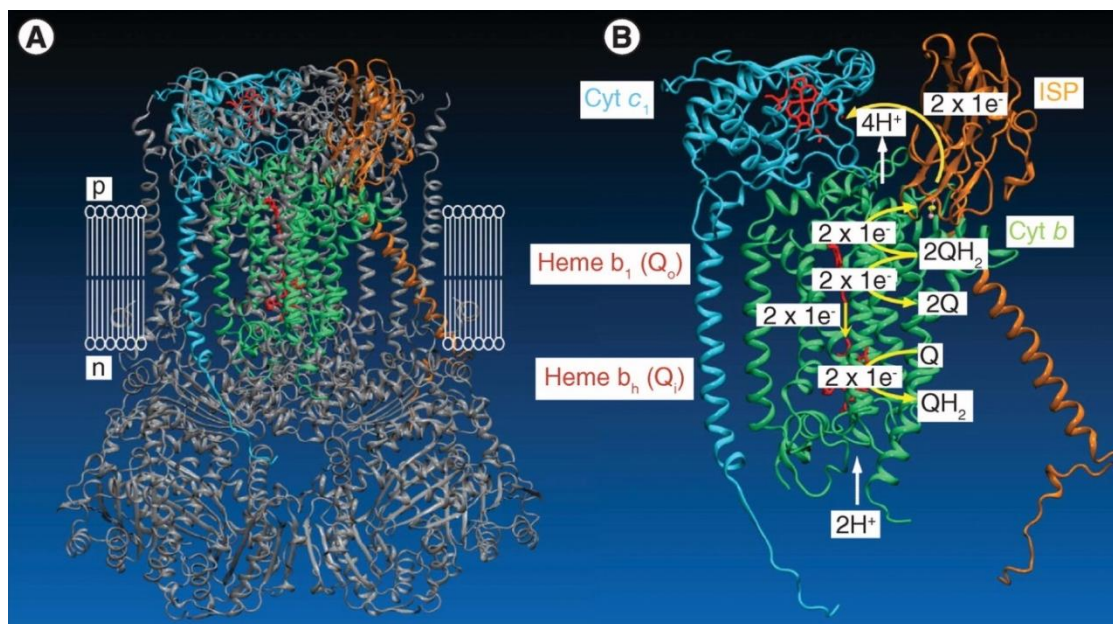


Figure 2.2 The cytochrome bc_1 complex. Cytochrome *b*, cytochrome c_1 and the Rieske ISP protein are represented in green, cyan and orange, respectively. Hemes of cytochrome *b* and cytochrome c_1 are shown in red wireframe, with the iron (pink) and sulphur (yellow) atoms of the Rieske [2Fe2S] cluster represented in spacefill. (A) Ribbon model (gray) of the homodimeric structure of the yeast cytochrome bc_1 complex (PDB code 3CX5). (B) The structure and Q-cycle mechanism of the catalytic core of the bc_1 complex. Electron transfers to and from ubiquinol (QH_2) and ubiquinone (Q) are represented by yellow arrows. Proton movements are indicated by white arrows³.

2.2.2 The inhibitors of *Pf* cytochrome bc_1

There are several quinol antagonists serving as inhibitors to the cytochrome bc_1 Q_o site such as aforementioned stigmatellin (**38**) and myxothiazol (**39**). Some bind at Q_i site such as naturally occurring antibiotic antimycin A (**40**). These compounds potentially abolish the bc_1 protonmotive activity leading to the collapse

of the mitochondrial membrane potential and cell death¹¹; however, they are not species selective, and therefore, their toxicity limits its therapeutic uses¹².

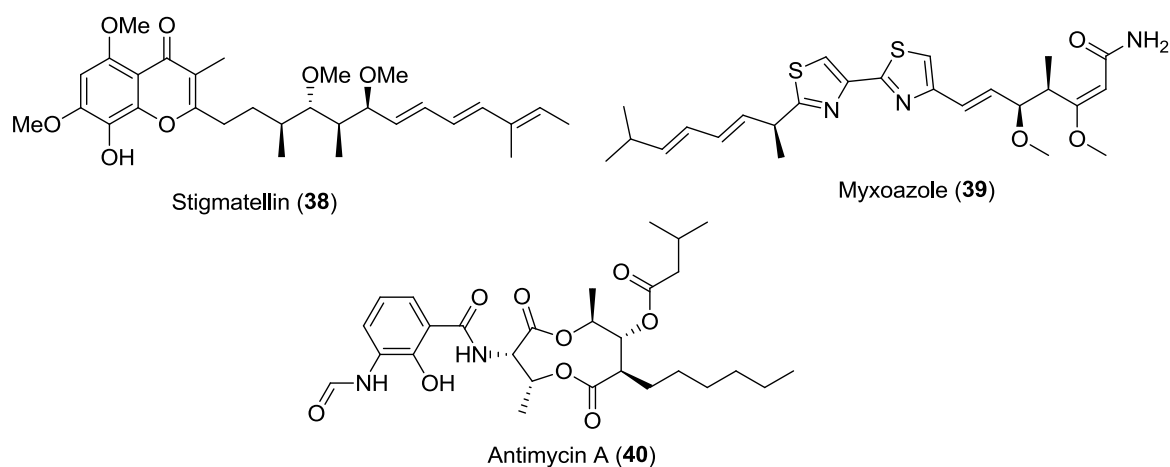


Figure 2.3 Inhibitors of *Pf* cytochrome bc_1

Atovaquone

The *Plasmodium bc₁* is the only component of the ETC that clinically served as an antimalarial target¹³. Atovaquone (ATQ)(8) is the only established chemotherapy targeting *Pfbc₁*¹⁴. The discovery and development of ATQ is described in detail elsewhere¹⁵. In brief, it began after the outbreak of World War II due to a shortage of quinine¹⁶. A large number of hydroxynaphthoquinones were discovered with modest antimalarial activity in duck models, but were inactive in malaria patients due to their poor absorption and rapid metabolism¹⁷. The programme was revisited in 1960s and it led to the discovery of intravenously administered lapinone¹⁸. The Wellcome Research Laboratories reinvestigated the potential of quinones as antimalarial agents in 1980s. The study was designed to develop a quinone with a good metabolic stability combined with good antimalarial activity. Several quinones from this programme demonstrated an excellent potency of nanomolar concentration against *P.falciparum*¹⁹, but only ATQ was found to be inert to human liver microsomes²⁰.

Due to its rapid emergence of resistance during its clinical development, the use of ATQ as monotherapy is discouraged. ATQ is consequently used as a fixed-dose combination with proguanil (marketed as Malarone)²¹ for treating children

and adults with uncomplicated malaria²², or as chemoprophylaxis for preventing malaria in travellers²³. Despite its excellent activity and good metabolic stability, the high cost of production and its poor absorption limit its widespread use. The search for cheaper alternatives demonstrating a little cross resistance and better pharmacokinetics properties has led to the discovery of several active chemotypes, for example, pyridones, acridone analogues, and quinolones^{3,10}.

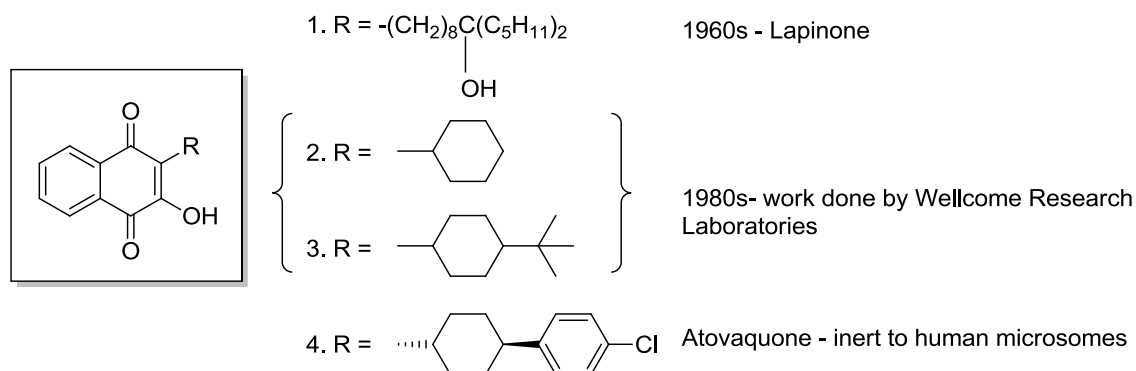


Figure 2.4 The discovery and development of atovaquone^{6a}

Pyridones

Discovered in 1960s, clopidol, one of the well-known anticoccidial agents acting as an inhibitor of parasite mitochondrial respiration, was the starting point for the research in this class. Clopidol (**41**) also maintains activity against atovaquone-resistant strains suggesting that pyridones may bind at the different site in the Q_o pocket¹⁰.

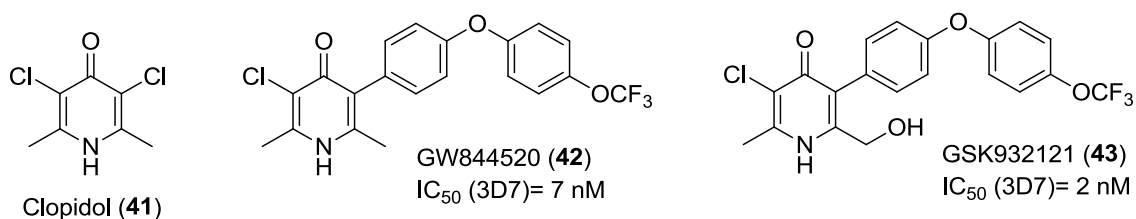


Figure 2.5 Antimalarial pyridones

In 2006, GSK reported the preclinical SAR of a new class 4-pyridones²⁴. In collaboration with Yeates et al., a series of substituted clopidol were developed²⁵. It

was found that GW844520, with a flexible phenoxyphenyl side chain, is well tolerated with an IC_{50} (3D7) of 7 nM. However, its development was terminated owing to unexpected cardiotoxicity²⁶. This adverse effect may be related to off-target binding of human bc_1 function. Further investigation led to the discovery of another candidate GSK932121 which was found to be highly potent against multidrug resistant *Pf* in a murine model²⁷. GSK932121 went into clinical trials in December 2008, but it was later suspended by the MMV due to its toxicity issues³.

Acridine related compounds

A number of acridinediones as potent bc_1 inhibitors were developed by the Walter Reed Army Institute of Research. Moreover, their mode of action has also been proved to be heme-binding and prevention of detoxifying crystallisation²⁸. A small change in their structures affects not only the potency but also the mechanism of action. Highly potent floxacrine and WR249685 show *in vitro* antimalarial IC_{50} activity of 140 and 15 nM, respectively. It was found that floxacrine is active through heme-binding processes whilst the latter acts as a selective inhibitor of *Pfbc_1*²⁹.

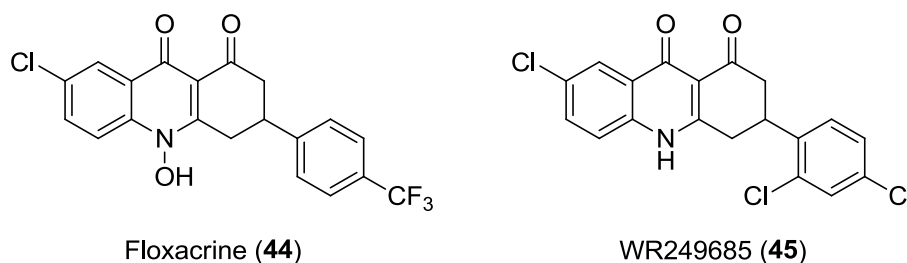
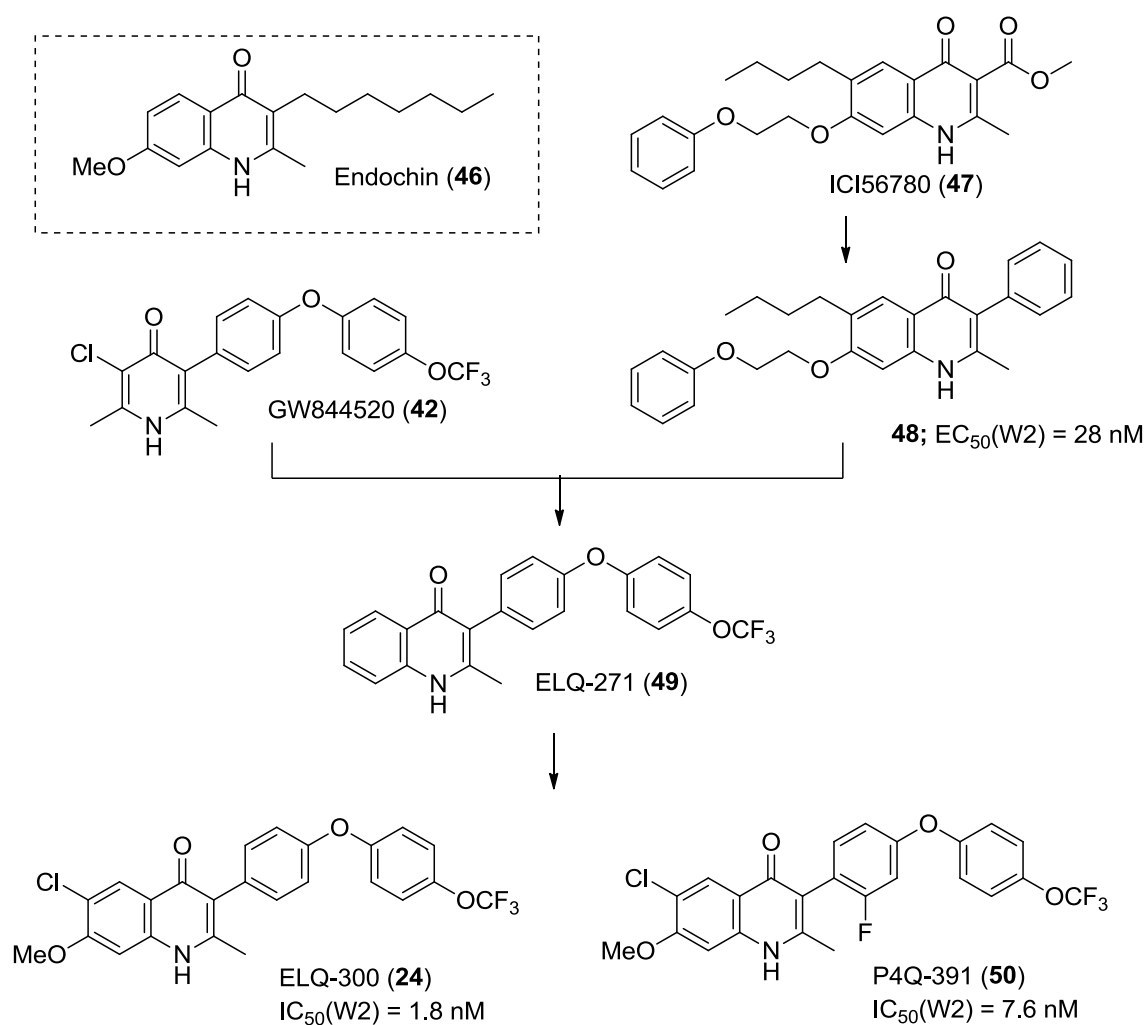


Figure 2.6 Antimalarial acridinediones

Quinolones

There are a large number of recent publications based on the development of antimalarial quinolones³⁰. The most advance development amongst this class is ELQ-300. Starting from endochin which possesses prophylactic and therapeutic property in avian *Plasmodia*³¹, the related quinolone ICI56780 were discovered in the 1960s with *in vivo* activity in rodent models^{30a}. The Manetsch group reported a similar compound with a phenyl substitution at C3 and it shows an EC_{50} = 28 nM

against W2 strain and of 31 nM against the atovaquone-resistant strain TM90-C2B³². Winter *et al.* has also developed a series of highly potent endochin-like quinolones (ELQ) with an aim of improving potency and metabolic stability³³. The optimisation of aryl substituent has led to the discovery of multiple potent derivatives that are active against drug-resistant strains. Replacement of the phenyl side chain with the side chain from aforesaid GW844520 gave ELQ-271 which possessed an improved metabolic stability. Most recently, a diarylether quinolone ELQ-300 was identified and selected as a preclinical candidate by MMV. The back-up compound P4Q-391 containing a fluorine atom in the diarylether side chain has also been fully investigated for its biological activity^{30c}.



Scheme 2.1 Rational development of endochin-like quinolones

ELQ-300 is a selective potent *Plasmodium bc₁* inhibitor and shows a superior antiparasitoid activity *in vitro* and *in vivo* against blood stage and liver stage of malaria. This class of compound, however, does have limitation due to its poor aqueous solubility, and this has an effect on its pharmacokinetics. Formulation approaches are currently in progress to resolve this^{30c}.

2.3 *Plasmodium falciparum* type II NADH:ubiquinone oxidoreductase (*Pf*NDH2)

2.3.1 The introduction to *Pf*NDH2

Due to the fact that the parasite lacks the NADH dehydrogenase which converts NADH to NAD⁺, it instead uses type II NADH:ubiquinone oxidoreductase (*Pf*NDH2)^{5a}. *Pf*NDH2 is a single subunit (52 kDa) mitochondrial enzyme catalysing an electron transfer from NADH to ubiquinone or CoQ³⁴. *Pf*NDH2 is a principal electron donor linking the fermentative glycolysis where NADHs are produced to the generation of mitochondrial membrane potential. Thanks to the absence of NDH2 in humans, *Pf*NDH2 is therefore an attractive promising target in the development of antimalarials.

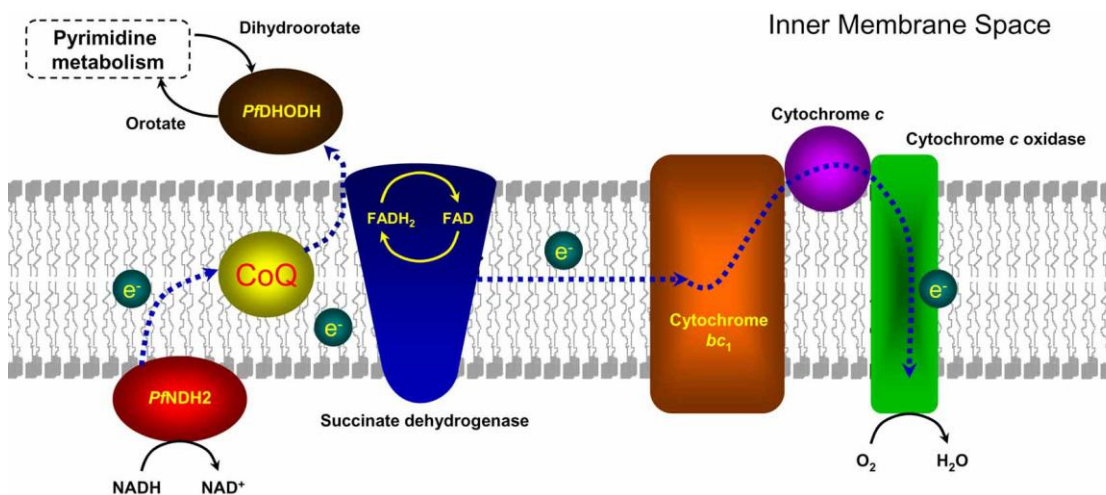
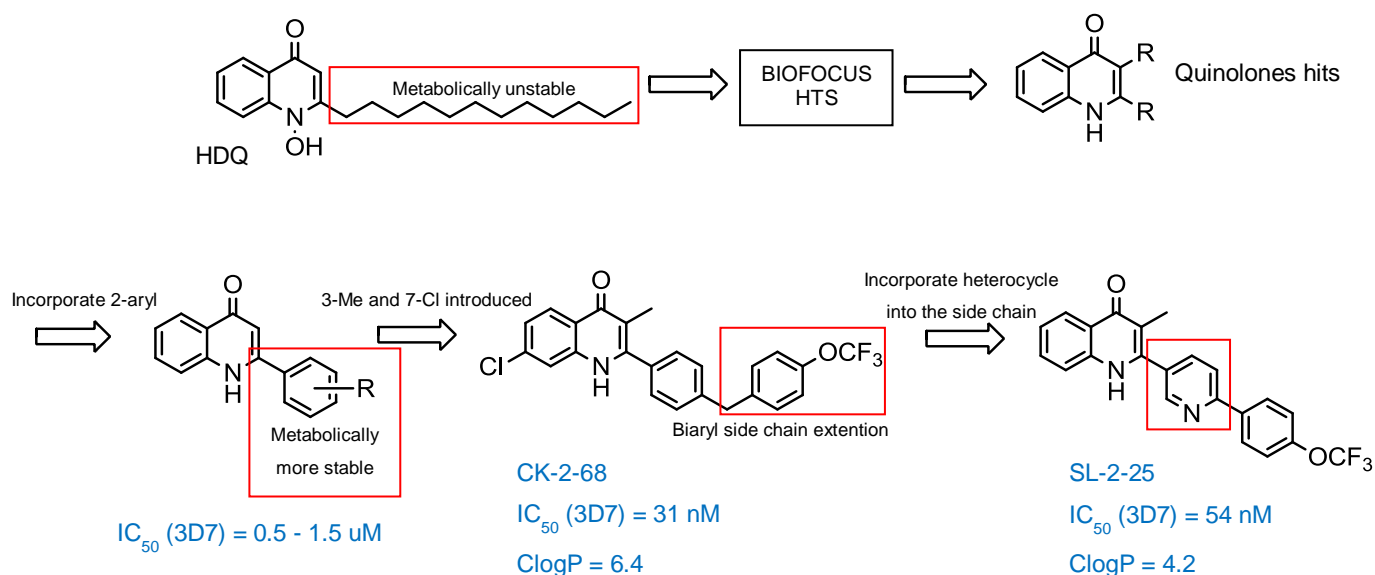


Figure 2.7 *Pf*NDH2¹

2.3.2 The discovery and development of *Pf*NDH2 inhibitors

*Pf*NDH2 has only one known inhibitor, HDQ or hydroxyl-2-dodecyl-4-(1H)-quinolone. A high-throughput screening against *Pf*NDH2 was set up using recombinant *Pf*NDH2 expressed in an *Escherichia Coli* model³⁵. The focused library

was selected from a commercial library of ~750,000 compounds (BioFocus DPI), and compounds were predicted to possess favourable absorption, distribution, metabolism, excretion, and toxicity characteristics³⁶. Following a preliminary screening, 419 actives (>30% inhibition at 20 μM) were retested in triplicate, and from these, 150 compounds were progressed for potency determination (10-point concentration curves, 1:3 dilution). From the active compounds tested for potency, 22 compounds had IC_{50} values falling between 11–40 μM , and 24 compounds had IC_{50} values <10 μM and purity >70%. Several distinct chemotypes were obtained from the screen. The quinolone core was selected as the key template for further SAR development³⁷.



Scheme 2.2 The development of selective *Pf*NDH2 inhibitors

Initial studies have focused on 2-monoaryl quinolones; however, it was impossible to achieve activity below 500 nM against the 3D7 strain of *P.falciparum*. Replacing the metabolically vulnerable HDQ side chain with a longer bisaryl or phenoxy aryl has provided derivatives with improved both antimalarial and *Pf*NDH2 activity. Introduction of a methyl substituent at position 3 manipulates the twists of the 2-aryl side chain, alters the torsion angle (presumably leading to a reduction in aggregation) and results in better overall solubility and greatly enhanced activity. This medicinal chemistry strategy generated more than 60 compounds, as exemplified by CK-2–68 with activity of 31 nM against the *P. falciparum* 3D7 strain and 16 nM against *Pf*NDH2. Preliminary animal studies of CK-2-68 reveals that a

reduction of ClogP and enhancement in aqueous solubility are required in order to orally administer the drug without any need of prodrug approach³⁷.

Heterocycle incorporation into the quinolone side chain gave a series of compounds containing a pyridine group. Introduction of a pyridyl group reduces ClogP; improves aqueous solubility, and allows the possibility of salt formation. These structural changes led to the identification of SL-2-25 with an IC₅₀ in the nanomolar range versus both the enzyme and whole-cell *Pf*³⁸. Further detail on its development will be extensively discussed in the following chapter.

2.4 2-Aryl quinolones targeting both *Pf*NDH2 and *Pfbc*₁: the dual inhibition

Although the initial studies on 2-ary quinolones were focused on optimization of activity versus *Pf*NDH2, during hit-to-lead development, it was found that optimized compounds with nanomolar activity versus *Pf*NDH2 were also active at the parasite *bc*₁ complex. This dual inhibitory effect is also seen with the starting compound for this program, HDQ, suggesting that the quinolone pharmacophore is a privileged scaffold for inhibition of both targets. Such multiple-target drugs are seen increasingly as having added therapeutic benefit over drugs acting exclusively at one site³⁹.

Manipulation of quinolone core to impart some selectivity is possible. When comparing the 2-aryl and 3-aryl series of compounds, 2-aryl quinolones provide *Pf*NDH2 inhibition levels of less than 20 nM, whereas the 3-aryl counterparts have *Pf*NDH2 inhibition levels greater than 200 nM. However, 3-aryl quinolones demonstrate high levels of *bc*₁ inhibition^{30b}. As a result of the potential of this template, the potent lead compound from this series is currently in the MMV pipeline.

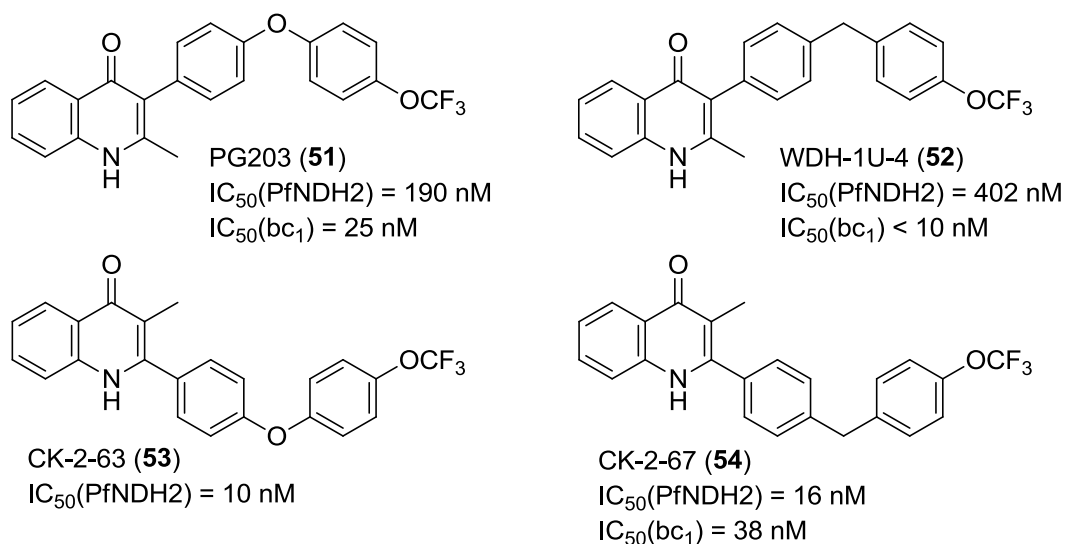
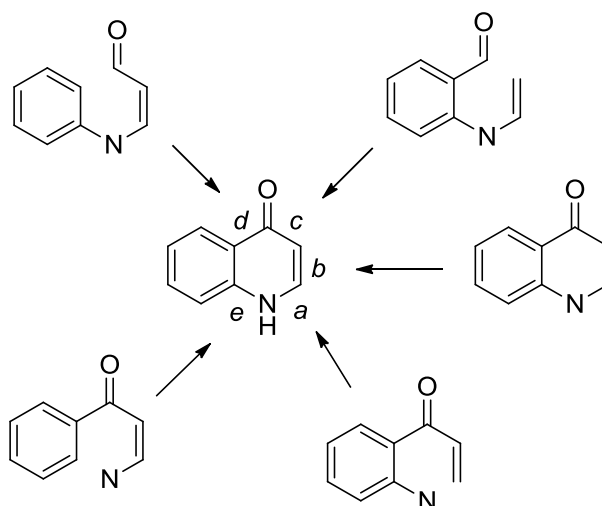


Figure 2.8 The 2-aryl quinolones provide greater levels of PfNDH2 inhibition, whereas 3-aryl counterparts possess high levels of bc_1 inhibition

2.5 Chemistry of 4-quinolones

As 4-quinolones are the main target being focused in the next few chapters, a literature search shows that there are several ways to construct and modify the 4-quinolone skeleton. Those synthetic methods were well examined and discussed⁴⁰; some are widely used; however, in this part, the method based on the annulation of quinolone B-ring will be discussed and summarised.

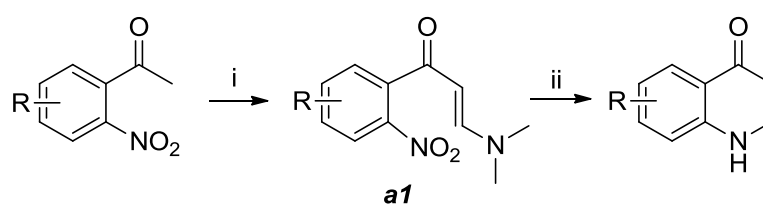
Many cyclisation methods are well known for the production of 4-quinolone. All the reactions can be categorised into five strategies depending on the formation of which bond (*a*, *b*, *c*, *d* or *e*) leading to ring closure. In this thesis, these methods were used and applied towards the synthesis of corresponding targeted 4-quinolones.



Scheme 2.3 Quinolone cyclisation

2.5.1 Cyclisation of bond *a*

Ring closure of bond *a* requires the corresponding *o*-carbonyl-aniline starting material bearing an electrophilic group at β -position which can be either vinyl or carbonyl. This method was successfully proved by the synthesis of 2,3-unsubstituted quinolones. The starting enamine **a1** produced by reacting *o*-nitroacetophenone with dimethyl formamide dimethyl acetal in DMF underwent cyclisation under reducing environment with 10% Pd-C as catalyst⁴¹.

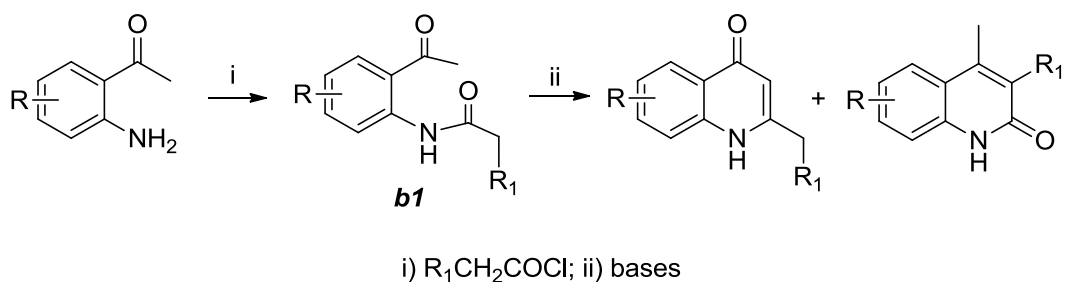


i) $(\text{MeO})_2\text{CHNMe}_2$, DMF; ii) 10% Pd-C, cyclohexane, EtOH

Scheme 2.4 Cyclisation of bond *a*

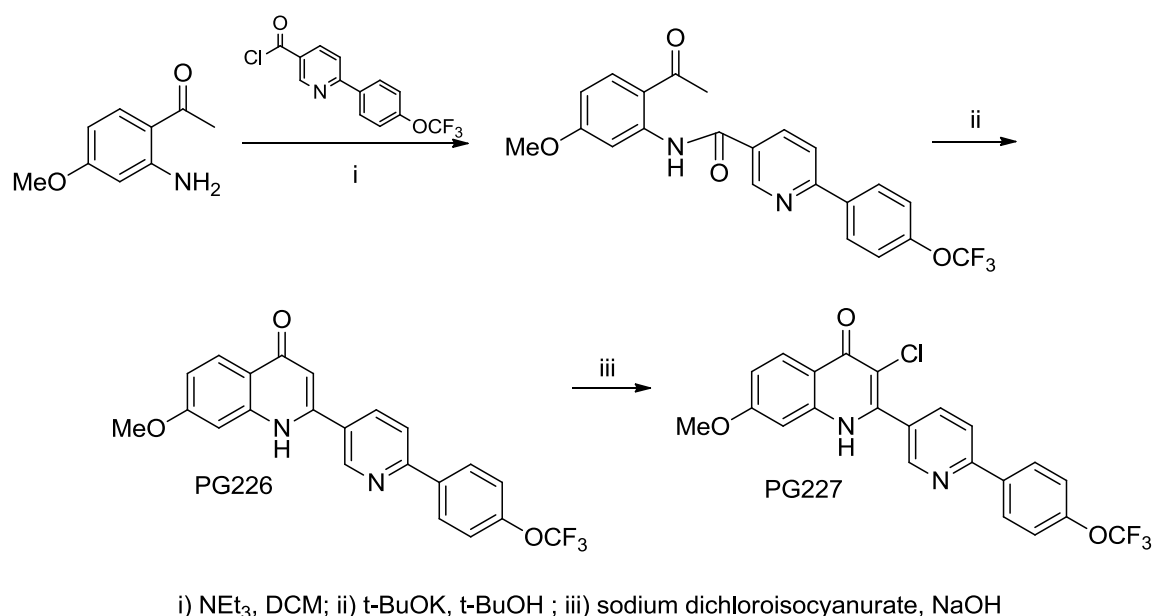
2.5.2 Cyclisation of bond *b*

This type of closure needs the synthesis of intermediate *b1* which its cyclisation of bond *b* leads to the formation of a 4-quinolone ring.



Scheme 2.5 Camps cyclisation

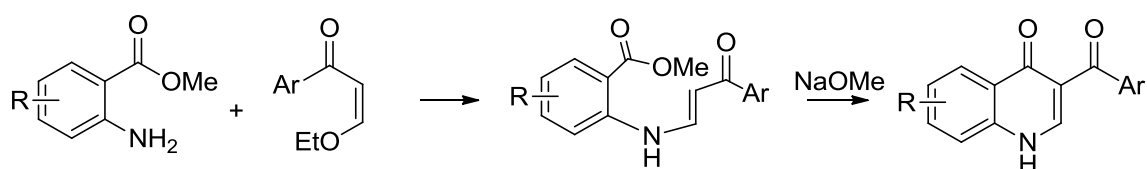
To begin with, the aniline of choices can be acetylated with various reagents by the Friedel-Craft's mechanism. The resulting acetophenone then reacts with corresponding acyl chlorides to form amides. After treated with base, the amides compounds undergo cyclisation with the formation of 4-quinolones. The ring closure takes place in the presence of strong bases such as $NaOEt^{42}$, $t-BuOK$ in $t-BuOH^{43}$, $NaOH^{44}$, or LDA in THF^{45} . This process is also known as the Camps cyclisation⁴⁶. With this method, 2-aryl-4-quinolones containing various substituents on the benzene ring can be obtained. The successful example from these strategies includes the original synthesis of highly potent quinolone lead - PG227 shown in the later chapter in this thesis.



Scheme 2.6 The original PG227 synthesis

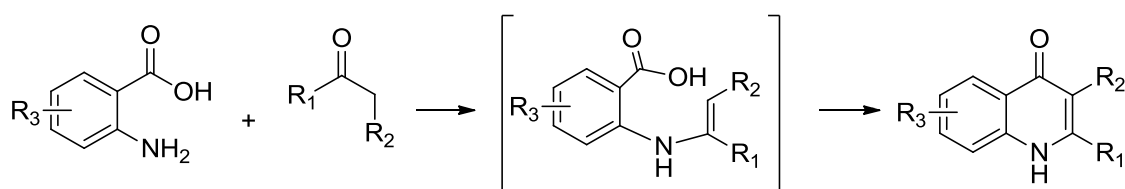
2.5.3 Cyclisation of bond c

The ring closure at bond *c* requires enamine derivatives of benzoic acid as a starting material. The reaction of methyl anthranilate and aryl vinyl ketones under various conditions gives the enamine in moderate yields. The cyclisation takes place in the presence of base such as NaOMe to obtain the desired 4-quinolone⁴⁷.



Scheme 2.7 Cyclisation of bond *c*

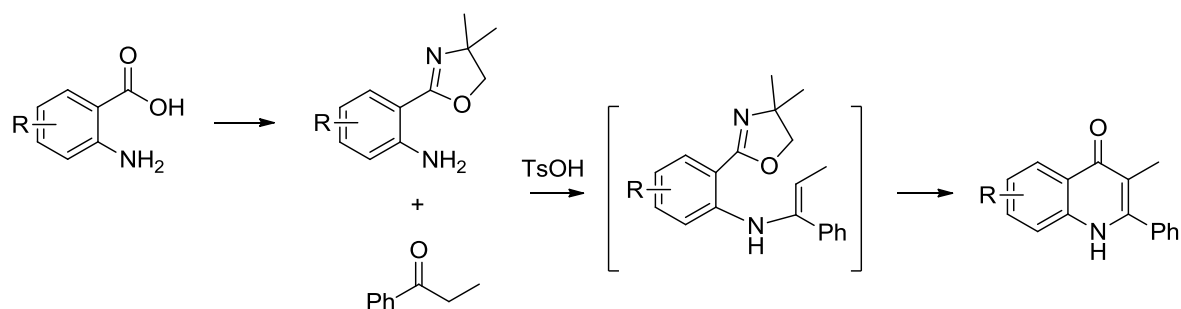
The Niementowski reaction is also known to produce 4-quinolones through the cyclisation at bond *c*. Niementowski found 2-phenyl-4-hydroxyquinoline product which later tautomerise to quinolone from the reaction of anthranilic acids and acetophenones at 120–130 °C. The reaction is thought to begin with the formation of a Schiff base, and then proceed via an intra-molecular condensation to make an imine intermediate. There is then a loss of water that leads to a ring closing and formation of the quinoline derivative⁴⁸.



Scheme 2.8 Niementowski reaction

The alternative and rather unusual method published in 2006 by Luo *et al.*⁴⁹ involves the reaction between propiophenones and *o*-oxazoline-substituted anilines in boiling absolute butanol in the presence of catalytic tosic acid under inert atmosphere. The reaction proceeds through the formation of enamine adduct. The detailed mechanism was discussed in the original paper⁴⁹. Shown in the next chapter, this method is extensively used to synthesise a library of 2-ary-4-

quinolones as the synthesis gives promising yields. It is also easy to handle and suitable to use in divergent synthesis.

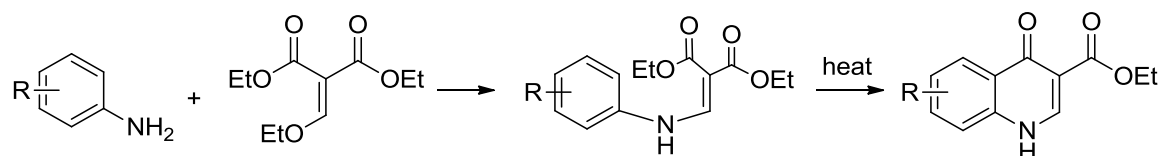


Scheme 2.9 Synthesis of 4-quinolones described by Luo *et al.*

2.5.4 Cyclisation of bond *d*

The synthesis of 4-quinolone mainly relies on this bond *d* cyclisation as seen in a large number of publications.

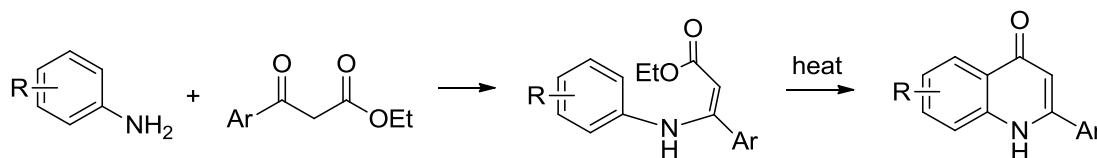
As with other methods, the enamines required for the synthesis are produced by a condensation of substituted anilines with various electron-withdrawing alkenes such as methylenemalonate derivatives. The cyclisation of the enamines also known as the Gould-Jacobs reaction⁵⁰ occurs in relatively high temperature in such high-boiling-point solvents as biphenyl ether^{47, 51}, biphenyl^{5c}, and Dowtherm A⁵², or by using polyphosphoric acid⁴⁰. The yields of the targeted quinolones are generally moderate to good, and the product purification is rather easy. As an example, this method is also used in the synthesis towards quinolone esters described in relevant publication^{52b}.



Scheme 2.10. Gould-Jacobs reaction

An alternative approach to construct the quinolone core is described by the Conrad-Limpach reaction. The Conrad-Limpach synthesis is the condensation of

anilines with β -ketoesters to form 4-quinolones via a Schiff base. The mechanism is based on the thermocyclisation at such high temperature as the Gould-Jacobs reaction⁵³. The advantage of this reaction is that the 3-ester is not required in the final product and 2-substituent can be varied. This synthetic strategy is also used in the alternative synthetic route towards PG227.

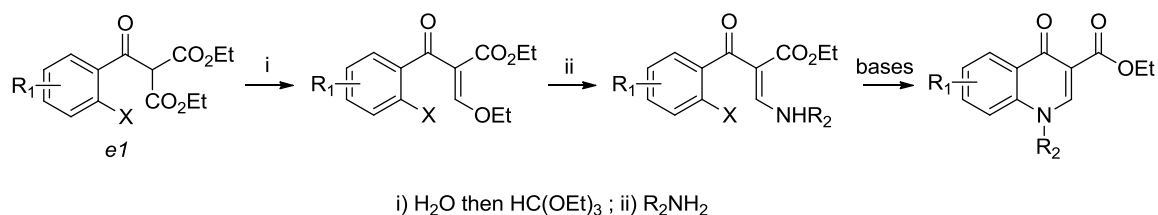


Scheme 2.11 Conrad–Limpach synthesis

2.5.5 Cyclisation of bond e

Several publications reporting the use of this approach towards the synthesis of quinolones includes the ring closure of aminovinyl phenyl ketones. The reaction involves the replacement of halogen atom at the *ortho* position of aryl ring.

The derivatives *e1* was hydrolysed and decarboxylated, and the product was then reacted further to obtain aminovinyl phenyl ketones. The cyclisation leading to the formation of quinolones can be accomplished by the use of various basic reagents such as NaOEt in EtOH, KF in DMF, carbonate salts in DMF, or triethylamine in DMF⁴⁰.



Scheme 2.12 Cyclisation of bond e

2.6 Conclusion

The mitochondrial electron transport chain of *Plasmodium falciparum* is an attractive target for chemotherapy. Two enzymes in the pathway - *Pfbc1* and *PfNDH2* - are druggable target enzymes. The dual inhibition of both enzymes can be

seen in 2-aryl quinolone pharmacophore giving added therapeutic benefit. The development from this series leading to the discovery of potent lead compound is currently in the MMV pipeline. Several cyclisation methods are well used and applied towards the synthesis of corresponding targeted 4-quinolones.

2.7 Reference

- Rodrigues, T.; Lopes, F.; Moreira, R., Inhibitors of the mitochondrial electron transport chain and de novo pyrimidine biosynthesis as antimalarials: The present status. *Current medicinal chemistry* **2010**, *17* (10), 929-56.
- Mather, M. W.; Henry, K. W.; Vaidya, A. B., Mitochondrial drug targets in apicomplexan parasites. *Current drug targets* **2007**, *8* (1), 49-60.
- Nixon, G. L.; Pidathala, C.; Shone, A. E.; Antoine, T.; Fisher, N.; O'Neill, P. M.; Ward, S. A.; Biagini, G. A., Targeting the mitochondrial electron transport chain of *Plasmodium falciparum*: new strategies towards the development of improved antimalarials for the elimination era. *Future medicinal chemistry* **2013**, *5* (13), 1573-91.
- Vaidya, A. B.; Mather, M. W., Mitochondrial evolution and functions in malaria parasites. *Annual review of microbiology* **2009**, *63*, 249-67.
- (a) Fisher, N.; Bray, P. G.; Ward, S. A.; Biagini, G. A., The malaria parasite type II NADH:quinone oxidoreductase: an alternative enzyme for an alternative lifestyle. *Trends in parasitology* **2007**, *23* (7), 305-10; (b) Fry, M.; Webb, E.; Pudney, M., Effect of mitochondrial inhibitors on adenosinetriphosphate levels in *Plasmodium falciparum*. *Comparative biochemistry and physiology. B, Comparative biochemistry* **1990**, *96* (4), 775-82; (c) Balabaskaran Nina, P.; Morrisey, J. M.; Ganesan, S. M.; Ke, H.; Pershing, A. M.; Mather, M. W.; Vaidya, A. B., ATP synthase complex of *Plasmodium falciparum*: dimeric assembly in mitochondrial membranes and resistance to genetic disruption. *The Journal of biological chemistry* **2011**, *286* (48), 41312-22.
- (a) Hunte, C.; Palsdottir, H.; Trumpower, B. L., Protonmotive pathways and mechanisms in the cytochrome bc1 complex. *FEBS letters* **2003**, *545* (1), 39-46; (b) Crofts, A. R., The cytochrome bc1 complex: function in the context of structure. *Annual review of physiology* **2004**, *66*, 689-733; (c) Kessl, J. J.; Lange, B. B.; Merbitz-Zahradnik, T.; Zwicker, K.; Hill, P.; Meunier, B.; Palsdottir, H.; Hunte, C.; Meshnick, S.; Trumpower, B. L., Molecular basis for atovaquone binding to the cytochrome bc1 complex. *The Journal of biological chemistry* **2003**, *278* (33), 31312-8.
- (a) Solmaz, S. R.; Hunte, C., Structure of complex III with bound cytochrome c in reduced state and definition of a minimal core interface for electron transfer. *The Journal of biological chemistry* **2008**, *283* (25), 17542-9; (b) Zara, V.; Conte, L.; Trumpower, B. L., Evidence that the assembly of the yeast cytochrome bc1 complex involves the formation of a large core structure in the inner mitochondrial membrane. *The FEBS journal* **2009**, *276* (7), 1900-14.
- Cape, J. L.; Bowman, M. K.; Kramer, D. M., Understanding the cytochrome bc complexes by what they don't do. The Q-cycle at 30. *Trends in plant science* **2006**, *11* (1), 46-55.
- Mitchell, P., The protonmotive Q cycle: a general formulation. *FEBS letters* **1975**, *59* (2), 137-9.

10. Barton, V.; Fisher, N.; Biagini, G. A.; Ward, S. A.; O'Neill, P. M., Inhibiting Plasmodium cytochrome bc1: a complex issue. *Current opinion in chemical biology* **2010**, *14* (4), 440-6.
11. Berry, E. A.; Huang, L. S., Conformationally linked interaction in the cytochrome bc(1) complex between inhibitors of the Q(o) site and the Rieske iron-sulfur protein. *Biochimica et biophysica acta* **2011**, *1807* (10), 1349-63.
12. Stocks, P. A.; Barton, V.; Antoine, T.; Biagini, G. A.; Ward, S. A.; O'Neill, P. M., Novel inhibitors of the Plasmodium falciparum electron transport chain. *Parasitology* **2014**, *141* (1), 50-65.
13. Fry, M.; Pudney, M., Site of action of the antimalarial hydroxynaphthoquinone, 2-[trans-4-(4'-chlorophenyl) cyclohexyl]-3-hydroxy-1,4-naphthoquinone (566C80). *Biochemical pharmacology* **1992**, *43* (7), 1545-53.
14. Srivastava, I. K.; Morrissey, J. M.; Darrouzet, E.; Daldal, F.; Vaidya, A. B., Resistance mutations reveal the atovaquone-binding domain of cytochrome b in malaria parasites. *Molecular microbiology* **1999**, *33* (4), 704-11.
15. Nixon, G. L.; Moss, D. M.; Shone, A. E.; Laloo, D. G.; Fisher, N.; O'Neill, P. M.; Ward, S. A.; Biagini, G. A., Antimalarial pharmacology and therapeutics of atovaquone. *The Journal of antimicrobial chemotherapy* **2013**, *68* (5), 977-85.
16. Fieser, L. F.; Richardson, A. P., Naphthoquinone antimalarials; correlation of structure and activity against *P. lophurae* in ducks. *Journal of the American Chemical Society* **1948**, *70* (10), 3156-65.
17. (a) Fieser, L. F.; Chang, F. C.; et al., Naphthoquinone antimalarials; metabolic oxidation products. *The Journal of pharmacology and experimental therapeutics* **1948**, *94* (2), 85-96; (b) Fieser, L. F.; Heymann, H.; Seligman, A. M., Naphthoquinone antimalarials; metabolic degradation. *The Journal of pharmacology and experimental therapeutics* **1948**, *94* (2), 112-24.
18. (a) Fieser, L. F.; Schirmer, J. P.; Archer, S.; Lorenz, R. R.; Pfaffenbach, P. I., Naphthoquinone antimalarials. XXIX. 2-hydroxy-3-(omega-cyclohexylalkyl)-1,4-naphthoquinones. *Journal of medicinal chemistry* **1967**, *10* (4), 513-7; (b) Fawaz, G.; Haddad, F. S., The effect of lapinone (M-2350) on *P. vivax* infection in man. *The American journal of tropical medicine and hygiene* **1951**, *31* (5), 569-71.
19. (a) Hudson, A. T.; Randall, A. W.; Fry, M.; Ginger, C. D.; Hill, B.; Latter, V. S.; McHardy, N.; Williams, R. B., Novel anti-malarial hydroxynaphthoquinones with potent broad spectrum anti-protozoal activity. *Parasitology* **1985**, *90* (Pt 1), 45-55; (b) Hudson, A. T.; Pether, M. J.; Randall, A. W.; Fry, M.; Latter, V. S.; Mchardy, N., In vitro Activity of 2-Cycloalkyl-3-Hydroxy-1,4-Naphthoquinones against *Theileria*, *Eimeria* and *Plasmodia* Species. *European journal of medicinal chemistry* **1986**, *21* (4), 271-275.
20. Hudson, A. T.; Dickins, M.; Ginger, C. D.; Gutteridge, W. E.; Holdich, T.; Hutchinson, D. B. A.; Pudney, M.; Randall, A. W.; Latter, V. S., 566c80 - a Potent Broad-Spectrum Antiinfective Agent with Activity against Malaria and Opportunistic Infections in Aids Patients. *Drugs under experimental and clinical research* **1991**, *17* (9), 427-435.
21. Canfield, C. J.; Pudney, M.; Gutteridge, W. E., Interactions of atovaquone with other antimalarial drugs against *Plasmodium falciparum* in vitro. *Experimental parasitology* **1995**, *80* (3), 373-81.
22. Osei-Akoto, A.; Orton, L.; Owusu-Ofori, S. P., Atovaquone-proguanil for treating uncomplicated malaria. *The Cochrane database of systematic reviews* **2005**, (4), CD004529.
23. Laloo, D. G.; Hill, D. R., Preventing malaria in travellers. *Bmj* **2008**, *336* (7657), 1362-6.
24. Xiang, H.; McSurdy-Freed, J.; Moorthy, G. S.; Hugger, E.; Bambal, R.; Han, C.; Ferrer, S.; Gargallo, D.; Davis, C. B., Preclinical drug metabolism and pharmacokinetic evaluation of GW844520, a novel anti-malarial mitochondrial electron transport inhibitor. *Journal of pharmaceutical sciences* **2006**, *95* (12), 2657-2672.

25. Yeates, C. L.; Batchelor, J. F.; Capon, E. C.; Cheesman, N. J.; Fry, M.; Hudson, A. T.; Pudney, M.; Trimming, H.; Woolven, J.; Bueno, J. M.; Chicharro, J.; Fernandez, E.; Fiandor, J. M.; Gargallo-Viola, D.; de las Heras, F. G.; Herreros, E.; Leon, M. L., Synthesis and structure-activity relationships of 4-pyridones as potential antimalarials. *Journal of medicinal chemistry* **2008**, *51* (9), 2845-2852.
26. Bueno, J. M.; Manzano, P.; Garcia, M. C.; Chicharro, J.; Puente, M.; Lorenzo, M.; Garcia, A.; Ferrer, S.; Gomez, R. M.; Fraile, M. T.; Lavandera, J. L.; Fiandor, J. M.; Vidal, J.; Herreros, E.; Gargallo-Viola, D., Potent antimalarial 4-pyridones with improved physico-chemical properties. *Bioorganic & medicinal chemistry letters* **2011**, *21* (18), 5214-5218.
27. Bueno, J. M.; Herreros, E.; Angulo-Barturen, I.; Ferrer, S.; Fiandor, J. M.; Gamo, F. J.; Gargallo-Viola, D.; Derimanov, G., Exploration of 4(IH)-pyridones as a novel family of potent antimalarial inhibitors of the plasmodial cytochrome bcl. *Future medicinal chemistry* **2012**, *4* (18), 2311-2323.
28. Biagini, G. A.; Fisher, N.; Berry, N.; Stocks, P. A.; Meunier, B.; Williams, D. P.; Bonar-Law, R.; Bray, P. G.; Owen, A.; O'Neill, P. M.; Ward, S. A., Acridinediones: selective and potent inhibitors of the malaria parasite mitochondrial bc1 complex. *Molecular pharmacology* **2008**, *73* (5), 1347-55.
29. Calderon, F.; Wilson, D. M.; Gamo, F. J., Antimalarial drug discovery: recent progress and future directions. *Progress in medicinal chemistry* **2013**, *52*, 97-151.
30. (a) Ryley, J. F.; Peters, W., The antimalarial activity of some quinolone esters. *Annals of tropical medicine and parasitology* **1970**, *64* (2), 209-22; (b) Biagini, G. A.; Fisher, N.; Shone, A. E.; Mubarak, M. A.; Srivastava, A.; Hill, A.; Antoine, T.; Warman, A. J.; Davies, J.; Pidathala, C.; Amewu, R. K.; Leung, S. C.; Sharma, R.; Gibbons, P.; Hong, D. W.; Pacorel, B.; Lawrenson, A. S.; Charoensutthivarakul, S.; Taylor, L.; Berger, O.; Mbekeani, A.; Stocks, P. A.; Nixon, G. L.; Chadwick, J.; Hemingway, J.; Delves, M. J.; Sinden, R. E.; Zeeman, A. M.; Kocken, C. H.; Berry, N. G.; O'Neill, P. M.; Ward, S. A., Generation of quinolone antimalarials targeting the Plasmodium falciparum mitochondrial respiratory chain for the treatment and prophylaxis of malaria. *Proceedings of the National Academy of Sciences of the United States of America* **2012**, *109* (21), 8298-303; (c) Nilsen, A.; LaCrue, A. N.; White, K. L.; Forquer, I. P.; Cross, R. M.; Marfurt, J.; Mather, M. W.; Delves, M. J.; Shackleford, D. M.; Saenz, F. E.; Morrissey, J. M.; Steuten, J.; Mutka, T.; Li, Y.; Wirjanata, G.; Ryan, E.; Duffy, S.; Kelly, J. X.; Sebayang, B. F.; Zeeman, A. M.; Noviyanti, R.; Sinden, R. E.; Kocken, C. H.; Price, R. N.; Avery, V. M.; Angulo-Barturen, I.; Jimenez-Diaz, M. B.; Ferrer, S.; Herreros, E.; Sanz, L. M.; Gamo, F. J.; Bathurst, I.; Burrows, J. N.; Siegl, P.; Guy, R. K.; Winter, R. W.; Vaidya, A. B.; Charman, S. A.; Kyle, D. E.; Manetsch, R.; Riscoe, M. K., Quinolone-3-diarylethers: a new class of antimalarial drug. *Science translational medicine* **2013**, *5* (177), 177ra37.
31. (a) Kikuth, W.; Mudrowreichenow, L., *Uber Kausalprophylaktisch Bei Vogelmalaria Wirksame Substanzen. *Zeitschrift Fur Hygiene Und Infektionskrankheiten* **1947**, *127* (1-2), 151-165; (b) Salzer, W.; Timmler, H.; Andersag, H., Uber Einen Neuen, Gegen Vogelmalaria Wirksamen Verbindungstypus. *Chem Ber-Recl* **1948**, *81* (1), 12-19.
32. Cross, R. M.; Namelikonda, N. K.; Mutka, T. S.; Luong, L.; Kyle, D. E.; Manetsch, R., Synthesis, antimalarial activity, and structure-activity relationship of 7-(2-phenoxyethoxy)-4(1H)-quinolones. *Journal of medicinal chemistry* **2011**, *54* (24), 8321-7.
33. Winter, R.; Kelly, J. X.; Smilkstein, M. J.; Hinrichs, D.; Koop, D. R.; Riscoe, M. K., Optimization of endochin-like quinolones for antimalarial activity. *Experimental parasitology* **2011**, *127* (2), 545-51.
34. Biagini, G. A.; Viriyavejakul, P.; O'Neill P, M.; Bray, P. G.; Ward, S. A., Functional characterization and target validation of alternative complex I of Plasmodium falciparum mitochondria. *Antimicrobial agents and chemotherapy* **2006**, *50* (5), 1841-51.
35. Sharma, R.; Lawrenson, A. S.; Fisher, N. E.; Warman, A. J.; Shone, A. E.; Hill, A.; Mbekeani, A.; Pidathala, C.; Amewu, R. K.; Leung, S.; Gibbons, P.; Hong, D. W.; Stocks, P.; Nixon, G. L.; Chadwick, J.; Shearer, J.; Gowers, I.; Cronk, D.; Parel, S. P.; O'Neill, P. M.; Ward,

- S. A.; Biagini, G. A.; Berry, N. G., Identification of novel antimalarial chemotypes via chemoinformatic compound selection methods for a high-throughput screening program against the novel malarial target, PfNDH2: increasing hit rate via virtual screening methods. *Journal of medicinal chemistry* **2012**, *55* (7), 3144-54.
36. Lipinski, C. A., Drug-like properties and the causes of poor solubility and poor permeability. *Journal of pharmacological and toxicological methods* **2000**, *44* (1), 235-49.
37. Pidathala, C.; Amewu, R.; Pacorel, B.; Nixon, G. L.; Gibbons, P.; Hong, W. D.; Leung, S. C.; Berry, N. G.; Sharma, R.; Stocks, P. A.; Srivastava, A.; Shone, A. E.; Charoensutthivarakul, S.; Taylor, L.; Berger, O.; Mbekeani, A.; Hill, A.; Fisher, N. E.; Warman, A. J.; Biagini, G. A.; Ward, S. A.; O'Neill, P. M., Identification, design and biological evaluation of bisaryl quinolones targeting Plasmodium falciparum type II NADH:quinone oxidoreductase (PfNDH2). *Journal of medicinal chemistry* **2012**, *55* (5), 1831-43.
38. Leung, S. C.; Gibbons, P.; Amewu, R.; Nixon, G. L.; Pidathala, C.; Hong, W. D.; Pacorel, B.; Berry, N. G.; Sharma, R.; Stocks, P. A.; Srivastava, A.; Shone, A. E.; Charoensutthivarakul, S.; Taylor, L.; Berger, O.; Mbekeani, A.; Hill, A.; Fisher, N. E.; Warman, A. J.; Biagini, G. A.; Ward, S. A.; O'Neill, P. M., Identification, design and biological evaluation of heterocyclic quinolones targeting Plasmodium falciparum type II NADH:quinone oxidoreductase (PfNDH2). *Journal of medicinal chemistry* **2012**, *55* (5), 1844-57.
39. Hopkins, A. L., Network pharmacology: the next paradigm in drug discovery. *Nature chemical biology* **2008**, *4* (11), 682-90.
40. Boteva, A. A.; Krasnykh, O. P., The Methods of Synthesis, Modification, and Biological Activity of 4-Quinolones (Review). *Chem Heterocycl Com+* **2009**, *45* (7), 757-785.
41. Tois, J.; Vahermo, M.; Koskinen, A., Novel and convenient synthesis of 4(1H)quinolones. *Tetrahedron Lett* **2005**, *46* (5), 735-737.
42. Sui, Z. H.; Nguyen, V. N.; Altom, J.; Fernandez, J.; Hilliard, J. J.; Bernstein, J. I.; Barrett, J. F.; Ohemeng, K. A., Synthesis and topoisomerase inhibitory activities of novel aza-analogues of flavones. *European journal of medicinal chemistry* **1999**, *34* (5), 381-387.
43. (a) Hadjeri, M.; Peiller, E. L.; Beney, C.; Deka, N.; Lawson, M. A.; Dumontet, C.; Boumendjel, A., Antimitotic activity of 5-hydroxy-7-methoxy-2-phenyl-4-quinolones. *Journal of medicinal chemistry* **2004**, *47* (20), 4964-4970; (b) Xia, Y.; Yang, Z. Y.; Xia, P.; Hackl, T.; Hamel, E.; Mauger, A.; Wu, J. H.; Lee, K. H., Antitumor agents. 211. Fluorinated 2-phenyl-4-quinolone derivatives as antimitotic antitumor agents. *Journal of medicinal chemistry* **2001**, *44* (23), 3932-3936.
44. Jones, C. P.; Anderson, K. W.; Buchwald, S. L., Sequential Cu-catalyzed amidation-base-mediated camp cyclization: A two-step synthesis of 2-aryl-4-quinolones from o-halophenones. *Journal of Organic Chemistry* **2007**, *72* (21), 7968-7973.
45. Li, L.; Wang, H. K.; Kuo, S. C.; Wu, T. S.; Lednicer, D.; Lin, C. M.; Hamel, E.; Lee, K. H., Antitumor Agents .150. 2',3',4',5',5,6,7-Substituted 2-Phenyl-4-Quinolones and Related-Compounds - Their Synthesis, Cytotoxicity, and Inhibition of Tubulin Polymerization. *Journal of medicinal chemistry* **1994**, *37* (8), 1126-1135.
46. Manske, R. H., The chemistry of quinolines. *Chemical reviews* **1942**, *30* (1), 113-144.
47. Stern, E.; Millet, R.; Depreux, P.; Henichart, J. P., A versatile and efficient synthesis of 3-aryl-1,4-dihydroquinolin-4-ones. *Tetrahedron Lett* **2004**, *45* (50), 9257-9259.
48. Meyer, J. F.; Wagner, E. C., The Niementowski reaction. The use of methyl anthranilate or isatoic anhydride with substituted amides or amidines in the formation of 3-substituted-4-keto-3, 4-dihydroquinazolines. The course of the reaction. *Journal of Organic Chemistry* **1942**, *8* (3), 239-252.
49. Luo, F. T.; Ravi, V. K.; Xue, C. H., The novel reaction of ketones with o-oxazoline-substituted anilines. *Tetrahedron* **2006**, *62* (40), 9365-9372.
50. Gould, R. G.; Jacobs, W. A., The Synthesis of Certain Substituted Quinolines and 5,6-Benzoquinolines. *Journal of the American Chemical Society* **1939**, *61* (10), 2890-2895.

51. (a) Lauer, W. M.; Arnold, R. T.; Tiffany, B.; Tinker, J., The Synthesis of Some Chloromethoxyquinolines. *Journal of the American Chemical Society* **1946**, *68* (7), 1268-1269; (b) Stern, E.; Muccioli, G. G.; Millet, R.; Goossens, J. F.; Farce, A.; Chavatte, P.; Poupaert, J. H.; Lambert, D. M.; Depreux, P.; Henichart, J. P., Novel 4-oxo-1,4-dihydroquinoline-3-carboxamide derivatives as new CB2 cannabinoid receptors agonists: Synthesis, pharmacological properties and molecular modeling. *Journal of medicinal chemistry* **2006**, *49* (1), 70-79; (c) Stern, E.; Muccioli, G. G.; Bosier, B.; Hamtiaux, L.; Millet, R.; Poupaert, J. H.; Henichart, J. P.; Depreux, P.; Goossens, J. F.; Lambert, D. M., Pharmacomodulations around the 4-oxo-1,4-dihydroquinoline-3-carboxamides, a class of potent CB2-selective cannabinoid receptor ligands: Consequences in receptor affinity and functionality. *Journal of medicinal chemistry* **2007**, *50* (22), 5471-5484.
52. (a) Winter, R. W.; Kelly, J. X.; Smilkstein, M. J.; Dodean, R.; Hinrichs, D.; Riscoe, M. K., Antimalarial quinolones: synthesis, potency, and mechanistic studies. *Experimental parasitology* **2008**, *118* (4), 487-97; (b) Cowley, R.; Leung, S.; Fisher, N.; Al-Helal, M.; Berry, N. G.; Lawrenson, A. S.; Sharma, R.; Shone, A. E.; Ward, S. A.; Biagini, G. A.; O'Neill, P. M., The development of quinolone esters as novel antimalarial agents targeting the Plasmodium falciparum bc(1) protein complex. *Medchemcomm* **2012**, *3* (1), 39-44.
53. Brouet, J. C.; Gu, S.; Peet, N. P.; Williams, J. D., A Survey of Solvents for the Conrad-Limpach Synthesis of 4-Hydroxyquinolones. *Synthetic communications* **2009**, *39* (9), 5193-5196.

Chapter III: Lead optimisation of antimalarial 2-aryl quinolones

Chapter III : Lead optimisation of antimalarial 2-aryl quinolones

	page
3.1 From CK-2-67 and SL-2-25 to next generation lead compounds	54
3.2 Results and discussion	55
3.2.1 General synthesis towards 2-aryl quinolones	55
3.2.2 Lead optimisation I: incorporation of a polar head group	59
3.2.3 Lead optimisation II: pyridyl side chain regiochemistry	63
3.2.4 Lead optimisation III: end-capped substituents	68
3.2.5 6-Cl-7-OMe-2-aryl quinolone analogue	70
3.2.6 Drug resistant parasite inhibition profiles	73
3.2.7 Aqueous solubility profiles	73
3.2.8 Metabolic stability profiles	75
3.2.9 Potential off-target toxicity	76
3.2.10 Molecular modelling studies	77
3.3 Conclusion	88
3.4 Experimental	90
3.4.1 General	90
3.4.2 Synthesis	91
3.4.3 Biology	131
3.4.4 Molecular Modeling	135
3.5 References	137

Lead optimisation of antimalarial 2-aryl quinolones

3.1 From CK-2-67 and SL-2-25 to next generation lead compounds

As previously described in Chapter II and relevant publications¹, the 2-aryl quinolone template is a privileged drug scaffold that can inhibit both *Pfbc*₁ and *Pf*NDH2 resulting in potent antimalarial activity. Initial studies within our group showed that CK-2-67 and SL-2-25, lead compounds from this programme, possess IC₅₀s in the nanomolar range against the blood stage of *P.falciparum* malaria and have the capacity to inhibit two key enzymes in the respiratory pathway with potent activity in whole-cell assays¹. Preliminary *in vivo* studies confirm these inhibitors as drug-like with properties consistent with a potential role in malaria control and eradication².

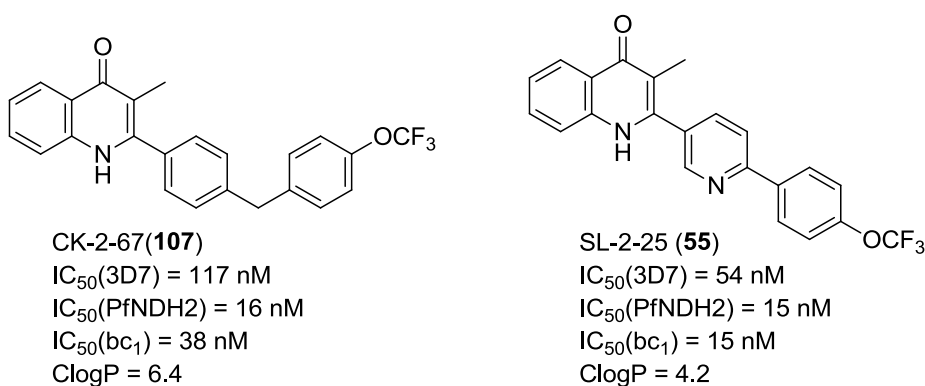


Figure 3.1 Two lead compounds at the starting point of this research

Despite these findings, the problem found within this class is that they generally have poor aqueous solubility due to the planar aggregation *via* π - π stacking of their ring systems, a phenomena that results in tight crystal packing and a high melting point³. To deliver a molecule with improved drug-like properties, it was apparent that the partition coefficient (ClogP) needed to be reduced and aqueous solubility needed to be increased. There are several regions within the lead structures that can be optimised to improve their solubility whilst activity is maintained (**Figure 3.2**).

(i) Incorporation of a hydroxyl group into the A-ring at one of the available positions. The additional benefit of the hydroxyl group is that it offered the option

of exploring prodrugs for this series by derivatisation to provide either phosphate or carbamate pro-drugs as demonstrated in a relevant publication^{1b}. Since the corresponding methoxy analogues were prepared en route, these compounds were also screened against *P.falciparum*.

(ii) In case of pyridyl side chain (SL-2-25's side chain), the pyridyl regiochemistry can also be altered. Any changes in pyridyl regiochemistry affect not only the pKa of pyridyl nitrogen but also the side chain flexibility which could lead to an increase in solubility by disruption of π - π stacking interactions.

(iii) From previous studies⁴, the *p*-OCF₃ substituent on the D-ring had been identified to provide excellent antimalarial. Recent studies on related quinolone series revealed some advantages in 3,4-dichloro substitution and for this reason this substitution pattern was also planned.

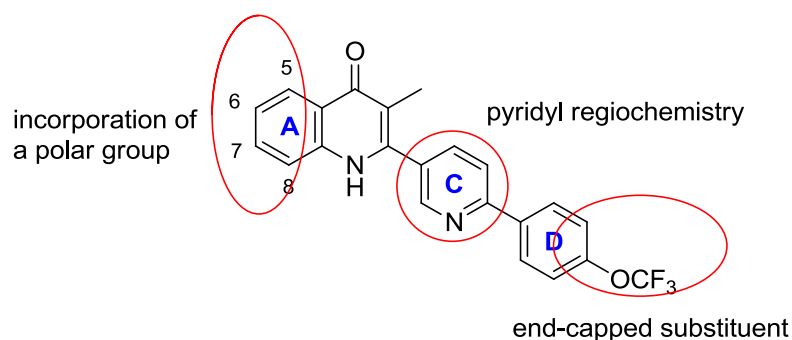


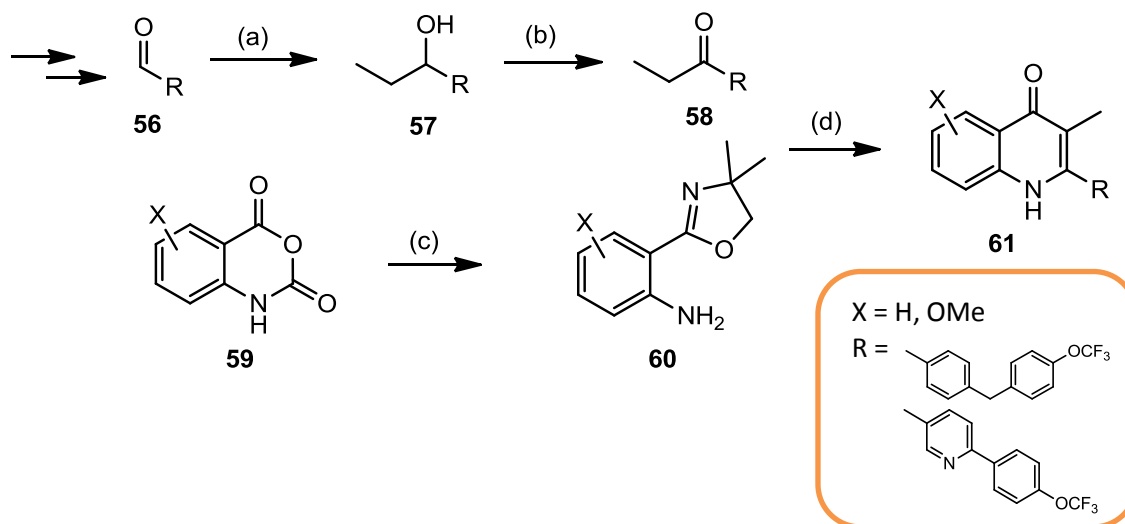
Figure 3.2 Rationale of lead optimisation

3.2 Results and discussion

3.2.1 General synthesis towards 2-aryl quinolones

Following the programme on antimalarial 2-aryl quinolones, the 2-aryl quinolone core can be synthesised according to the relevant publications by O'Neill *et al.*¹ The synthesis of 2-aryl quinolones series was accomplished in 5-7 steps from commercially available starting materials. The synthesis started from a well-renowned Suzuki reaction constructing C-C bond between aromatic halides and boronic acids or ester to obtain aldehyde **56** in excellent yields. A solution of EtMgBr was utilised in a Grignard reaction extending two more carbon atoms and the

carbonyl was simultaneously transformed to alcohols **57** in 32-83% yields. Alcohol **57** was then oxidised using a mild oxidant, which can be either PCC or DMP⁵, to yield corresponding ketone **58** in good yields.

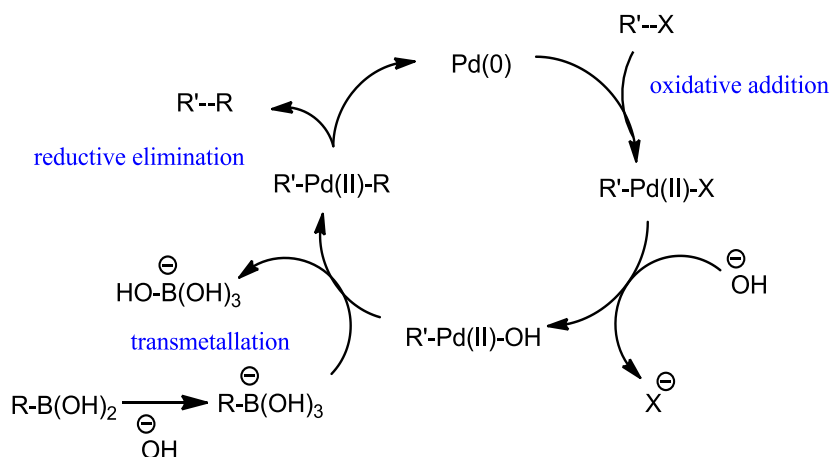


Scheme 3.1 Reagents : (a) EtMgBr, THF, 0 °C, under N₂, 1 h (b) DMP, wet DCM, 15 mins or PCC, DCM, 2 h (c) 2-amino-2-methyl-propanol, ZnCl₂, PhCl, 135 °C (d) CF₃SO₃H, *n*-BuOH, under N₂, 130 °C, 1 day.

Oxazole **60** was prepared in yields of 31-98% from the respective isatoic anhydride **59** which was synthesised by adding diphosgene into methoxy-substituted anthranilic acid. Reaction of oxazole **60** and ketone **58** in the presence of zinc chloride and trifluoromethane sulfonic acid gave the desired quinolones **61** in 4-62% yields⁶.

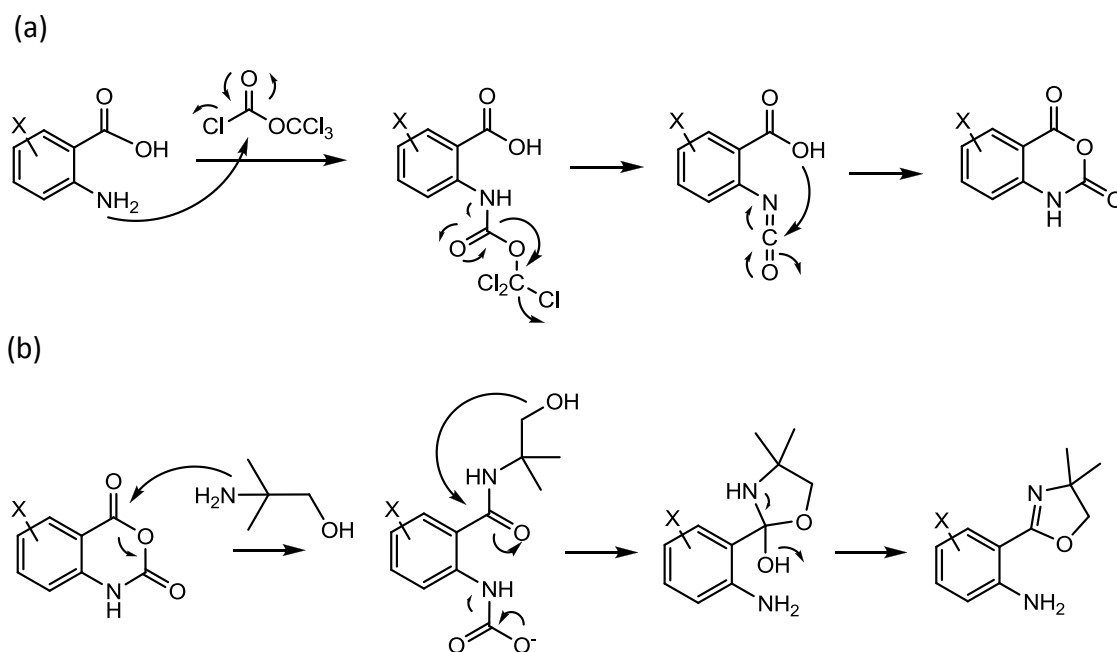
Synthesis of bisaryl and pyridyl side chain analogues

The Suzuki coupling reaction involves the reaction between an aryl or vinyl boronic acid and aryl or vinyl halide catalysed by a palladium (0) complex in the presence of a base. The mechanism of the Suzuki reaction is best viewed from the perspective of the palladium catalyst. The first step is the oxidative addition of palladium to the less hindered halide to form the palladium (II) species. Reaction with base and transmetalation with the boronate complex forms the organopalladium species. Reductive elimination of the desired product restores the original palladium (0) catalyst which completes the catalytic cycle.

**Scheme 3.2** Suzuki coupling

Several types of side chain were prepared via Suzuki coupling; however, the pyridyl side chain later gained more attention due to the fact that a salt could be readily produced by a protonation of the pyridyl nitrogen.

Synthesis of *o*-oxazoline-substituted aniline



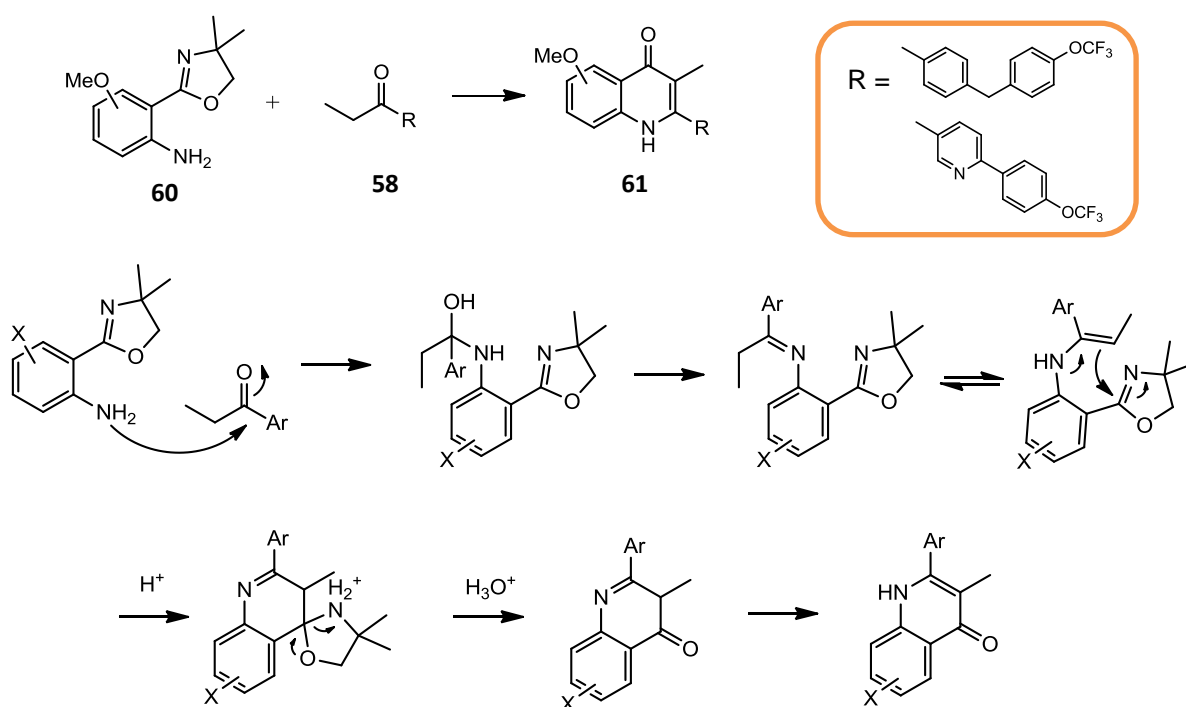
Scheme 3.3 (a) Reaction of diphosgene with methoxy-substituted anthranilic acid and (b) the mechanism of the synthesis of *o*-oxazoline-substituted aniline

The synthesis of *o*-oxazoline-substituted aniline from isatoic anhydride was reported by Giri⁷. The mechanism is shown in **Scheme 3.3**. Substituted isatoic

anhydrides were not commercially available from any sources thus they were prepared from the corresponding substituted anthranilic acid by reacting with diphosgene.

Instead of phosgene, diphosgene was employed in this synthesis as it is more conveniently handled. The reaction of diphosgene with amino group gives isocyanates which further react with intramolecular carboxylic acid to finally yield anhydrides according to **Scheme 3.3**. The anhydrides were poorly soluble in any solvents resulting in poorly defined NMR spectra.

Cyclisation of bond c

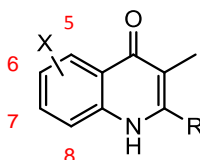


Scheme 3.4 The reaction mechanism between ketones and *o*-oxazoline-substituted aniline.

The original method published in 2006 involves the reaction of propiophenone and *o*-oxazoline-substituted aniline in boiling butanol in the presence of a strong acid under an inert atmosphere⁶. Though there are slight modifications over times¹⁻², a library of 2-aryl quinolones were prepared from a reaction between oxazole **60** and ketone **58** in the presence of triflic acid. The reaction mechanism illustrated in **Scheme 3.4**.

3.2.2 Lead optimisation I: incorporation of a polar head group

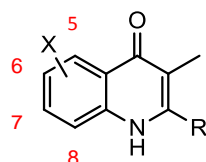
As noted earlier, the first focus of this investigation was the incorporation of a polar head group. Firstly, a library of methoxy-substituted 2-aryl quinolones with either a bisaryl or pyridyl side chain was investigated and synthesised according to **Scheme 3.1** and the yields can be summarised in **Table 3.1**.



Compound	R	X	No. of steps	% Yield 57	% Yield 58	% Yield 60	% Yield 61
61a	-PhpCH ₂ PhpOCF ₃	5-OMe	6	42	89	98	8
61b	-PhpCH ₂ PhpOCF ₃	6-OMe	6	42	89	48	28
61c	-PhpCH ₂ PhpOCF ₃	7-OMe	6	42	89	73	29
61d	-PhpCH ₂ PhpOCF ₃	8-OMe	6	42	89	30	27
61e		5-OMe	6	67	69	98	4
61f		6-OMe	6	67	69	48	22
61g		7-OMe	6	67	69	73	51
61h		8-OMe	6	67	69	30	25

Table 3.1 Yields for the synthesis of compounds **61a-61h**

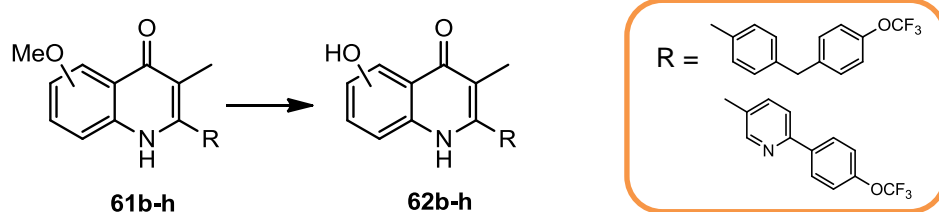
All methoxy derivatives were tested against *Pf3D7*, and antimalarial *in vitro* data shown in the **Table 3.2** below reveals that optimal activity can be achieved by the introduction of a methoxy group to the 7-position (see entries **61c** and **61g**). The potency obviously increases 3-8 folds when 7-OMe attached. A clear trend is seen in pyridyl series where 7-methoxylation provides optimal activity (see **61g**). It is noteworthy that 7-OMe is also present in stigmatellin (**38**) and endochin (**46**) both of which possess good antimalarial activity through the inhibition of *bc*₁ complex (see chapter II).



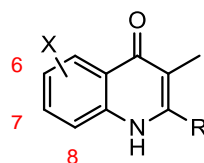
Compound	R	X	IC ₅₀ (nM) 3D7 ± SD
CK-2-67	-PhpCH ₂ PhpOCF ₃	7-H	117
SL-2-25		7-H	54 ± 6
61a	-PhpCH ₂ PhpOCF ₃	5-OMe	664 ± 80
61b	-PhpCH ₂ PhpOCF ₃	6-OMe	465 ± 39
61c	-PhpCH ₂ PhpOCF ₃	7-OMe	13 ± 2
61d	-PhpCH ₂ PhpOCF ₃	8-OMe	381 ± 45
61e		5-OMe	> 1000
61f		6-OMe	> 1000
61g		7-OMe	14 ± 2
61h		8-OMe	> 1000

Table 3.2 *In vitro* antimalarial activity of methoxy-substituted quinolones

Some selected quinolones were demethylated using BBr₃ in dichloromethane⁸ to obtain hydroxyl analogues **62b-h** in 10-69 % yields and their antimalarial activities were assessed and displayed in the **Table 3.3** below. It was found that the OH-substituted quinolones showed moderate activity. When compared to their methoxylated products, OH substitution is less favourable.



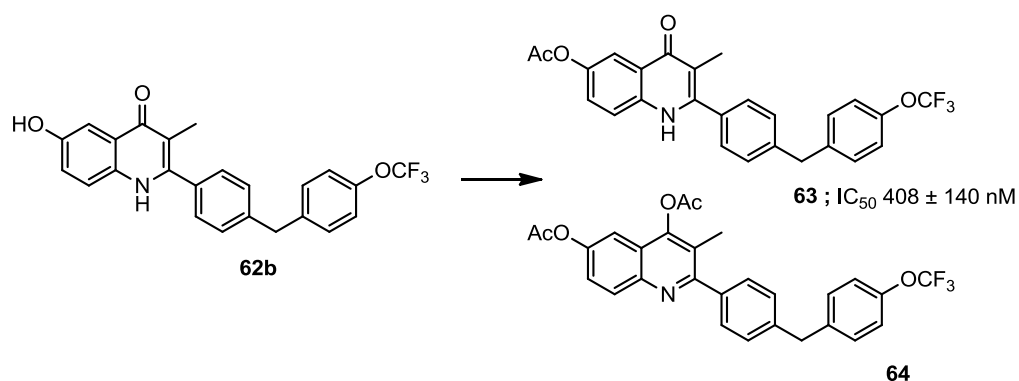
Scheme 3.5 Demethylation of methoxy quinolone; *Reagent*: BBr₃, DCM, rt, overnight, 10-69 %.



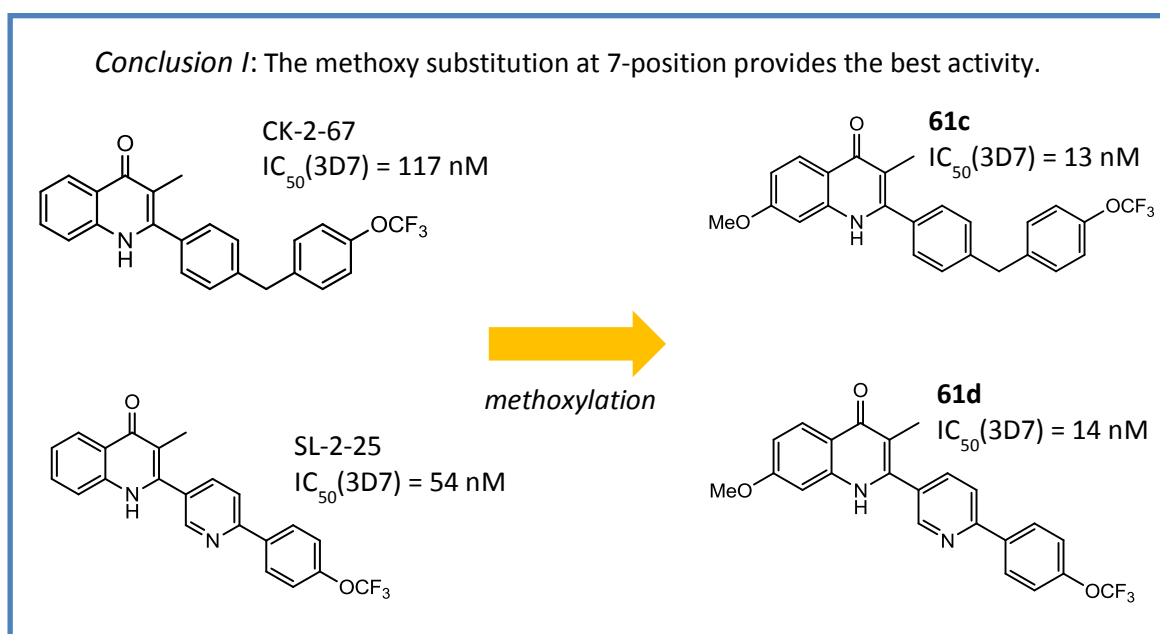
Compound	R	X	IC ₅₀ (nM) 3D7 ± SD
CK-2-67	-PhpCH ₂ PhpOCF ₃	7-H	117
SL-2-25		7-H	54 ± 6
62b	-PhpCH ₂ PhpOCF ₃	6-OH	465 ± 39
62c	-PhpCH ₂ PhpOCF ₃	7-OH	139 ± 20
62d	-PhpCH ₂ PhpOCF ₃	8-OH	819 ± 50
62f		6-OH	280 ± 50
62g		7-OH	202 ± 79
62h		8-OH	> 1000

Table 3.3 *In vitro* antimalarial activity of hydroxy-substituted quinolones

Acetylation can be used to prepare a prodrug with better pharmacokinetics property as exemplified by the development of antiviral famciclovir. Famciclovir is the diacetate ester prodrug of penciclovir⁹. The oral bioavailability increased from 4% for penciclovir to 75% for famciclovir¹⁰. Acetate prodrug **63** was also preliminarily investigated to find any advantages in physico-chemical properties when the acetate moiety is attached. Acetylation can be achieved using acetyl chloride in the presence of triethylamine in DCM. When an excess amount of acetyl chloride is used, diacetate quinolone **64** was found and, in this case, both **63** and **64** were submitted for antimalarial assessment. They show moderate antiplasmodial properties and, therefore, were not pursued further.



Scheme 3.6 Acetylation of hydroxyl quinolones; *Reagent:* AcCl, DMF, DCM, rt.



The presence of an OMe group on the A ring is tolerated with substitution at the 7-position greatly enhancing activity. **61c** has activity of 13 nM while CK-2-67 devoid of 7-OMe moiety shows an IC_{50} of 117 nM. Comparing to SL-2-25, **61d** exhibits antimalarial activity of 14 nM.

3.2.3 Lead optimisation II: pyridyl side chain regiochemistry

After it was found that 7-OMe provides the most active derivative, the research aim then shifts into the investigation of side chain's regiochemistry. The pyridyl side chain gains more attraction as the pyridyl moiety contains an ionisable nitrogen atom which could further improve solubility by forming a protonated salt.

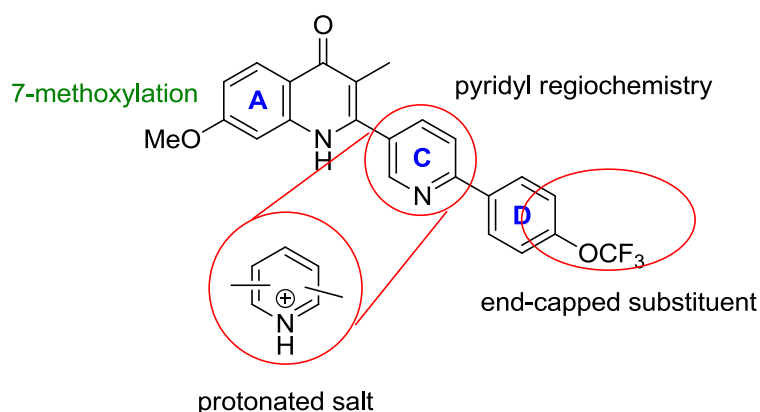


Figure 3.3 Rationale of lead optimisation (continued)

It was documented that *meta*-substituted bisaryl quinolone **108** possessing a more flexible linker is well tolerated as demonstrated an improved *in vitro* antimalarial activity against drug-sensitive and –resistant parasites^{1a}. The result suggests that flexibility of a particular side chain may affect compound activity.

(**Figure 3.5**)

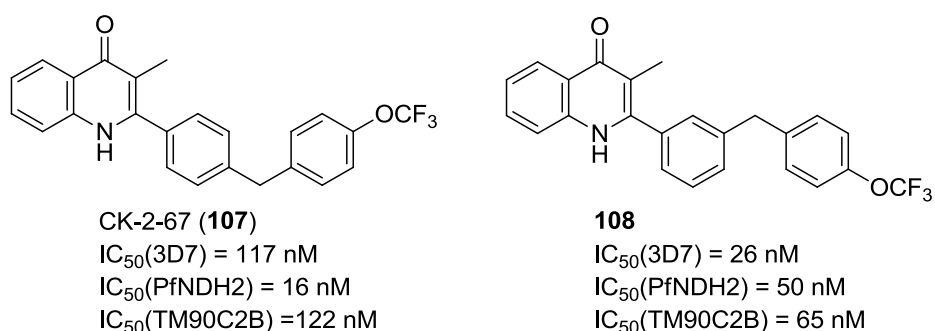
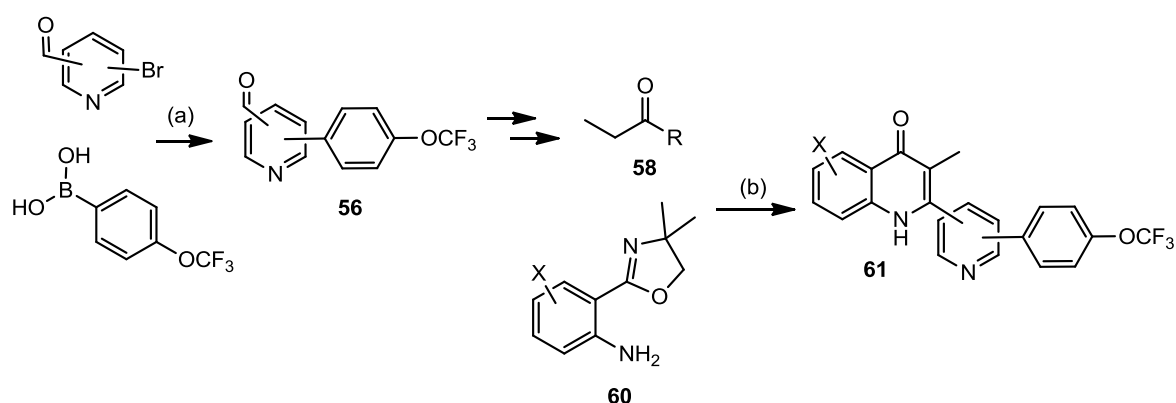


Figure 3.4 The effect of flexible aryl side chain towards antimalarial activity

Looking in detail at pyridyl regiochemistry in the lead molecule, it was found that several types of substitution could be investigated. When two substituents located on the opposite side of pyridyl ring (*para*-substitution) *i.e.* 2,5-disubstituted

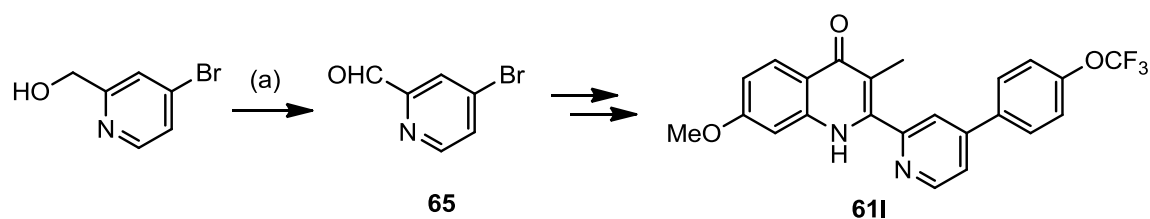
pyridine, the resulting straight-type side chains are rigid, lack flexibility resulting in poor aqueous solubility. On the other hand, another disubstitution pattern (*meta*-substitution) will provide more flexible and rotatable molecule (*i.e.* 3,5-disubstituted pyridine). The flexible side chain also resembles the structural characteristics observed in substrates like endochin (**46**) and stigmatellin (**38**). In addition to flexibility enhancement, it was well documented that desymmetrisationⁱ by changing the substitution pattern on an aromatic ring can enhance aqueous solubility³ thus it was hypothesised that the incorporation of *meta*-disubstituted pyridine will provide more water-soluble quinolones.



Scheme 3.7 Brief synthetic route towards pyridyl regioisomers; *Reagents* : (a) Pd(PPh₃)₄, K₂CO₃, THF, H₂O, under N₂, 80 °C, overnight (b) CF₃SO₃H, *n*-BuOH, under N₂, 130 °C, 1 day.

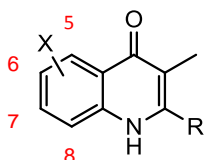
Based on similar chemistry (**Scheme 3.1** and **3.7**), the synthesis of more flexible side chain was accomplished from commercially available starting materials apart from **61I** for which the precursor aldehyde could not be purchased. The aldehyde **65** was made from the oxidation of respective alcohol in the presence of DMP in 66% yield⁵ (**Scheme 3.8**).

ⁱ **Desymmetrisation** in stereochemistry is the modification of a molecule that results in the loss of one or more symmetry elements.



Scheme 3.8 Alcohol oxidation; *Reagent*: (a) wet DMP, DCM, rt., 30 min, 66%.

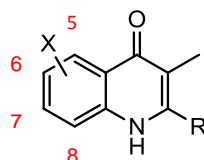
Analogues **61i** – **61s** with a flexible pyridyl side chain at the 2-position were synthesised according to **Scheme 3.1**, and the yields can be summarised in **Table 3.4**. In this case, both 7-H and 7-OMe analogues were synthesised and submitted for antimalarial assessment to attest the previous hypothesis claiming that 7-methoxylation provides highly active derivatives.



Compound	R	X	No. of steps	% Yield 58	% Yield 59	% Yield 60	% Yield 61
61i		7-OMe	6	32	92	73	34
61j		7-OMe	6	73	47	73	40
61k		7-OMe	6	55	99	73	34
61l		7-OMe	7	32	66	73	42
61m		7-OMe	6	37	97	73	62
61p		7-H	5	32	92	31	54
61q		7-H	5	73	47	31	55
61r		7-H	5	55	99	31	56
61s		7-H	5	37	97	31	62

Table 3.4 Yields for the synthesis of compounds **61i-61s**

The resulting compounds were assayed against *P.falciparum* malaria and the *in vitro* data is shown in **Table 3.5**. It was found that some pyridyl regioisomers of **61g** (eg. **61i** and **61k**) exhibit potent activity against the 3D7 parasite. Although 7-methoxylation provides the best activity, it is noteworthy that analogues **61p** and **61r**, which lack this substituent, are also potent nanomolar active antimalarials.



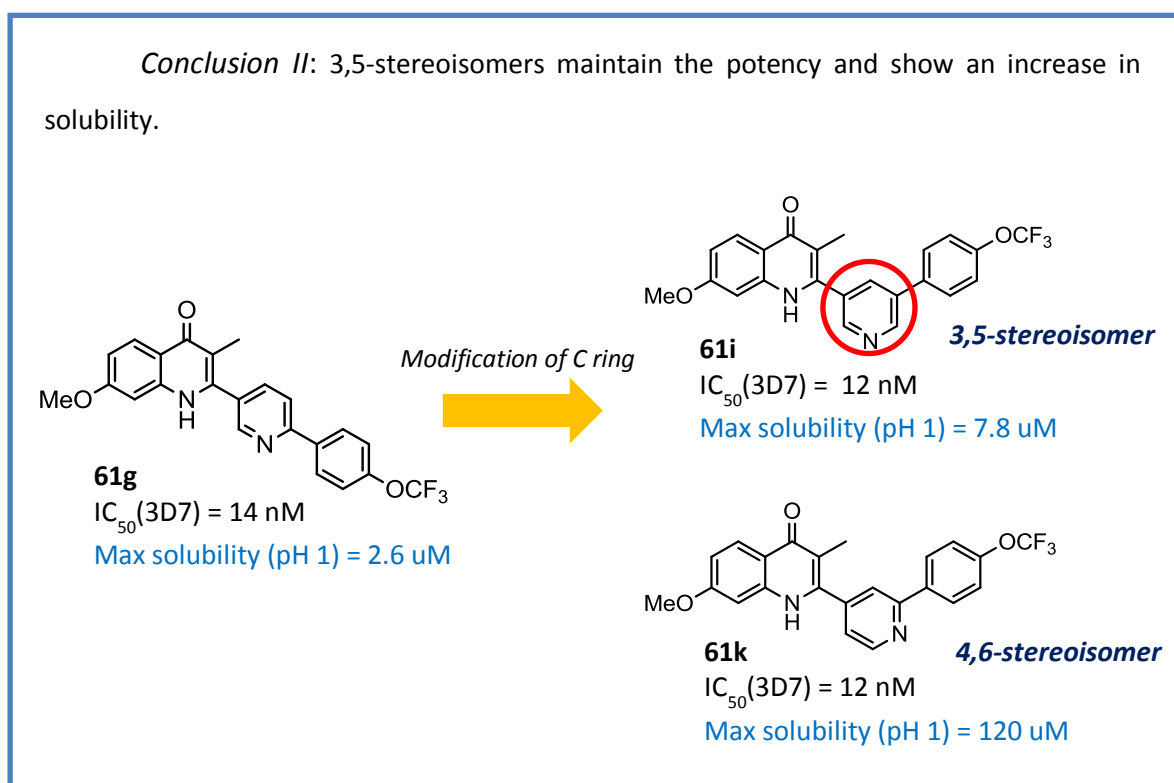
Compound	R	X	IC ₅₀ (nM) 3D7 ± SD
61g		7-OMe	14 ± 2
61i		7-OMe	12 ± 3
61j		7-OMe	149 ± 5
61k		7-OMe	12 ± 3
61l		7-OMe	150 ± 10
61m		7-OMe	> 1000
61p		7-H	41 ± 2
61q		7-H	390 ± 30
61r		7-H	21 ± 5
61s		7-H	> 1000

Table 3.5 *In vitro* antimalarial activity of quinolones **61i-61s**.

Looking in details at their molecular structures, **61m** and **61s** which possess a 7-OMe and a rigid side chain (*para*- substitution) devoid of flexibility show poor antimalarial activities. On the other hand, **61i** – **61l** and **61p** - **61r** containing more

flexible side chains (*meta*- substitution) exhibit good to outstanding efficacy against the 3D7 parasite. The pyridyl nitrogen position also plays a role in activity. Compounds containing a nitrogen atom located away from a quinolone core (**61i**, **61k**, **61p** and **61r**) seem to exhibit greater potency. It is possibly due to the fact that N-H of quinolone is important in target protein binding as demonstrated in molecular modelling studies described later in this chapter. Any disruption from pyridyl nitrogen towards this moiety (i.e. steric clash between pyridyl N and N-H) may abolish potency.

These compounds were also screened for aqueous solubility and any potential toxicity which will be discussed in later sections. It was apparent that 3,5-stereoisomers (**61i** and **61p**) show a good safety profile and an increase in solubility comparing to other stereoisomers.



3.2.4 Lead optimisation III: end-capped substituents

Following previous studies, the *p*-OCF₃ substituent on the D-ring has been identified to provide excellent antimalarial activity. More recent works on a related quinolones series revealed some advantages in 3,4-dichloro substitution⁴ and for this reason this substitution pattern was investigated within the quinolone D-ring side-chain in analogues **61n - o**.

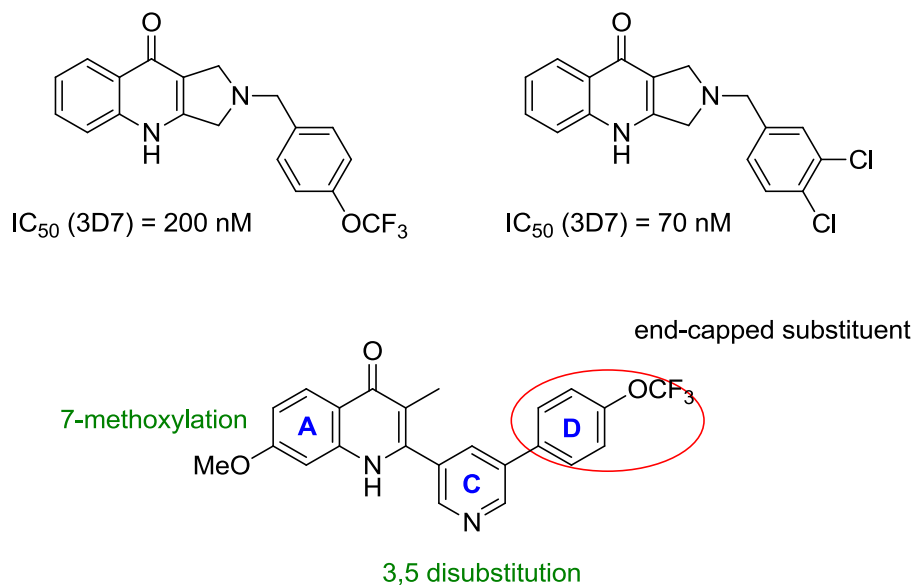
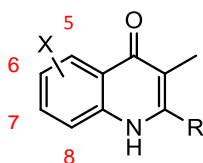


Figure 3.5 Rationale of lead optimisation (continued)

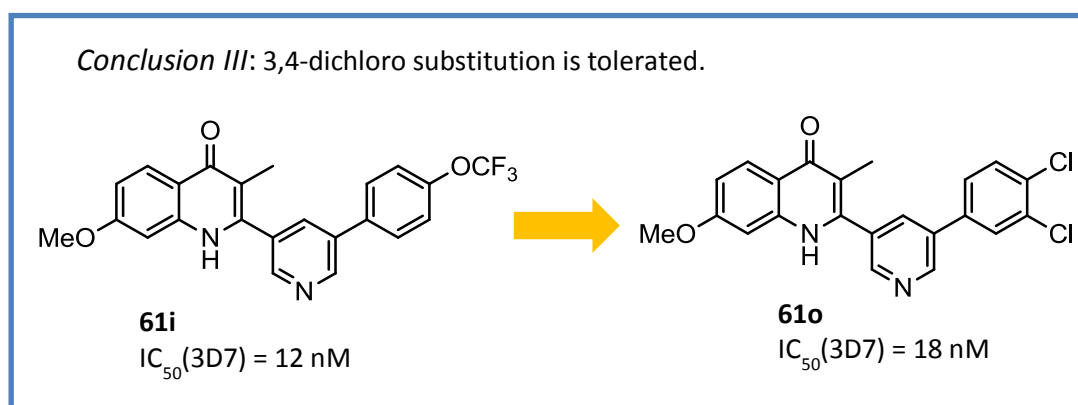
Bearing in mind that 7-OMe and 3,5-disubstituted pyridyl were found to provide analogues which possess an outstanding potency and a good physico-chemical property profile, within this scope, three 3,4-dichlorophenyl analogues were investigated. The synthesis towards 3,4-dichloro analogues can be done using aforementioned chemistry starting from commercially available 3,4-dichlorophenylboronic acid (**Scheme 3.1** and **3.7**). The yields are summarised in the **Table 3.6** and these compounds submitted for antimalarial *in vitro* assay.



Compound	R	X	No. of steps	% Yield 57	% Yield 58	% Yield 60	% Yield 61	IC ₅₀ (nM) 3D7 ± SD
61n		7-OMe	6	83	69	73	23	200 ± 10
61o		7-OMe	6	65	33	73	17	18 ± 3
61t		7-H	5	65	33	31	25	40

Table 3.6 Yields and *in vitro* antimalarial activity of 3,4-dichlorophenyl quinolones

The *in vitro* assay revealed that 3,4-dichlorophenyl substitution is tolerated as seen in **61o** and **61t** both of which show excellent antimalarial efficacy. **61o** expresses an activity as low as 18 nM against 3D7 parasite with improved toxicity, solubility and stability profiles as described later. Further biological experiments regarding this compound are in progress.



3.2.5 6-Cl-7-OMe-2-aryl quinolone analogue

During the course of this project, the related quinolone ELQ-300 (**24**) featuring 6-Cl and 7-OMe substituents on the A-ring was identified. ELQ-300 is a selective potent *Plasmodium bc₁* inhibitor and shows a superior antiplasmodial activity *in vitro* and *in vivo* against blood stage and liver stages of malaria¹¹. It is evident that, by replacing a H atom with a halogen atom at the 6-position on the quinolone core, more potent derivatives were found. With this strategy combining with the fact that 7-methoxylation provide the most active derivative, **61u** was synthesised following a general synthetic route used for 2-aryl quinolone.

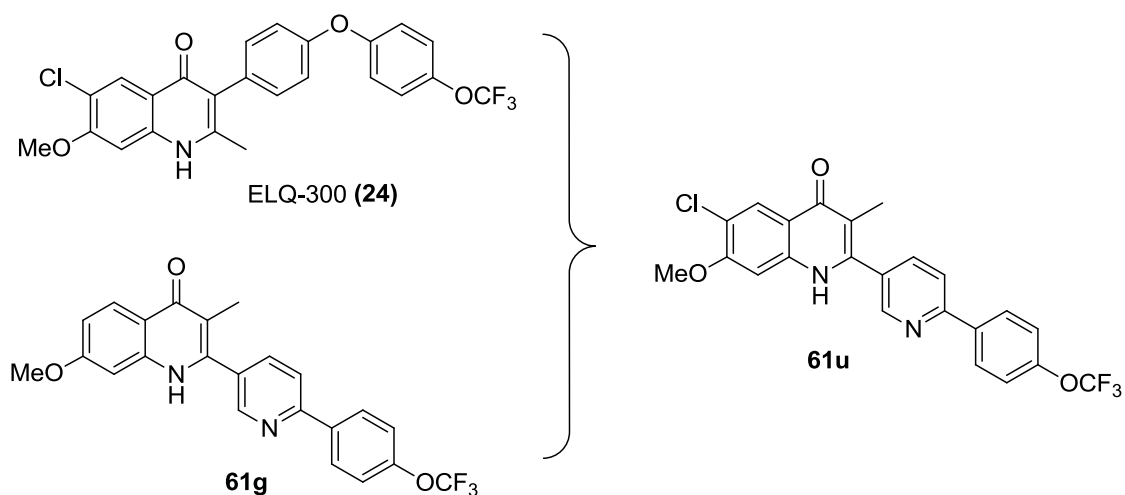
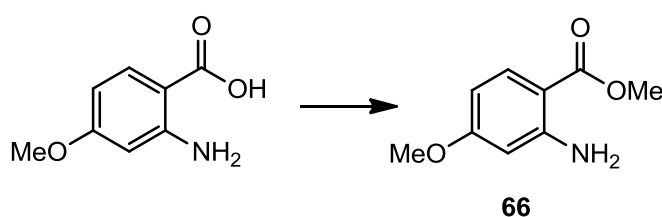


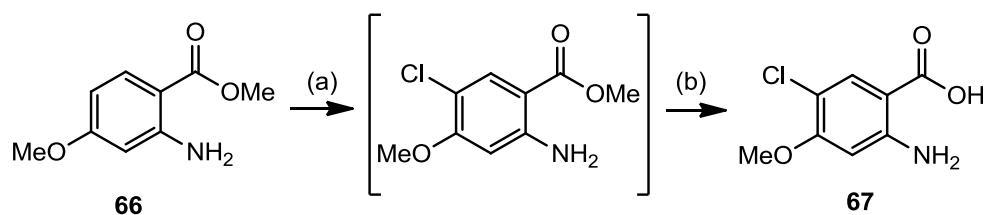
Figure 3.6 The chemical structure of **61u** based on a quinolone scaffold that resembles the structural characteristic of ELQ-300 and **61g**

Unfortunately, 5-chloro-4-methoxyanthranilic acid was not commercially available at that time, therefore, the synthesis of this anthranilic acid was then required. Starting from 4-methoxyanthranilic acid, the reaction of the carboxylic acid with methyl iodide in the presence of potassium carbonate gave methyl ester **66** in good yield¹².



Scheme 3.9 Reagent: MeI, K₂CO₃, DMF, 2 h, rt, 81%.

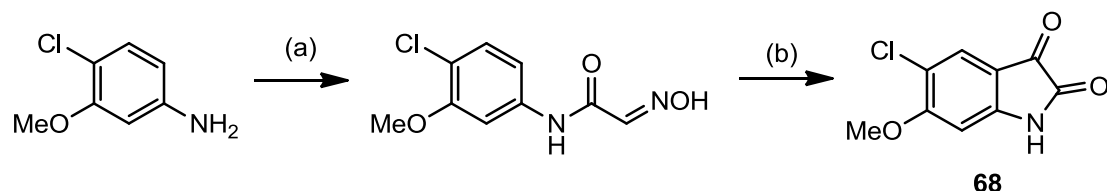
A chlorine atom was then added by using sulfuryl chloride in chloroform¹². The sulfur dioxide produced was passed through a water trap. Once there was no gas bubbling out from the reaction, the intermediate methyl ester was saponified with 1 M NaOH solution to give the desired anthranilic acid **67** in 19% yield. The product can be purified by column chromatography. The total yield for this synthetic route was poor and therefore an alternative approach was investigated.



Scheme 3.10 Reagent: (a) SO_2Cl_2 , CHCl_3 , 0°C , 30 min (b) 1 M aq. NaOH, 1 h, 19% over 2 steps.

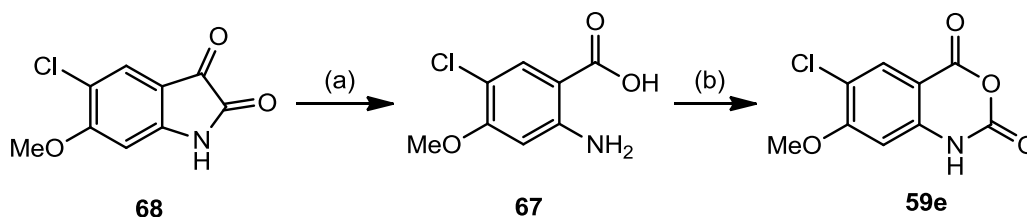
A literature search shows that anthranilic acid can be made from the corresponding starting aniline *via* isatin formation¹³. The Sandmeyer isatin synthesis discovered in 1919 is known to produce isatin through the cyclisation of the condensation product of chloral hydrate, aniline and hydroxylamine in sulfuric acid. Isatin can be oxidised to give a corresponding anthranilic acid^{13a}.

According to the known reaction above, the synthesis begins with the reaction between the 4-chloro-3-methoxyaniline and chloral hydrate under acidic condition^{13c, d}. The oxime product appeared as a dark brown solid was formed in excellent yield. Due to the fact that this compound has poor solubility in organic solvent, only its $^1\text{H-NMR}$ was obtained.



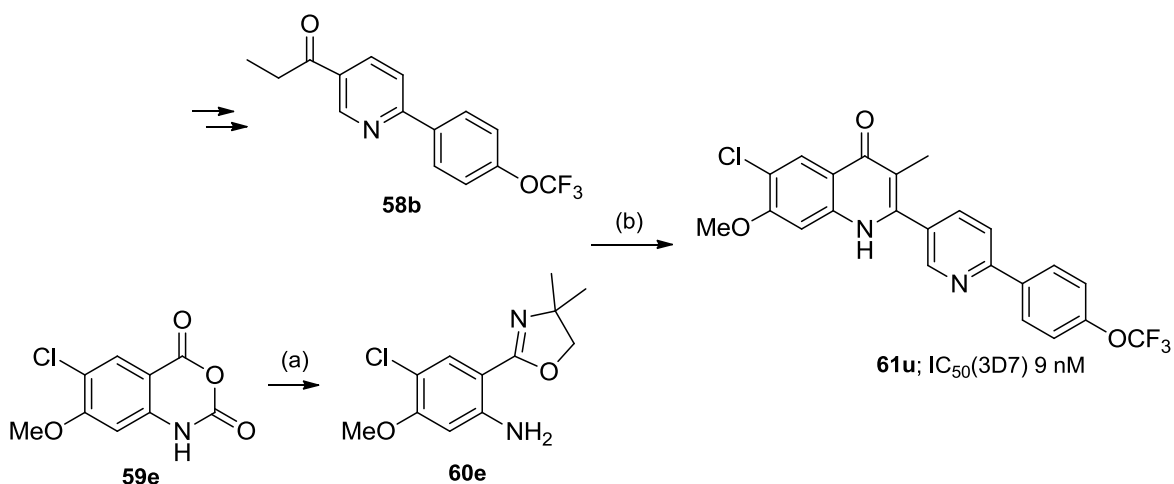
Scheme 3.11 Reagent: (a) Na_2SO_4 , chloral hydrate, concentrated HCl, $\text{NH}_2\text{OH}\cdot\text{HCl}$, water, 100°C , 3 h, 94%. (b) H_2SO_4 , $90\text{--}105^\circ\text{C}$, 25 min, 79%.

The cyclisation of this oxime in warm sulfuric acid yields isatin **68** or indolinedione in 79% conversion^{13c, d}. The solid was collected and dried. Without any purification its ¹H-NMR showed high purity. The oxidation of isatin **68** in a diluted solution of hydrogen peroxide under basic condition gave the corresponding anthranilic acid **67** in good yield^{13c, d}. The spectroscopic and elemental analysis data were consistent to the pure sample obtained from a different synthetic route.



Scheme 3.12 Reagent: (a) aq. 4 M NaOH, 3% H₂O₂, ice bath, 45 min, 83% (b) CCl₃COCl, THF, H₂O, 0°C, 2 h, 47%

The synthesis then follows the general synthesis described in **Scheme 3.1** and **3.13** starting from anthranilic acid **59e** which was made from **67** using diphosgene. Yields were reported in the experimental section in this chapter. Compound **61u** with 6-Cl and 7-OMe substituents were obtained and it was assayed for antimalarial activity. The *in vitro* data shows high potency against *Plasmodium* 3D7 parasite with an IC₅₀ of 9 nM. With this promising activity, this compound is now under further biological experiments.



Scheme 3.13 Reagents: (a) 2-amino-2-methyl-propanol, ZnCl₂, PhCl, 135 °C, 19% (b) CF₃SO₃H, *n*-BuOH, under N₂, 130 °C, 1 day, 19%.

3.2.6 Drug resistant parasite inhibition profiles

Drug resistance is a major threat in malaria control and elimination as noted in the first chapter. New drugs should provide a better safety profile and show no cross resistanceⁱⁱ with current drugs¹⁴. In addition to the *Pf3D7* testing, some selected compounds were tested against drug resistant strains of *P. falciparum* including chloroquine resistant W2 and atovaquone resistant TM90C2B (**Table 3.7**). **61i** and **61k**, both contain flexible side chains, showed excellent activities against both W2 and TM90C2B strains which are comparable to marketed drugs and our current lead - SL-2-25. Notably, against the atovaquone resistant strain TM90C2B both **61i** and **61k** express excellent activity and show no cross resistance with atovaquone. It suggests that flexible **61i** and **61k** bind to the target in a different manner to atovaquone.

Compound	IC ₅₀ (nM) W2	IC ₅₀ (nM) TM90C2B
chloroquine	12.3	14.5
atovaquone	0.30	9908
SL-2-25	48	156
61i	4.0	8.2
61k	4.2	7.0

Table 3.7 Drug resistant parasites inhibition profiles of selected quinolones

3.2.7 Aqueous solubility profiles

Aqueous solubility is important for drug candidates. A literature search showed that aqueous solubility can be inferred by changes to ClogP, melting point, and HPLC retention time³. Previous research indicates that quinolones generally

ⁱⁱ **Cross resistance** is a resistance to a particular drug that often results in resistance to other drugs, usually from a similar chemical class, to which the pathogen may not have been exposed.

have poor aqueous solubility due to the planar aggregation *via* π - π stacking of their ring system¹. Several strategies can be used to improve their solubility. Here, the incorporation of and modification of pyridyl side chain was explored with an aim of solubility enhancement. Some derivatives exhibited higher potency and those compounds were subjected to 96-well plate aqueous solubility assessment. The experiment was run in three different solutions according to their acidity.

Compound	Max Solubility (μ M)			pKa	Melting Point °C
	pH1	pH7.4	Media		
SL-2-25 (55)	3.2	<1	48	< 1.5	277-278
61i	7.8	<1	64	< 2.0	255-258
61g	2.6	<1	44	< 1.5	324-325
61k	120	<1	98	< 2.5	245-247
61p	140	3.6	59	< 2.5	217-220
61r	79	2.1	92	ND	244-246
61o	15	14	100	< 2.0	290-292

*Media = culture media (10% serum-based culture medium (RPMI-1640 supplemented with 25 mM HEPES and 4 μ g/ml gentamicin))

Table 3.8 Aqueous solubility profiles of selected quinolones

The results are shown in **Table 3.8**. At pH1, where the nitrogen lone pair can be protonated, **61p** has the best aqueous solubility amongst the selected quinolones which correlated with its low melting point. Although **61g** gave excellent activity, it is worth noting that a high melting point is observed which possibly reflects a decrease in aqueous solubility. Looking in detail at the side chain, substitution on pyridyl exclusively affected both antimalarial activity and solubility. The presence of the *meta*-pyridyl substitution (3,5-disubstituted pyridyl) seems to provide potent derivatives and also a good range of solubility (**61i** and **61k**). The relationship between melting point and solubility can be used within the pharmacophore to preliminarily compare their solubility.

3.2.8 Metabolic stability profiles

Selected potent quinolones were also submitted for their *in vitro* metabolic stability. Drug metabolism is a chemical transformation of pharmaceutical substances into more hydrophilic products which can be readily excreted by living organisms. The human liver is the most important site of drug metabolism in the body. Approximately 60 % of marketed compounds are cleared by hepatic CYP-mediated metabolism¹⁵. Subcellular fractions such as liver microsomes are useful *in vitro* models of hepatic clearance as they contain many of the drug metabolising enzymes found in the liver¹⁶. On the other hand, hepatocytes contain the full complement of hepatic drug metabolising enzymes (both phase I and phase II) maintained within the intact cell¹⁷. They are used as primary screens in the early drug discovery process. High clearance compounds are generally considered to be unfavourable as they are likely to be rapidly cleared *in vivo* resulting in a short half-life¹⁸.

Compound	Human Mics CL _{int} ($\mu\text{L}/\text{min}/\text{mg}$)	Rat Heps CL _{int} ($\mu\text{L}/\text{min}/10^6$)
SL-2-25 (55)	20.6	ND
61i	25.9	1.2
61o	14	4.9
61p	12.5	1.8
61r	7.7	2.5
61t	5.6	9.9

Table 3.9 Selected compounds solubility and metabolic stability profiles

Human microsomal stability assessment shows how stable the drug is when enters CYP450 oxidation stage, while rat hepatocytic clearance shows the compound stability in both phase I and phase II metabolism. The result shows that **61r** and **61t** show very low intrinsic clearance in human microsomal assay ($\ll 20 \mu\text{L}/\text{min}/\text{mg}$ protein)^{16, 18}, whereas **61i**, **61o**, **61p** and **61r** exhibit low hepatocytic clearance in the assay ($< 7 \mu\text{L}/\text{min}/10^6$ cell)¹⁷⁻¹⁸.

61i, **61o**, and **61p** are likely to be metabolised in human microsome as moderate clearances found. It is possibly due to the fact that their pyridyl nitrogen atoms are more exposed to the oxidative enzyme resulting in the *N*-oxidation products. Comparing between 7-OMe (**61i** and **61o**) and 7-H (**61p**, **61r**, **61t**) analogues, 7-OMe compounds are more sensitive to metabolism as a possible result of 7-*O*-demethylation. 3,4-dichlorophenyl compounds (**61o**, **61t**) are more stable in human microsomal media than their *p*-OCF₃ counterparts. It is likely due to the fact that the *ortho* oxidation is prohibited by this substituent. **61r** would be expected to be subject to very slow clearance *in vivo*¹⁸.

3.2.9 Potential off-target toxicity

Previous antimalarial projects that have focused on the development of *bc*₁ inhibitors have had to be terminated because of safety concerns regarding drug cardiotoxicity¹⁹. Therefore, a bovine heart *bc*₁ counterscreen was established to investigate any potential mammalian mitochondrial toxicity²⁰. Some highly potent compounds were assessed *in vitro*, using bovine heart *bc*₁ inhibition as displayed in **Table 3.10**.

Compound	IC ₅₀ (3D7)(nM)	Bovine heart <i>bc</i> ₁ (% inhibition at 100 nM)	Bovine heart <i>bc</i> ₁ (% inhibition at 1 μM)
SL-2-25	54	ND	60
61g	14	55	98
61i	12	19	81
61k	12	63	85
61o	18	13	20
61p	41	20	25
61r	21	52	81

Bovine heart *bc*₁ inhibition, IC₅₀ for SL-2-25 (**55**) = 890 nM and atovaquone = 83 nM

Table 3.10 Enzyme and parasite inhibition profiles of selected quinolones.

The single-point inhibition experiments were run at two different concentrations of select compounds – 100 nM and 1 μM. A low % inhibition

represents that the compound is less active in the bovine heart bc_1 screen. The general trend when 7-H compounds are compared to the 7-OMe counterparts is a reduction in inhibition of the bovine heart bc_1 complex. It is evident that the 7-OMe group plays a role in parasitic activity but it shows the drawback of the bovine heart bc_1 inhibition. Generally, the substitutions on pyridyl ring as in **61i**, **61o** and **61p** provide less toxic derivatives. In cases of **61o** and **61p**, given the preliminary data above, it is expected that their IC_{50} values are greater than 1 μ M making these compounds even safer than SL-2-25.

3.2.10 Molecular modelling studies

In addition to the chemical synthesis and antimalarial assessment of analogues, molecular modelling studies also performed to predict the way which a molecule is likely to interact with potential protein targets. The approach can be used either as a method to forecast those compounds most likely to give good results when synthesised, or to rationalise the observed results for existing compounds and suggest further development.

There are a number of docking software available either free, online or *via* licence needed. GOLD (Generic Optimisation for Ligand Docking) was chosen for this study²¹ as it has been used by relevant publications regarding the molecular docking at Q_o site of the bc_1 complex²². The molecular docking performed by GOLD is scored according to factors such as hydrogen bonding, van der Waals interaction, ligand strain, and steric clashes generating a term called GoldScore.

Although the protein crystal structure for *P.falciparum* bc_1 is not available, details of ATQ binding to cytochrome *b* have been elucidated based on studies performed on model organism and molecular modelling. The studies including EPR spectroscopy of the Rieske [2Fe2S] cluster, site-directed mutagenesis of model organism cytochrome *b* and gene sequencing of ATQ resistant *Plasmodium* species have demonstrated that ATQ is most likely a competitive inhibitor of the parasite's cytochrome *b* at quinol oxidation (Q_o) site²³. After ATQ monotherapy was

introduced to the market, subsequent *P.falciparum* parasites with a point mutation at Y268 were found in infected patients and it leads to 9,000-fold increase in IC₅₀²⁴. Position 268 in cytochrome *b* is highly conserved across all phyla and is located in the 'ef' helix component of the Q_o site, which is involved in quinol binding^{19, 23a}. It can be inferred that mutations at Y268 in Q_o site connect to the ATQ resistance²⁴⁻²⁵. Recently the X-ray structure of mitochondrial cytochrome *bc*₁ from yeast (*Saccharomyces cerevisiae*) with ATQ reveals that ATQ bound in the catalytic Q_o site (3.0-Å resolution) (PDB code 4PD4)²⁶.

Even though the crystallographic structure of *P.falciparum bc*₁ is not available, known *bc*₁ inhibitors were re-docked *in silico* using the high resolution crystal structure of yeast *bc*₁ protein (1.9-Å resolution) (PDB code 3CX5). The rationale for using the yeast protein is that it shares 40% homology with *P.falciparum* and the Q_o region is well conserved between the two proteins^{2, 23b}. The yeast *bc*₁ complex was originally co-crystallised with natural occurring stigmatellin binding at the Q_o site. Using the GOLD docking programme, stigmatellin can be removed and other compounds then docked into the same binding site.

Docking Solution	Goldscore	Reference.RMSD
1	88.5148	1.9451
2	104.7243	1.2493
3	79.3534	3.7428
4	94.5962	1.1509
5	91.8883	1.3194
6	97.6777	1.8039
7	96.4232	1.7432
8	97.5787	2.0191
9	84.7930	1.3627
10	107.2751	0.7892

Table 3.11 3CX5 protein validation results by stigmatellin re-docking mode

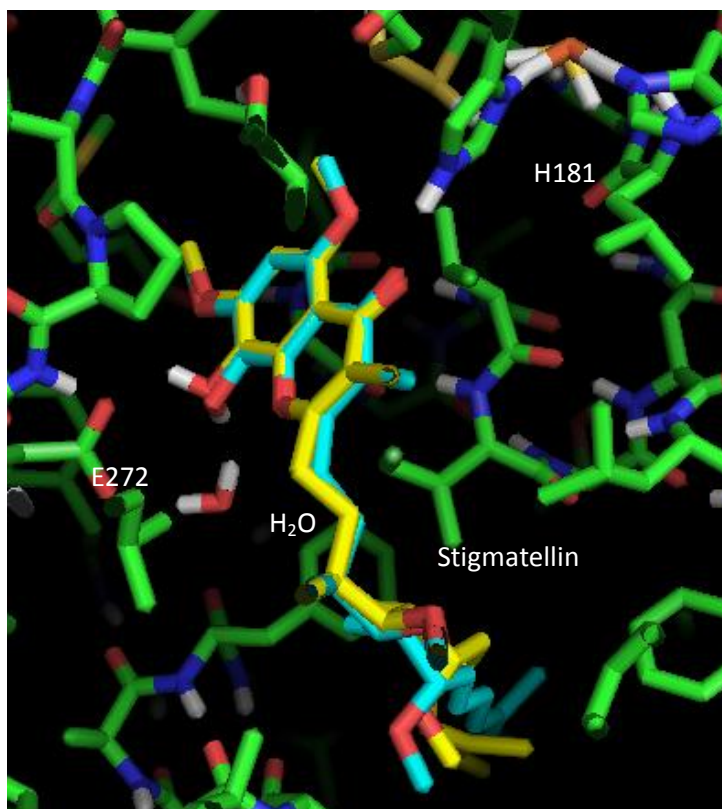


Figure 3.7 *In silico* re-docking mode for 3CX5 Q₀ site with stigmatellin. The crystallographic ligand was shown in cyan and the highest scoring result was shown in yellow

Therefore, in order to validate the chosen protein configuration, stigmatellin was docked into the Q₀ active site and the docking result shows that the highest score docking pose for stigmatellin, entry 10 in **Table 3.11**, has an RMSD of less than 1 Å with an average RMSD of 1.71 Å which is within 2 Å standard for a successful docking. In fact only two poses, entry 2 and 8, have RMSD values of greater than 2 Å. With an average Goldscore of 94.2, these results can be considered as a validation of ligand orientation and the docking method, meaning that any docking for other ligands using this approach are likely to be accurate. A simple outlying image also shows that the re-docking pose aligns in a similar way to the crystallographic ligand (**Figure 3.7**).

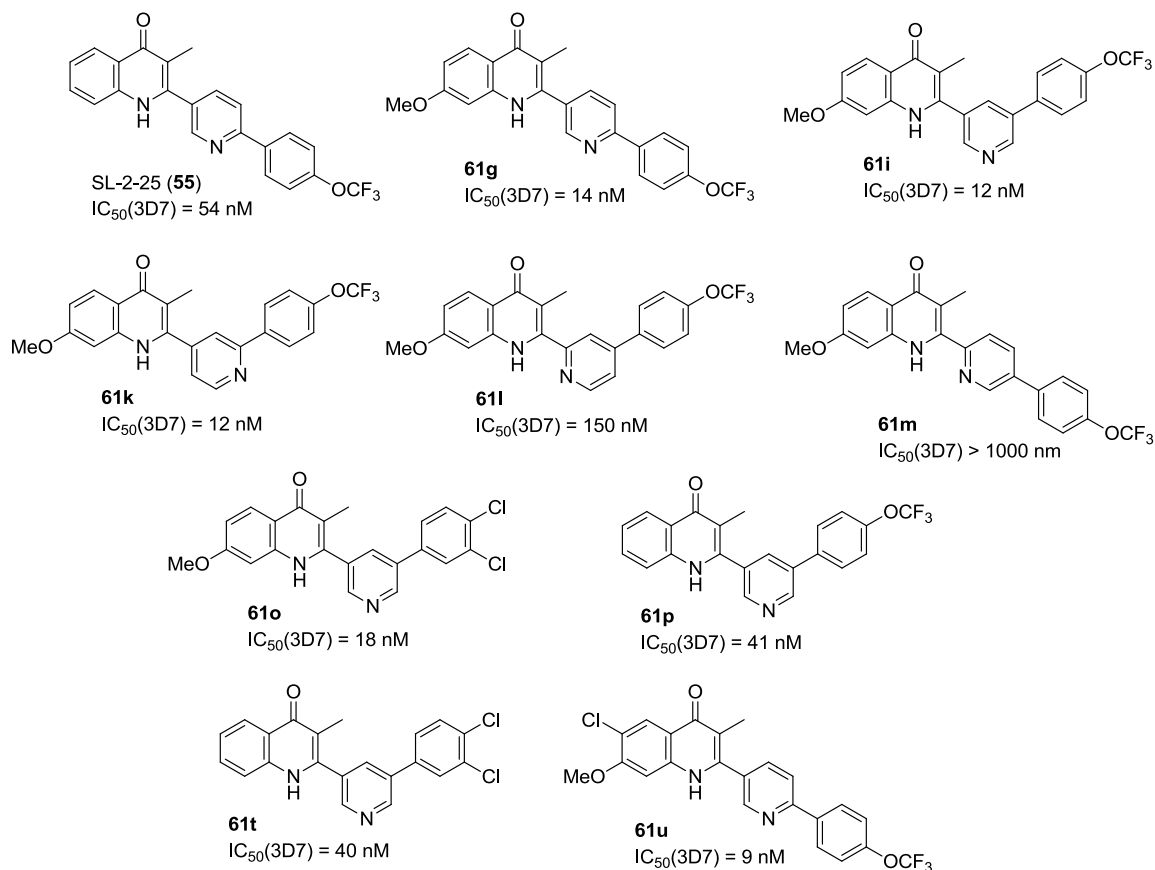


Figure 3.8 4-Quinolones employed in molecular docking

Having established the method, some highly active quinolones were selected for docking. To prepare quinolones for docking into the active site, their three dimensional structures were constructed and their minimal energy optimised using the Spartan'08 molecular mechanics programme. The files were then imported to GOLD and those molecules were docked into the Q_o site using the configuration previously validated by a successful re-docking of stigmatellin. For each quinolone, ten docking poses including its Goldscore were obtained for comparison and analysis. The quinolones used in molecular docking experiments are depicted below.

SL-2-25 (**55**), the initial lead compound in the programme, has very good potency and was the starting point of this research; therefore, it was selected as the benchmark for comparison. The compound did not score highest in the Goldscore amongst synthesised quinolones; the average score was only 57.07. It was found that there are a few poses where the compound did not locate in the correct

binding position. It is probably due to the fact that this compound contains a rigid side chain and lacks flexibility in some orientations.

Docking solution	Goldscore
1	55.7294
2	58.9367
3	53.0100
4	58.1072
5	57.2962
6	57.5820
7	56.2343
8	56.8088
9	57.4782
10	59.5537

Table 3.12 Docking results for SL-2-25 on 3CX5 protein.

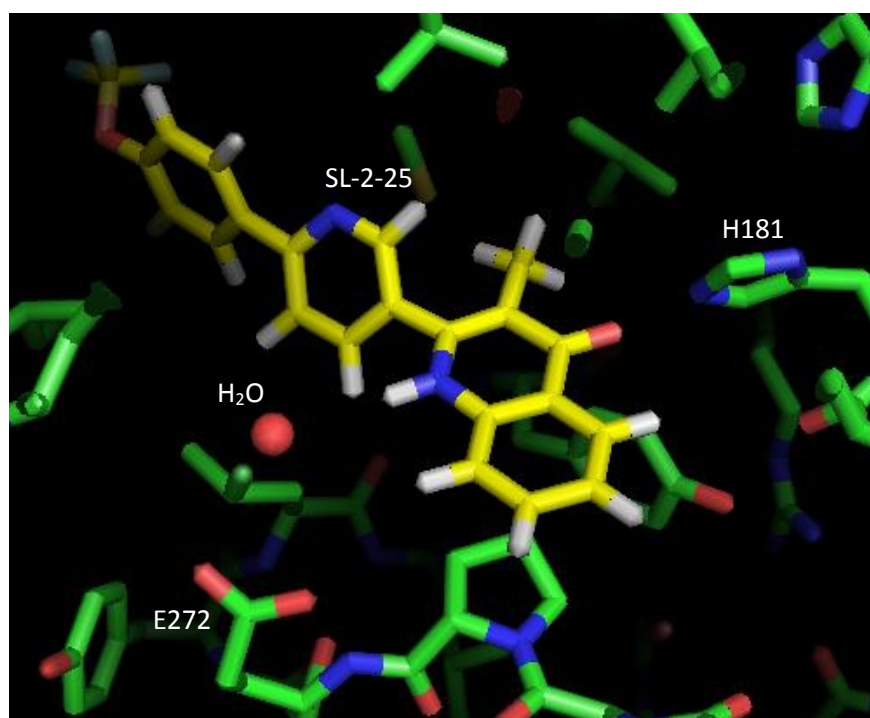


Figure 3.9 *In silico* docking mode for 3CX5 Q₀ site with SL-2-25. The selected SL-2-25 pose is depicted with carbons shown in yellow.

Using the same technique, quinolone analogues **61g**, **61i**, **61k**, **61l**, **61m**, **61o**, **61p**, **61t**, and **61u** were selected and their dockings were performed. A Goldscore for each quinolones was generated and presented in the **Table 3.13** with measured antimalarial IC₅₀s.

The best fit docking pose can be presented as the quinolone core inside the binding pocket and the 2-aryl side chain in the hydrophobic tunnel. In general, it was found that all quinolone bind tightly to the protein (average Goldscore > 60 in most cases). The essential interactions for strong binding are the hydrogen bond between H181 linked to Rieske protein and quinolone's carbonyl, the water-mediated hydrogen bond between E272 and N-H of quinolone, and surprisingly the interaction of 7-methoxy with a methionine residue. This binding mode not only results in a collapse of mitochondrial membrane potential but also impacts on metabolic enzymes that depend on the electron transport chain such as DHODH²⁷.

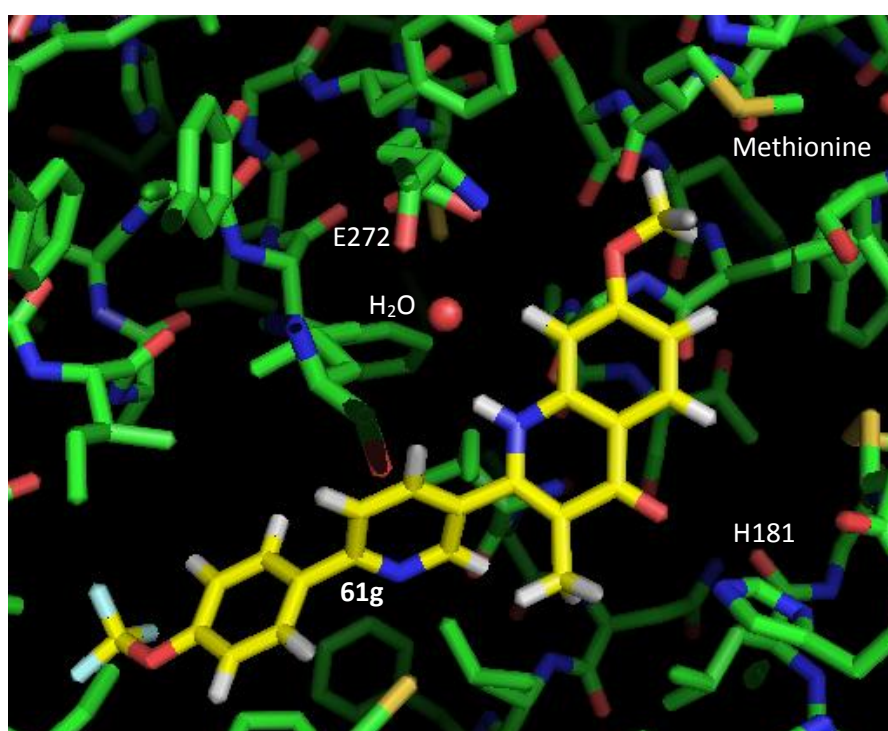


Figure 3.10 *In silico* docking mode for 3CX5 Q_o site with **61g**. The highest scoring pose is depicted with carbons shown in yellow.

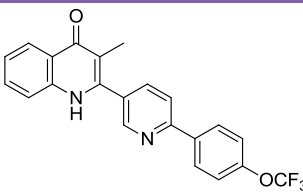
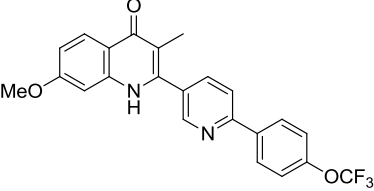
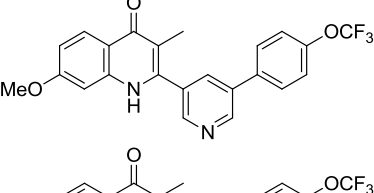
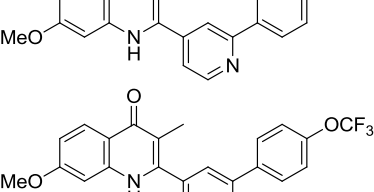
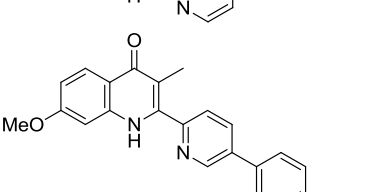
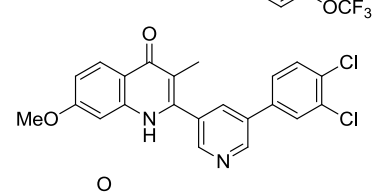
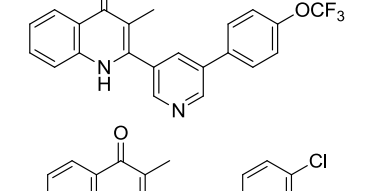
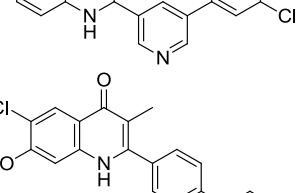
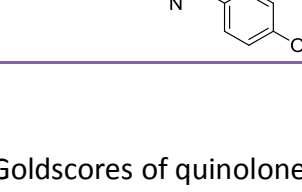

Compound	Structure	IC ₅₀ (nM)	Average Goldscore
SL-2-25 (55)		54	57.07
61g		14	62.86
61i		12	78.38
61k		12	72.10
61l		150	73.13
61m		>1000	68.48
61o		18	79.77
61p		41	67.97
61t		40	72.34
61u		9	56.10

Table 3.13 IC₅₀s and Goldscores of quinolone analogue (3CX5)

There is a rather clear trend we can observe that quinolones containing a flexible side chain and a 7-OMe (**61i**, **61k**, **61l**, and **61o**) seem to possess a higher Goldscore indicating that these structural features are important in bc_1 Q_o site binding.

The 7-OMe group can form a H-bond with a methionine residue at the end of the Q_o pocket which may act to tether the compound into the active site. This combined with strong H181 and water-mediated E272 interaction makes a more potent inhibitor. This is reflected by the higher GoldScore values for **61g** over SL-2-25. Similar relationships were found which **61i**, **61o** (7-OMe) possess higher Goldscores than **61p** and **61t** (7-H), respectively.

As described earlier, a long chain at C2 appears to be crucial for good antimalarial activity and physico-chemical properties. Obviously the *meta*-substituted analogues (**61i**, **61k**, **61l**, **61o**, **61p**, and **61t**) fit well into the Q_o pocket, much more easily than the *para*-substituted analogue (**61g**, **61m**, and **61u**) as demonstrated by higher Goldscores observed. For example, going from **61m** to **61l** the activity was restored. This can be supported by the large increase in the GoldScore value for **61l** suggesting the preferential binding of the *meta*-analogue. Also, a simple understanding and inspection of the Q_o site and the ligands in the pocket shows that the *meta*-analogue simply fits better, with less strain, as in **61m** the *p*-OCF₃ appears to sit in a little pocket which may bring about a strong steric clash, and given the compounds rigid nature there would be no way to circumvent this interaction without the compounds falling out of the pocket.

The difference in pyridyl regiochemistry as demonstrated in **61i**, **61k** and **61l** doesn't seem to have major negative effects on Goldscores which disagrees with the observed antimalarial activity. Comparison of the docking results between 3,4-dichloro substitution and *p*-OCF₃ on D ring shows a little advantage of a 3,4-dichloro moiety as demonstrated by greater Goldscores observed for **61o**, **61t** (3,4-dichloro substitution) than **61i** and **61p** (*p*-OCF₃), respectively.

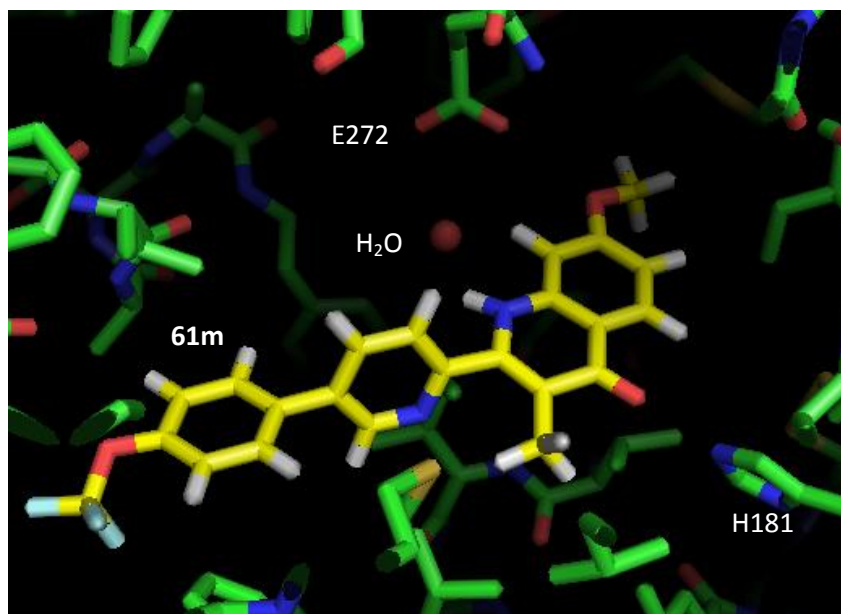


Figure 3.11 *In silico* docking mode for 3CX5 Q_o site with **61m**. The highest scoring pose is depicted with carbons shown in yellow.

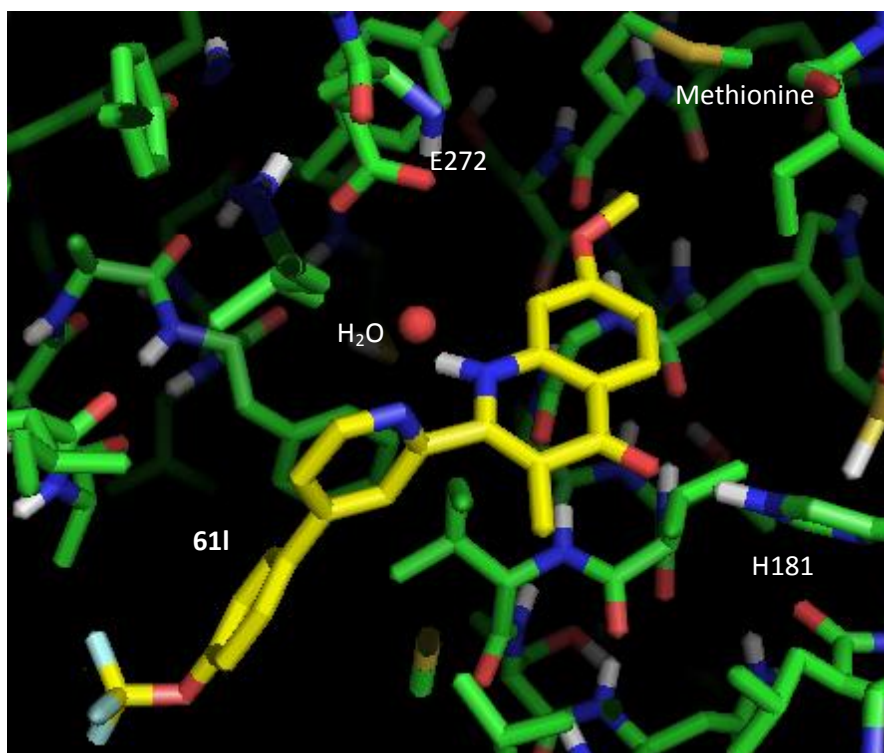


Figure 3.12 *In silico* docking mode for 3CX5 Q_o site with **61l**. The highest scoring pose is depicted with carbons shown in yellow.

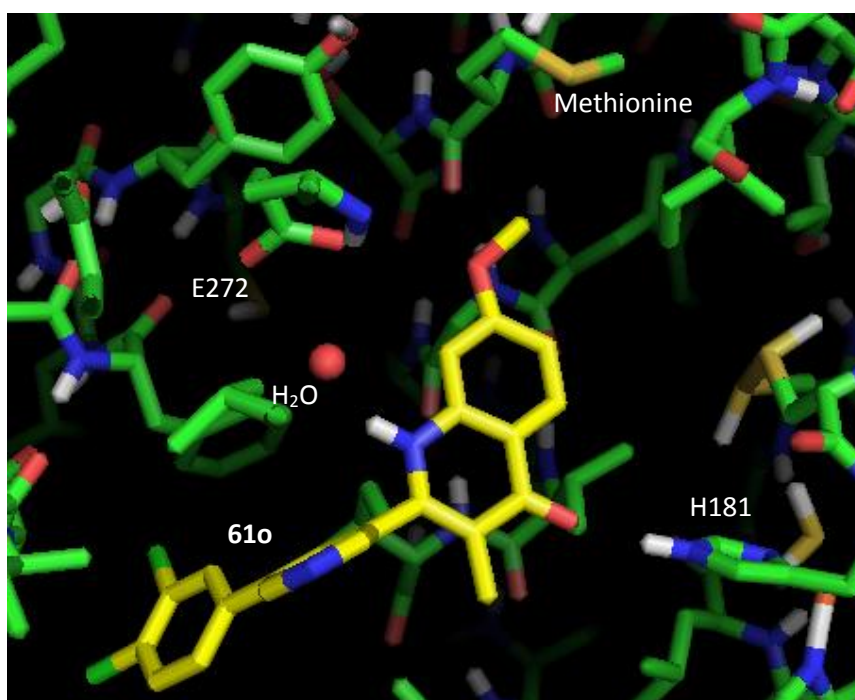


Figure 3.13 *In silico* docking mode for 3CX5 Q₀ site with **61o**. The highest scoring pose is depicted with carbons shown in yellow.

Another homology model of cytochrome *bc*₁ based on the primary sequence Q02768 and the 1KYO *S. cerevisiae* *bc*₁ complex template was created with the PHYRE online homology modelling tool²⁸. 1KYO is a 2.97 Å resolution crystal structure of cytochrome *bc*₁ complex co-crystallised with the ligand stigmatellin. After validation and structural refinement using the WHATIF web interface and SYBYL-X 1.1 Biopolymer module, respectively²⁹, the model was used to explore the binding mode of quinolone analogues within the Q₀ active site.

Using GOLD and the methods described earlier, stigmatellin was removed from the crystal and the model was validated by the re-docking mode of stigmatellin. The re-docking result shows that stigmatellin has an average Goldscore of 94.6 with an RMSD of 2.53 suggesting a rather successful method. Quinolone compounds were then docked into to binding site and their Goldscores were summarised in the **Table 3.14**.

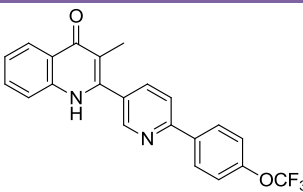
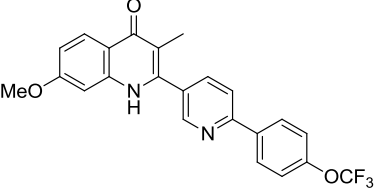
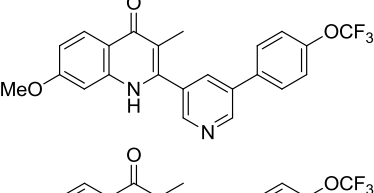
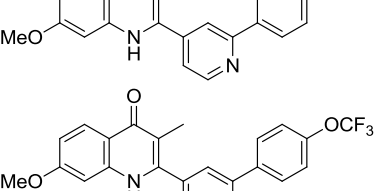
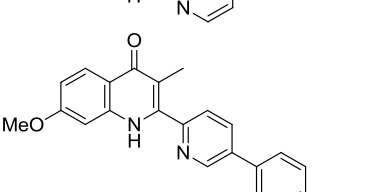
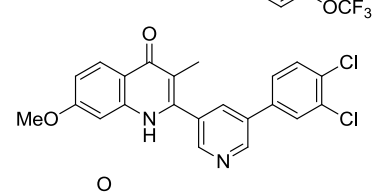
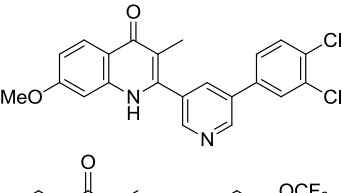
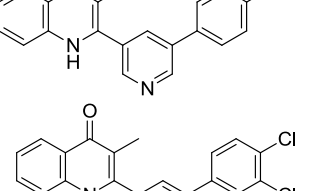
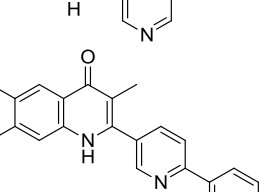
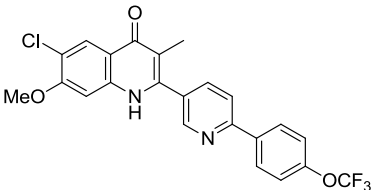
Compound	Structure	IC ₅₀ (nM)	Average Goldscore
SL-2-25 (55)		54	76.73
61g		14	83.85
61i		12	85.06
61k		12	83.62
61l		150	84.16
61m		>1000	84.25
61o		18	84.18
61p		41	84.30
61t		40	76.12
61u		9	79.03

Table 3.14 IC₅₀s and Goldscores of quinolone analogue (1KYO)

Similar to 3CX5 model, tight bindings between quinolones and the 1KYO model were found with an average Goldscore > 75 in all case. A clear trend was also observed that quinolones containing a 7-OMe possess a higher Goldscore demonstrating that the methoxy moiety is critical in both *in vitro* activity and *in silico* docking.

Using this model, all molecular docking provides a similar range of Goldscores suggesting that the procedure used is not suitable to differentiate or predict the antimalarial activity from *in silico* modeling. On the other hand, with all Goldscore higher > 75, it can be proposed that all quinolone tightly binds to the *bc*₁ target in this model giving the nanomolar potency except for inactive **61m**.

3.3 Conclusion

To conclude, a 5-7 step synthesis of a library of 2-aryl quinolones with potent antimalarial activity has been prepared. *In vitro* antimalarial assessment of these quinolone revealed the advantages of the 7-methoxy moiety. The potency increases 3-8 folds when the 7-OMe group is attached. Further lead optimisation led to the identification of a more flexible quinolone **61i** retaining high potency against the 3D7 strain of *P. falciparum*. The structure also possesses greater aqueous solubility and low potential for off-target toxicity.

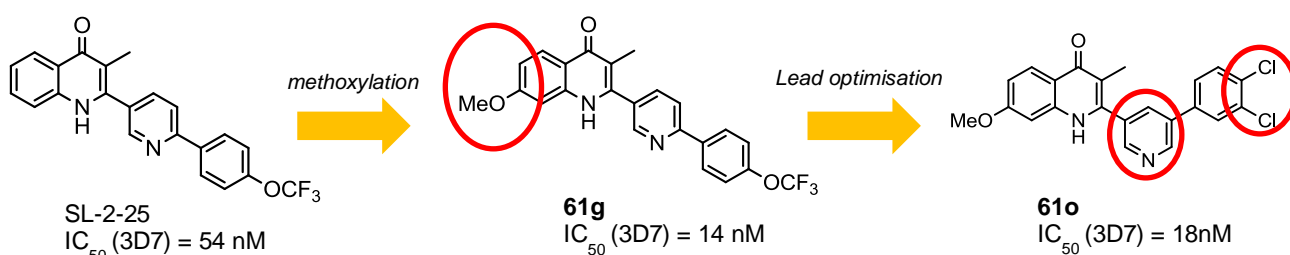


Figure 3.14 Lead optimisation of 2-aryl quinolones based on SL-2-25

Following a similar study on related quinolones, 3,4-dichloro analogues were briefly investigated and it shows the advantage of 3,4-dichloro moiety over *p*-OCF₃.

This led to the discovery of **61o** possessing an outstanding potency against 3D7 strain of *P. falciparum* of 18 nM. It shows even lower bovine *bc*₁ inhibition potency when compare to other quinolones. *In vivo* assessment and DMPK studies are also currently ongoing.

Featuring 6-Cl and 7-OMe substituents, **61u** was identified with an *in vitro* IC₅₀ potency of 9 nM against *Plasmodium*. With respect to SAR, it would be interesting to synthesise some quinolone analogues based on the structural characteristics of **61u** and **61o**, for example, **61v** which resembles flexible side chain, 3,4-dichlorophenyl and 6-Cl-7-OMe features (**Figure 3.15**). **61v** is expected to possess high potency with good solubility and safety profiles.

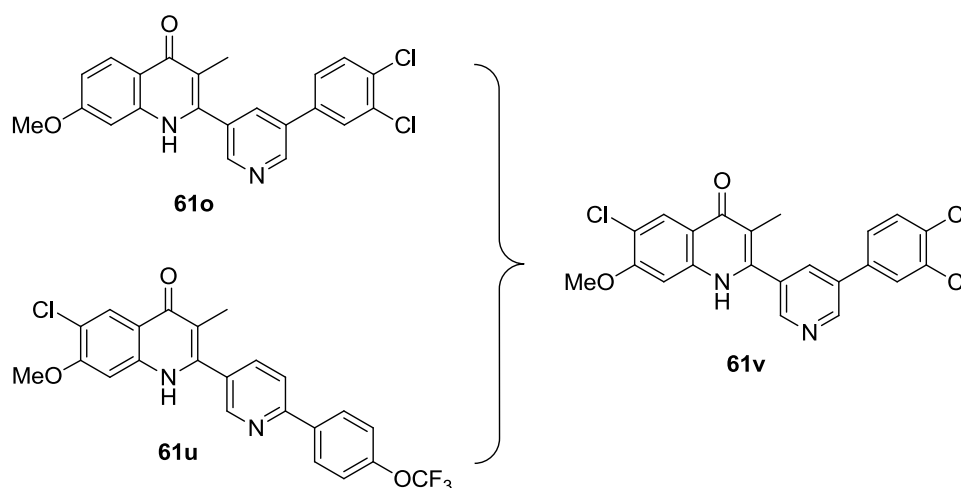


Figure 3.15 **61v** resembles the structural characteristics of **61u** and **61o**

Molecular modelling was employed to predict the way in which quinolone molecules bind to the target *bc*₁ protein. Several models based on the yeast *bc*₁ protein complex were generated, validated and used. *In silico* molecular modelling shows that all quinolones bind tightly to the protein. The essential interactions for strong binding are the hydrogen bond between histidine residue linked to the Rieske protein and the quinolone carbonyl, and the water-mediated hydrogen bond between glutamate and N-H of quinolone as demonstrated earlier.

3.4 Experimental

3.4.1 General

Air- and moisture-sensitive reactions were carried out in oven-dried glassware sealed with rubber septa under nitrogen from a balloon. Sensitive liquids and reagents were transferred via syringe. Reactions were stirred using Teflon-coated magnetic stir bars. All commercial reagents were used without further purifications. Organic solutions were concentrated under vacuum using Buchi rotary evaporator.

Anhydrous solvents were either purchased from reliable commercial sources or distilled from a still prior to use under inert gas atmosphere. THF was distilled from Na with benzophenone as an indicator. DCM was distilled from CaH₂. All reagents were purchased from reliable commercial sources and were used without any purification unless otherwise indicated. TLC analysis was performed to confirm the reagents purity.

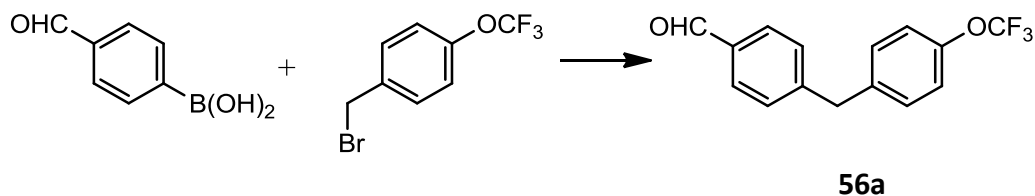
TLC was performed on 0.25 mm thickness Merck silica gel 60 with fluorescent indicator at 254 nm and visualised under UV light. UV inactive compounds were stained and visualised using iodine, *p*-anisaldehyde, or potassium permanganate solution followed by gentle heating. Flash column chromatography was performed using normal phase silica gel purchased from Sigma-Aldrich.

NMR spectra were recorded in a solution of CDCl₃ or DMSO-*d*₆ on a Bruker AMX400 spectrometer (¹H 400 MHz, ¹³C 100 MHz). Chemical shifts (δ) were expressed in ppm relative to tetramethylsilane (TMS) used as an internal standard. *J* coupling constants are in hertz (Hz) and the multiplicities were designed as follows: s, singlet; d, doublet; t, triplet; q, quartet; dd, double of doublet; m, multiplet. Mass spectra were recorded on either a Micromass LCT Mass Spectrometer using electrospray ionisation (ESI) or Trio-1000 Mass Spectrometer using chemical ionisation (CI). Reported mass values are within error limits of ±5 ppm. Elemental analysis (%C, %H, %N) was performed in the University of Liverpool microanalysis

laboratory. All melting points were determined with Gallenkamp melting point apparatus and were uncorrected.

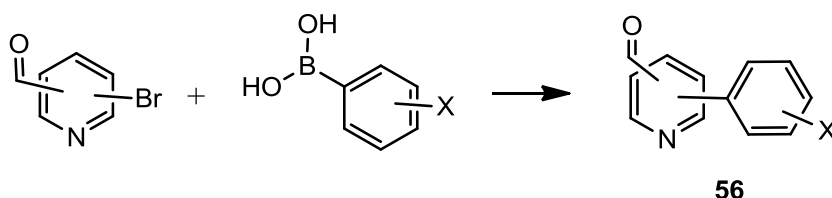
3.4.2 Synthesis

Preparation of **4-(4-(trifluoromethoxy)benzyl)benzaldehyde, 56a**



To a solution of 1-(bromomethyl)-4-(trifluoromethoxy)benzene (1.03 g, 1.1 eq), Pd(PPh₃)₄ (180 mg, 0.025 eq), and potassium carbonate (2.84 g, 3.3 eq) in THF (35 mL) and H₂O (15 mL) under an N₂ atmosphere was added 4-formylphenylboronic acid (1.59 g, 1.0 eq). The reaction was allowed to stir and heated to reflux condition (80 °C) overnight. After that the mixture was allowed to cool to room temperature and evaporated to remove solvent. The residue was redissolved in EtOAc, passed through a silica pad to obtain a dark brown oil after solvent removal. Purification by column chromatography (eluting with 10% EtOAc/*n*-Hexane) gave **56a** (1.65 g, 94%) as a white solid. ¹H NMR (400 MHz, CDCl₃) δ 9.99 (s, 1H, COH), 7.83 (d, *J* = 8.2 Hz, 2H, Ar), 7.34 (d, *J* = 8.1 Hz, 2H, Ar), 7.20 (d, *J* = 8.8 Hz, 2H, Ar), 7.15 (d, *J* = 8.4 Hz, 2H, Ar), 4.06 (s, 2H, ArCH₂Ar); ¹³C NMR (100 MHz, CDCl₃) δ 192.3, 148.0, 138.8, 135.3, 130.6, 130.6, 129.9, 121.6, 41.7. MS (CI) : *m/z* calculated for C₁₅H₁₁O₂F₃ ([M]⁺) 280.1, found 280.3.

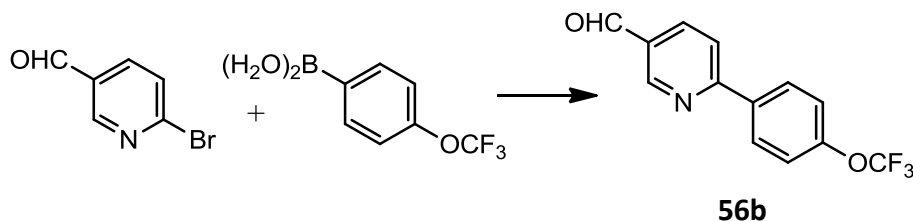
General procedure 1



To a solution of selected aromatic aldehyde (1.0 eq), Pd(PPh₃)₄ (0.08 eq) and potassium carbonate (3.3 eq) in THF (25 mL) and H₂O (10 mL) under N₂ atmosphere was added phenylboronic acids (1.1 eq). The reaction was allowed to stir and

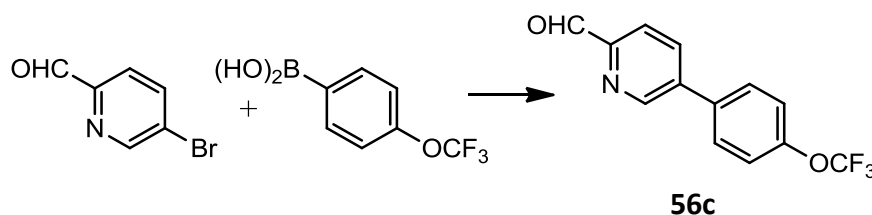
heated to reflux condition (80 °C) overnight. After the mixture was allowed to cool to room temperature, water (20 mL) was poured into the mixture. Extraction with EtOAc (3 x 30 mL), washing with brine and drying over MgSO₄ gave the crude after solvent evaporation. Purification was performed by column chromatography (eluting with 10-30% EtOAc/*n*-Hexane).

Preparation of 6-(4-(trifluoromethoxy)phenyl)nicotinaldehyde, **56b**

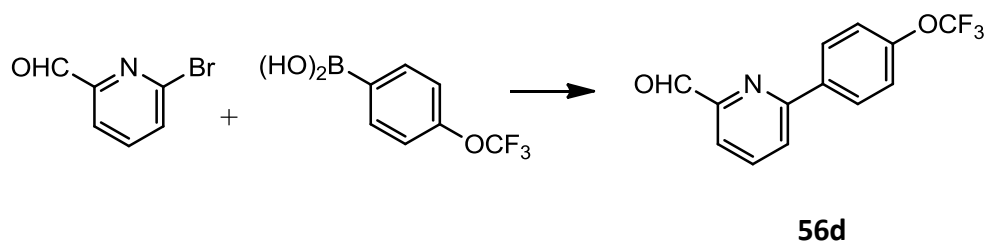


6-Bromonicotinaldehyde (835 mg, 5 mmol) was treated following **the General procedure 1** gave **56b** (1.06 g, 88%) as a pale yellow solid. ¹H NMR (400 MHz, CDCl₃) δ 10.16 (s, 1H, COH), 9.14 (d, *J* = 1.5 Hz, 1H), 8.26 (dd, *J* = 8.2, 2.2 Hz, 1H), 8.14 (d, *J* = 8.9 Hz, 2H), 7.90 (d, *J* = 8.3 Hz, 1H), 7.37 (d, *J* = 8.1 Hz, 2H); ¹³C NMR (100 MHz, CDCl₃) δ 190.78, 161.07, 152.82, 137.17, 136.88, 130.43, 129.57, 121.60, 120.91. ESI-HRMS: *m/z* calculated for C₁₄H₁₃NO₃F₃ ([M+MeOH+H]⁺) 300.0848, found 300.0849.

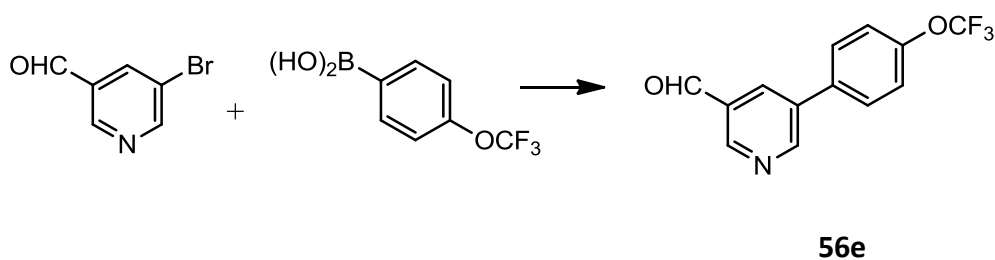
Preparation of 5-(4-(trifluoromethoxy)phenyl)picolinaldehyde, **56c**



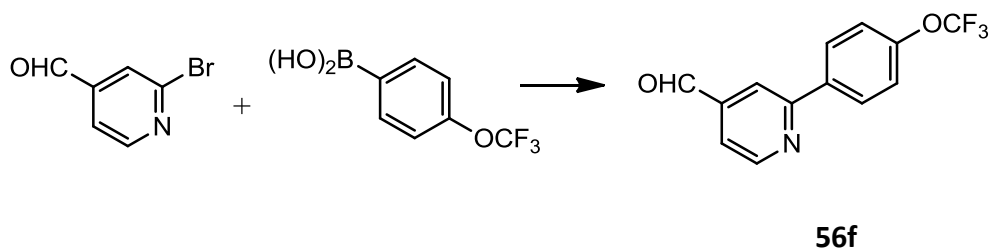
5-Bromopicolinaldehyde (930 mg, 5 mmol) was treated following **the General procedure 1** gave **56c** (1.30 g, 98%) as a pale yellow solid. ¹H NMR (400 MHz, CDCl₃) δ 10.14 (s, 1H), 9.00 (dd, *J* = 1.9, 1.0 Hz, 1H), 8.09 – 8.00 (m, 2H), 7.68 (d, *J* = 8.7 Hz, 2H), 7.38 (d, *J* = 8.0 Hz, 2H). ¹³C NMR (100 MHz, CDCl₃) δ 193.31, 152.23, 148.98, 139.74, 135.64, 129.36, 128.09, 122.26, 122.14. ESI-HRMS: *m/z* calculated for C₁₃H₉NO₂F₃ ([M+H]⁺) 268.0585, found 268.0587.

Preparation of **6-(4-(trifluoromethoxy)phenyl)picolinaldehyde, 56d**

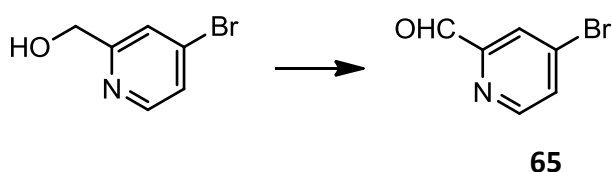
6-Bromopicolinaldehyde (930 mg, 5 mmol) was treated following the **General procedure 1** gave **56d** (1.20 g, 89%) as yellow needles. ^1H NMR (400 MHz, CDCl_3) δ 10.16 (d, $J = 0.6$ Hz, 1H), 8.18 – 8.10 (m, 2H), 7.97 – 7.90 (m, 3H), 7.36 (dd, $J = 8.9, 0.9$ Hz, 2H). ^{13}C NMR (101 MHz, CDCl_3) δ 194.03, 156.90, 153.22, 150.79, 150.77, 138.41, 137.10, 128.96, 124.68, 121.61, 120.45. ESI-HRMS: m/z calculated for $\text{C}_{13}\text{H}_8\text{NO}_2\text{F}_3\text{Na}$ ($[\text{M}+\text{Na}]^+$) 290.0405, found 290.0406.

Preparation of **5-(4-(trifluoromethoxy)phenyl)nicotinaldehyde, 56e**

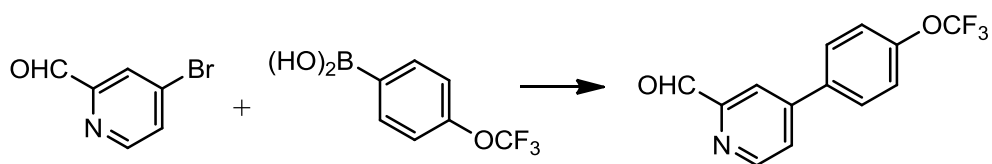
5-Bromonicotinaldehyde (2.4 g, 13 mmol) was treated following the **General procedure 1** gave **56e** (3.4 g, 99%) as a white solid. ^1H NMR (400 MHz, CDCl_3) δ 10.21 (s, 1H), 9.09 (d, $J = 1.7$ Hz, 1H), 9.07 (d, $J = 2.2$ Hz, 1H), 8.34 (t, $J = 2.1$ Hz, 1H), 7.67 (d, $J = 8.8$ Hz, 2H), 7.38 (d, $J = 8.0$ Hz, 2H). ^{13}C NMR (101 MHz, CDCl_3) δ 190.92, 153.38, 151.41, 150.24, 136.48, 135.40, 134.04, 131.82, 129.17, 122.18. ESI-HRMS: m/z calculated for $\text{C}_{14}\text{H}_{13}\text{NO}_3\text{F}_3$ ($[(\text{M}+\text{MeOH})+\text{H}]^+$) 300.0848, found 300.0847.

Preparation of **2-(4-(trifluoromethoxy)phenyl)isonicotinaldehyde, 56f**

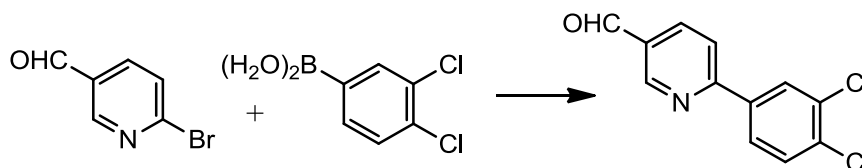
2-Bromoisonicotinaldehyde (2.6 g, 14 mmol) was treated following the **General procedure 1** gave **56f** (3.52 g, 94%) as a colourless oil. ^1H NMR (400 MHz, CDCl_3) δ 10.14 (s, 1H), 8.94 (dd, $J = 4.9, 0.6$ Hz, 1H), 8.17 – 8.02 (m, 3H), 7.65 (dd, $J = 4.9, 1.4$ Hz, 1H), 7.34 (d, $J = 8.0$ Hz, 2H). ^{13}C NMR (101 MHz, CDCl_3) δ 191.74, 158.01, 151.60, 150.82, 150.81, 143.00, 137.13, 128.95, 121.55, 121.44, 118.94. ESI-HRMS: m/z calculated for $\text{C}_{14}\text{H}_{13}\text{NO}_3\text{F}_3$ ($[(\text{M}+\text{MeOH})+\text{H}]^+$) 300.0848, found 300.0853.

Preparation of **4-bromopicolinaldehyde, 65**

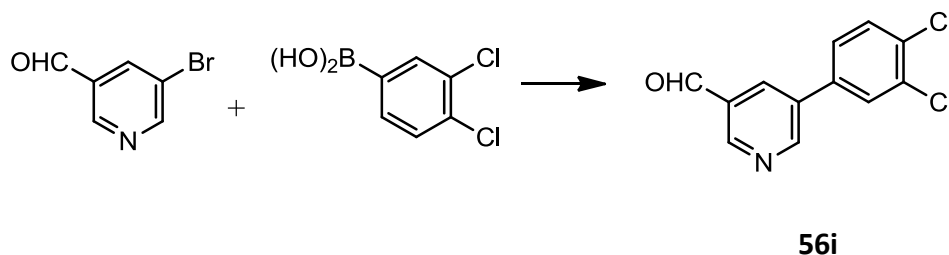
Wet DCM (10 mL) was added slowly to the stirring solution of (4-bromopyridin-2-yl)methanol (658 mg, 3.5 mmol) and DMP (1.5 eq) in DCM (15 mL). The cloudy mixture was left for an hour then diluted with ether, concentrated on rotavap. The residue was then taken up in 30 mL of ether and then washed with 20 mL of 1:1 mixture of 10% $\text{Na}_2\text{S}_2\text{O}_3$ and sat. NaHCO_3 , followed by water and brine. The aqueous washings were back-extracted with ether. The combined organic layers were dried over MgSO_4 and evaporated to dryness. Purification was achieved by column chromatography (eluting with 40% EtOAc/*n*-Hexane) to afford 4-bromopicolinaldehyde (432 mg, 66%) as a yellow oil. ^1H NMR (400 MHz, CDCl_3) δ 10.04 (s, 1H), 8.61 (dd, $J = 5.2, 0.4$ Hz, 1H), 8.12 (dd, $J = 1.9, 0.5$ Hz, 1H), 7.69 (dd, $J = 5.2, 2.0$ Hz, 1H). ^{13}C NMR (101 MHz, CDCl_3) δ 192.42, 154.06, 151.27, 134.57, 131.31, 125.52.

Preparation of **4-(4-(trifluoromethoxy)phenyl)picolinaldehyde, 56g****56g**

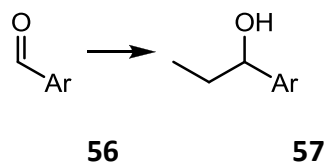
4-Bromopicolinaldehyde, **65** (550 mg, 2.96 mmol) was treated following the **General procedure 1** gave **56g** (610 mg, 83%) as a yellow solid. ^1H NMR (400 MHz, CDCl_3) δ 10.15 (s, 1H), 8.85 (dd, $J = 5.1, 0.7$ Hz, 1H), 8.17 (dd, $J = 1.9, 0.7$ Hz, 1H), 7.75 – 7.67 (m, 3H), 7.37 (d, $J = 8.0$ Hz, 2H). ^{13}C NMR (101 MHz, CDCl_3) δ 193.73, 151.23, 148.68, 129.06, 125.76, 122.03, 119.70, 117.74. ESI-HRMS: m/z calculated for $\text{C}_{13}\text{H}_8\text{NO}_2\text{F}_3\text{Na}$ ($[\text{M}+\text{Na}]^+$) 290.0405, found 290.0409.

Preparation of **6-(3,4-dichlorophenyl)nicotinaldehyde, 56h****56h**

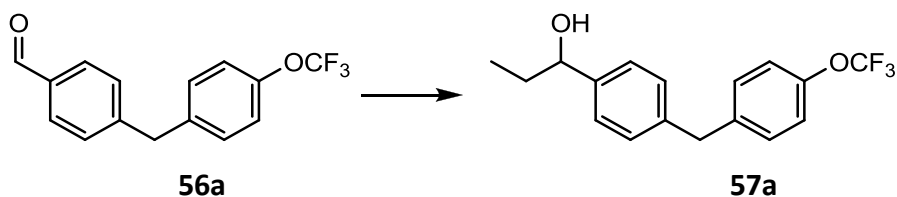
6-Bromonicotinaldehyde (986 mg, 5.3 mmol) and 3,4-dichlorobenzeneboronic acid (1.09 g, 5.7 mmol) was treated following the **General procedure 1** gave **56h** (1.04 g, 78%) as a white solid. ^1H NMR (400 MHz, CDCl_3) δ 10.15 (s, 1H), 9.13 (d, $J = 2.1$ Hz, 1H), 8.28 – 8.21 (m, 2H), 7.93 (dd, $J = 8.4, 2.1$ Hz, 1H), 7.88 (d, $J = 8.2$ Hz, 1H), 7.59 (d, $J = 8.4$ Hz, 1H). ^{13}C NMR (101 MHz, CDCl_3) δ 190.54, 159.94, 152.72, 138.20, 137.28, 135.16, 133.89, 131.36, 130.74, 129.85, 126.89, 120.81. MS (CI): m/z calculated for $\text{C}_{12}\text{H}_8^{35}\text{Cl}_2\text{NO}$ ($[\text{M}+\text{H}]^+$) 252.0, found 252.1(100%), 254.0(79), 256.2(11).

Preparation of 5-(3,4-dichlorophenyl)nicotinaldehyde, **56i**

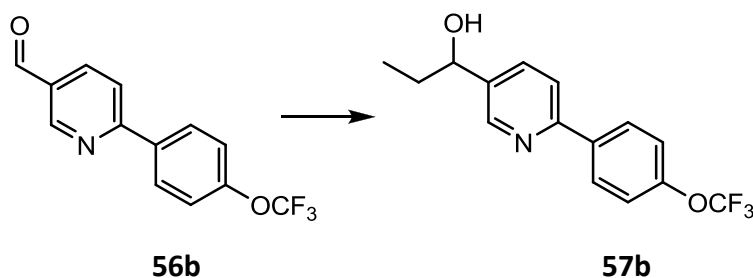
5-Bromonicotinaldehyde (930 mg, 5 mmol) and 3,4-dichlorobenzeneboronic acid (1.07 g, 5.5 mmol) was treated following the **General procedure 1** gave **56i** (987 mg, 78%) as a yellow solid. ^1H NMR (400 MHz, CDCl_3) δ 10.21 (s, 1H), 9.09 (d, $J = 0.8$ Hz, 1H), 9.05 (d, $J = 1.6$ Hz, 1H), 8.31 (t, $J = 2.2$ Hz, 1H), 7.73 (d, $J = 2.1$ Hz, 1H), 7.60 (d, $J = 8.3$ Hz, 1H), 7.47 (dd, $J = 8.3, 2.2$ Hz, 1H). ^{13}C NMR (101 MHz, CDCl_3) δ 190.73, 179.85, 153.27, 151.83, 136.72, 134.14, 133.89, 133.85, 131.76, 129.48, 128.08, 126.78. MS (CI): m/z calculated for $\text{C}_{12}\text{H}_8\text{Cl}_2\text{NO}$ ($[\text{M}+\text{H}]^+$) 252.0, found 252.2(100%), 254.2(66), 256.2(11).

General procedure 2.

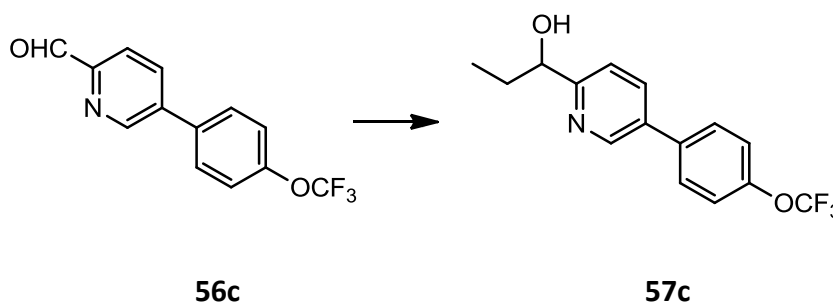
Aldehyde **56** (1.0 eq) was dissolved in THF (30 mL) and cooled down to 0 °C under N_2 atmosphere. 1.0 M Ethylmagnesium bromide solution (1.5 eq) was added dropwise to the mixture and the reaction was allowed to stir at 0 °C for 1 hour. The solution was then quenched with 1M HCl (30 mL) and extracted with ether (3 x 30 mL). The combined organic layer was washed with brine and dried over MgSO_4 . The solution was then evaporated under vacuum. The purification was performed using column chromatography eluted with 10% increasing to 40% EtOAc/*n*-Hexane.

Preparation of **1-(4-(4-(trifluoromethoxy)benzyl)phenyl)propan-1-ol, 57a**

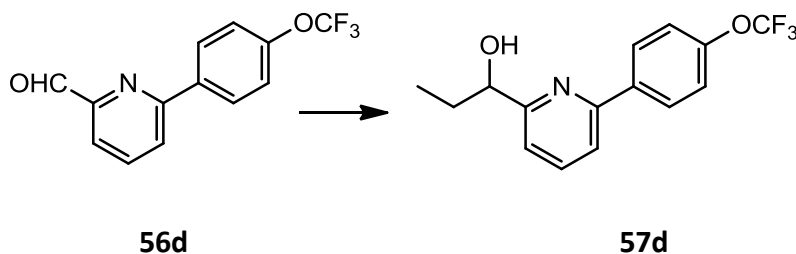
56a (1.59 g, 5.67 mmol) was treated following the **General procedure 2** to give **57a** as a pale yellow oil (734 mg, 42%). ^1H NMR (400 MHz, CDCl_3) δ 7.27 (d, $J = 8.0$ Hz, 2H), 7.18 (s, $J = 8.8$ Hz, 2H), 7.17 – 7.09 (m, 4H), 4.57 (t, $J = 6.6$ Hz, 1H), 3.96 (s, 2H), 1.85 – 1.66 (m, 2H), 0.91 (t, $J = 7.4$ Hz, 3H); ^{13}C NMR (100 MHz, CDCl_3) δ 142.71, 139.84, 139.69, 130.11, 128.93, 126.28, 121.03, 75.79, 40.88, 31.86, 10.19. ESI-HRMS: m/z calculated for $\text{C}_{17}\text{H}_{17}\text{O}_2\text{F}_3\text{Na}$ ($[\text{M}+\text{Na}]^+$) 333.1078, found 333.1066.

Preparation of **1-(6-(4-(trifluoromethoxy)phenyl)pyridin-3-yl)propan-1-ol, 57b**

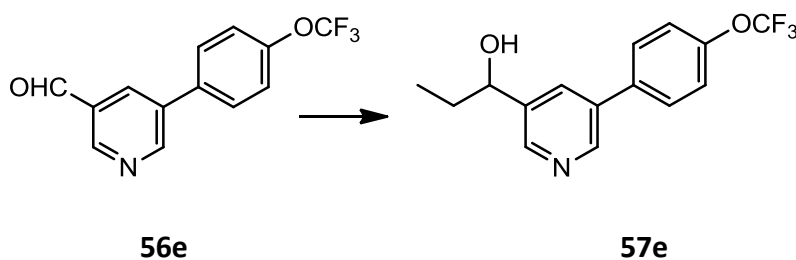
56b (1.28 g, 4.8 mmol) was treated following the **General procedure 2** to give **57b** as a white solid (954 mg, 67%). ^1H NMR (400 MHz, CDCl_3) δ 8.64 (d, $J = 2.1$ Hz, 1H), 8.02 (d, $J = 9.0$ Hz, 2H), 7.79 (ddd, $J = 8.2, 2.3, 0.5$ Hz, 1H), 7.71 (dd, $J = 8.2, 0.6$ Hz, 1H), 7.32 (dd, $J = 8.9, 0.9$ Hz, 2H), 4.73 (td, $J = 6.8, 3.0$ Hz, 1H), 1.93 – 1.75 (m, 2H), 0.97 (t, $J = 7.4$ Hz, 3H); ^{13}C NMR (101 MHz, CDCl_3) δ 155.76, 148.37, 138.17, 134.97, 128.72, 121.49, 120.62, 73.89, 32.35, 10.32. ESI-HRMS: m/z calculated for $\text{C}_{15}\text{H}_{15}\text{NO}_2\text{F}_3$ ($[\text{M}+\text{H}]^+$) 298.1055, found 298.1060.

Preparation of 1-(5-(4-(trifluoromethoxy)phenyl)pyridin-2-yl)propan-1-ol, **57c**

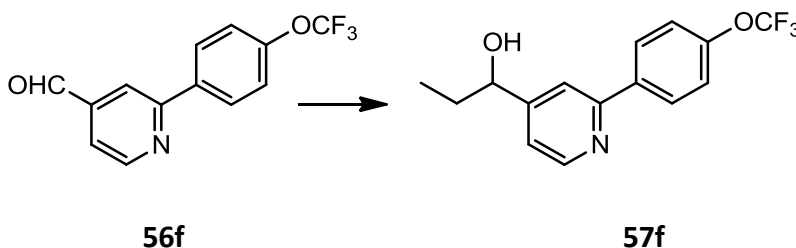
56c (1.20 g, 4.49 mmol) was treated following the **General procedure 2** to give **57c** as a yellow oil (503 mg, 38%). ^1H NMR (400 MHz, CDCl_3) δ 8.75 (d, $J = 1.8$ Hz, 1H), 7.86 (dd, $J = 8.1, 2.3$ Hz, 1H), 7.60 (d, $J = 8.8$ Hz, 2H), 7.39 – 7.29 (m, 3H), 4.76 (s, 1H), 4.03 (d, $J = 4.6$ Hz, 1H), 1.94 (dq, $J = 14.8, 7.4, 4.6$ Hz, 1H), 1.83 – 1.70 (m, 1H), 0.99 (t, $J = 7.4$ Hz, 3H). ^{13}C NMR (101 MHz, CDCl_3) δ 161.70, 146.92, 136.74, 135.51, 134.47, 128.93, 121.99, 120.78, 74.14, 31.76, 9.84. ESI-HRMS: m/z calculated for $\text{C}_{15}\text{H}_{15}\text{NO}_2\text{F}_3$ ($[\text{M}+\text{H}]^+$) 298.1055, found 298.1053.

Preparation of 1-(6-(4-(trifluoromethoxy)phenyl)pyridin-2-yl)propan-1-ol, **57d**

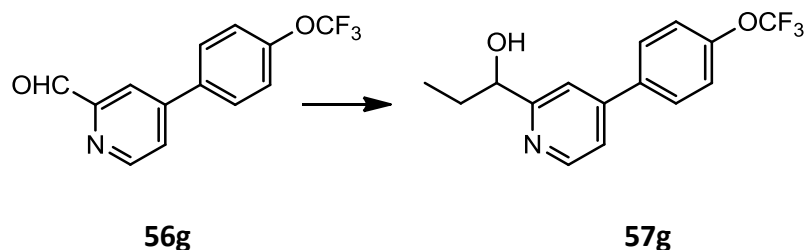
56d (1.0 g, 3.74 mmol) was treated following the **General procedure 2** to give **57d** as a yellow oil (816 mg, 73%). ^1H NMR (400 MHz, CDCl_3) δ 8.05 (d, $J = 8.8$ Hz, 2H), 7.78 (t, $J = 7.8$ Hz, 1H), 7.63 (d, $J = 7.8$ Hz, 1H), 7.33 (d, $J = 8.0$ Hz, 2H), 7.21 (d, $J = 7.7$ Hz, 1H), 4.76 (dd, $J = 11.7, 5.0$ Hz, 1H), 4.46 (d, $J = 5.5$ Hz, 1H), 1.95 (dq, $J = 14.8, 7.4, 4.6$ Hz, 1H), 1.82 – 1.69 (m, 1H), 0.98 (t, $J = 7.4$ Hz, 3H). ^{13}C NMR (101 MHz, CDCl_3) δ 162.21, 154.70, 150.36, 138.03, 137.85, 128.77, 121.49, 119.58, 119.24, 73.89, 31.80, 9.77. ESI-HRMS: m/z calculated for $\text{C}_{15}\text{H}_{14}\text{NO}_2\text{F}_3\text{Na}$ ($[\text{M}+\text{Na}]^+$) 320.0874, found 320.0877.

Preparation of 1-(5-(4-(trifluoromethoxy)phenyl)pyridin-3-yl)propan-1-ol, **57e**

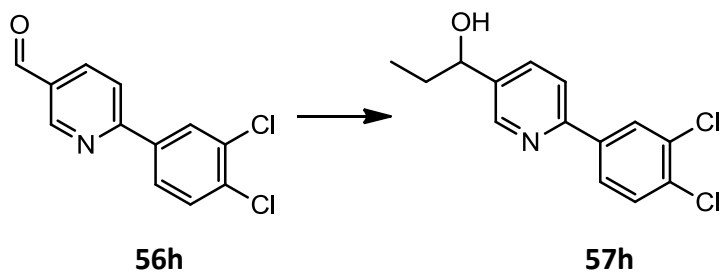
56e (4.0 g, 15.0 mmol) was treated following the **General procedure 2** to give **57e** as a yellow oil (3.11 g, 77%). ¹H NMR (400 MHz, CDCl₃) δ 8.73 (s, 1H), 8.57 (s, 1H), 7.88 (s, 1H), 7.62 (d, *J* = 8.8 Hz, 2H), 7.34 (d, *J* = 8.5 Hz, 2H), 4.77 (t, *J* = 6.2 Hz, 1H), 2.11 (s, 1H), 1.96 – 1.76 (m, 2H), 0.98 (t, *J* = 7.4 Hz, 3H). ¹³C NMR (101 MHz, CDCl₃) δ 149.68, 147.70, 147.47, 140.20, 136.90, 135.62, 132.34, 129.05, 121.97, 73.92, 32.52, 10.35. ESI HRMS: *m/z* calculated for C₁₅H₁₅NO₂F₃ ([M+H]⁺) 298.1055, found 298.1051.

Preparation of 1-(2-(4-(trifluoromethoxy)phenyl)pyridin-4-yl)propan-1-ol, **57f**

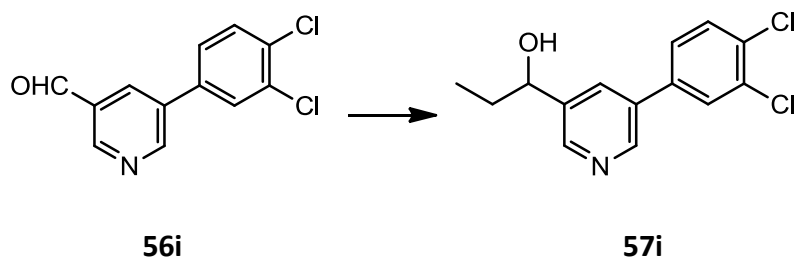
56f (3.62 g, 13.5 mmol) was treated following the **General procedure 2** to give **57f** as a yellow oil (2.17 g, 54%). ¹H NMR (400 MHz, CDCl₃) δ 8.57 (dd, *J* = 5.1, 0.7 Hz, 1H), 7.97 (d, *J* = 8.9 Hz, 2H), 7.68 – 7.62 (m, 1H), 7.28 (dd, *J* = 8.9, 0.9 Hz, 2H), 7.17 (ddd, *J* = 5.1, 1.5, 0.5 Hz, 1H), 4.65 (t, *J* = 6.3 Hz, 1H), 2.83 (s, 1H), 1.85 – 1.70 (m, 2H), 0.95 (t, *J* = 7.4 Hz, 3H). ¹³C NMR (101 MHz, CDCl₃) δ 156.59, 155.08, 150.29, 149.99, 138.33, 128.86, 121.39, 120.22, 118.14, 74.72, 32.18, 10.11. ESI HRMS: *m/z* calculated for C₁₅H₁₅NO₂F₃ ([M+H]⁺) 298.1055, found 298.1056.

Preparation of **1-(4-(4-(trifluoromethoxy)phenyl)pyridin-2-yl)propan-1-ol, 57g**

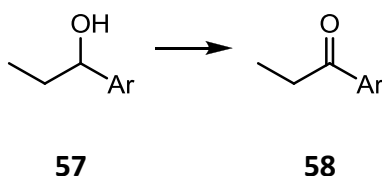
56g (640 mg, 2.39 mmol) was treated following the **General procedure 2** to give **57g** as a yellow oil (221 mg, 31%). ^1H NMR (400 MHz, CDCl_3) δ 8.61 (d, J = 5.2 Hz, 1H), 7.66 (d, J = 8.8 Hz, 2H), 7.44 (s, 1H), 7.39 (dd, J = 5.2, 1.6 Hz, 1H), 7.34 (d, J = 8.1 Hz, 2H), 4.84 – 4.70 (m, 1H), 4.01 (s, 1H), 1.94 (dq, J = 14.8, 7.5, 4.8 Hz, 1H), 1.85 – 1.71 (m, 1H), 0.99 (t, J = 7.4 Hz, 3H). ^{13}C NMR (101 MHz, CDCl_3) δ 163.35, 149.21, 148.15, 137.31, 129.03, 121.88, 120.73, 118.61, 117.74, 74.47, 31.84, 9.86. ESI HRMS: m/z calculated for $\text{C}_{15}\text{H}_{15}\text{NO}_2\text{F}_3$ ($[\text{M}+\text{H}]^+$) 298.1055, found 298.1064.

Preparation of **1-(6-(3,4-dichlorophenyl)pyridin-3-yl)propan-1-ol, 57h**

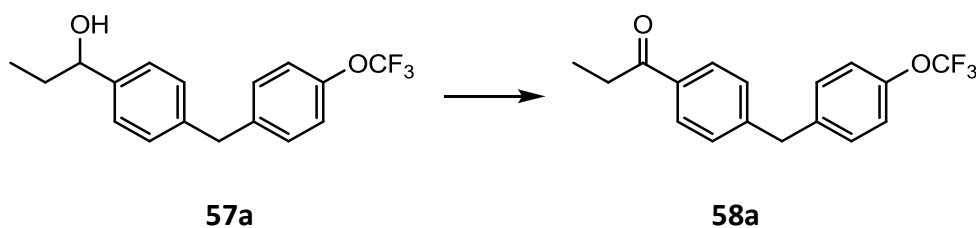
56h (1.0 g, 3.97 mmol) was treated following the **General procedure 2** to give **57h** as a colourless oil (934 mg, 83%). ^1H NMR (400 MHz, CDCl_3) δ 8.63 (d, J = 2.2 Hz, 1H), 8.13 (d, J = 2.1 Hz, 1H), 7.83 (dd, J = 8.4, 2.1 Hz, 1H), 7.79 (ddd, J = 8.2, 2.3, 0.4 Hz, 1H), 7.69 (dd, J = 8.2, 0.6 Hz, 1H), 7.53 (d, J = 8.4 Hz, 1H), 4.73 (td, J = 6.6, 3.6 Hz, 1H), 1.96 (d, J = 3.6 Hz, 1H), 1.85 (qd, J = 13.7, 7.4 Hz, 2H), 0.97 (t, J = 7.4 Hz, 3H). ^{13}C NMR (101 MHz, CDCl_3) δ 154.60, 148.43, 139.46, 139.32, 135.02, 133.48, 131.08, 129.15, 126.28, 120.49, 117.73, 73.82, 32.36, 10.25. ESI-HRMS: m/z calculated for $\text{C}_{14}\text{H}_{14}\text{NO}^{35}\text{Cl}_2$ ($[\text{M}+\text{H}]^+$) 282.0452, found 282.0445.

Preparation of 1-(5-(3,4-dichlorophenyl)phenyl)pyridin-3-yl)propan-1-ol, **57i**

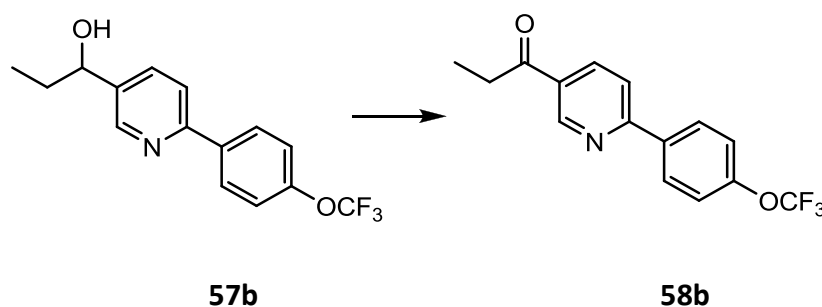
56i (673 mg, 2.67 mmol) was treated following the **General procedure 2** to give **57i** as a yellow oil (490 mg, 65%). ^1H NMR (400 MHz, CDCl_3) δ 8.71 (d, $J = 2.2$ Hz, 1H), 8.58 (d, $J = 2.0$ Hz, 1H), 7.86 (t, $J = 1.9$ Hz, 1H), 7.68 (d, $J = 2.1$ Hz, 1H), 7.56 (d, $J = 8.3$ Hz, 1H), 7.43 (dd, $J = 8.3, 2.2$ Hz, 1H), 4.77 (td, $J = 6.7, 2.7$ Hz, 1H), 2.02 (d, $J = 3.1$ Hz, 1H), 1.93 – 1.78 (m, 2H), 0.99 (t, $J = 7.4$ Hz, 3H). ^{13}C NMR (101 MHz, CDCl_3) δ 147.48, 147.11, 134.24, 133.35, 131.76, 131.07, 129.03, 127.69, 126.39, 73.45, 32.16, 9.89. ESI-HRMS: m/z calculated for $\text{C}_{14}\text{H}_{14}\text{NO}^{35}\text{Cl}_2$ ($[\text{M}+\text{H}]^+$) 282.0452, found 282.0447.

General procedure 3.

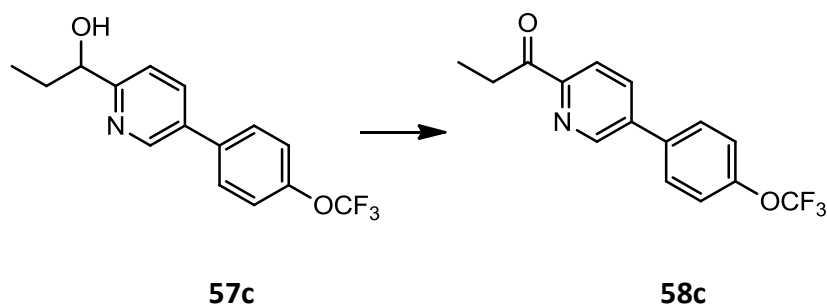
To a stirred solution of alcohol **57** (1.0 eq) in DCM (30 mL), PCC (1.5 eq) was added and the mixture was allowed to stir under N_2 atmosphere for 2 hours at ambient temperature. The reaction was then quenched and diluted by adding ether (60 mL). The solution was passed through a silica pad to get rid of any precipitate. The filtrate was concentrated under vacuum to yield the crude product as clear yellow oil which was further purified by column chromatography (eluting with 10% EtOAc/*n*-Hexane) to give the product.

Preparation of 1-(4-(4-(trifluoromethoxy)benzyl)phenyl)propan-1-one, **58a**

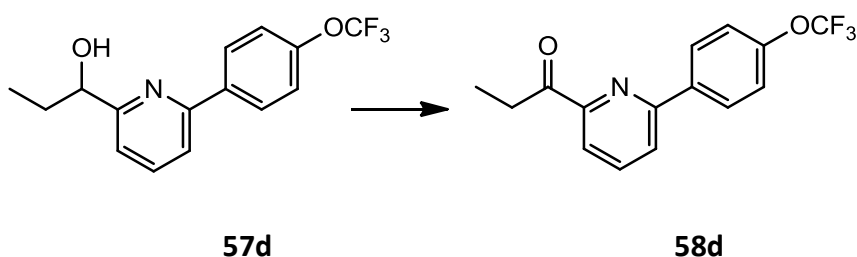
57a (734 mg, 2.36 mmol) was oxidised according to the **General procedure 3** to give **58a** as a white solid (649 mg, 89%). ^1H NMR (400 MHz, CDCl_3) δ 7.91 (d, $J = 8.3$ Hz, 2H), 7.26 (d, $J = 8.4$ Hz, 3H), 7.19 (d, $J = 8.8$ Hz, 2H), 7.14 (d, $J = 8.2$ Hz, 2H), 2.98 (q, $J = 7.2$ Hz, 2H), 1.22 (t, $J = 7.3$ Hz, 3H); ^{13}C NMR (100 MHz, CDCl_3) δ 200.81, 148.20, 146.13, 139.25, 135.64, 130.58, 129.48, 128.83, 121.58, 41.53, 32.15, 8.67. ESI-HRMS: m/z calculated for $\text{C}_{17}\text{H}_{15}\text{O}_2\text{F}_3\text{Na}$ ($[\text{M}+\text{Na}]^+$) 331.0922, found 331.0928.

Preparation of 1-(6-(4-(trifluoromethoxy)phenyl)pyridin-3-yl)propan-1-one, **58b**

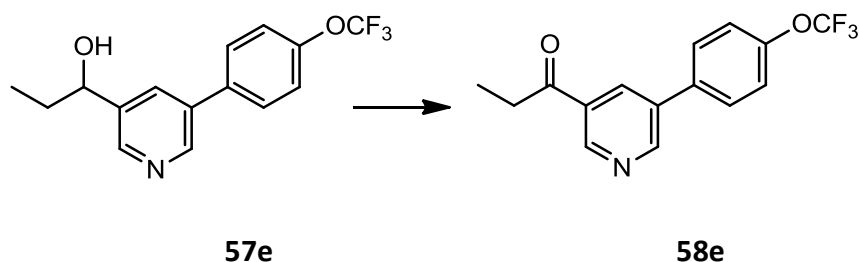
57b (954 mg, 3.21 mmol) was oxidised according to the **General procedure 3** to give **58b** as a pale yellow solid (654 mg, 69%). ^1H NMR (400 MHz, CDCl_3) δ 9.24 (d, $J = 1.4$ Hz, 1H), 8.32 (dd, $J = 8.3, 2.0$ Hz, 1H), 8.11 (d, $J = 8.8$ Hz, 2H), 7.82 (d, $J = 8.3$ Hz, 1H), 7.35 (d, $J = 8.1$ Hz, 2H), 3.06 (q, $J = 7.2$ Hz, 2H), 1.28 (t, $J = 7.2$ Hz, 3H); ^{13}C NMR (100 MHz, CDCl_3) δ 199.55, 159.62, 151.00, 150.16, 137.14, 136.81, 130.97, 129.30, 122.12, 121.54, 120.47, 32.60, 8.35. ESI-HRMS: m/z calculated for $\text{C}_{15}\text{H}_{13}\text{NO}_2\text{F}_3$ ($[\text{M}+\text{H}]^+$) 296.0898, found 296.0899.

Preparation of 1-(5-(4-(trifluoromethoxy)phenyl)pyridin-2-yl)propan-1-one, **58c**

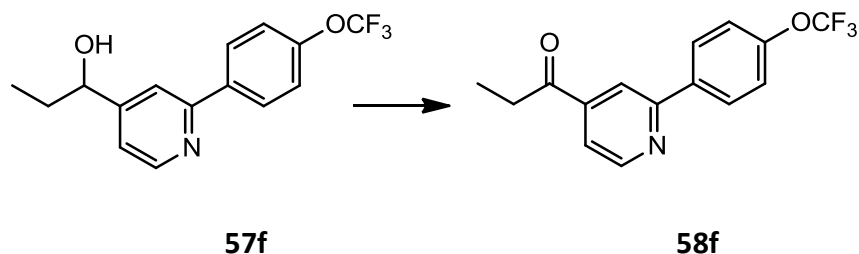
57c (474 mg, 1.59 mmol) was oxidised according to the **General procedure 3** to give **58c** as a pale yellow solid (457 mg, 97 %). ^1H NMR (400 MHz, CDCl_3) δ 8.88 (dd, $J = 2.3, 0.6$ Hz, 1H), 8.14 (dd, $J = 8.1, 0.7$ Hz, 1H), 7.99 (dd, $J = 8.1, 2.3$ Hz, 1H), 7.66 (d, $J = 8.8$ Hz, 2H), 7.37 (d, $J = 8.8$ Hz, 2H), 3.28 (q, $J = 7.3$ Hz, 2H), 1.25 (t, $J = 7.3$ Hz, 3H). ^{13}C NMR (101 MHz, CDCl_3) δ 202.55, 152.77, 150.16, 147.67, 138.79, 136.06, 135.47, 129.21, 122.32, 122.09, 31.62, 8.40. ESI-HRMS: m/z calculated for $\text{C}_{15}\text{H}_{12}\text{NO}_2\text{F}_3\text{Na}$ ($[\text{M}+\text{Na}]^+$) 318.0718, found 318.0718.

Preparation of 1-(5-(4-(trifluoromethoxy)phenyl)pyridin-2-yl)propan-1-one, **58d**

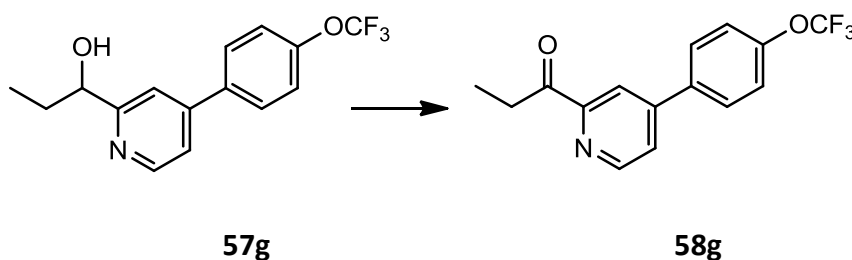
57d (815 mg, 2.74 mmol) was oxidised according to the **General procedure 3** to give **58d** as a pale yellow solid (767 mg, 95 %). ^1H NMR (400 MHz, CDCl_3) δ 8.14 (d, $J = 8.9$ Hz, 2H), 8.00 (dd, $J = 6.1, 2.7$ Hz, 1H), 7.94 – 7.89 (m, 2H), 7.36 (dd, $J = 8.9, 0.9$ Hz, 2H), 3.37 (q, $J = 7.3$ Hz, 2H), 1.26 (t, $J = 7.3$ Hz, 3H). ^{13}C NMR (101 MHz, CDCl_3) δ 200.56, 153.68, 138.29, 128.81, 123.67, 121.58, 120.60, 31.56, 8.40. ESI-HRMS: m/z calculated for $\text{C}_{15}\text{H}_{12}\text{NO}_2\text{F}_3\text{Na}$ ($[\text{M}+\text{Na}]^+$) 318.0718, found 318.0722.

Preparation of 1-(5-(4-(trifluoromethoxy)phenyl)pyridin-3-yl)propan-1-one, **58e**

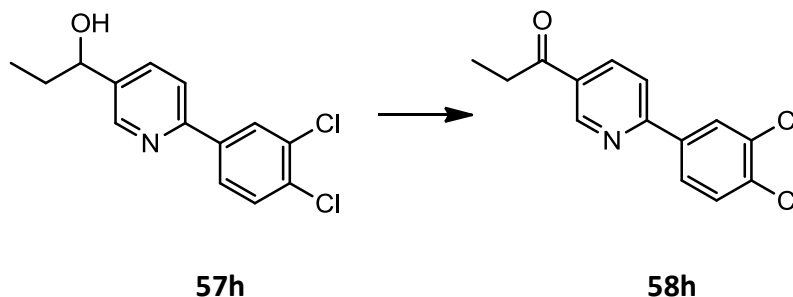
57e (963 mg, 3.24 mmol) was oxidised according to the **General procedure 3** to give **58e** as a pale yellow solid (725 mg, 76 %). ^1H NMR (400 MHz, CDCl_3) δ 9.17 (d, $J = 2.0$ Hz, 1H), 8.98 (d, $J = 2.3$ Hz, 1H), 8.41 (t, $J = 2.2$ Hz, 1H), 7.65 (d, $J = 8.8$ Hz, 2H), 7.37 (d, $J = 8.0$ Hz, 2H), 3.10 (q, $J = 7.2$ Hz, 2H), 1.29 (t, $J = 7.2$ Hz, 3H). ^{13}C NMR (101 MHz, CDCl_3) δ 199.73, 152.00, 150.05, 148.85, 135.97, 135.91, 133.88, 132.48, 129.14, 122.11, 32.84, 8.32. ESI HRMS: m/z calculated for $\text{C}_{15}\text{H}_{13}\text{NO}_2\text{F}_3$ ($[\text{M}+\text{H}]^+$) 296.0898, found 296.0899.

Preparation of 1-(2-(4-(trifluoromethoxy)phenyl)pyridin-4-yl)propan-1-one, **58f**

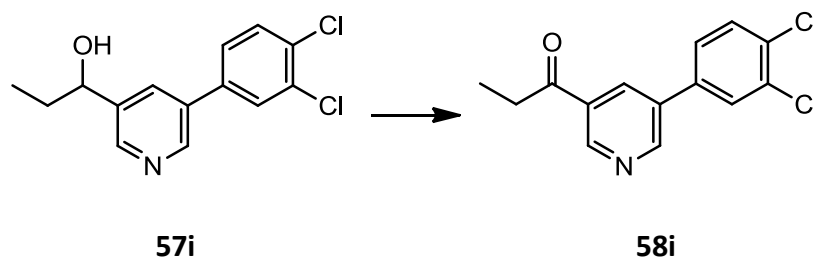
57f (2.0 g, 6.73 mmol) was oxidised according to the **General procedure 3** to give **58f** as a pale yellow solid (1.21 g, 61 %). ^1H NMR (400 MHz, CDCl_3) δ 8.86 (dd, $J = 5.0, 0.8$ Hz, 1H), 8.18 – 8.15 (m, 1H), 8.09 (d, $J = 8.9$ Hz, 2H), 7.68 (dd, $J = 5.0, 1.5$ Hz, 1H), 7.35 (d, $J = 8.0$ Hz, 2H), 3.07 (q, $J = 7.2$ Hz, 2H), 1.27 (t, $J = 7.2$ Hz, 3H). ^{13}C NMR (101 MHz, CDCl_3) δ 200.43, 157.77, 151.29, 144.23, 137.65, 128.95, 121.56, 120.23, 118.07, 32.75, 8.21. ESI HRMS: m/z calculated for $\text{C}_{15}\text{H}_{13}\text{NO}_2\text{F}_3$ ($[\text{M}+\text{H}]^+$) 296.0898, found 296.0895.

Preparation of 1-(4-(4-(trifluoromethoxy)phenyl)pyridin-2-yl)propan-1-one, **58g**

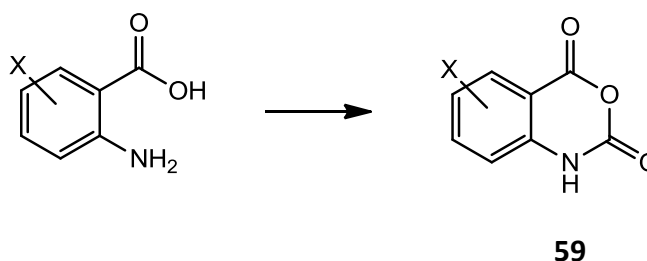
57g (280 mg, 0.94 mmol) was oxidised according to the **General procedure 3** to give **58g** as a pale yellow solid (184 mg, 66 %). ^1H NMR (400 MHz, CDCl_3) δ 8.73 (dd, $J = 5.1, 0.7$ Hz, 1H), 8.25 (dd, $J = 1.9, 0.7$ Hz, 1H), 7.72 (d, $J = 8.9$ Hz, 2H), 7.65 (dd, $J = 5.1, 1.9$ Hz, 1H), 7.36 (dd, $J = 8.8, 0.9$ Hz, 2H), 3.29 (q, $J = 7.3$ Hz, 2H), 1.25 (t, $J = 7.3$ Hz, 3H). ^{13}C NMR (101 MHz, CDCl_3) δ 202.94, 169.50, 154.52, 150.01, 148.37, 136.57, 129.02, 124.89, 121.95, 119.87, 117.73, 31.69, 8.39. ESI HRMS: m/z calculated for $\text{C}_{15}\text{H}_{12}\text{NO}_2\text{F}_3\text{Na}$ ($[\text{M}+\text{Na}]^+$) 318.0718, found 318.0724.

Preparation of 1-(6-(3,4-dichlorophenyl)pyridin-2-yl)propan-1-one, **58h**

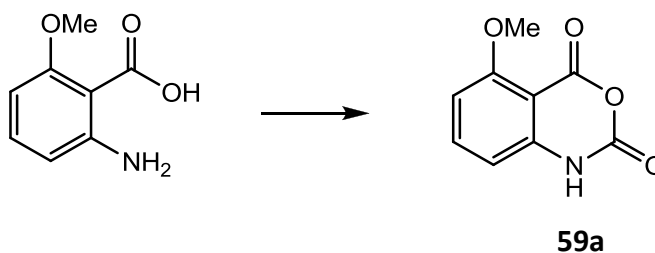
57h (512 mg, 2.13 mmol) was oxidised according to the **General procedure 3** to give **58h** as a pale yellow solid (354 mg, 69 %). ^1H NMR (400 MHz, CDCl_3) δ 9.23 (dd, $J = 2.2, 0.8$ Hz, 1H), 8.31 (dd, $J = 8.3, 2.3$ Hz, 1H), 8.21 (d, $J = 2.1$ Hz, 1H), 7.90 (dd, $J = 8.4, 2.1$ Hz, 1H), 7.81 (dd, $J = 8.3, 0.8$ Hz, 1H), 7.57 (d, $J = 8.4$ Hz, 1H), 3.06 (q, $J = 7.2$ Hz, 2H), 1.28 (t, $J = 7.2$ Hz, 3H). ^{13}C NMR (101 MHz, CDCl_3) δ 199.01, 169.12, 158.13, 149.78, 138.08, 136.50, 133.39, 130.93, 130.89, 129.25, 126.31, 120.00, 32.25, 7.95. ESI-HRMS: m/z calculated for $\text{C}_{14}\text{H}_{12}\text{NO}^{35}\text{Cl}_2$ ($[\text{M}+\text{H}]^+$) 280.0296, found 280.0290.

Preparation of 1-(5-(3,4-dichlorophenyl)pyridin-2-yl)propan-1-one, **58i**

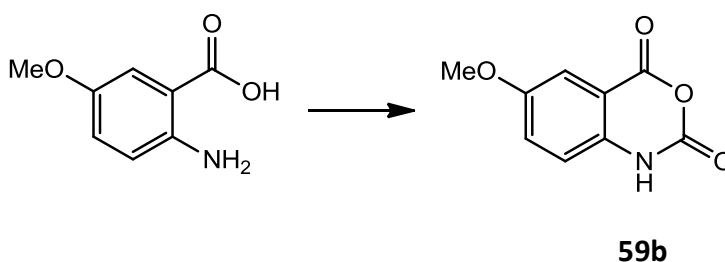
57i (490 mg, 1.73 mmol) was treated following the **General procedure 3** to give **58i** as a brown solid (160 mg, 33%). ^1H NMR (400 MHz, CDCl_3) δ 9.17 (s, 1H), 8.97 (s, 1H), 8.38 (s, 1H), 7.71 (d, $J = 2.1$ Hz, 1H), 7.59 (d, $J = 8.3$ Hz, 1H), 7.46 (dd, $J = 8.3, 2.1$ Hz, 1H), 3.09 (q, $J = 7.2$ Hz, 2H), 1.29 (t, $J = 7.2$ Hz, 3H). ^{13}C NMR (101 MHz, CDCl_3) δ 199.17, 169.12, 151.41, 148.82, 136.82, 133.62, 133.36, 133.20, 131.27, 129.09, 126.42, 32.46, 7.92. ESI-HRMS: m/z calculated for $\text{C}_{14}\text{H}_{12}\text{NO}^{35}\text{Cl}_2$ ($[\text{M}+\text{H}]^+$) 280.0296, found 282.0294.

General procedure 4.

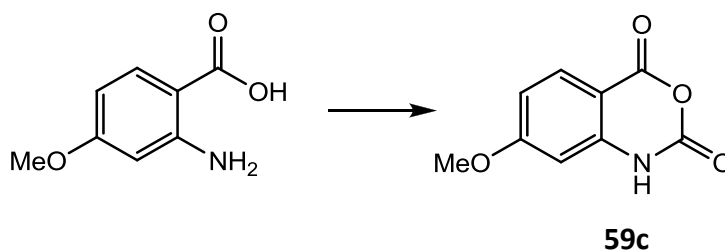
To a stirred solution of substituted anthranilic acid (1.0 eq) in THF (20 mL) and H_2O (20 mL), CCl_3COCl (1.5 eq) was added dropwisely at 0°C . After the addition, the reaction was then allowed to raise the temperature to room temperature and stirred for 2 hours. The reaction mixture was evaporated to remove THF. The precipitate was filtered, washed successively with water, collected and dried under vacuum to give the desire product **59**.

Preparation of **5-methoxy-1H-benzo[d][1,3]oxazine-2,4-dione, 59a**

2-Amino-6-methoxybenzoic acid (2.50 g, 15 mmol) was reacted as in the **General procedure 4** to give **59a** as pale brown crystal (1.78 g, 61%). $^1\text{H NMR}$ (400 MHz, CDCl_3) δ 8.01 (s, 1H), 7.59 (t, $J = 8.3$ Hz, 1H), 6.74 (d, $J = 8.5$ Hz, 1H), 6.56 (dd, $J = 8.1, 0.8$ Hz, 1H), 4.01 (s, 3H).

Preparation of **6-methoxy-1H-benzo[d][1,3]oxazine-2,4-dione, 59b**

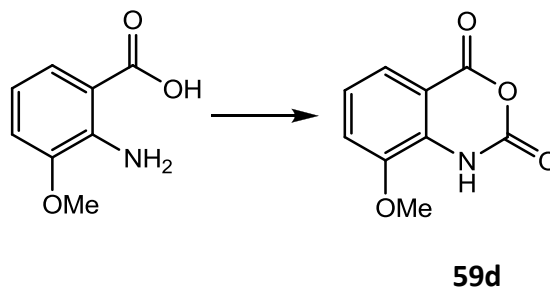
2-Amino-5-methoxybenzoic acid (2.50 g, 15 mmol) was treated as the **General procedure 4** to give **59b** as pale yellow solid (1.92 g, 66%). $^1\text{H NMR}$ (400 MHz, CDCl_3) δ 7.76 (s, 1H), 7.51 (d, $J = 2.9$ Hz, 1H), 7.29 (dd, $J = 8.9, 2.9$ Hz, 1H), 6.96 (d, $J = 8.8$ Hz, 1H), 3.87 (s, 3H).

Preparation of **7-methoxy-1H-benzo[d][1,3]oxazine-2,4-dione, 59c**

2-Amino-4-methoxybenzoic acid (2.50 g, 15 mmol) was reacted as in the **General procedure 4** to give **59c** as a pale brown solid (2.03 g, 70%). $^1\text{H NMR}$ (400 MHz, CDCl_3) δ 8.67 (s, 1H), 8.01 (d, $J = 8.9$ Hz, 1H), 6.82 (dd, $J = 8.9, 2.3$ Hz, 1H), 6.46

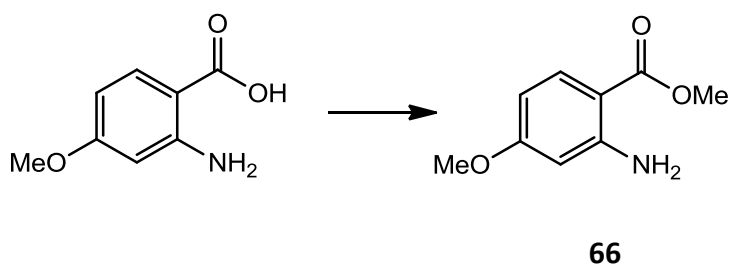
(d, $J = 2.3$ Hz, 1H), 3.92 (s, 3H). Elemental Analysis Calculated for $C_9H_7NO_4$: C, 55.96; H, 3.65; N, 7.25. Found: C, 53.36; H, 3.92; N, 6.88.

Preparation of **8-methoxy-1H-benzo[d][1,3]oxazine-2,4-dione, 59d**



2-Amino-3-methoxybenzoic acid (2.50 g, 15 mmol) was reacted as in the **General procedure 4** to give **59d** as an off-white solid (2.12 g, 73%). ^1H NMR (400 MHz, CDCl_3) δ 8.02 (s, 1H), 7.67 (ddd, $J = 7.2, 2.0, 0.6$ Hz, 1H), 7.24 – 7.15 (m, 2H), 3.98 (s, 3H).

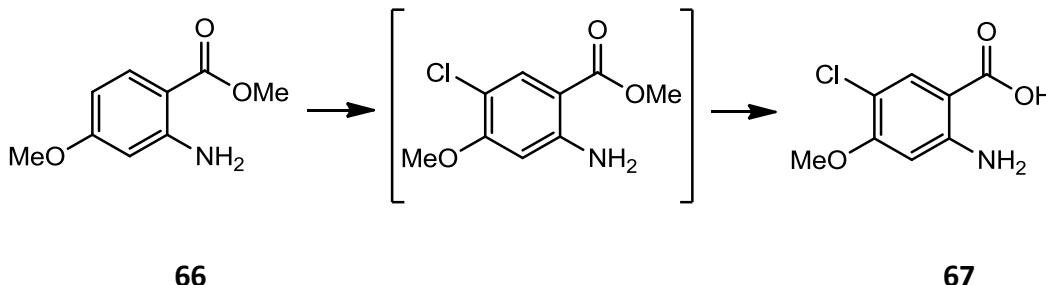
Preparation of **methyl 2-amino-4-methoxybenzoate, 66**³⁰



2-Amino-4-methoxybenzoic acid (3.34 g, 20 mmol, 1.0 eq) was dissolved in DMF (40 mL) then K_2CO_3 (8.3 g, 60 mmol, 3.0 eq) was added. Iodomethane was then added and the reaction's colour was changed to brown. Being stirred for 2 h, 5% citric acid solution (50 mL) was poured into and extracted with EtOAc. The aqueous layer was extracted several times with EtOAc. The combined organic layer was washed with water, bicarb, brine and dried over MgSO_4 . The crude was purified by column chromatography (20-30% EtOAc/Hexane) to give methyl 2-amino-4-methoxybenzoate as a white solid (2.96g, 81%); mp = 72 -75 °C; ^1H NMR (400 MHz, CDCl_3) δ 7.80 (d, $J = 8.9$ Hz, 1H), 6.26 (dd, $J = 9.0, 2.5$ Hz, 1H), 6.16 (d, $J = 2.5$ Hz, 1H), 3.84 (s, 3H), 3.80 (s, 3H). ^{13}C NMR (101 MHz, CDCl_3) δ 168.68, 164.67, 152.00,

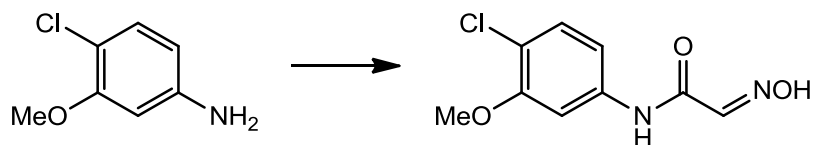
133.48, 105.41, 100.35, 55.63, 51.75, 31.34. Elemental Analysis Calculated for $C_9H_{11}NO_3$: C, 59.66; H, 6.12; N, 7.73. Found: C, 59.54; H, 6.18; N, 7.68.

Preparation of **2-amino-5-chloro-4-methoxybenzoic acid**¹²



Sulfuryl chloride (1.46 mL, 18 mmol, 1.2 eq) was added dropwise to a cooled solution of methyl 2-amino-4-methoxybenzoate, **66** (2.72 g, 15 mmol, 1.0 eq) in 30 mL of chloroform at 0 °C. The sulfur dioxide produced was passes through a water trap. After being stirred for 30 min, the reaction was refluxed for 2 h. The darken solution was evaporated. The crude methyl ester was saponified with 40 mL of 1 M NaOH solution for an hour. After cooling, acidification, the brown precipitate was extracted into EtOAc and purified on column chromatography (gradually increase polarity from 40% EtOAc/Hexane to 100% EtOAc then 5% MeOH/EtOAc) to give 2-amino-5-chloro-4-methoxybenzoic acid as a yellow solid (582 mg, 19%); mp = 209 - 210 °C; ¹H NMR (400 MHz, MeOD) δ 7.69 (s, 1H), 6.33 (s, 1H), 3.82 (s, 3H). ¹³C NMR (101 MHz, MeOD) δ 175.40, 165.68, 158.91, 138.46, 115.29, 109.79, 104.69, 61.41. Elemental Analysis Calculated for $C_8H_8ClNO_3$: C, 47.66; H, 4.00; N, 6.95. Found: C, 47.79; H, 4.03; N, 6.86.

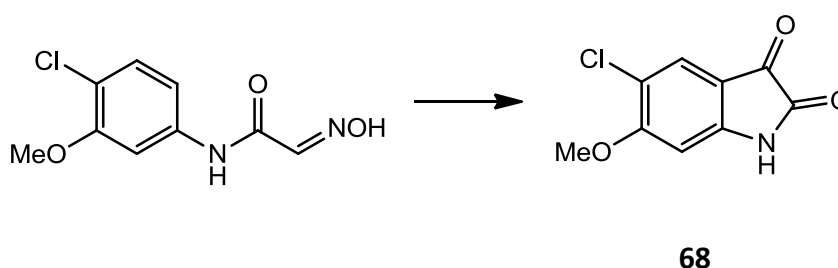
Preparation of **N-(4-chloro-3-methoxyphenyl)-2-(hydroxyimino)acetamide**



To a suspension of 4-chloro-3-methoxyaniline (4.73 g, 30 mmol) and conc. HCl (6 mL) in 23 mL of water was added a mixture of Na_2SO_4 (32 g) and chloral hydrate (5.11 g, 30.9 mmol) in 100 mL of water, followed by a solution of $NH_2OH.HCl$ (6.32 g, 90.9 mmol) in 25 mL of water. The suspension was then heated

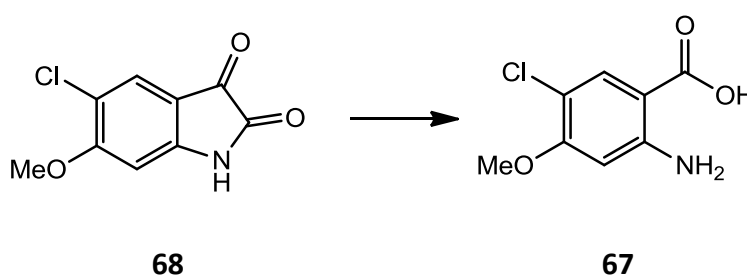
to 100 °C for 3 h. The reaction was allowed to cool overnight. The solid was filtered off, washed with water, and re-dissolved in 1% NaOH solution (700 mL). The alkaline solution was then acidified with 20 mL conc. HCl and diluted with water (100 mL). The solid was collected, washed with water and dried to obtain N-(4-chloro-3-methoxyphenyl)-2-(hydroxyimino)acetamide as a dark brown solid (6.45 g, 94%); ¹H NMR (400 MHz, CDCl₃) δ 7.58 (d, *J* = 2.2 Hz, 1H), 7.54 (s, 1H), 7.29 (d, *J* = 8.5 Hz, 1H), 6.95 (dd, *J* = 8.5, 2.3 Hz, 1H), 3.92 (s, 3H).

Preparation of 5-chloro-6-methoxyindoline-2,3-dione



Sulfuric acid (18 mL) was heated to 90 °C. N-(4-chloro-3-methoxyphenyl)-2-(hydroxyimino)acetamide (4.0 g, 17.5 mmol) was added slowly in 10 mins. The resulting brown solution was heated to 105 °C for a further 15 min. The reaction was cooled and poured in to 150 mL iced cold water. The solid was collected by filtration, washed with water and dried to give 5-chloro-6-methoxyindoline-2,3-dione as a dark brown solid (2.93 g, 79%); ¹H NMR (400 MHz, CDCl₃) δ 7.60 (s, 1H), 6.50 (s, 1H), 4.02 (s, 3H).

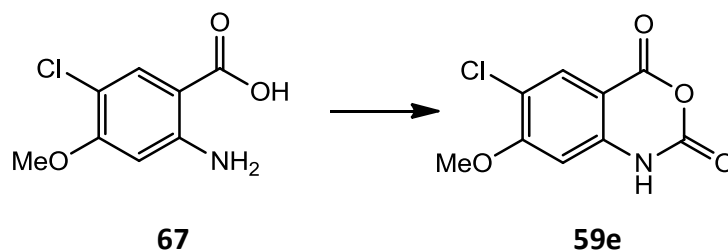
Preparation of 2-amino-5-chloro-4-methoxybenzoic acid



5-Chloro-6-methoxyindoline-2,3-dione (2.93 g, 13.8 mmol) was suspended in aq. NaOH (4 M, 25 mL). 3% H₂O₂ (25 mL) was added slowly while stirring. After cooling down in cold water for 45 min., the dark mixture was treated with 40 mL of

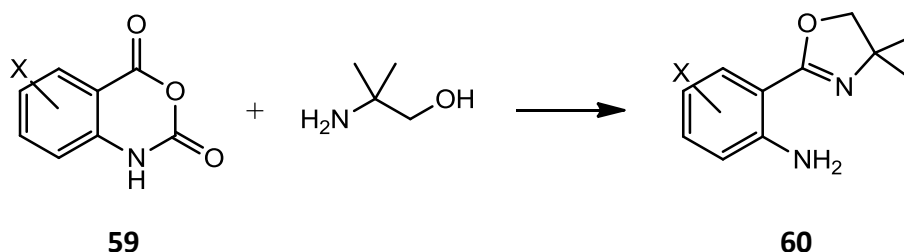
4 N sulfuric acid. The precipitate was collected, washed with water, then re-dissolved in 2% NaHCO₃ solution (150 mL). The brown insoluble material was removed by filtration, and the filtrate was acidified with 4 N sulfuric acid (10 mL). The product was collected, washed with water, and dried at 100 °C to give 2-amino-5-chloro-4-methoxybenzoic acid as a yellow solid (2.33 g, 83%).

Preparation of **6-chloro-7-methoxy-1H-benzo[d][1,3]oxazine-2,4-dione, 59e**



2-Amino-5-chloro-4-methoxybenzoic acid (2.22 g, 11 mmol) was reacted as in the **General procedure 4** to give **59e** as a yellow solid (1.17 g, 47%). ¹H NMR (400 MHz, MeOD) δ 7.91 (s, 1H), 6.66 (s, 1H), 3.96 (s, 3H). Elemental Analysis Calculated for C₉H₆ClNO₄: C, 47.49; H, 2.66; N, 6.15. Found: C, 47.47; H, 2.72; N, 6.09.

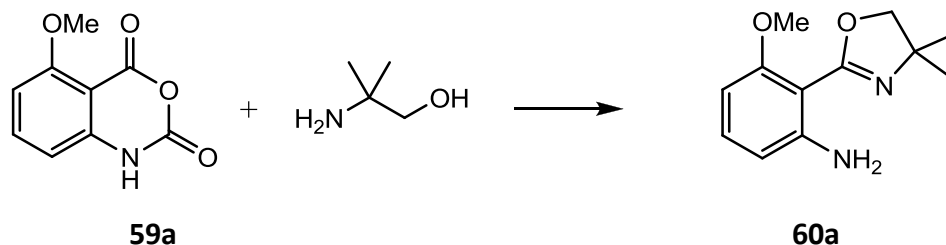
General procedure 5.



The isatoic anhydride **59** (1.0 eq) was dissolved in chlorobenzene under nitrogen and stirred for 5 minutes. 2-amino-2-methylpropan-1-ol (1.5 eq) was added to the mixture, followed by addition of anhydrous zinc chloride (20 mol%). The resulting mixture was slowly heated to remove gas and then to reflux at 130 °C for 24 hours. The mixture was allowed to cool to room temperature and the solvent was removed under vacuum. EtOAc (30 mL) was added to the residue and washed with brine. The aqueous layer was then extracted with EtOAc thrice. The combined organic layer was dried over MgSO₄, and the solvent was evaporated to yield dark

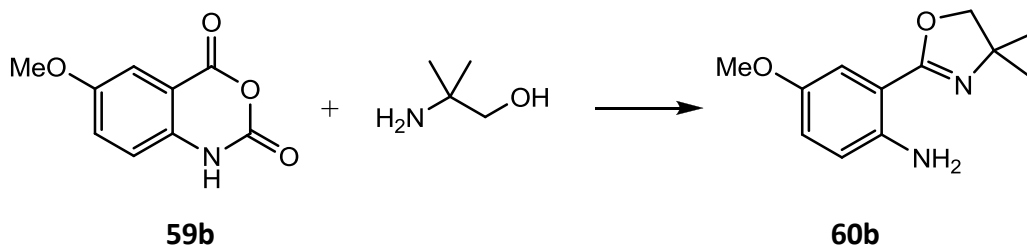
brown oil which was further purified by column chromatography (eluting with 20% EtOAc/*n*-Hexane)

Preparation of **2-(4,4-dimethyl-4,5-dihydrooxazol-2-yl)-3-methoxyaniline, 60a**

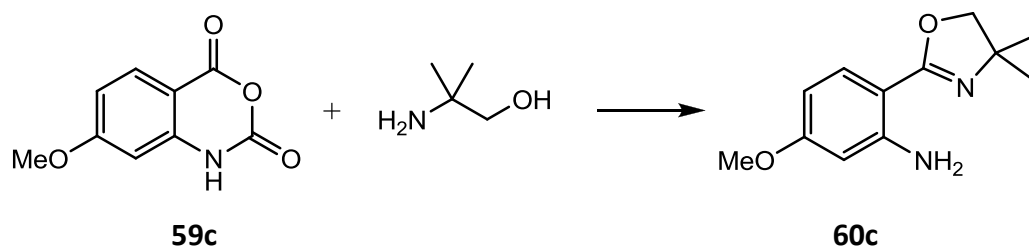


59a (1.28 g, 4.8 mmol) was treated following the **General procedure 5** but eluted the column with 50% EtOAc in *n*-Hexane to give **60a** as a yellow oil (1.66 g, 98%). ¹H NMR (400 MHz, CDCl₃) δ 7.76 (s, 2H), 7.08 (t, *J* = 8.2 Hz, 1H), 6.32 (dd, *J* = 8.2, 1.0 Hz, 1H), 6.21 (dd, *J* = 8.2, 0.7 Hz, 1H), 3.86 (s, 3H), 3.66 (s, 2H), 1.37 (s, 6H); ¹³C NMR (100 MHz, CDCl₃) δ 169.22, 159.02, 151.61, 132.21, 111.46, 105.74, 99.72, 71.39, 56.58, 56.42, 25.38.

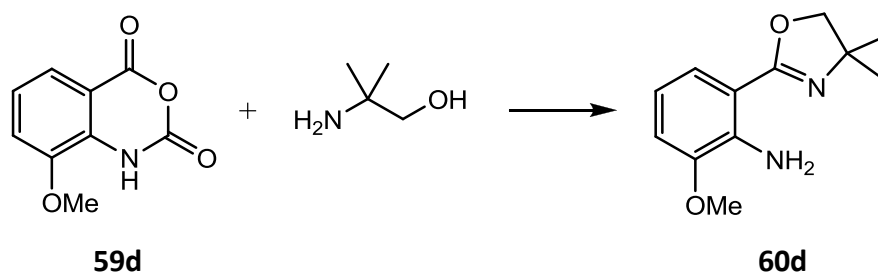
Preparation of **2-(4,4-dimethyl-4,5-dihydrooxazol-2-yl)-4-methoxyaniline, 60b**



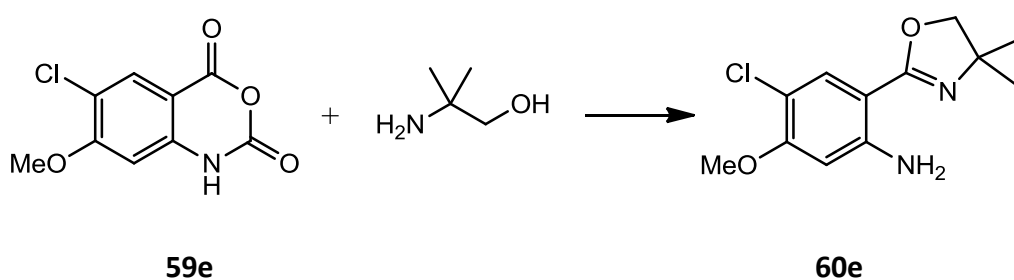
59b (1.93 g, 9.9 mmol) was treated following the **General procedure 5** to afford **60b** as pale-yellow solid (1.06 g, 48.4%). ¹H NMR (400 MHz, CDCl₃) δ 7.21 (d, *J* = 3.0 Hz, 1H), 6.86 (dd, *J* = 8.8, 3.0 Hz, 1H), 6.66 (d, *J* = 8.8 Hz, 1H), 5.76 (s, 2H), 4.00 (s, 2H), 3.76 (s, 3H), 1.37 (s, 6H); ¹³C NMR (100 MHz, CDCl₃) δ 162.22, 150.98, 143.41, 120.80, 117.60, 112.71, 109.86, 68.37, 56.32, 29.13. Elemental Analysis Calculated for C₁₂H₁₆N₂O₂: C, 65.43; H, 7.32; N, 12.72. Found: C, 65.45; H, 7.46; N, 12.65.

Preparation of **2-(4,4-dimethyl-4,5-dihydrooxazol-2-yl)-5-methoxyaniline, 60c**

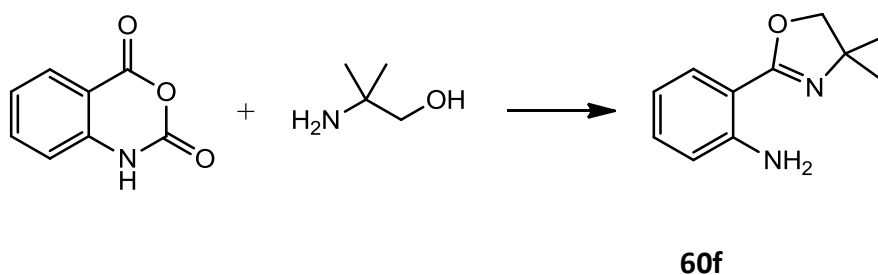
59c (2.0 g, 10.3 mmol) was treated as in the **General procedure 5** to give **60c** as a white solid (454 mg, 19.9%). ^1H NMR (400 MHz, CDCl_3) δ 7.59 (d, $J = 8.8$ Hz, 1H), 6.25 (dd, $J = 8.8, 2.5$ Hz, 1H), 6.18 (d, $J = 2.4$ Hz, 1H), 6.14 (s, 2H), 3.96 (s, 2H), 3.78 (s, 3H), 1.35 (s, 6H); ^{13}C NMR (100 MHz, CDCl_3) δ 162.94, 162.29, 150.57, 131.39, 103.87, 103.49, 99.63, 68.02, 55.54, 29.19. ESI-HRMS: m/z calculated for $\text{C}_{12}\text{H}_{17}\text{N}_2\text{O}_2$ ($[\text{M}+\text{H}]^+$) 221.1285, found 221.1285.

Preparation of **2-(4,4-dimethyl-4,5-dihydrooxazol-2-yl)-6-methoxyaniline, 60d**

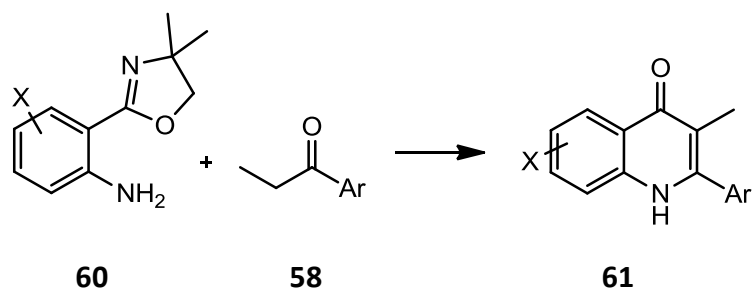
59d (2.13 g, 11.0 mmol) was treated as in the **General procedure 5** to give **60d** as a yellow solid (740 mg, 30.5%). ^1H NMR (400 MHz, CDCl_3) δ 7.30 (dd, $J = 8.1, 1.3$ Hz, 1H), 6.81 (dd, $J = 7.9, 1.2$ Hz, 1H), 6.59 (t, $J = 8.0$ Hz, 1H), 6.31 (s, 2H), 3.99 (s, 2H), 3.87 (s, 3H), 1.37 (s, 6H); ^{13}C NMR (100 MHz, CDCl_3) δ 162.56, 147.16, 139.84, 121.44, 114.99, 111.91, 109.15, 68.21, 56.15, 29.17. Elemental Analysis Calculated for $\text{C}_{12}\text{H}_{16}\text{N}_2\text{O}_2$: C, 65.43; H, 7.32; N, 12.72. Found: C, 65.46; H, 7.42; N, 12.63.

Preparation of **4-chloro-2-(4,4-dimethyl-4,5-dihydrooxazol-2-yl)-5-methoxyaniline, 60e****60e**

59e (1.02 g, 4.5 mmol) was treated as in the **General procedure 5** to give **60e** as a yellow solid (221 mg, 19%). ^1H NMR (400 MHz, CDCl_3) δ 7.67 (s, 1H), 6.28 (s, 2H), 6.20 (s, 1H), 3.99 (s, 2H), 3.87 (s, 3H), 1.36 (s, 6H); Elemental Analysis calculated for $\text{C}_{12}\text{H}_{15}\text{ClN}_2\text{O}_2$: C, 56.58; H, 5.94; N, 11.00. Found: C, 56.29; H, 6.10; N, 10.56.

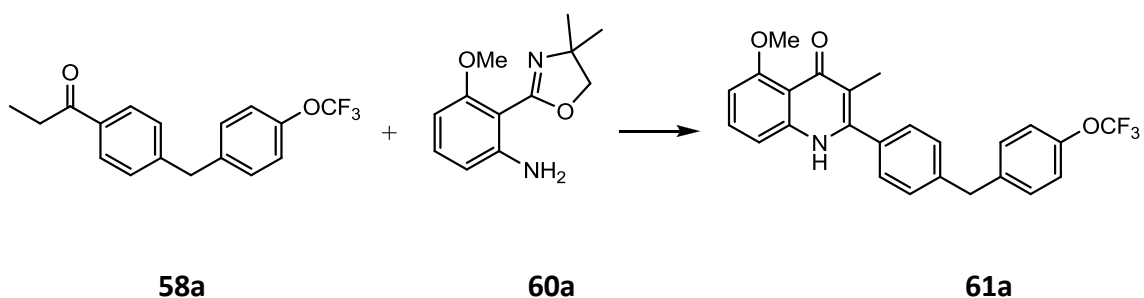
Preparation of **2-(4,4-dimethyl-4,5-dihydrooxazol-2-yl)aniline, 60f**

Isatoic anhydride (10 g, 61 mmol) which is commercially available was treated as in the **General procedure 5** to give **60f** as an off-white solid (3.62 g, 31.2%) ^1H NMR (400 MHz, CDCl_3) δ 7.67 (dd, $J = 7.9, 1.6$ Hz, 1H), 7.22 – 7.15 (m, 1H), 6.69 (dd, $J = 8.2, 1.0$ Hz, 1H), 6.65 (ddd, $J = 8.0, 7.2, 1.1$ Hz, 1H), 6.08 (s, 2H), 3.99 (s, 2H), 1.36 (s, 6H). ^{13}C NMR (101 MHz, CDCl_3) δ 162.44, 148.88, 132.25, 129.85, 116.41, 116.00, 109.73, 68.23, 29.15. Elemental Analysis calculated for $\text{C}_{11}\text{H}_{14}\text{N}_2\text{O}$: C, 69.45; H, 7.42; N, 14.73. Found: C, 69.49; H, 7.42; N, 14.77.

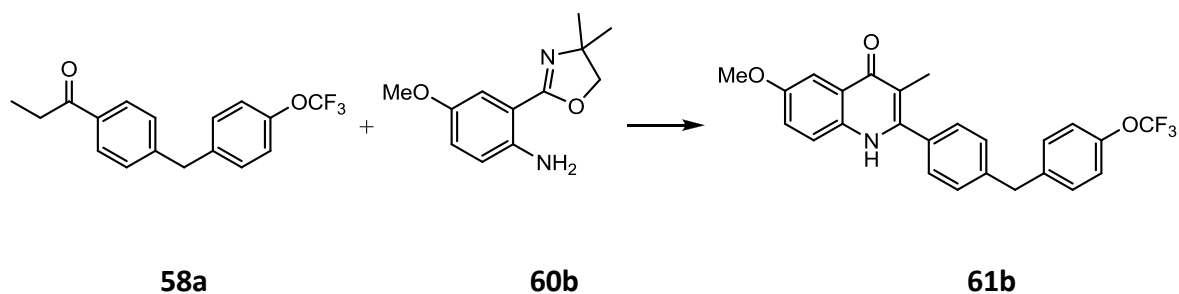
General procedure 6.

To a solution of *o*-oxazoline-substituted anilines **60** (1.1 eq, 1.1 mmol) and ketones **58** (1.0 eq, 1.0 mmol) in dry *n*-butanol (15 mL) was added trifluoromethane sulfonic acid (20 mol %) and the mixture was allowed to stir under reflux (135 °C) for 24 hours. The reaction was cooled to room temperature and the solvent evaporated under vacuum. Saturated sodium carbonate solution (20 mL) was added. The aqueous solution was extracted with EtOAc (3 x 20 mL), washed with brine, dried over MgSO₄, and concentrated under vacuum. The crude mixture was purified either trituration with EtOAc or by column chromatography to give quinolones **61**.

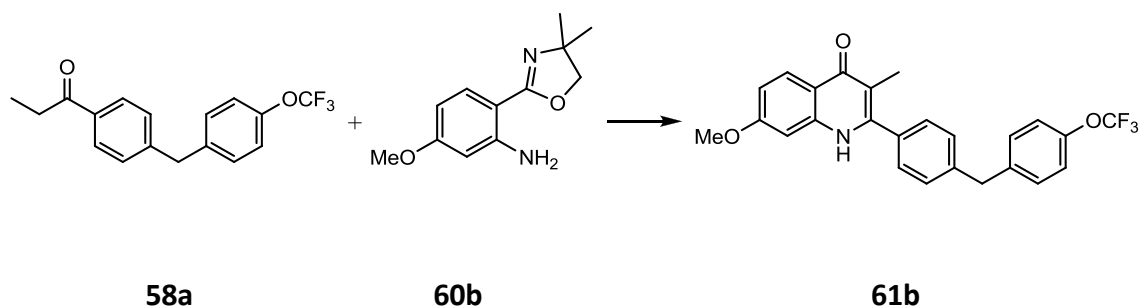
Preparation of **5-methoxy-3-methyl-2-(4-(4-(trifluoromethoxy)benzyl)phenyl)quinolin-4(1H)-one, 61a**



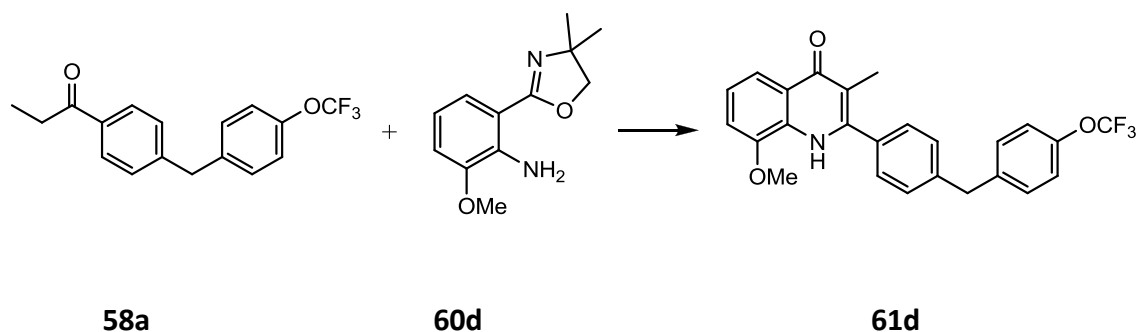
58a (308 mg, 1.0 mmol) was reacted with **60a** (235 mg, 1.2 mmol) as in the **General procedure 6** eluted with 2-5% MeOH in DCM to give **61a** as a light brown powder (20 mg, 8%). ¹H NMR (400 MHz, DMSO) δ 11.17 (s, 1H), 7.48 – 7.36 (m, 7H), 7.32 (d, *J* = 7.9 Hz, 2H), 7.08 (d, *J* = 7.8 Hz, 1H), 6.68 (d, *J* = 8.0 Hz, 1H), 4.08 (s, 2H), 3.79 (s, 3H), 1.78 (s, 3H). ES HRMS: *m/z* calculated for C₂₅H₂₁NO₃F₃ ([M+H]⁺) 440.1474, found 440.1473

Preparation of **6-methoxy-3-methyl-2-(4-(4-(trifluoromethoxy)benzyl)phenyl)quinolin-4(1H)-one, 61b**

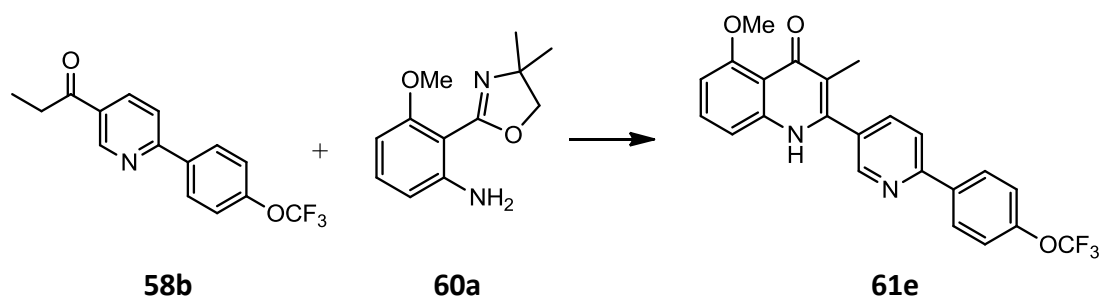
58a (462 mg, 1.5 mmol) was reacted with **60b** (396 mg, 1.8 mmol) as in the **General procedure 6** eluted with 50-80% EtOAc in DCM to give **61b** as a pale yellow powder (185 mg, 28%). mp = 238 - 240 °C. ¹H NMR (400 MHz, DMSO) δ 11.51 (s, 1H), 7.53 (d, *J* = 9.1 Hz, 1H), 7.50 (d, *J* = 3.0 Hz, 1H), 7.45 (m, 6H), 7.32 (d, *J* = 7.9 Hz, 2H), 7.26 (dd, *J* = 9.0, 3.0 Hz, 1H), 4.09 (s, 2H), 3.83 (s, 3H), 1.89 (s, 3H). ES HRMS: *m/z* calculated for C₂₅H₂₁NO₃F₃ ([M+H]⁺) 440.1474, found 440.1479

Preparation of **7-methoxy-3-methyl-2-(4-(4-(trifluoromethoxy)benzyl)phenyl)quinolin-4(1H)-one, 61c**

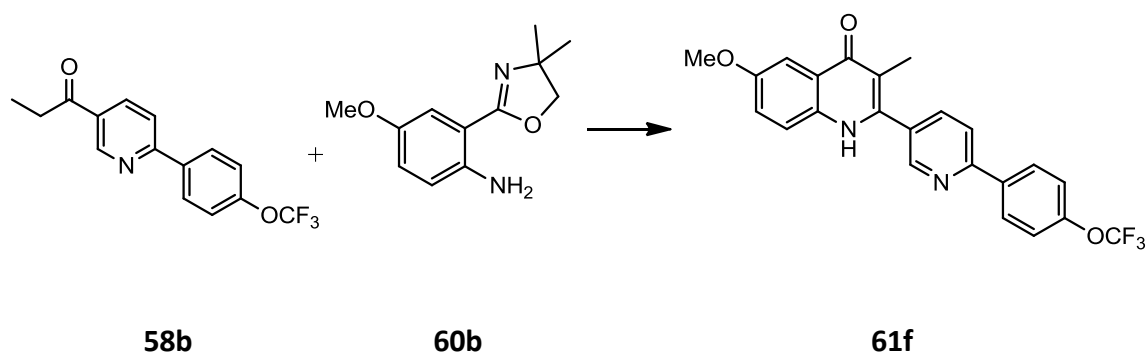
58a (397 mg, 1.29 mmol) was reacted with **60c** (190 mg, 0.86 mmol) as in the **General procedure 6** eluted with 20-50% EtOAc in DCM to give **61c** as a white solid (110 mg, 29%). mp = 225 - 228 °C. ¹H NMR (400 MHz, DMSO) δ 11.34 (s, 1H), 8.01 (d, *J* = 9.0 Hz, 1H), 7.51 - 7.42 (m, 6H), 7.33 (d, *J* = 7.9 Hz, 2H), 6.99 (d, *J* = 2.4 Hz, 1H), 6.89 (dd, *J* = 9.0, 2.4 Hz, 1H), 4.10 (s, 2H), 3.81 (s, 3H), 1.86 (s, 3H). ¹³C NMR (101 MHz, DMSO) δ 176.61, 161.89, 147.36, 142.60, 141.52, 141.01, 133.44, 130.89, 129.52, 129.18, 127.15, 121.56, 117.93, 115.03, 114.21, 113.24, 99.09, 83.96, 55.64, 12.44. ES HRMS: *m/z* calculated for C₂₅H₂₁NO₃F₃ ([M+H]⁺) 440.1474, found 440.1492.

Preparation of **8-methoxy-3-methyl-2-(4-(4-(trifluoromethoxy)benzyl)phenyl)quinolin-4(1H)-one, 61d**

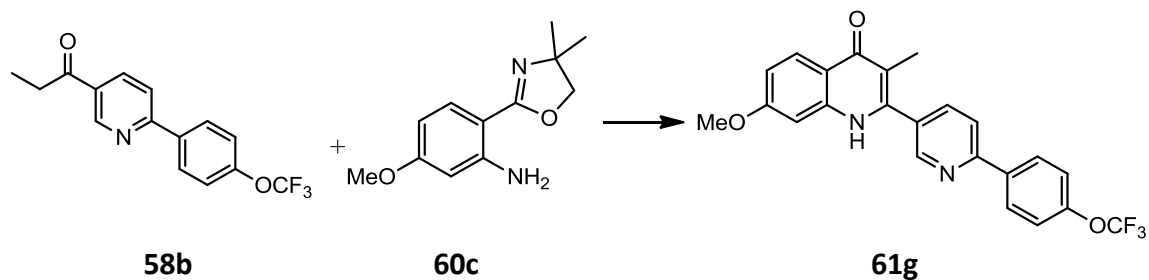
58a (370 mg, 1.2 mmol) was reacted with **60d** (317 mg, 1.4 mmol) as in the **General procedure 6** eluted with 80% EtOAc in DCM to give **61d** as a pale yellow powder (128 mg, 27%). mp = 131 - 133 °C. ¹H NMR (400 MHz, DMSO) δ 10.66 (s, 1H), 7.68 (dd, *J* = 7.9, 1.5 Hz, 1H), 7.45 (d, *J* = 8.7 Hz, 2H), 7.42 (s, 4H), 7.32 (d, *J* = 7.9 Hz, 2H), 7.23 (t, *J* = 7.8 Hz, 1H), 7.18 (dd, *J* = 7.8, 1.5 Hz, 1H), 4.08 (s, 2H), 3.90 (s, 3H), 1.84 (s, 3H). ES HRMS: *m/z* calculated for C₂₅H₂₁NO₃F₃ ([M+H]⁺) 440.1474, found 440.1490.

Preparation of **5-methoxy-3-methyl-2-(6-(4-(trifluoromethoxy)phenyl)pyridin-3-yl)quinolin-4(1H)-one, 61e**

58b (309 mg, 1.04 mmol) was reacted with **60a** (235 mg, 1.2 mmol) as in the **General procedure 6** eluted with 10% MeOH in DCM to give **61e** as a light brown powder (18 mg, 4%). ¹H NMR (400 MHz, DMSO) δ 11.40 (s, 1H), 8.86 (s, 1H), 8.33 (d, *J* = 8.8 Hz, 2H), 8.22 (d, *J* = 8.1 Hz, 1H), 8.12 (dd, *J* = 8.1, 2.1 Hz, 1H), 7.54 (d, *J* = 8.0 Hz, 2H), 7.48 (t, *J* = 8.1 Hz, 1H), 7.10 (d, *J* = 8.1 Hz, 1H), 6.73 (d, *J* = 7.9 Hz, 1H), 3.82 (s, 3H), 1.86 (s, 3H). ES HRMS: *m/z* calculated for C₂₃H₁₈N₂O₃F₃ ([M+H]⁺) 427.1270, found 427.1271

Preparation of **6-methoxy-3-methyl-2-(6-(4-(trifluoromethoxy)phenyl)pyridin-3-yl)quinolin-4(1H)-one, 61f**

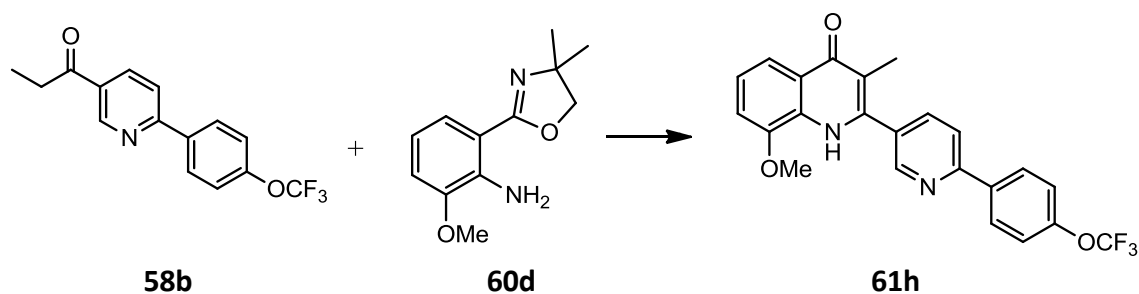
58b (309 mg, 1.04 mmol) was reacted with **60b** (235 mg, 1.2 mmol) as in the **General procedure 6** eluted with 5% MeOH in DCM to give **61f** as a white solid (119 mg, 22%). mp = 312 - 314 °C. ^1H NMR (400 MHz, DMSO) δ 11.77 (s, 1H), 8.89 (s, 1H), 8.34 (d, J = 8.9 Hz, 2H), 8.24 (d, J = 8.1 Hz, 1H), 8.16 (dd, J = 8.1, 2.3 Hz, 1H), 7.56 (m, 4H), 7.31 (dd, J = 9.0, 3.0 Hz, 1H), 3.86 (s, 3H), 1.97 (s, 3H); ^{13}C NMR (100 MHz, DMSO) δ 176.24, 155.70, 155.44, 149.77, 149.70, 143.99, 138.52, 137.47, 134.71, 130.37, 129.16, 124.43, 122.59, 121.73, 120.34, 114.45, 104.26, 55.69, 12.54. ES HRMS: m/z calculated for $\text{C}_{23}\text{H}_{18}\text{N}_2\text{O}_3\text{F}_3$ $[\text{M}+\text{H}]^+$ requires 427.1270, found 427.1248.

Preparation of **7-methoxy-3-methyl-2-(6-(4-(trifluoromethoxy)phenyl)pyridin-3-yl)quinolin-4(1H)-one, 61g**

58b (253 mg, 0.86 mmol) was reacted with **60c** (126 mg, 0.57 mmol) as in the **General procedure 6** eluted with 50-80% EtOAc in DCM to give **61g** as a pale yellow solid (126 mg, 52%). mp = 324 - 325 °C. ^1H NMR (400 MHz, DMSO) δ 11.60 (s, 1H), 8.88 (d, J = 1.9 Hz, 1H), 8.34 (d, J = 8.8 Hz, 2H), 8.24 (d, J = 8.2 Hz, 1H), 8.15 (dd, J = 8.2, 2.2 Hz, 1H), 8.04 (d, J = 8.9 Hz, 1H), 7.55 (d, J = 8.3 Hz, 2H), 6.99 (d, J = 2.3 Hz, 1H), 6.93 (dd, J = 9.0, 2.3 Hz, 1H), 3.84 (s, 3H), 1.93 (s, 3H). ^{13}C NMR (101

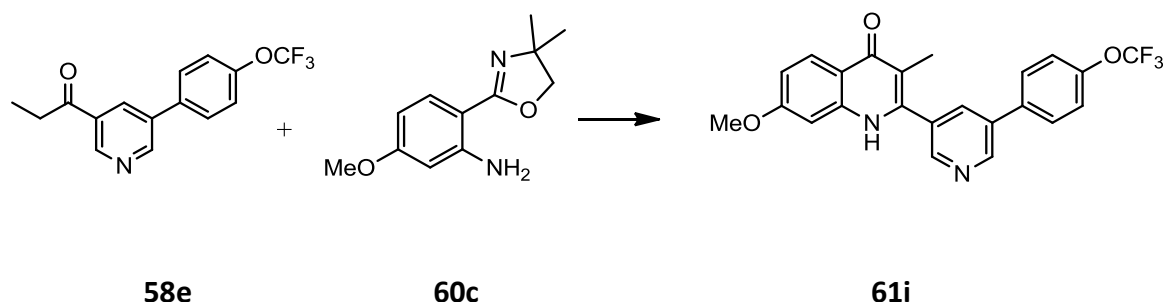
MHz, DMSO) δ 162.06, 155.43, 149.75, 138.46, 130.34, 129.16, 129.16, 121.74, 121.74, 120.36, 118.03, 115.22, 113.59, 99.02, 55.72, 12.32. ES HRMS: m/z calculated for $C_{23}H_{18}N_2O_3F_3$ ($[M+H]^+$) 427.1270, found 427.1287.

Preparation of **8-methoxy-3-methyl-2-(6-(4-(trifluoromethoxy)phenyl)pyridin-3-yl)quinolin-4(1H)-one, 61h**



58b (350 mg, 1.2 mmol) was reacted with **60d** (317 mg, 1.4 mmol) as in the **General procedure 6** eluted with 80% EtOAc in DCM to give **61h** as a pale yellow solid (124 mg, 25%). mp = 182 - 185 °C. 1H NMR (400 MHz, DMSO) δ 11.11 (s, 1H), 8.78 (d, J = 1.6 Hz, 1H), 8.33 (d, J = 8.9 Hz, 2H), 8.18 (dd, J = 8.2, 0.5 Hz, 1H), 8.05 (dd, J = 8.2, 2.3 Hz, 1H), 7.72 (dd, J = 7.8, 1.6 Hz, 1H), 7.54 (d, J = 8.1 Hz, 2H), 7.27 (t, J = 7.8 Hz, 1H), 7.23 (dd, J = 7.9, 1.6 Hz, 1H), 3.94 (s, 3H), 1.89 (s, 3H). ES HRMS: m/z calculated for $C_{23}H_{18}N_2O_3F_3$ ($[M+H]^+$) 427.1270, found 427.1268

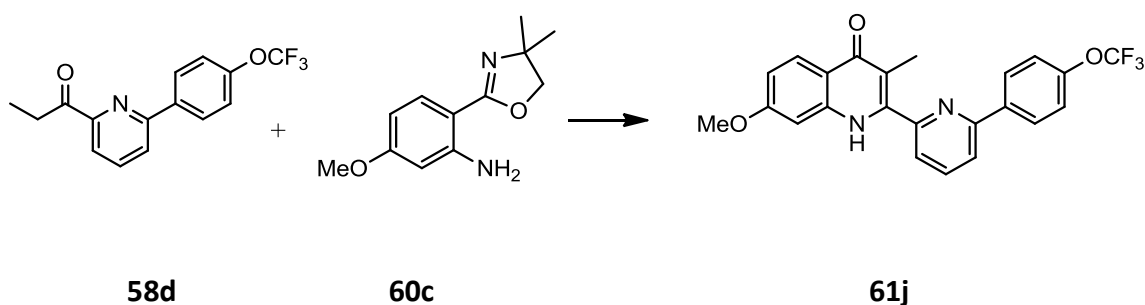
Preparation of **7-methoxy-3-methyl-2-(5-(4-(trifluoromethoxy)phenyl)pyridin-3-yl)quinolin-4(1H)-one, 61i**



58e (295 mg, 1.0 mmol) was reacted with **60c** (242 mg, 1.1 mmol) as in the **General procedure 6** eluted with 5% MeOH in DCM to give **61i** as a pale yellow solid (145 mg, 34%).; mp = 255 - 258 °C; 1H NMR (400 MHz, DMSO) δ 11.57 (s, 1H), 9.10 (d, J = 2.2 Hz, 1H), 8.80 (d, J = 2.0 Hz, 1H), 8.35 (t, J = 2.2 Hz, 1H), 8.05 (d, J = 9.0 Hz,

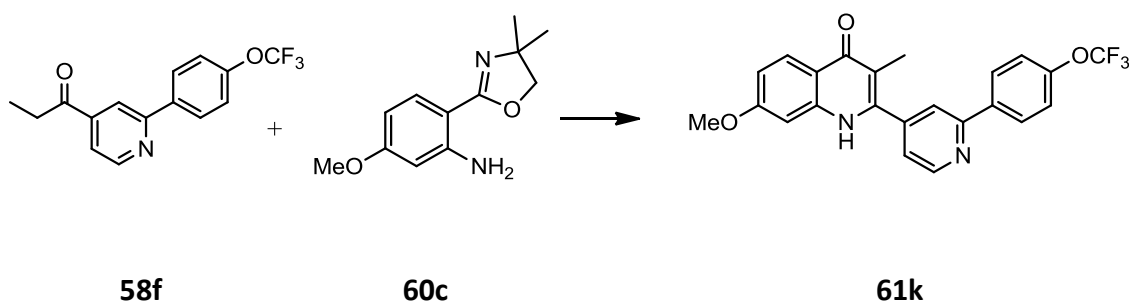
1H), 8.01 (d, $J = 8.9$ Hz, 2H), 7.55 (d, $J = 7.9$ Hz, 2H), 6.97 (d, $J = 2.3$ Hz, 1H), 6.93 (dd, $J = 8.9, 2.4$ Hz, 1H), 3.84 (s, 3H), 1.94 (s, 3H). ^{13}C NMR (101 MHz, DMSO) δ 176.55, 162.10, 148.91, 148.65, 144.18, 141.70, 136.05, 135.12, 134.25, 131.44, 129.57, 127.30, 122.10, 118.06, 115.27, 113.58, 99.03, 55.73, 12.31. ESI HRMS: m/z calculated for $\text{C}_{23}\text{H}_{18}\text{N}_2\text{O}_3\text{F}_3$ ($[\text{M}+\text{H}]^+$) 427.1270, found 427.1272.

Preparation of **7-methoxy-3-methyl-2-(6-(4-(trifluoromethoxy)phenyl)pyridin-2-yl)quinolin-4(1H)-one, 61j**



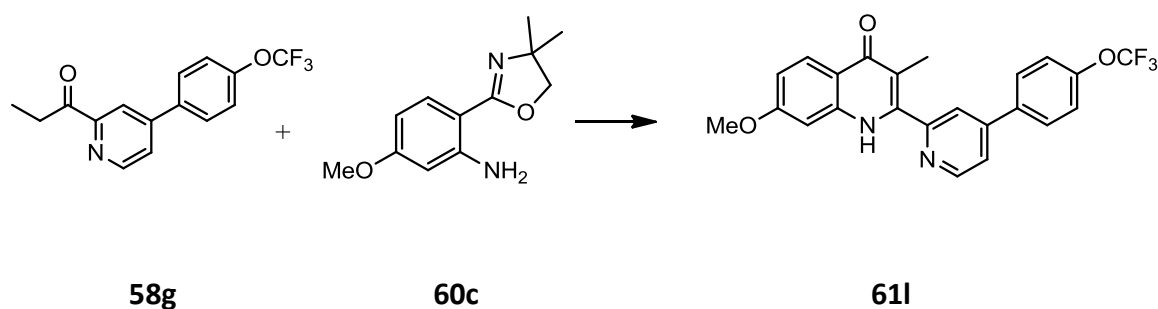
58d (205 mg, 0.69 mmol) was reacted with **60c** (205 mg, 0.93 mmol) as in the **General procedure 6** eluted with 100% EtOAc to give **61j** as an off-white solid (118 mg, 40%); mp = 200 - 204 °C; ^1H NMR (400 MHz, DMSO) δ 11.51 (s, 1H), 8.34 (d, $J = 8.9$ Hz, 2H), 8.21 - 8.13 (m, 2H), 8.05 (d, $J = 9.0$ Hz, 1H), 7.76 (dd, $J = 7.2, 1.2$ Hz, 1H), 7.55 (d, $J = 8.1$ Hz, 2H), 7.14 (d, $J = 2.4$ Hz, 1H), 6.93 (dd, $J = 9.0, 2.4$ Hz, 1H), 3.85 (s, 3H), 2.03 (s, 3H). ^{13}C NMR (101 MHz, DMSO) δ 162.12, 155.14, 153.17, 148.43, 145.48, 142.92, 141.59, 138.72, 137.69, 129.37, 127.24, 121.65, 121.29, 113.66, 99.20, 55.73, 12.22. ESI HRMS: m/z calculated for $\text{C}_{23}\text{H}_{18}\text{N}_2\text{O}_3\text{F}_3$ ($[\text{M}+\text{H}]^+$) 427.1270, found 427.1282.

Preparation of **7-methoxy-3-methyl-2-(2-(4-(trifluoromethoxy)phenyl)pyridin-4-yl)quinolin-4(1H)-one, 61k**

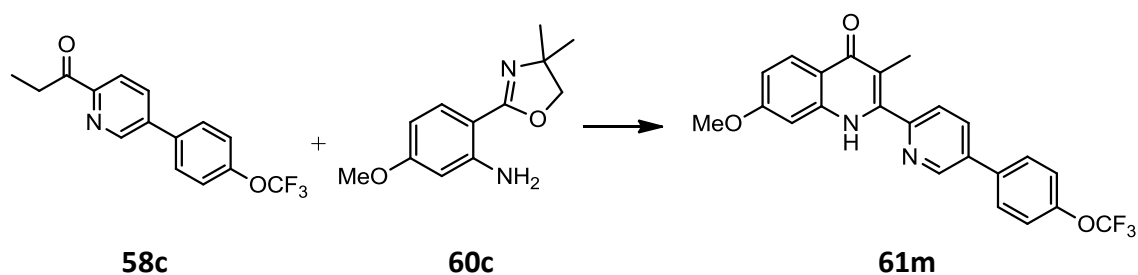


58f (295 mg, 1.0 mmol) was reacted with **60c** (242 mg, 1.1 mmol) as in the **General procedure 6** eluted with 100% EtOAc to give **61l** as a white solid (147 mg, 34%); mp = 245 - 247 °C; ¹H NMR (400 MHz, DMSO) δ 11.56 (s, 1H), 8.89 (d, *J* = 5.0 Hz, 1H), 8.34 (d, *J* = 8.9 Hz, 2H), 8.22 (s, 1H), 8.06 (d, *J* = 9.0 Hz, 1H), 7.60 (dd, *J* = 5.0, 1.5 Hz, 1H), 7.53 (d, *J* = 8.0 Hz, 2H), 7.00 (d, *J* = 2.4 Hz, 1H), 6.94 (dd, *J* = 9.0, 2.4 Hz, 1H), 3.85 (s, 4H), 1.93 (s, 3H). ¹³C NMR (101 MHz, DMSO) δ 176.55, 162.14, 155.48, 150.40, 144.93, 144.15, 141.66, 137.67, 129.18, 127.29, 123.24, 121.61, 120.71, 118.07, 114.70, 113.66, 111.41, 99.11, 55.74, 12.18. ESI HRMS: *m/z* calculated for C₂₃H₁₈N₂O₃F₃ ([M+H]⁺) 427.1270, found 427.1266.

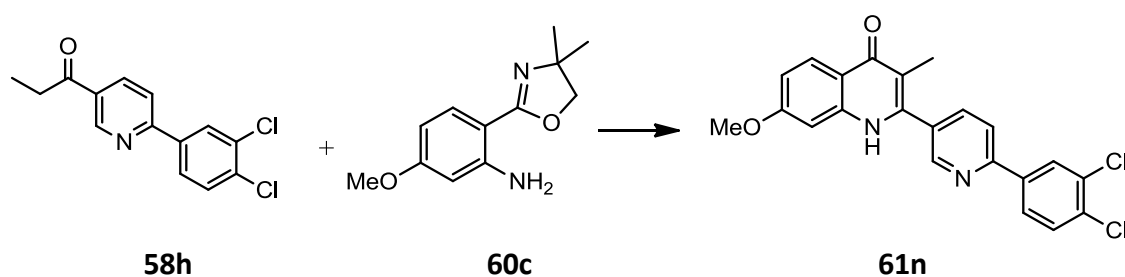
Preparation of **7-methoxy-3-methyl-2-(4-(4-(trifluoromethoxy)phenyl)pyridin-2-yl)quinolin-4(1H)-one, 61l**



58g (184 mg, 0.62 mmol) was reacted with **60c** (151 mg, 0.68 mmol) as in the **General procedure 6** eluted with 100% EtOAc to give **61l** as a white solid (113 mg, 42%); mp = 188 - 190 °C; ¹H NMR (400 MHz, DMSO) δ 11.51 (s, 1H), 8.89 (d, *J* = 4.9 Hz, 1H), 8.12 - 8.03 (m, 4H), 7.93 (dd, *J* = 5.2, 1.8 Hz, 1H), 7.57 (d, *J* = 8.1 Hz, 2H), 7.13 (d, *J* = 2.4 Hz, 1H), 6.93 (dd, *J* = 9.0, 2.4 Hz, 1H), 3.85 (s, 3H), 2.03 (s, 3H). ¹³C NMR (101 MHz, DMSO) δ 176.96, 154.22, 150.65, 146.84, 145.47, 141.58, 136.32, 129.68, 127.25, 122.74, 122.09, 118.04, 115.03, 113.52, 99.27, 55.72, 12.17. ESI HRMS: *m/z* calculated for C₂₃H₁₈N₂O₃F₃ ([M+H]⁺) 427.1270, found 427.1284.

Preparation of **7-methoxy-3-methyl-2-(5-(4-(trifluoromethoxy)phenyl)pyridin-2-yl)quinolin-4(1H)-one, 61m**

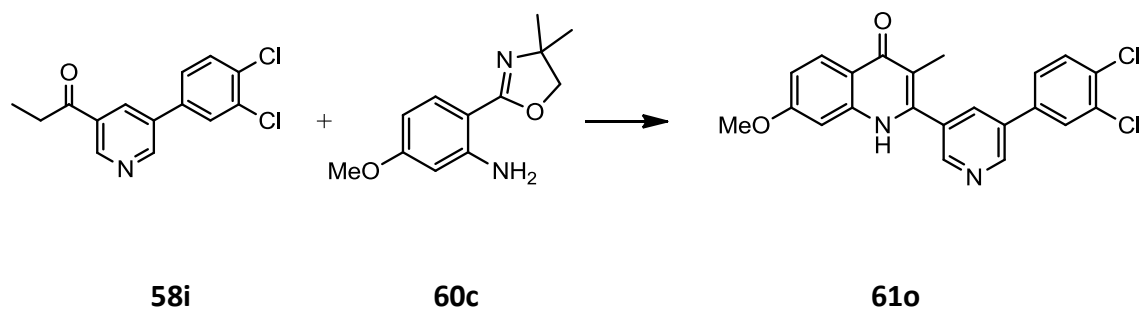
58c (265 mg, 0.90 mmol) was reacted with **60c** (268 mg, 1.22 mmol) as in the **General procedure 6** eluted with 100% EtOAc to give **61m** as a pale yellow solid (237 mg, 62%).; mp = 255 - 258 °C; ^1H NMR (400 MHz, DMSO) δ 11.52 (s, 1H), 9.16 (dd, J = 2.4, 0.7 Hz, 1H), 8.36 (dd, J = 8.2, 2.4 Hz, 1H), 8.05 (d, J = 9.0 Hz, 1H), 8.01 (d, J = 8.8 Hz, 2H), 7.89 (dd, J = 8.2, 0.7 Hz, 1H), 7.57 (d, J = 8.0 Hz, 2H), 7.17 (d, J = 2.4 Hz, 1H), 6.93 (dd, J = 9.0, 2.4 Hz, 1H), 3.85 (s, 3H), 2.04 (s, 3H). ^{13}C NMR (101 MHz, DMSO) δ 176.94, 162.12, 160.44, 152.40, 148.00, 145.09, 141.61, 136.03, 135.40, 134.83, 129.55, 127.22, 125.48, 122.17, 118.00, 114.96, 113.51, 99.35, 55.72, 12.27. ES HRMS: m/z calculated for $\text{C}_{23}\text{H}_{18}\text{N}_2\text{O}_3\text{F}_3$ ($[\text{M}+\text{H}]^+$) 427.1270, found 427.1281.

Preparation of **7-methoxy-3-methyl-2-(6-(3,4-dichlorophenyl)pyridin-3-yl)quinolin-4(1H)-one, 61n**

58h (195 mg, 0.70 mmol) was reacted with **60c** (126 mg, 0.66 mmol) as in the **General procedure 6** eluted with EtOAc to give **61n** as a pale yellow solid (63 mg, 23%).; mp = 268 - 270 °C; ^1H NMR (400 MHz, DMSO) δ 11.56 (s, 1H), 8.89 (d, J = 1.7 Hz, 1H), 8.47 (d, J = 2.1 Hz, 1H), 8.31 (d, J = 8.0 Hz, 1H), 8.22 (dd, J = 8.5, 2.1 Hz, 1H), 8.15 (dd, J = 8.2, 2.3 Hz, 1H), 8.05 (d, J = 9.0 Hz, 1H), 7.83 (d, J = 8.5 Hz, 1H),

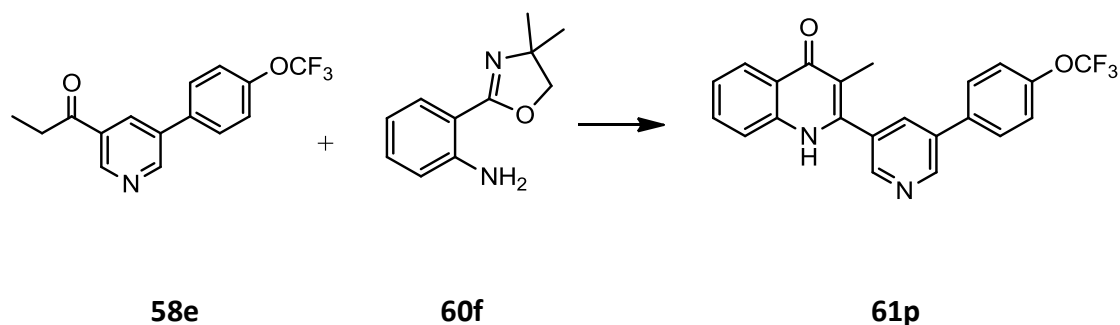
6.99 (d, $J = 2.2$ Hz, 1H), 6.94 (dd, $J = 9.0, 2.4$ Hz, 1H), 3.85 (s, 3H), 1.93 (s, 3H). ES HRMS: m/z calculated for $C_{22}H_{17}N_2O_2^{35}Cl_2$ ($[M+H]^+$) 411.0667, found 411.0683.

Preparation of **7-methoxy-3-methyl-2-(5-(3,4-dichlorophenyl)pyridin-3-yl)quinolin-4(1H)-one, 61o**



58i (168 mg, 0.60 mmol) was reacted with **60c** (146 mg, 0.66 mmol) as in the **General procedure 6** washed with EtOAc to give **61o** as a pale yellow solid (90 mg, 36%).; mp = 290 - 292 °C; 1H NMR (400 MHz, DMSO) δ 11.59 (s, 1H), 9.15 (d, $J = 2.2$ Hz, 1H), 8.81 (d, $J = 1.9$ Hz, 1H), 8.43 (t, $J = 2.1$ Hz, 1H), 8.22 (d, $J = 2.2$ Hz, 1H), 8.05 (d, $J = 8.9$ Hz, 1H), 7.91 (dd, $J = 8.4, 2.2$ Hz, 1H), 7.82 (d, $J = 8.5$ Hz, 1H), 6.98 (d, $J = 2.3$ Hz, 1H), 6.94 (dd, $J = 8.9, 2.4$ Hz, 1H), 3.85 (s, 3H), 1.93 (s, 3H). ESI HRMS: m/z calculated for $C_{22}H_{17}N_2O_2^{35}Cl_2$ ($[M+H]^+$) 411.0667, found 411.0668.

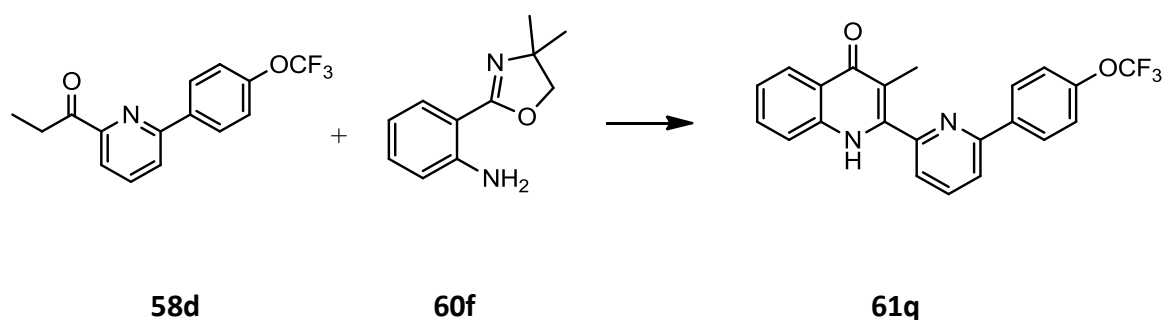
Preparation of **3-methyl-2-(5-(4-(trifluoromethoxy)phenyl)pyridin-3-yl)quinolin-4(1H)-one, 61p**



58e (238 mg, 0.81 mmol) was reacted with **60c** (217 mg, 1.14 mmol) as in the **General procedure 6** eluted with 100% EtOAc and 5% MeOH in EtOAc to give **61p** as a pale yellow solid (172 mg, 54%).; mp = 217 - 220 °C; 1H NMR (400 MHz, DMSO) δ 11.77 (s, 1H), 9.12 (d, $J = 2.3$ Hz, 1H), 8.82 (d, $J = 2.0$ Hz, 1H), 8.38 (t, $J = 2.1$

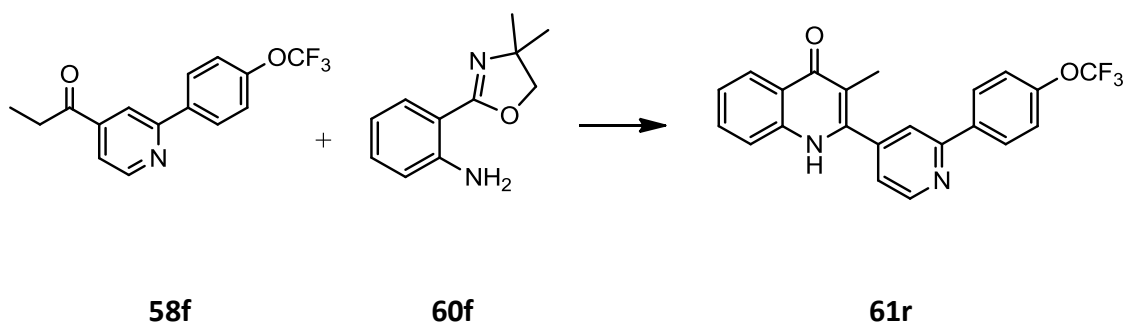
Hz, 1H), 8.16 (dd, $J = 8.1, 1.2$ Hz, 1H), 8.01 (d, $J = 8.8$ Hz, 2H), 7.66 (ddd, $J = 8.3, 6.9, 1.5$ Hz, 1H), 7.59 (d, $J = 7.9$ Hz, 1H), 7.56 (d, $J = 8.0$ Hz, 2H), 7.34 (ddd, $J = 8.1, 6.9, 1.1$ Hz, 1H), 1.96 (s, 3H). ^{13}C NMR (101 MHz, DMSO) δ 176.99, 148.91, 148.72, 144.73, 139.94, 136.04, 135.18, 134.24, 131.88, 131.39, 129.59, 125.39, 123.50, 123.25, 122.13, 118.48, 115.63, 12.44. ES HRMS: m/z calculated for $\text{C}_{22}\text{H}_{16}\text{N}_2\text{O}_2\text{F}_3$ ($[\text{M}+\text{H}]^+$) 397.1164, found 397.1169.

Preparation of **3-methyl-2-(6-(4-(trifluoromethoxy)phenyl)pyridin-2-yl)quinolin-4(1H)-one, 61q**



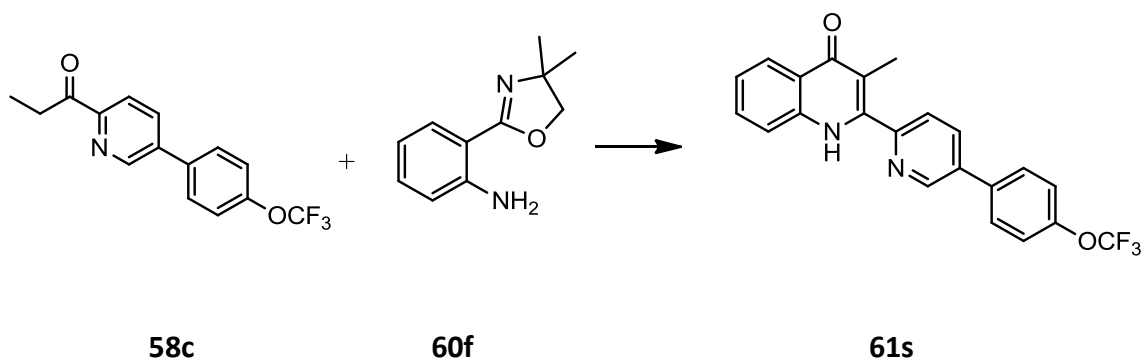
58d (303 mg, 1.0 mmol) was reacted with **60f** (224 mg, 1.1 mmol) as in the **General procedure 6** eluted with 100% EtOAc and 5% MeOH in EtOAc to give **61q** as an off-white solid (225 mg, 55%); mp = 187 - 192 °C; ^1H NMR (400 MHz, DMSO) δ 11.74 (s, 1H), 8.33 (d, $J = 8.9$ Hz, 2H), 8.21 (dd, $J = 8.0, 1.1$ Hz, 1H), 8.19 - 8.13 (m, 2H), 7.78 (dd, $J = 7.3, 1.1$ Hz, 1H), 7.71 (d, $J = 7.7$ Hz, 1H), 7.66 (ddd, $J = 8.3, 6.7, 1.5$ Hz, 1H), 7.54 (d, $J = 8.1$ Hz, 2H), 7.33 (ddd, $J = 8.1, 6.7, 1.3$ Hz, 1H), 2.03 (s, 3H). ^{13}C NMR (101 MHz, DMSO) δ 177.40, 155.13, 153.18, 146.02, 139.81, 138.77, 137.65, 131.88, 129.35, 125.37, 124.41, 123.47, 123.19, 121.67, 121.34, 118.72, 115.13, 12.27. ES HRMS: m/z calculated for $\text{C}_{22}\text{H}_{16}\text{N}_2\text{O}_2\text{F}_3$ ($[\text{M}+\text{H}]^+$) 397.1164, found 397.1179.

Preparation of **3-methyl-2-(2-(4-(trifluoromethoxy)phenyl)pyridin-4-yl)quinolin-4(1H)-one, 61r**



58f (135 mg, 0.56 mmol) was reacted with **60f** (121 mg, 0.64 mmol) as in the **General procedure 6** eluted with 100% EtOAc to give **61r** as a white solid (101 mg, 56%); mp = 244 - 246 °C; ¹H NMR (400 MHz, DMSO) δ 11.78 (s, 1H), 8.90 (dd, *J* = 4.9, 0.7 Hz, 1H), 8.35 (d, *J* = 8.9 Hz, 2H), 8.26 (s, 1H), 8.16 (dd, *J* = 8.2, 1.1 Hz, 1H), 7.67 (ddd, *J* = 8.3, 6.8, 1.5 Hz, 1H), 7.63 (dd, *J* = 5.0, 1.5 Hz, 1H), 7.60 (d, *J* = 7.8 Hz, 1H), 7.53 (d, *J* = 8.1 Hz, 2H), 7.34 (ddd, *J* = 8.1, 6.8, 1.2 Hz, 1H), 1.95 (s, 3H). ¹³C NMR (101 MHz, DMSO) δ 150.42, 144.11, 139.89, 131.93, 129.18, 125.38, 123.52, 123.32, 123.28, 123.24, 121.64, 120.74, 118.56, 114.98, 12.30. ES HRMS: *m/z* calculated for C₂₂H₁₆N₂O₂F₃ ([M+H]⁺) 397.1164, found 397.1171.

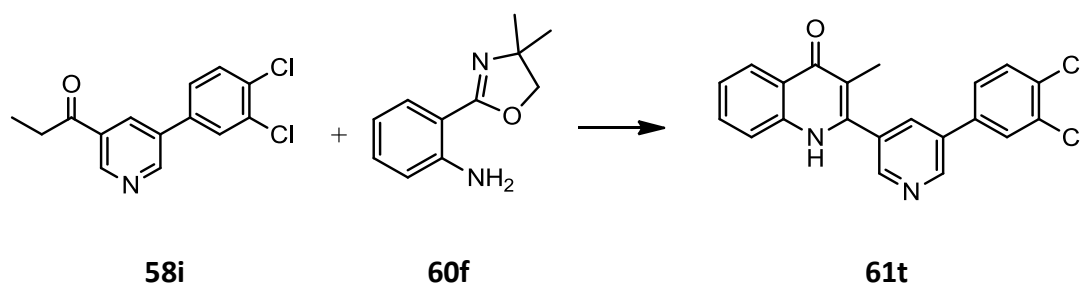
Preparation of **3-methyl-2-(5-(4-(trifluoromethoxy)phenyl)pyridin-2-yl)quinolin-4(1H)-one, 61s**



58c (298 mg, 1.0 mmol) was reacted with **60f** (213 mg, 1.1 mmol) as in the **General procedure 6** eluted with 100% EtOAc to give **61s** as a pale yellow solid (248 mg, 62%); mp = 239 - 241 °C; ¹H NMR (400 MHz, DMSO) δ 11.74 (s, 1H), 9.18 (d, *J* = 1.7 Hz, 1H), 8.37 (dd, *J* = 8.2, 2.4 Hz, 1H), 8.15 (dd, *J* = 8.1, 1.3 Hz, 1H), 8.01 (d, *J* = 8.8

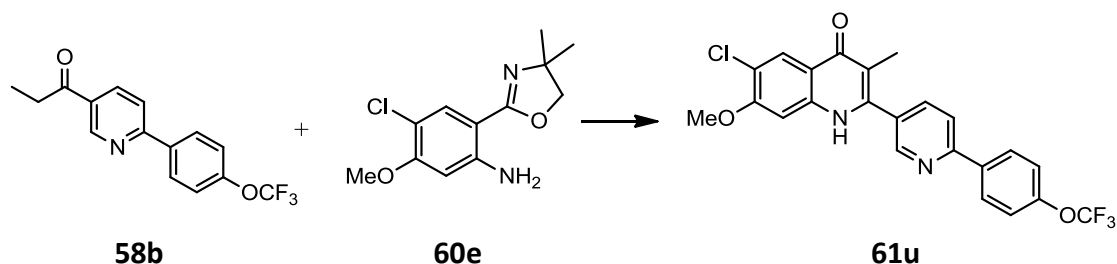
Hz, 2H), 7.91 (d, $J = 8.2$ Hz, 1H), 7.72 (d, $J = 8.1$ Hz, 1H), 7.65 (ddd, $J = 8.4, 6.9, 1.5$ Hz, 1H), 7.58 (d, $J = 8.0$ Hz, 2H), 7.33 (ddd, $J = 8.0, 6.9, 1.1$ Hz, 1H), 2.05 (s, 3H). ^{13}C NMR (101 MHz, DMSO) δ 152.42, 148.07, 145.65, 139.86, 136.04, 135.44, 134.90, 131.88, 129.57, 125.56, 125.34, 123.43, 123.17, 122.21, 118.74, 115.25, 12.36. ES HRMS: m/z calculated for $\text{C}_{22}\text{H}_{16}\text{N}_2\text{O}_2\text{F}_3$ ($[\text{M}+\text{H}]^+$) 397.1164, found 397.1178.

Preparation of **3-methyl-2-(5-(3,4-dichlorophenyl)pyridin-3-yl)quinolin-4(1H)-one, 61t**



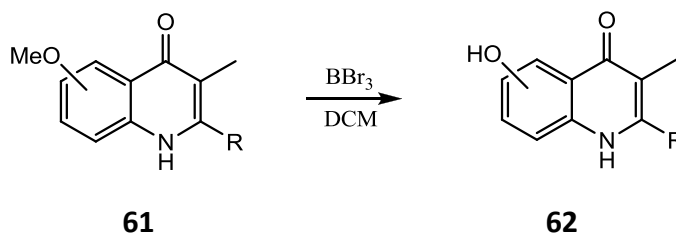
58i (168 mg, 0.60 mmol) was reacted with **60e** (126 mg, 0.66 mmol) as in the **General procedure 6** washed with EtOAc to give **61t** as a pale yellow solid (58 mg, 25%); mp = 270 - 272 °C; ^1H NMR (400 MHz, DMSO) δ 11.75 (s, 1H), 9.15 (d, $J = 2.3$ Hz, 1H), 8.82 (d, $J = 2.0$ Hz, 1H), 8.45 (t, $J = 2.1$ Hz, 1H), 8.22 (d, $J = 2.1$ Hz, 1H), 8.15 (dd, $J = 8.0, 0.8$ Hz, 1H), 7.91 (dd, $J = 8.4, 2.2$ Hz, 1H), 7.81 (d, $J = 8.4$ Hz, 1H), 7.66 (ddd, $J = 8.3, 6.9, 1.5$ Hz, 1H), 7.59 (d, $J = 8.0$ Hz, 1H), 7.33 (ddd, $J = 8.0, 6.9, 1.1$ Hz, 1H), 1.95 (s, 3H). HRMS (CI): m/z calculated for $\text{C}_{21}\text{H}_{14}\text{N}_2\text{O}^{35}\text{Cl}_2$ ($[\text{M}+\text{H}]^+$) 381.0556, found 381.0553.

Preparation of **6-chloro-7-methoxy-3-methyl-2-(6-(4-(trifluoromethoxy)phenyl)pyridin-3-yl)quinolin-4(1H)-one, 61u**



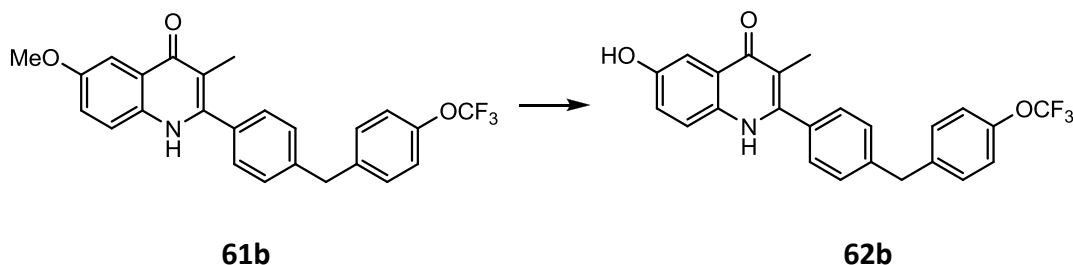
58b (127 mg, 0.43 mmol) was reacted with **60e** (100 mg, 0.39 mmol) as in the **General procedure 6** washed with EtOAc to give **61u** as a white solid (35 mg, 19%); mp = 294 - 295 °C; $^1\text{H NMR}$ (400 MHz, DMSO) δ 11.85 (s, 1H), 8.89 (d, J = 1.8 Hz, 1H), 8.34 (d, J = 8.9 Hz, 2H), 8.25 (d, J = 8.4 Hz, 1H), 8.16 (dd, J = 8.2, 2.3 Hz, 1H), 8.07 (s, 1H), 7.55 (d, J = 8.1 Hz, 2H), 7.18 (s, 1H), 3.94 (s, 3H), 1.95 (s, 3H). ES HRMS: m/z calculated for $\text{C}_{23}\text{H}_{17}\text{N}_2\text{O}_3\text{F}_3^{35}\text{Cl}$ ($[\text{M}+\text{H}]^+$) 461.0880, found 461.0884.

General procedure 7



To a solution of **61** (1.0 eq) in anhydrous DCM at 0 °C was added 1M solution of BBr_3 in DCM (0.6 ml, 3.0 eq), the reaction mixture was allowed to warm to room temp and continued stirring for 24 hr. The reaction mixture was quenched with cold water and extracted with ethyl acetate. The combined organic extracts were washed with brine and dried over MgSO_4 and concentrated *in vacuo* to yield a brown solid which was purified by column chromatography (5% to 10% MeOH in DCM) to give **62**.

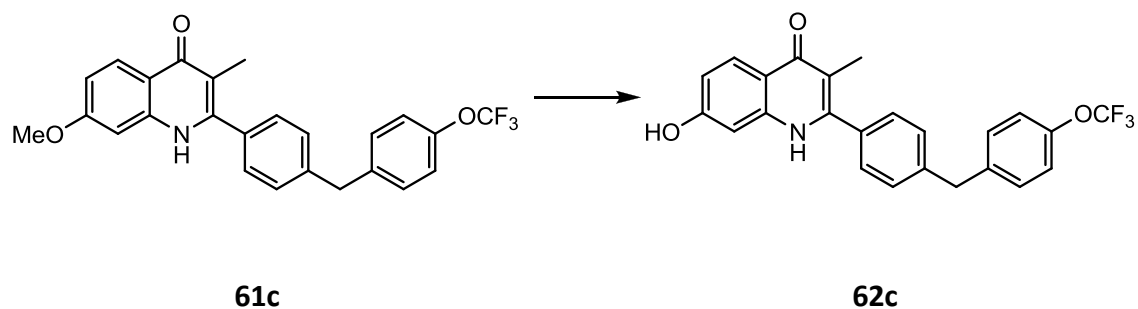
Preparation of **6-hydroxy-3-methyl-2-(4-(4-(trifluoromethoxy)benzyl)phenyl)quinolin-4(1H)-one, 62b**



61b (120 mg, 0.27 mmol) was treated as in the **General procedure 7** to give **62b** as a light brown solid (78 mg, 67%). mp = 245 - 248 °C $^1\text{H NMR}$ (400 MHz, DMSO) δ 11.40 (s, 1H), 9.58 (s, 1H), 7.49 – 7.40 (m, 8H), 7.32 (d, J = 7.9 Hz, 2H), 7.11 (dd, J = 8.9, 2.8 Hz, 1H), 4.09 (s, 2H), 1.86 (s, 3H). $^{13}\text{C NMR}$ (101 MHz, DMSO) δ

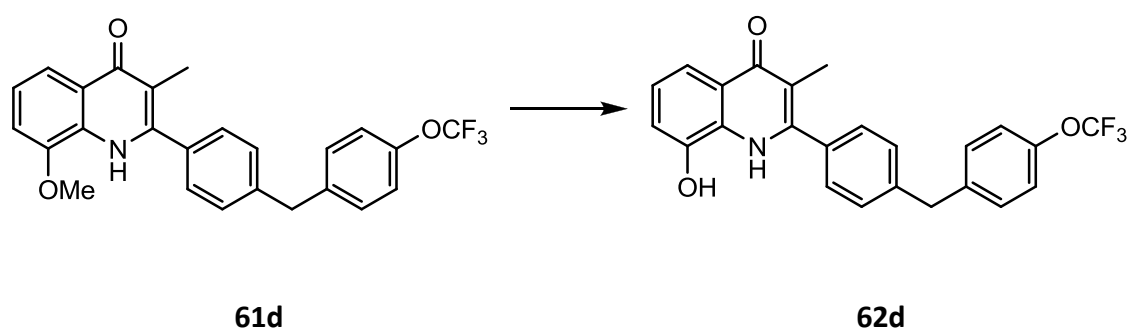
176.31, 153.51, 146.96, 142.48, 141.01, 133.62, 133.54, 130.88, 129.53, 129.13, 124.75, 122.05, 121.55, 119.99, 112.89, 107.46, 12.61. ES HRMS: m/z calculated for $C_{24}H_{19}NO_3F_3$ ($[M+H]^+$) 426.1317, found 426.1308.

Preparation of **7-hydroxy-3-methyl-2-(4-(4-(trifluoromethoxy)benzyl)phenyl)quinolin-4(1H)-one, 62c**

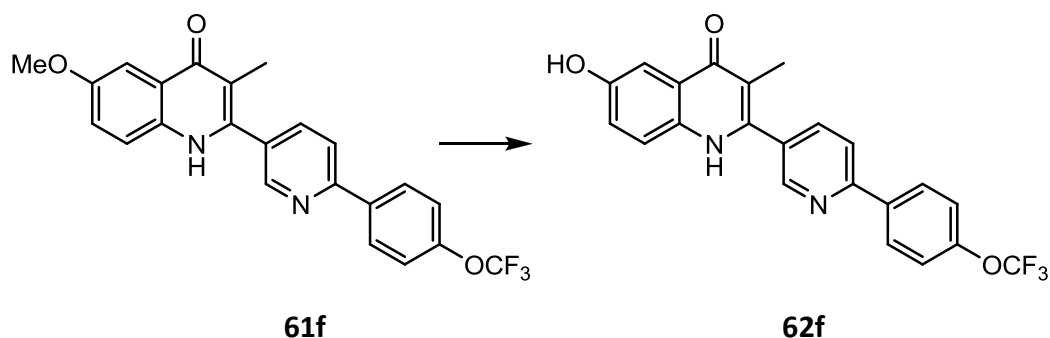


61c (80 mg, 0.18 mmol) was treated as in the **General procedure 7** to give **62c** as a light brown solid (40 mg, 51%). mp = 258 - 260 °C 1H NMR (400 MHz, DMSO) δ 11.15 (s, 1H), 10.11 (s, 1H), 7.93 (d, J = 8.8 Hz, 1H), 7.46 – 7.41 (m, 6H), 7.35 – 7.29 (m, 2H), 6.85 (d, J = 2.2 Hz, 1H), 6.74 (dd, J = 8.8, 2.3 Hz, 1H), 4.08 (s, 2H), 1.83 (s, 3H). ES HRMS: m/z calculated for $C_{24}H_{19}NO_3F_3$ ($[M+H]^+$) 426.1317, found 426.1333.

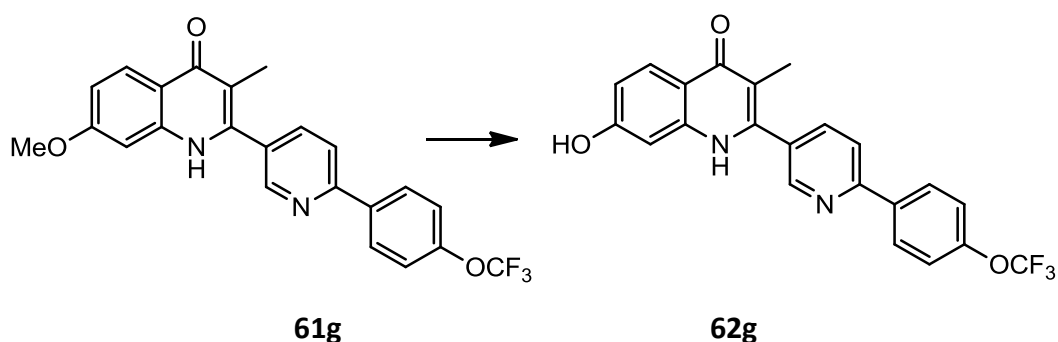
Preparation of **8-hydroxy-3-methyl-2-(4-(4-(trifluoromethoxy)benzyl)phenyl)quinolin-4(1H)-one, 62d**



61d (90 mg, 0.2 mmol) was treated as in the **General procedure 7** to give **62d** as a light brown solid (60 mg, 69%). mp = 226 - 230 °C 1H NMR (400 MHz, DMSO) δ 10.38 (s, 2H), 7.56 (dd, J = 8.1, 1.3 Hz, 1H), 7.48 – 7.37 (m, 6H), 7.32 (d, J = 7.9 Hz, 2H), 7.10 (t, J = 7.8 Hz, 1H), 7.01 (dd, J = 7.6, 1.3 Hz, 1H), 4.08 (s, 2H), 1.85 (s, 3H). ES HRMS: m/z calculated for $C_{24}H_{19}NO_3F_3$ ($[M+H]^+$) 426.1317, found 426.1309.

Preparation of **6-hydroxy-3-methyl-2-(6-(4-(trifluoromethoxy)phenyl)pyridin-3-yl)quinolin-4(1H)-one, 62f**

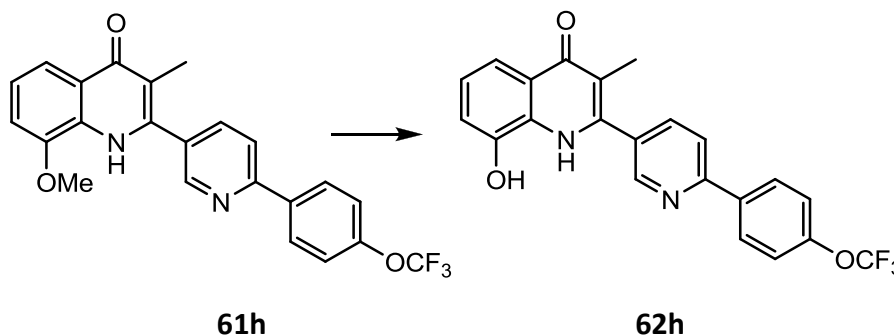
61f (79 mg, 0.18 mmol) was treated as in the **General procedure 7** to give **62f** as a white solid (10 mg, 10%). mp = decomposed at > 250 °C. ^1H NMR (400 MHz, DMSO) δ 11.61 (s, 1H), 9.62 (s, 1H), 8.87 (dd, J = 2.3, 0.8 Hz, 1H), 8.33 (d, J = 8.9 Hz, 2H), 8.22 (d, J = 7.6 Hz, 1H), 8.13 (dd, J = 8.2, 2.3 Hz, 1H), 7.54 (d, J = 8.0 Hz, 2H), 7.48 (d, J = 8.9 Hz, 1H), 7.46 (d, J = 2.8 Hz, 1H), 7.16 (dd, J = 8.9, 2.8 Hz, 1H), 1.93 (s, 3H). ES HRMS: m/z calculated for $\text{C}_{22}\text{H}_{16}\text{N}_2\text{O}_3\text{F}_3$ ($[\text{M}+\text{H}]^+$) 413.1113, found 413.1117.

Preparation of **7-hydroxy-3-methyl-2-(6-(4-(trifluoromethoxy)phenyl)pyridin-3-yl)quinolin-4(1H)-one, 62g**

61g (82 mg, 0.18 mmol) was treated as in the **General procedure 7** to give **62g** as a white solid (55 mg, 68%). ^1H NMR (400 MHz, MeOD) δ 8.81 (dd, J = 2.2, 1.0 Hz, 1H), 8.33 – 8.20 (m, 3H), 8.17 – 8.13 (m, 1H), 8.11 (dd, J = 8.2, 1.0 Hz, 1H), 8.08 (dd, J = 8.2, 2.2 Hz, 1H), 7.45 (dd, J = 8.9, 0.9 Hz, 2H), 6.92 (dd, J = 8.9, 2.3 Hz, 1H), 6.89 (m, 1H), 2.06 (s, 3H); ^{13}C NMR (101 MHz, MeOD) δ 199.27, 178.62, 161.39, 156.56, 155.27, 150.26, 149.03, 145.49, 141.82, 137.97, 137.26, 130.10, 128.66,

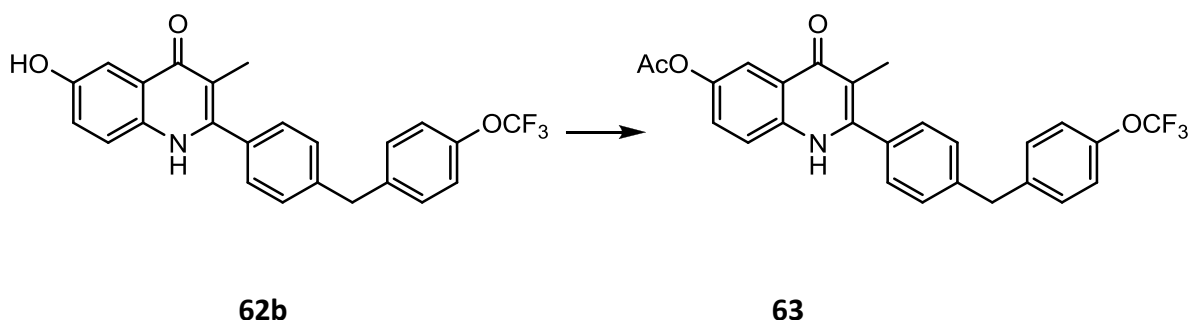
126.87, 120.95, 120.26, 117.19, 115.18, 114.82, 112.86, 100.31, 11.01; ES HRMS: m/z calculated for $C_{22}H_{16}N_2O_3F_3$ ($[M+H]^+$) 413.1113, found 413.1102.

Preparation of **8-hydroxy-3-methyl-2-(6-(4-(trifluoromethoxy)phenyl)pyridin-3-yl)quinolin-4(1H)-one, 62h**



61h (90 mg, 0.18 mmol) was treated as in the **General procedure 7** to give **62h** as a light brown solid (35 mg, 40%). mp = 154 - 156 °C 1H NMR (400 MHz, DMSO) δ 11.00 (s, 1H), 10.53 (s, 1H), 8.79 (d, J = 1.8 Hz, 1H), 8.33 (d, J = 8.8 Hz, 2H), 8.17 (d, J = 7.8 Hz, 1H), 8.06 (dd, J = 8.1, 2.2 Hz, 1H), 7.59 (dd, J = 8.2, 1.2 Hz, 1H), 7.54 (d, J = 8.1 Hz, 2H), 7.14 (t, J = 7.8 Hz, 1H), 7.05 (dd, J = 7.7, 1.4 Hz, 1H), 1.89 (s, 3H). ES HRMS: m/z calculated for $C_{22}H_{16}N_2O_3F_3$ ($[M+H]^+$) 413.1113, found 413.1109

Preparation of **3-methyl-4-oxo-2-(4-(4-(trifluoromethoxy)benzyl)phenyl)-1,4-dihydroquinolin-6-yl acetate, 63**



To a stirred solution of **62b** (42.7 mg, 0.10 mmol) in dry DCM was added Et_3N (0.12 mmol) and the mixture was stirred for 15 min at room temp. Acetyl Chloride (0.12 mmol) was then added and reacted for an hour. The reaction was quenched with water and extracted with ethyl acetate. The combined organic layer

was washed with brine, dried over MgSO_4 and concentrated under vacuum to yield a crude which was further purified by column chromatography (5% MeOH in DCM) to give **63** (33 mg, 70%) as a pale brown solid. ^1H NMR (400 MHz, DMSO) δ 11.65 (s, 1H), 7.78 (d, $J = 2.7$ Hz, 1H), 7.61 (d, $J = 9.0$ Hz, 1H), 7.51 – 7.42 (m, 6H), 7.40 (dd, $J = 9.0, 2.7$ Hz, 1H), 7.32 (d, $J = 7.9$ Hz, 2H), 4.10 (s, 2H), 2.30 (s, 3H), 1.89 (s, 3H). ES HRMS: m/z calculated for $\text{C}_{26}\text{H}_{21}\text{NO}_4\text{F}_3$ ($[\text{M}+\text{H}]^+$) 468.1423, found 468.1434 and m/z calculated for $\text{C}_{26}\text{H}_{20}\text{NO}_4\text{F}_3\text{Na}$ ($[\text{M}+\text{Na}]^+$) 490.1242, found 490.1248.

3.4.3 Biology

This part of work was done in collaboration with the Liverpool School of Tropical Medicine. Biological-related experiments were carried out by Dr Alison (Shone) Crowther, Dr Paul Bedingfield, and Dr Gemma Nixon under a supervision of Professor Giancarlo Biagini and Professor Stephen Ward.

Parasite culture

Laboratory strains of *P. falciparum* were cultured in human erythrocytes following Trager and Jensen method³¹ with modifications³². The parasites were retrieved from cryopreserved stock by thawing in water bath at 37°C until completion. 1 ml of 3.5% NaCl solution was gently added to thawed blood. The solution was centrifuged at slow speed and supernatant was removed. The culture was then initialised by adding 10 mL of 10% serum-based culture medium (RPMI-1640 supplemented with 25 mM HEPES and 4 $\mu\text{g}/\text{ml}$ gentamicin). The parasites were maintained in fresh human erythrocytes at 37°C under a low oxygen atmosphere (3% CO_2 , 4% O_2 , and 93% N_2). The culture was daily evaluated for parasitemia and parasite stages using Giemsa-stained microscopy method.

Drug sensitivity assay

Drug-sensitivity phenotypes of *P. falciparum* strains 3D7, W2, and TM90C2B (Thailand) have been described previously^{2, 33}. *In vitro* antimalarial activity of quinolones was assessed by the SYBR Green I fluorescence-based method³². The assay was set up in 96-well plates by Hamilton Star robotic platform with two-fold

dilutions of each drug across the plate at a final concentration of 2% parasitemia at 0.5% haematocrit (v/v). The dilution series was initiated at a concentration of 1 μM ranging to 0.61 nM. ATQ and CQ were used as positive control (IC_{50} (3D7) = 0.9 and 11 nM, respectively). The plates were incubated for 48 hours under a culture condition. The assay was terminated by frozen at -20°C overnight. Growth proliferation was determined by SYBR Green method. The half maximal inhibitory concentration (IC_{50}) was calculated using 'ic50' package in R programming software.

Solubility assay

Test compounds

The compounds have so far been tested in pH 7.4 (phosphats) and pH 1 (FIXANAL) buffers and in culture media. 20 μl of 10mM stock compound in DMSO was added to 980 μl of each medium in Eppendorf's. This gives a final concentration of 200 μM compound and 2% DMSO. Blanks were also made using 20 μl of DMSO in 980 μl media. For best results the experiment carries out in triplicate. The samples were rotated at room temperature over night to allow equilibration.

Using a needle the compounds were drawn up into a small syringe and passed through a 0.22 μm MILLEX GP PES membrane syringe end filter. The PES membrane in the filter is important to reduce the binding of the test compound. 200 μl of the resulting solution was transferred to a well in a UV 96 well plate (see materials).The spectrum was then read every 2nM between 200 and 400nM and the blank for each buffer was deducted.

Calibration curve

Two calibration curves of the test compounds were made using 50% DMSO and 50% buffer. pH 1 buffer was used for the pH1 samples and pH 7.4 buffer was used for the pH 7.4 and the media samples. (NB- once the DMSO was added the pH was readjusted using HCl and NaOH to counteract any variation from the dilution.)

In a UV 96 well plate a dilution series was made up for each compound using 200 μM as the top concentration with 1 in 3 dilutions i.e. 200 μM , 66.66 μM , 22.22 μM , 7.41 μM , 2.50 μM , 0.82 μM , 0.27 μM , 0.091 μM , 0 μM . The final volume in

each well was 200 μ l. This was again read on the spectrophotometer between 200 and 400nm every 2nm. The blank was deducted and a peak was selected from the graph. The absorbances at the peak's wavelength were plotted against concentration to produce a calibration curve. The maximum concentration of the compounds in the media and buffer solutions was read off the calibration curve using the absorbance at the corresponding wavelength.

pKa determination protocol

Using FIXANAL[®] buffer concentrates from Sigma-Aldrich buffers 10 buffers were made at pH 1-10. Test compounds were made up at 100 μ M in DMSO. 30 μ L of 100 μ M stock was added to 270 μ L buffer in a UV 96 well plate to give 300 μ l of 10 μ M compound in 10% DMSO pH buffer. Control wells were also made up with buffer and just 10% DMSO.

A spectrum scan was carried out on the plate reader every 2 nm between 200 and 400 nm. The control absorbance was deducted from the readings and graphs of wavelength against absorbance were plotted for each pH. Where the spectrum changes from one profile to another determines the pKa. The pKa value was determined by plotting the pH at key wavelengths and determining the 'IC₅₀' (bearing in mind that pH is already a logarithmic scale).

Metabolic stability

Pooled human liver microsomes (pooled male and female) were purchased from a reputable commercial supplier. Alternative species and strains are available upon request. Microsomes are stored at -80°C prior to use.

Microsomes (final protein concentration 0.5mg/mL), 0.1M phosphate buffer pH7.4 and test compound (final substrate concentration = 3 μ M; final DMSO concentration = 0.25%) are pre-incubated at 37°C prior to the addition of NADPH (final concentration = 1mM) to initiate the reaction. The final incubation volume is 25 μ L. A control incubation is included for each compound tested where 0.1M phosphate buffer pH7.4 is added instead of NADPH (minus NADPH). Two control

compounds are included with each species. All incubations are performed singularly for each test compound.

Each compound is incubated for 0, 5, 15, 30 and 45min. The control (minus NADPH) is incubated for 45min only. The reactions are stopped by the addition of 50 μ L methanol containing internal standard at the appropriate time points. The incubation plates are centrifuged at 2,500rpm for 20min at 4 °C to precipitate the protein. Following protein precipitation, the sample supernatants are combined in cassettes of up to 4 compounds and analysed using LC-MS/MS conditions.

From a plot of ln peak area ratio (compound peak area/internal standard peak area) against time, the gradient of the line is determined. Subsequently, half-life and intrinsic clearance are calculated using the equations below:

$$\text{Elimination rate constant (k)} = (- \text{gradient})$$

$$\text{Half-life (t}_{1/2}\text{) (min)} = 0.693/k$$

Intrinsic Clearance (CL_{int}) (μ L/min/mg protein) = V x 0.693/t_{1/2} where V=Incubation volume μ L/mg microsomal protein.

Bovine bc₁ counterscreen³⁴

Cytochrome *bc*₁ complex from bovine heart was isolated from mitochondrial membranes as described previously³⁵. Cytochrome *c* reductase activity measurements were assayed in 50 mM potassium phosphate, pH 7.5, 2 mM EDTA, 10 mM KCN, and 30 μ M equine cytochrome *c* (Sigma Chemical, Poole, Dorset, UK) at room temperature³⁶. Cytochrome *c* reductase activity was initiated by the addition of decylubiquinol (50 μ M). Reduction of cytochrome *c* was monitored in a Cary 4000 UV-visible spectrophotometer (Varian, Inc., Palo Alto, CA) at 550 versus 542 nm. Initial rates (computer-fitted as zero-order kinetics) were measured as a function of decylubiquinol concentration. The cytochrome *b* content of membranes was determined from the dithionite-reduced minus ferricyanide-oxidized difference spectra, using $\epsilon_{562-575} = 28.5 \text{ mM}^{-1} \text{ cm}^{-1}$.³⁷ Turnover rates of cytochrome *c* reduction were determined using $\epsilon_{550-542} = 18.1 \text{ mM}^{-1} \text{ cm}^{-1}$. Inhibitors of *bc*₁ activity were added without prior incubation. DMSO in the assays did not exceed 0.3% (v/v). Data

were collected and analyzed using an Online Instrument Systems Inc. computer interface and software.

3.4.4 Molecular Modeling

A homology model of *P. falciparum* cytochrome bc_1 complex was constructed using the PHYRE online homology modelling program²⁸. The *P. falciparum* cytochrome *b* primary sequence Q02768 was obtained from UNIPROT^{29a} used as the query sequence. A number of protein alignments and homology models were constructed by PHYRE and the model with the highest confidence (lowest E-value) was selected. The highest scoring *Pf* cytochrome *b* homology model was based on a *S. cerevisiae* cytochrome bc_1 complex template (PDB accession code: 1KYO). 1KYO is a 2.97 Å resolution crystal structure of cytochrome bc_1 complex co-crystallised with the ligand Stigmatellin A which is bound within the Q_o active site. The structure of the model was validated using WHATIF web interface^{29b}.

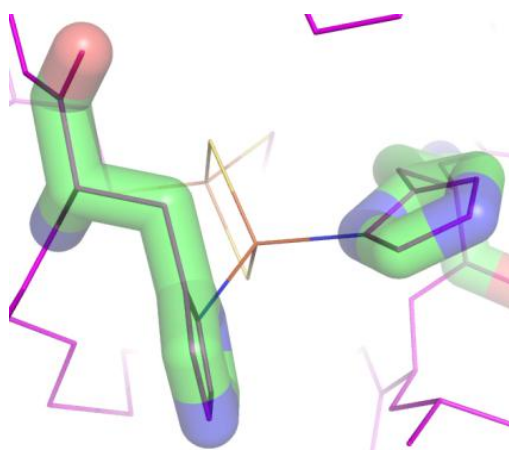


Figure 3.15 The above figure shows that *Pf* Rieske ISP homology model and the 1KYO Rieske are identical at the active site residues. The homology model ISP histidine equivalents to His161 and His181 are conserved from the 1KYO template. Given the homology model is primarily for docking purposes the accuracy Q_o site is a priority. It was easier to keep the original Rieske ISP from 1KYO than to use the *Pf* Rieske ISP homology model which contained long loop regions which could be inaccurate and cause more clashes with the cytochrome *b* homology model when orientated.

The resultant homology model of *Pf* cytochrome *b* was aligned with the original 1KYO structure with SYBYL using the alignment functions within Biopolymer module of SYBYL-X version 1.1. This enabled the *P. falciparum* cytochrome *b* to be combined with the *S. cerevisiae* Rieske iron-sulfur protein in the correct orientation as the Rieske ISP residues that constitute the bc_1 Q_o active site are invariant between the *S. cerevisiae* template and the *Plasmodium falciparum* sequences when aligned. This combined model was then checked, refined and minimised using the protein refinement modules with SYBYL's protein preparation tools.

The selected compounds were modelled *in silico* using either 3CX5 model or the modified 1KYO model described above in order to visualise the interactions between each analogue and the active site. Using GOLD, stigmatellin can be removed, protons were added and all crystallographic water molecules were removed, except for a specific water which has been described as key to the hydrogen bonding. The docking poses were optimised for the histidine and glutamate hydrogen bond interactions with quinolones. To prepare our quinolones ready to be docked into the model, three dimensional structures were constructed and their minimal energy optimised using the Spartan molecular mechanics programme. The files were then imported to GOLD and those molecules were docked into the Q_o site using the configuration previously validated by successful re-docking of stigmatellin. The key water was allowed to spin and translate from its original place with a radius of 2 Å. The docking was performed using the standard procedure and, for each quinolones, ten docking poses including its GoldScore were obtained for comparison and analysis.

3.5 References

1. (a) Pidathala, C.; Amewu, R.; Pacorel, B.; Nixon, G. L.; Gibbons, P.; Hong, W. D.; Leung, S. C.; Berry, N. G.; Sharma, R.; Stocks, P. A.; Srivastava, A.; Shone, A. E.; Charoensutthivarakul, S.; Taylor, L.; Berger, O.; Mbekeani, A.; Hill, A.; Fisher, N. E.; Warman, A. J.; Biagini, G. A.; Ward, S. A.; O'Neill, P. M., Identification, design and biological evaluation of bisaryl quinolones targeting Plasmodium falciparum type II NADH:quinone oxidoreductase (PfNDH2). *Journal of medicinal chemistry* **2012**, *55* (5), 1831-43; (b) Leung, S. C.; Gibbons, P.; Amewu, R.; Nixon, G. L.; Pidathala, C.; Hong, W. D.; Pacorel, B.; Berry, N. G.; Sharma, R.; Stocks, P. A.; Srivastava, A.; Shone, A. E.; Charoensutthivarakul, S.; Taylor, L.; Berger, O.; Mbekeani, A.; Hill, A.; Fisher, N. E.; Warman, A. J.; Biagini, G. A.; Ward, S. A.; O'Neill, P. M., Identification, design and biological evaluation of heterocyclic quinolones targeting Plasmodium falciparum type II NADH:quinone oxidoreductase (PfNDH2). *Journal of medicinal chemistry* **2012**, *55* (5), 1844-57.
2. Biagini, G. A.; Fisher, N.; Shone, A. E.; Mubarak, M. A.; Srivastava, A.; Hill, A.; Antoine, T.; Warman, A. J.; Davies, J.; Pidathala, C.; Amewu, R. K.; Leung, S. C.; Sharma, R.; Gibbons, P.; Hong, D. W.; Pacorel, B.; Lawrenson, A. S.; Charoensutthivarakul, S.; Taylor, L.; Berger, O.; Mbekeani, A.; Stocks, P. A.; Nixon, G. L.; Chadwick, J.; Hemingway, J.; Delves, M. J.; Sinden, R. E.; Zeeman, A. M.; Kocken, C. H.; Berry, N. G.; O'Neill, P. M.; Ward, S. A., Generation of quinolone antimalarials targeting the Plasmodium falciparum mitochondrial respiratory chain for the treatment and prophylaxis of malaria. *Proceedings of the National Academy of Sciences of the United States of America* **2012**, *109* (21), 8298-303.
3. Ishikawa, M.; Hashimoto, Y., Improvement in Aqueous Solubility in Small Molecule Drug Discovery Programs by Disruption of Molecular Planarity and Symmetry. *Journal of medicinal chemistry* **2011**, *54* (6), 1539-1554.
4. Lawrenson, A., Personal Communication. 2010.
5. Meyer, S. D.; Schreiber, S. L., Acceleration of the Dess-Martin Oxidation by Water. *Journal of Organic Chemistry* **1994**, *59* (24), 7549-7552.
6. Luo, F. T.; Ravi, V. K.; Xue, C. H., The novel reaction of ketones with o-oxazoline-substituted anilines. *Tetrahedron* **2006**, *62* (40), 9365-9372.
7. Giri, R.; Chen, X.; Hao, X. S.; Li, J. J.; Liang, J.; Fan, Z. P.; Yu, J. Q., Catalytic and stereoselective iodination of prochiral C-H bonds. *Tetrahedron-Asymmetry* **2005**, *16* (21), 3502-3505.
8. Hadjeri, M.; Mariotte, A. M.; Boumendjel, A., Alkylation of 2-phenyl-4-quinolones: Synthetic and structural studies. *Chem Pharm Bull* **2001**, *49* (10), 1352-1355.
9. (a) Gudmundsson, O. S.; Antman, M., Case Study: Famciclovir: A Prodrug of Penciclovir. *Biotechnol Pharm Asp* **2007**, *5*, 531-539; (b) Perry, C. M.; Wagstaff, A. J., Famciclovir - a Review of Its Pharmacological Properties and Therapeutic Efficacy in Herpesvirus Infections. *Drugs* **1995**, *50* (2), 396-415.
10. Rautio, J.; Kumpulainen, H.; Heimbach, T.; Oliyai, R.; Oh, D.; Jarvinen, T.; Savolainen, J., Prodrugs: design and clinical applications. *Nature reviews. Drug discovery* **2008**, *7* (3), 255-70.
11. Nilsen, A.; LaCrue, A. N.; White, K. L.; Forquer, I. P.; Cross, R. M.; Marfurt, J.; Mather, M. W.; Delves, M. J.; Shackelford, D. M.; Saenz, F. E.; Morrissey, J. M.; Steuten, J.; Mutka, T.; Li, Y.; Wirjanata, G.; Ryan, E.; Duffy, S.; Kelly, J. X.; Sebayang, B. F.; Zeeman, A. M.; Noviyanti, R.; Sinden, R. E.; Kocken, C. H.; Price, R. N.; Avery, V. M.; Angulo-Barturen, I.; Jimenez-Diaz, M. B.; Ferrer, S.; Herreros, E.; Sanz, L. M.; Gamo, F. J.; Bathurst, I.; Burrows, J. N.; Siegl, P.; Guy, R. K.; Winter, R. W.; Vaidya, A. B.; Charman, S. A.; Kyle, D. E.; Manetsch, R.; Riscoe, M. K., Quinolone-3-diarylethers: a new class of antimalarial drug. *Science translational medicine* **2013**, *5* (177), 177ra37.
12. Pfizer Alkoxy-substituted-6-chloro-quinazoline-2,4-diones US4287341, 1981.

13. (a) Sandmeyer, T., On iso-nitroacetanilide and its condensation to isatine. *Helvetica chimica acta* **1919**, 2, 234-242; (b) Sheibley, F. E.; McNulty, J. S., 3,5-Dichloroaniline in Sandmeyer Isatin Synthesis - 4,6-Dichloroanthranilic Acid. *Journal of Organic Chemistry* **1956**, 21 (2), 171-173; (c) Pokhodylo, N. T.; Matiychuk, V. S., Synthesis of New 1,2,3-Triazolo[1,5-a]quinazolinones. *J Heterocyclic Chem* **2010**, 47 (2), 415-420; (d) Seong, C. M.; Park, W. K.; Park, C. M.; Kong, J. Y.; Park, N. S., Discovery of 3-aryl-3-methyl-1H-quinoline-2,4-diones as a new class of selective 5-HT₆ receptor antagonists. *Bioorganic & medicinal chemistry letters* **2008**, 18 (2), 738-743.
14. Petersen, I.; Eastman, R.; Lanzer, M., Drug-resistant malaria: Molecular mechanisms and implications for public health. *FEBS letters* **2011**, 585 (11), 1551-1562.
15. McGinnity, D. F.; Soars, M. G.; Urbanowicz, R. A.; Riley, R. J., Evaluation of fresh and cryopreserved hepatocytes as in vitro drug metabolism tools for the prediction of metabolic clearance. *Drug Metab Dispos* **2004**, 32 (11), 1247-1253.
16. Cyprotex Microsomal stability. <http://www.cyprotex.com/admepk/in-vitro-metabolism/microsomal-stability/>.
17. Cyprotex Hepatocyte stability. <http://www.cyprotex.com/admepk/in-vitro-metabolism/hepatocyte-stability/>.
18. Houston, J. B., Utility of in vitro drug metabolism data in predicting in vivo metabolic clearance. *Biochemical pharmacology* **1994**, 47 (9), 1469-79.
19. Barton, V.; Fisher, N.; Biagini, G. A.; Ward, S. A.; O'Neill, P. M., Inhibiting Plasmodium cytochrome bc(1): a complex issue. *Current opinion in chemical biology* **2010**, 14 (4), 440-446.
20. Biagini, G. A.; Fisher, N.; Berry, N.; Stocks, P. A.; Meunier, B.; Williams, D. P.; Bonar-Law, R.; Bray, P. G.; Owen, A.; O'Neill, P. M.; Ward, S. A., Acridinediones: Selective and potent inhibitors of the malaria parasite mitochondrial bc(1) complex. *Molecular pharmacology* **2008**, 73 (5), 1347-1355.
21. (a) Adeniyi, A. A.; Ajibade, P. A., Comparing the Suitability of Autodock, Gold and Glide for the Docking and Predicting the Possible Targets of Ru(II)-Based Complexes as Anticancer Agents. *Molecules* **2013**, 18 (4), 3760-3778; (b) Verdonk, M. L.; Chessari, G.; Cole, J. C.; Hartshorn, M. J.; Murray, C. W.; Nissink, J. W. M.; Taylor, R. D.; Taylor, R., Modeling water molecules in protein-ligand docking using GOLD. *Journal of medicinal chemistry* **2005**, 48 (20), 6504-6515; (c) Verdonk, M. L.; Cole, J. C.; Hartshorn, M. J.; Murray, C. W.; Taylor, R. D., Improved protein-ligand docking using GOLD. *Proteins-Structure Function and Genetics* **2003**, 52 (4), 609-623.
22. Cowley, R.; Leung, S.; Fisher, N.; Al-Helal, M.; Berry, N. G.; Lawrenson, A. S.; Sharma, R.; Shone, A. E.; Ward, S. A.; Biagini, G. A.; O'Neill, P. M., The development of quinolone esters as novel antimalarial agents targeting the Plasmodium falciparum bc(1) protein complex. *Medchemcomm* **2012**, 3 (1), 39-44.
23. (a) Kessl, J. J.; Meshnick, S. R.; Trumppower, B. L., Modeling the molecular basis of atovaquone resistance in parasites and pathogenic fungi. *Trends in parasitology* **2007**, 23 (10), 494-501; (b) Nixon, G. L.; Moss, D. M.; Shone, A. E.; Laloo, D. G.; Fisher, N.; O'Neill, P. M.; Ward, S. A.; Biagini, G. A., Antimalarial pharmacology and therapeutics of atovaquone. *J Antimicrob Chemoth* **2013**, 68 (5), 977-985.
24. Fisher, N.; Majid, R. A.; Antoine, T.; Al-Helal, M.; Warman, A. J.; Johnson, D. J.; Lawrenson, A. S.; Ranson, H.; O'Neill, P. M.; Ward, S. A.; Biagini, G. A., Cytochrome b Mutation Y268S Conferring Atovaquone Resistance Phenotype in Malaria Parasite Results in Reduced Parasite bc(1) Catalytic Turnover and Protein Expression. *Journal of Biological Chemistry* **2012**, 287 (13), 9731-9741.
25. Kessl, J. J.; Ha, K. H.; Merritt, A. K.; Lange, B. B.; Hill, P.; Meunier, B.; Meshnick, S. R.; Trumppower, B. L., Cytochrome b mutations that modify the ubiquinol-binding pocket of the cytochrome bc(1) complex and confer anti-malarial drug resistance in *Saccharomyces cerevisiae*. *Journal of Biological Chemistry* **2005**, 280 (17), 17142-17148.

26. Birth, D.; Kao, W. C.; Hunte, C., Structural analysis of atovaquone-inhibited cytochrome bc(1) complex reveals the molecular basis of antimalarial drug action. *Nature communications* **2014**, *5*.
27. Painter, H. J.; Morrisey, J. M.; Mather, M. W.; Vaidya, A. B., Specific role of mitochondrial electron transport in blood-stage Plasmodium falciparum. *Nature* **2007**, *446* (7131), 88-91.
28. Kelley, L. A.; Sternberg, M. J. E., Protein structure prediction on the Web: a case study using the Phyre server. *Nat Protoc* **2009**, *4* (3), 363-371.
29. (a) Vriend, G., What If - a Molecular Modeling and Drug Design Program. *J Mol Graphics* **1990**, *8* (1), 52-56; (b) SYBYL-X 1.1 Software. www.tripos.com/sybylx.
30. Hinsberger, S.; Husecken, K.; Groh, M.; Negri, M.; Hauptenthal, J.; Hartmann, R. W., Discovery of novel bacterial RNA polymerase inhibitors: pharmacophore-based virtual screening and hit optimization. *Journal of medicinal chemistry* **2013**, *56* (21), 8332-8.
31. Trager, W.; Jensen, J. B., Human Malaria Parasites in Continuous Culture. *Science* **1976**, *193* (4254), 673-675.
32. Smilkstein, M.; Sriwilaijaroen, N.; Kelly, J. X.; Wilairat, P.; Riscoe, M., Simple and inexpensive fluorescence-based technique for high-throughput antimalarial drug screening. *Antimicrobial agents and chemotherapy* **2004**, *48* (5), 1803-1806.
33. (a) Bray, P. G.; Mungthin, M.; Ridley, R. G.; Ward, S. A., Access to hemozoin: The basis of chloroquine resistance. *Molecular pharmacology* **1998**, *54* (1), 170-179; (b) Suswam, E.; Kyle, D.; Lang-Unnasch, N., Plasmodium falciparum: The effects of atovaquone resistance on respiration. *Experimental parasitology* **2001**, *98* (4), 180-187.
34. Kessler, J. J.; Moskalev, N. V.; Gribble, G. W.; Nasr, M.; Meshnick, S. R.; Trumpower, B. L., Parameters determining the relative efficacy of hydroxy-naphthoquinone inhibitors of the cytochrome bc1 complex. *Biochimica et biophysica acta* **2007**, *1767* (4), 319-26.
35. Ljungdahl, P. O.; Pennoyer, J. D.; Robertson, D. E.; Trumpower, B. L., Purification of highly active cytochrome bc1 complexes from phylogenetically diverse species by a single chromatographic procedure. *Biochimica et biophysica acta* **1987**, *891* (3), 227-41.
36. Fisher, N.; Castleden, C. K.; Bourges, I.; Brasseur, G.; Dujardin, G.; Meunier, B., Human disease-related mutations in cytochrome b studied in yeast. *The Journal of biological chemistry* **2004**, *279* (13), 12951-8.
37. Vanneste, W. H., Molecular proportion of the fixed cytochrome components of the respiratory chain of Keilin-Hartree particles and beef heart mitochondria. *Biochimica et biophysica acta* **1966**, *113* (1), 175-8.

Chapter IV: Alternative synthetic route towards PG227

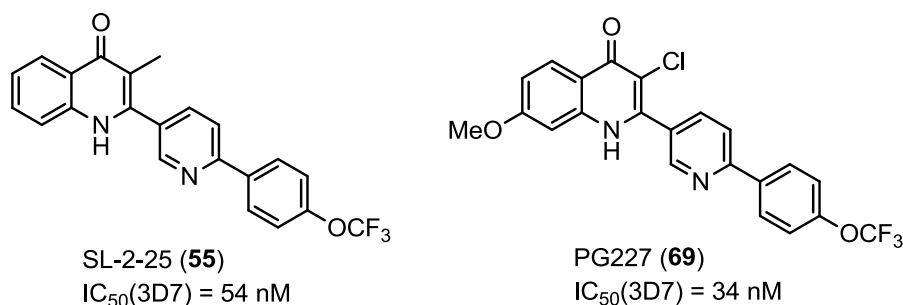
Chapter IV: Alternative synthetic route towards PG227

	page
4.1 Background	142
4.1.1 Pharmacological, physicochemical and pharmacokinetics profiles of PG227	144
4.1.2 The synthesis of PG227	147
4.2 Results and discussion	149
4.3 Conclusion	155
4.4 Experimental	156
4.5 References	164

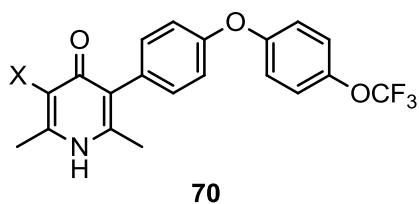
Alternative synthetic route towards PG227

4.1 Background

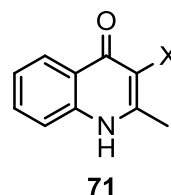
Shortly after the discovery of SL-2-25 (**55**), it became evident that the physico-chemical properties of this lead needed to be improved¹. The poor aqueous solubility of **55** impacts on the pharmacokinetic profile by limiting drug exposure making safety margin assessments in preclinical toxicological evaluations extremely difficult; this problem also occurred for the GSK pyridone programme and continues to hamper the development of the ELQ-300 series of quinolones. To resolve the insolubility problem, formulations of **55** including phosphate salt and morpholine prodrug were investigated, and they showed excellent *in vitro* activity and PK profiles in rodent models¹. However, to avoid the necessity of using a pro-drug approach, it was clear that further lead optimisation of the SL-2-25 scaffold was required. By increasing inherent drug potency, the possibility of reducing the oral dose to sub mg/kg levels, was considered as a possible development route for the quinolone series.



It is evident that the incorporation of halogen onto the pyridone or quinolone core can enhance the antimalarial activity. In the pyridone case (**70**), the work done by Yeates *et al.* showed that halogenation at C-3 increased *in vitro* activity about 5-fold and there was a little difference between 3-Br and 3-Cl (**Figure 4.1**)².



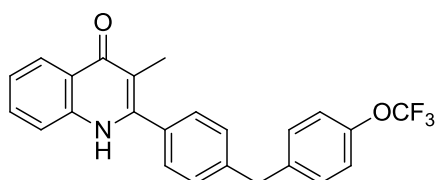
X = H : IC₅₀ (T9-96) = 0.16 μM
 Cl : IC₅₀ (T9-96) = 0.03 μM
 Br : IC₅₀ (T9-96) = 0.03 μM



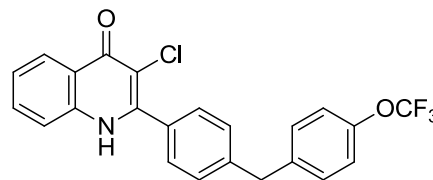
X = H (**71a**) IC₅₀ (TM90-C2B) = inactive
 Br (**71b**) IC₅₀ (TM90-C2B) = 77.6 nM

Figure 4.1 Comparison between 3-halogen and 3-H substitution on pyridone and quinolone

There are a few examples of 3-halogenated quinolones previously identified from the Manetsch group. While the 2-methyl-4-quinolone (**71a**) is completely devoid of antimalarial activity, introduction of a 3-bromo substituent brought the activity back to the quinolone **71**³. Comparing bisaryl quinolones **107** and **108**, the presence of chlorine atom at C-3 greatly enhances the *in vitro* whole-cell activity⁴. It is noteworthy that the reduction in *Pf*NDH2 inhibition is observed suggesting a possible change in molecular target such as the *bc*₁ complex.



CK-2-67 (**107**)
 IC₅₀(3D7) = 117 nM
 IC₅₀(*Pf*NDH2) = 16 nM



109
 IC₅₀(3D7) = 19 nM
 IC₅₀(*Pf*NDH2) = 137 nM

In the on-going programme focusing on antimalarial quinolones, PG227 (**69**) was first synthesised in the O'Neill group at the University of Liverpool. It exhibits high antiparasitic properties against both *in vivo* and *in vitro*, and also possesses good pharmacokinetics and bioavailability in rat model.

4.1.1 Pharmacological, physicochemical and pharmacokinetics profiles of PG227

Compared to SL-2-25, PG227 shows superior properties in many respects. PG227 is active against *Pfbc*₁ with an IC₅₀ of ~10 nM and against *PfNDH2*, with an IC₅₀ of ~150 nM. Addition to the standard testing, PG227 was assayed against drug resistant strains of *P. falciparum* including chloroquine resistant W2 and atovaquone resistant TM90C2B. PG227 shows excellent activities against both W2 and TM90C2B with an IC₅₀ of 4 and 5 nM, respectively, which are greater than SL-2-25's (IC₅₀ (W2) = 48 nM, IC₅₀ (TM90C2B) = 56 nM).

Compound	Vehicle	ED ₅₀ (mg/kg)	ED ₉₀ (mg/kg)
SL-2-25	PEG400	4.45	8.95
PG227	PEG400	0.13	0.26
ELQ300*	unknown	~0.25	~0.45

* estimated from a graph from presentation

Table 4.1 *In vivo* activity of the quinolones using Peter's Standard 4-Day test.

Drug	Vehicle	ED ₅₀ (mg/Kg)	ED ₉₀ (mg/Kg)
PG227	PEG400	0.46	0.59
PG227	GSK Vehicle	4.2	5.4
PG227 acetate Prodrug	PEG400	0.75	1.1
PG227 acetate Prodrug	GSK Vehicle	4.3	5.5
<i>PG227 (standard four day test)</i>	PEG400	0.13	0.26

Note : PG227 in PEG400, top dose cured the mice of infection (mice inspected 7 days after final dose)

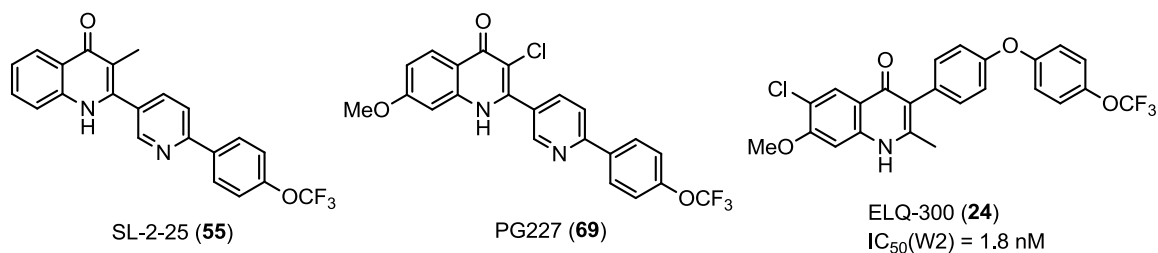
: GSK Vehicle: 01% Hydroxypropyl cyclodextrin, 10% EtOH, 10% propylene glycol, 40% PEG-400, 39% PBS.

Table 4.2 *In vivo* activity of the quinolones in the *Berghei* model –Using the modified Peter's Standard Four Day test (infect day 0 and begin dosing on day 3)

According to Peter's standard four-day test⁵ (**Table 4.1**), PG227 had an ED₅₀/ED₉₀ of 0.13 mg/kg and 0.26 mg/kg indicating far superior *in vivo* potency than SL-2-25 and ELQ-300. The choice of vehicle in the *in vivo* efficacy studies has a significant effect on PG227 efficacy. PEG400 vehicle appears to deliver the drug more efficiently than GSK vehicle resulting in lower ED₅₀ and ED₉₀ values. This vehicle effect is probably the result of the low solubility of PG227 with PEG400

providing an improved solubilisation for oral administration. Drug dosing on the day (standard Peter's) vs 3-day post infection has a two-fold effect on efficacy (entry 1 and 5 in **Table 4.2**).

The lead optimisation that led to PG227 included an assessment of the physicochemical, metabolic and pharmacokinetic properties to identify features that would limit oral bioavailability and exposure profiles. Early in this programme, it was realised that the most important limitation was very poor aqueous solubility. It was hoped that the pyridyl heterocycle would aid solubility since the nitrogen lone-pair can be protonated in an acidic environment; as can be seen in the **Table 4.3**, even at pH1, PG227 still has lower than expected solubility suggesting that the pKa of the pyridyl nitrogen $\ll 5$.



Compound	Max Solubility (μM)			pKa	Melting Point $^{\circ}\text{C}$	Caco-2 Permeability ($\text{cm} \times 10^{-6} \text{ s}^{-1}$)
	pH1	pH7.4	Media			
PG227	<1	<1	>150	LS*	345 (decomposed)	2.2
SL-2-25	3.2	<1	48	<1.5	277-278	14.8
ELQ300	<1	<1	40	ND	ND	ND
Atovaquone	<1	<1	>150	8.6	ND	ND

*LS = low solubility, ND = not determined

Table 4.3 Comparison between PG227, SL-2-25 ELQ-300 and atovaquone.

In addition to low aqueous solubility, PG227 exhibited very high binding (range: 99.7 to >99.9%) to proteins in human, dog, rat and mouse plasma and high binding (95.9%) to components in human liver microsomes at 0.5 mg/mL protein concentration. PG227 was stable in human, rat and mouse plasma and whole blood, and the apparent whole blood to plasma partitioning ratios across the three species

ranged from 0.59 to 0.71. PG227 exhibited low degradation in human, rat and mouse cryopreserved hepatocytes (**Table 4.4**) and therefore would be expected to be subject to low hepatic metabolic clearance *in vivo*.

	% Plasma Protein Bound	B/P ratio	Microsomal stability CL _{int} (μL/min/mg)	Hepatocytes degradation CL _{int} (μL/min/10 ⁶ cell)
Human	99.9	0.63 (S)	5.33 (t _{1/2} = 260 min)	<3.4
Dog	99.7	-	-	-
Rat	> 99.9	0.60 (S)	1.06	<1.8
Mouse	99.8	0.68 (S)	-	<1.9
Human Microsomes	95.9	-	-	-

*B:P = blood/plasma partition, S = stable in both blood and plasma

Table 4.4 Plasma Protein Binding, blood/plasma partitioning, microsomal stability and hepatocyte degradation of PG227

Cytochrome P450	IC ₅₀ (μM)
CYP1A2	> 20
CYP2C9	17.6
CYP2C19	> 20
CYP2D6	> 20
CYP3A4/5	> 20
Testosterone	> 20
Midazolam	>20

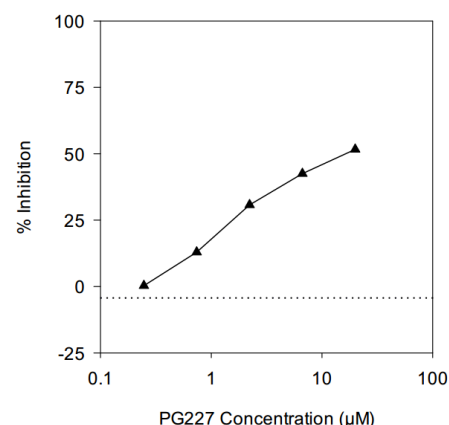


Table 4.5 A) Cytochrome P450 inhibition and **Figure 4.2** Percent inhibition plot for PG227 against CYP2C9-mediated tolbutamide methylhydroxylation in human liver microsomes.

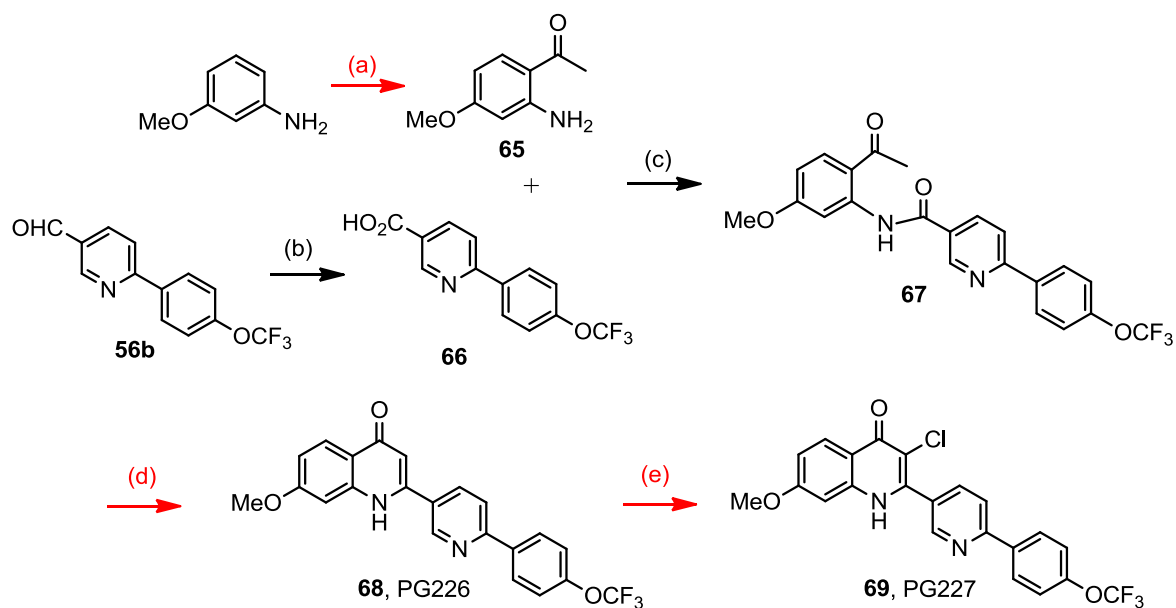
PG227 exhibited low inhibition against the five CYP isoforms with IC₅₀ values in the majority of cases being greater than the highest concentration tested in this assay (i.e. 20 μM; **Table 4.5**). Since there was no evidence of compound precipitation following spiking of PG227 into incubation buffer (in the absence of

microsomes) and since there was a concentration dependent increase in inhibition noted against CYP2C9 (**Figure 4.2**), the high IC₅₀ values observed for PG227 are likely to be due to lack of inhibitory effect rather than an artefact of limited solubility under the assay conditions.

In summary, PG227 is active against *P.falciparum* malaria with a greater potency *in vitro* and *in vivo* but still suffers from poor aqueous solubility. Based on the profile, MMV selected PG227 for further studies including an assessment of the *in vivo* activity in the *Pf*SCID model of infection. The original synthesis of PG227 gave a poor overall yield, and for this reason a new synthetic approach was required.

4.1.2 The synthesis of PG227

The original synthesis of PG227 includes the synthesis of two intermediates which were then coupled and cyclised. The first compound, 1-(2-amino-4-methoxyphenyl)ethanone, **65**, was successfully made by the Friedel-Crafts acylation of *m*-anisidine in the presence of boron trichloride. The carboxylic acid **66** was synthesised from the aldehyde **56b** by reacting with selenium dioxide in a solution of hydrogen peroxide. The coupling reaction between **65** and **66** gives the amide intermediate **67**. The cyclisation of **67** proceeds in a basic solution of *t*-BuOK in *t*-BuOH. The 3-chlorine atom was then added using sodium dichloroisocyanurate in NaOH as a chlorinating agent. The overall yield was low and unpredictable and was unsuitable for scale-up purposes.



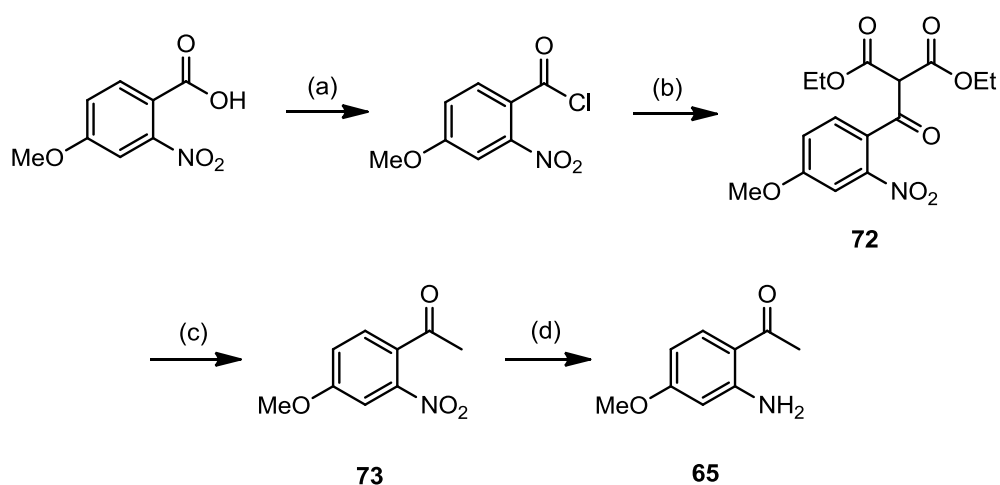
Scheme 4.1 Original synthesis of PG227 *Reagents* : (a) AcCl, BCl₃, DCM (b) SeO₂, H₂O₂, 2 h, 75 °C. (c) (COCl)₂, cat. DMF, DCM, 2 h, rt. then **65**, triethylamine, THF, overnight, rt. (d) *t*-BuOK, *t*-BuOH, overnight, 75 °C. (e) sodium dichloroisocyanurate, 1 M NaOH, MeOH, overnight, rt.

The key disadvantages of this route highlighted in red are (i) the Friedel-Crafts acylation, (ii) base-mediated cyclisation, and (iii) 3-chlorination. With respect to the Friedel-Crafts acylation, this chemistry gave variable yields with mixtures of products being obtained. The harsh condition used in the cyclisation step (d) was not suitable in a large-scale synthesis. For step (e), the 3-chlorination can only be done on a small-scale batch (less than 500-mg scale).

4.2 Result and discussion

In searching for an alternative approach towards compound **69**, a literature review showed that one of the intermediates can be made by another route involving cheaper starting materials and simpler chemistry⁶. The intermediate **65** which was previously made by the Friedel-Crafts acylation can also be prepared from its corresponding nitrobenzoic acid. The conversion of commercially available 4-methoxy-2-nitrobenzoic acid to its methyl ketone can be accomplished by transforming to its acyl chloride and reacted with a malonate ester carbanion.

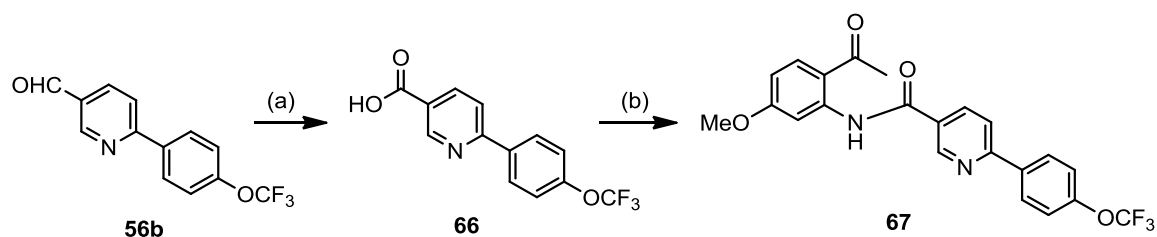
The resulting yellow oil of β -keto malonate **72** was then subjected to a double-decarboxylation procedure using a mixture of acetic acid and 4 N sulfuric acid solution to obtain the corresponding methyl ketone in good yield. The nitro moiety of **73** was then hydrogenated to the aniline **65** using iron dust in acetic acid. This alternative route can be used to prepare the intermediate in gram scale⁶. The overall yield from commercially available material is 34%.



Scheme 4.2 Reagents: (a) $(\text{COCl})_2$, cat. DMF, DCM, 2 h, rt. (b) diethyl malonate, NaOEt, THF, 1 h, 110 °C (c) AcOH, 4 N sulfuric acid, 4 h, 130 °C, 51% (over 3 steps). (d) iron dust, AcOH, EtOH, 1 h, 125 °C, 67%.

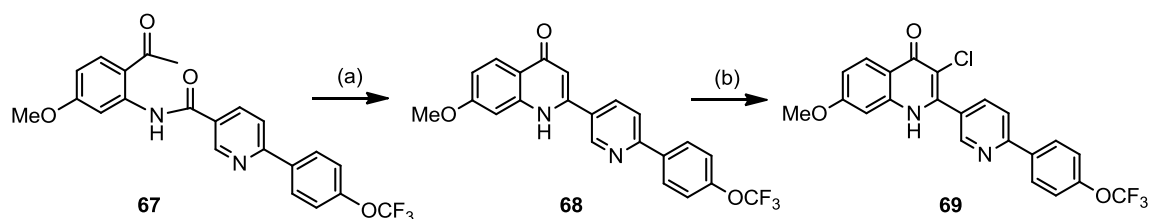
The pyridyl carboxylic acid **66** was made from the corresponding aldehyde **56b** according to the original method involving the use of SeO_2 in a solution of H_2O_2 ⁷. The amide coupling can be done by reaction of the acid chloride derived

from **66** with amine **65**. These two reactions worked well and gave good yields without any difficulties in purification.



Scheme 4.4 Reagents: (a) SeO_2 , H_2O_2 , 2 h, 75°C , 77 %. (b) $(\text{COCl})_2$, cat. DMF, DCM, 2 h, rt. then **11**, triethylamine, THF, overnight, rt, 95%.

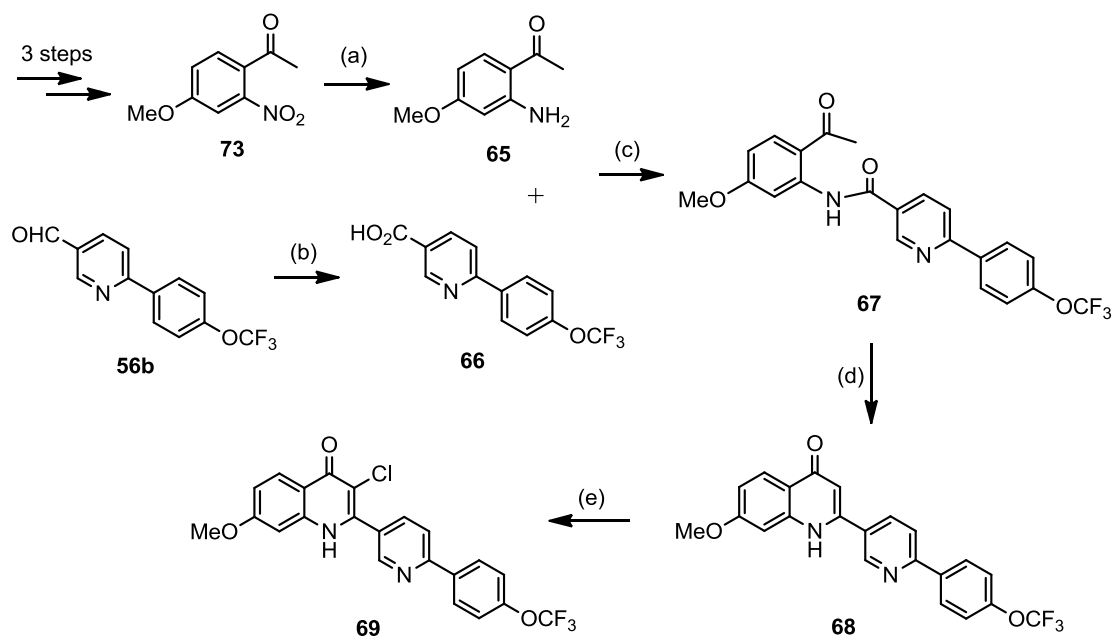
Several attempts were made to optimise the cyclisation step. A choice of bases, including NaOH and NaOEt, were used. Unfortunately, due to the insolubility and polarity of quinolones, it was difficult to purify and quantify the product using column chromatography. The cyclisation was found to proceed best with *t*-BuOK confirming earlier parallel work performed in the group. However, it was difficult to quantify the product as was contaminated with the base residue left from the reaction. As a result, spectroscopic spectra were poor and it was impossible to obtain a clean ^{13}C NMR spectrum due to insolubility even in DMSO; however, MS and ^1H NMR spectrum were identical to the previous work.



Scheme 4.5 Reagents: (a) *t*-BuOK, *t*-BuOH, overnight, 75°C . (b) sodium dichloroisocyanurate, 1 M NaOH, MeOH, overnight, rt.

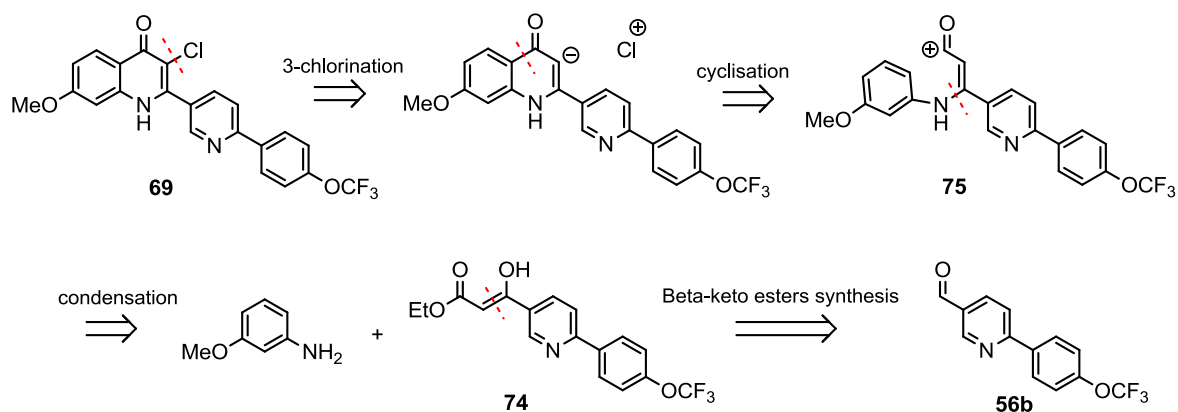
The 3-chlorination was accomplished by using sodium dichloroisocyanurate in 1 M NaOH as a chlorinating agent⁴. The yield of this step was acceptable with the product **69** seems the major product in the crude reaction mixture and the product could be purified by standard column chromatography. The HPLC trace and

elemental analysis also show that the product purity is more than 95%. The synthesis can be summarised in the scheme below.



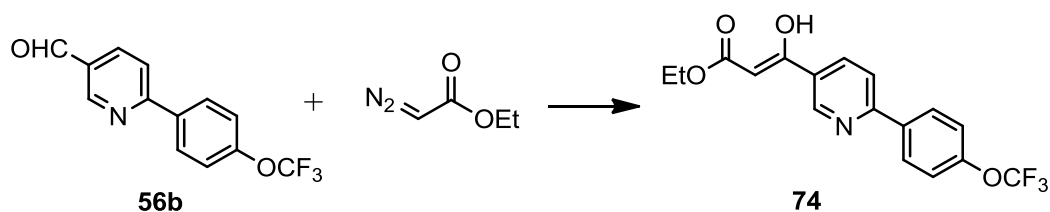
Scheme 4.6 Route A: Synthesis of PG227 via amide coupling. *Reagents:* (a) iron dust, AcOH, EtOH, 1 h, 125 °C. (b) SeO₂, H₂O₂, 2 h, 75 °C. (c) (COCl)₂, cat. DMF, DCM, 2 h, rt. then **65**, triethylamine, THF, overnight, rt. (d) *t*-BuOK, *t*-BuOH, overnight, 75 °C. (e) sodium dichloroisocyanurate, 1 M NaOH, MeOH, overnight, rt.

Overall, *Route A* still mainly relies on the original synthetic steps and attempts to optimise were met with moderate success. The aim of this research then turned to finding a novel synthetic approach towards PG227. A brief literature revisit in Chapter II showed that the quinolone can be successfully made by other approaches, for example, the Conrad-Limpach reaction. The Conrad-Limpach reaction involves the condensation of anilines with β -keto esters to form 4-quinolones via a Schiff base⁸. Based on this chemistry, the retrosynthetic analysis of PG227 can be drawn as below.



Scheme 4.7 The retrosynthetic analysis of PG227 - Route B

This synthesis requires the enamine intermediate whose cyclisation leads to the formation of quinolone core⁹. The enamine **75** can be made of *m*-anisidine and β -keto ester **74** which was synthesised from the corresponding aldehyde.

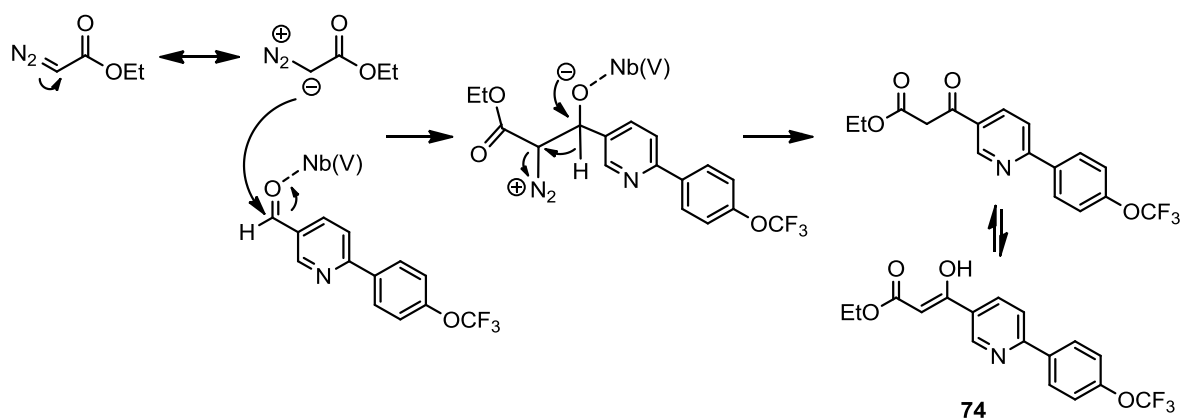


Scheme 4.8 Reagents: ethyl diazoacetate, cat. NbCl_5 , DCM, 3 days, rt., 43%.

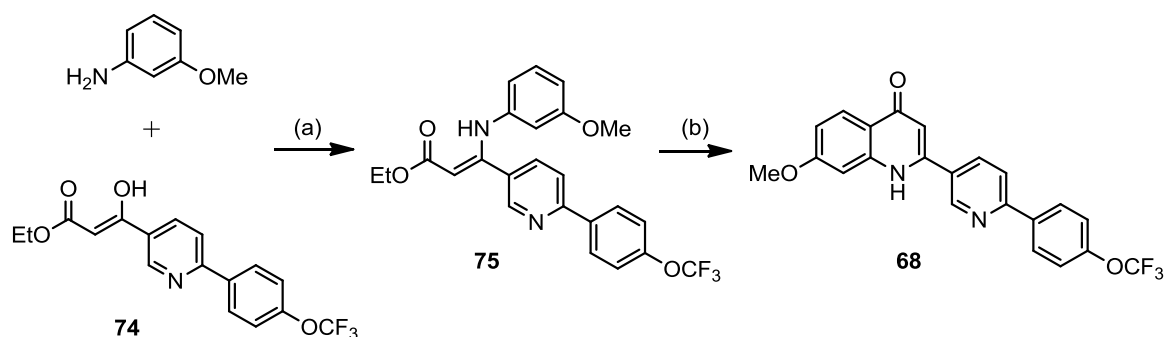
The aldehyde **56b** was made from commercially available boronic acid and nicotinaldehyde and it was previously reported in the Chapter III which is an excellent starting material for this synthesis as it can be prepared in multi-gram scale. Following a similar procedure^{1, 10}, the aldehyde reacts readily with ethyl diazoacetate in the presence of 5 mol% of NbCl_5 in dichloromethane to produce the corresponding β -keto esters in good yield with high selectivity. The chromatographic purification can be difficult as the product and starting material share a similar R_f in a range of 0.4-0.5 on TLC when eluted twice with 10% EtOAc in hexane. The conversion yield can be improved by adding a same proportion of ethyl diazoacetate to the reaction after a course of every 24 h. With this method, β -keto ester **74** can be prepared, and, according to the corresponding $^1\text{H-NMR}$ peaks at 12.61 and 5.75, its structure should be described as an enol

tautomer. The mechanism was also explained in the original work published in 2005¹⁰.

The reaction proceeds through the activated complexation between aldehyde and Nb(V). The nucleophilic diazoacetate then added to carbonyl carbon, the C=O bond was cleaved followed by 1,2-hydride shift with loss of N₂ resulting in the formation of β-keto ester.



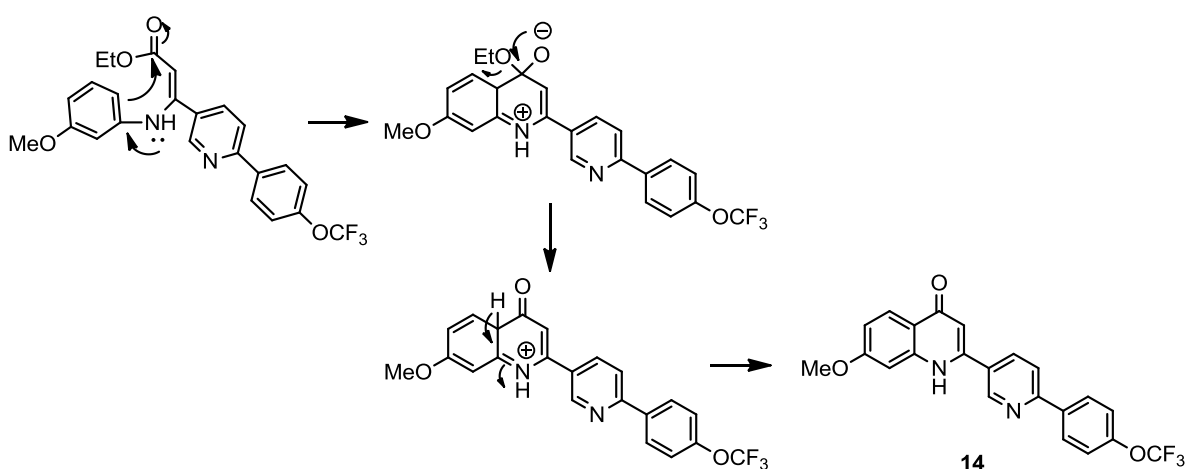
Scheme 4.9 Mechanism of Nb(V)-mediated synthesis of β-keto esters



Scheme 4.10 Reagents: (a) acetic acid, ethanol, 2 h, reflux, 50%. (b) Dowtherm A, 1 h, 240 °C, 64 %

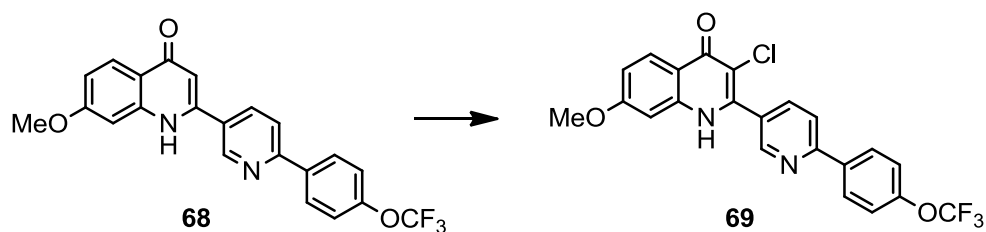
The Conrad-Limpach enamine intermediate **75** can be prepared from β-keto esters **74** and aniline in a solution of acetic acid in ethanol under a reflux condition⁹. The ring closure reaction of **75** then readily takes place in such a high-boiling-point solvent as Dowtherm A⁴. The advantage of this reaction is that the conversion yield is generally good and the product purification is easy. In this case, the resulting precipitate was collected and washed with hexane and ethyl acetate to give an off-

white solid of **68** without any further purification. Spectroscopic data were identical to previously reported. The mechanism can be depicted below.



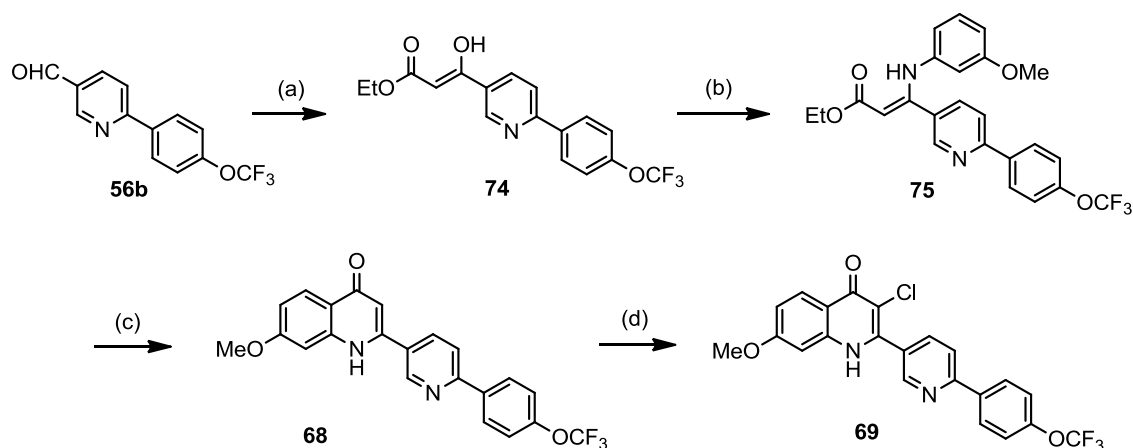
Scheme 4.11 Mechanism of the Conrad-Limpach cyclisation

N-Chlorosuccinimide (NCS) is used for chlorinations and as a mild oxidant. This reagent was reported to be able to replace sodium dichloroisocyanurate in 3-chlorination¹¹. **68** and NCS dissolved in warm acetic acid were left to react for 18 h. The reaction proceeded well with high conversion yield.



Scheme 4.12 Reagents: NCS, AcOH, DCM, 18 h, 35 °C, 60%.

The alternative synthesis towards PG227 can be accomplished in 5 steps from commercially available and cheap starting materials using alternative chemistries with the benefit of being able to enlarge the batch size. The summary of *Route B* synthesis *via* β -keto ester intermediate and the Conrad-Limpach cyclisation is displayed below. The overall yield was 7% over 5 steps starting from commercially available chemicals.



Scheme 4.13 *Route B: Synthesis of PG227 via β -keto ester and the Conrad-Limpach cyclisation.* Reagents: (a) ethyl diazoacetate, cat. NbCl_5 , DCM, 3 days, rt., 43%. (b) *m*-anisidine, acetic acid, ethanol, 2 h, reflux, 50%. (c) Dowtherm A, 1 h, 240 °C, 64 %. (d) NCS, AcOH, DCM, 18 h, 35 °C, 60%.

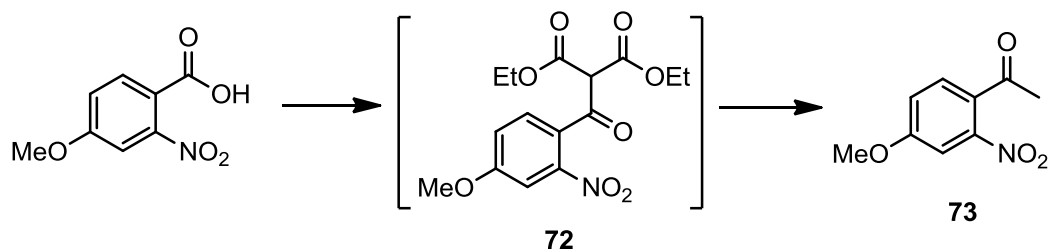
4.3 Conclusion

PG227 (**69**) exhibits an outstanding pharmacological properties amongst a series of quinolones made within the O'Neill group. Its original synthesis suffers from reproducibility and low overall yields. A literature search as described in Chapter II shows several synthetic preparations towards quinolone core and this provided the impetus for a new approach. PG227 now can be successfully made in a large-scale batch (multi-gram scale) using an alternative method for cyclisation. The 5-step synthesis of PG227 can be achieved from commercially available starting materials and the synthesis includes the synthesis of β -keto ester intermediate made from the corresponding aldehyde reacting with ethyl diazoacetate in the presence of NbCl_5 . The Conrad-Limpach cyclisation reaction was used to construct the quinolone core and the chlorination was done using NCS. The overall yield was 7%. This approach can also be used as a general scale-up synthetic route towards 2-aryl-3-chloro quinolone template.

4.4 Experimental

Route A: Synthesis of PG227 via amide coupling (see Scheme 4.6)

Preparation of **1-(4-methoxy-2-nitrophenyl)ethanone, 73**⁶



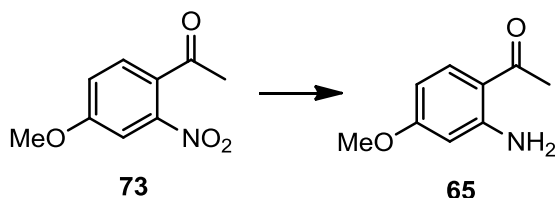
To a solution of 4-methoxy-2-nitrobenzoic acid (8.0 g, 40.8 mmol) in anhydrous DCM (60 mL) was added oxalyl chloride (5.2 mL, 7.77 g, 61 mmol) and a few drops of DMF. The reaction was left for 2 hours at room temperature and the progress was followed by TLC. Once the reaction completed, all solvent was evaporated to obtain corresponding benzoyl chloride which was used as such in the following step.

To a THF solution (50 mL) of diethyl malonate (6.8 mL, 7.2 g, 45 mmol) in an oven-dried two-neck flask equipped with a water condenser, NaOEt (3.06 g, 45 mmol) was added and the mixture was allowed to reflux at 110 °C for half an hour. The crude benzoyl chloride dissolved in THF (30 mL) was added to the stirred solution via septum. After being allowed to reflux for another half an hour, 4 N sulfuric acid solution was added until all solid disappeared. Extraction with ether, drying and removal of solvent gave crude yellow oil of diethyl 2-(4-methoxy-2-nitrobenzoyl)malonate, **72**.

The oil from previous step was allowed to reflux at 130 °C in acetic acid (50 mL) and 4 N sulfuric acid (25 mL) for 4 hours. Cooling, basification, extraction with ether yielded sticky oil which was purified by column chromatography over silica gel (40% EtOAc/Hexane) to yield 1-(4-methoxy-2-nitrophenyl)ethanone as pale yellow crystal (4.09 g, 51% over 2 steps). ¹H NMR (400 MHz, CDCl₃) δ 7.47 (d, *J* = 8.5 Hz, 1H), 7.43 (d, *J* = 2.5 Hz, 1H), 7.17 (dd, *J* = 8.5, 2.5 Hz, 1H), 3.92 (s, 3H), 2.52 (s, 3H). ¹³C NMR (101 MHz, CDCl₃) δ 198.57, 161.96, 148.72, 130.22, 128.27, 118.78, 109.91,

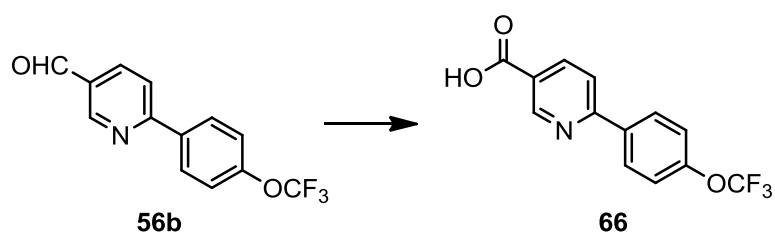
56.50, 29.52. Elemental Analysis calculated for $C_9H_9NO_4$: C, 55.39; H, 4.65; N, 7.18. Found: C, 54.95; H, 4.48; N, 7.05.

Preparation of **1-(2-amino-4-methoxyphenyl)ethanone, 65**⁶



1-(4-Methoxy-2-nitrophenyl)ethanone, **73** (3.9 g, 20 mmol) was added during one hour to a stirred solution of iron dust (3.3 g, 60 mmol), acetic acid (30 mL), and ethanol (30 mL). After being allowed to reflux at 125 °C for another hour, the mixture was filtered, concentrated, and dissolved in EtOAc. The organic layer was washed with bicarb., brine, dried over MgSO₄ and concentrated to give a crude. Purification was performed using column chromatography over silica gel (40% EtOAc/Hexane) to obtain 1-(2-amino-4-methoxyphenyl)ethanone (2.2 g, 67%); mp = 118.0 – 118.5 °C; ¹H NMR (400 MHz, CDCl₃) δ 7.64 (d, *J* = 9.0 Hz, 1H), 6.24 (dd, *J* = 9.0, 2.5 Hz, 1H), 6.09 (d, *J* = 2.5 Hz, 1H), 3.81 (s, 3H), 2.52 (s, 3H). ¹³C NMR (101 MHz, CDCl₃) δ 199.44, 164.74, 152.72, 134.51, 113.50, 105.02, 99.86, 55.64, 28.03. Elemental Analysis calculated for $C_9H_9NO_4$: C, 65.44; H, 6.71; N, 8.48. Found: C, 65.15; H, 6.69; N, 8.25.

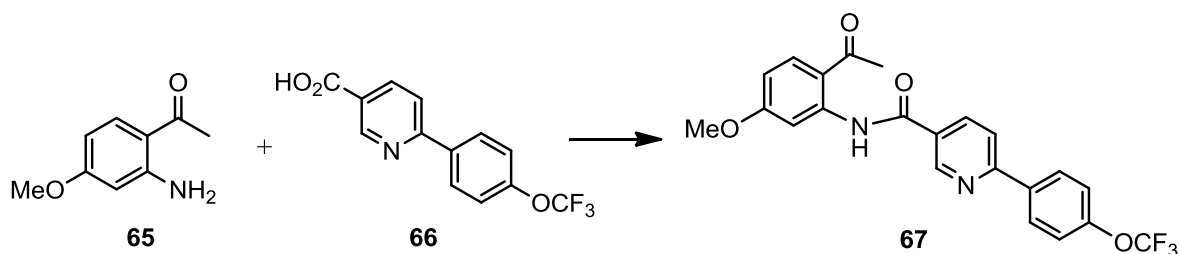
Preparation of **6-(4-(trifluoromethoxy)phenyl)nicotinic acid, 66**



To the THF solution (40 mL) of aldehyde **56b** (4.0 g, 15 mmol) was added SeO₂ (832 mg, 7.5 mmol) and H₂O₂ (3.8 mL of 27 % solution, 1.02 g, 30 mmol) and the mixture was refluxed for 2 hours at 75 °C. After that, the reaction was allowed to cool before a spatula of Pd/C (10%) was added to quench the excess H₂O₂. The mixture was filtered and the solvent removed. 2.5% NaHCO₃ solution was added

and extracted with EtOAc. The aqueous layer was acidified with 10% HCl and extracted with EtOAc. The organic layer was dried over MgSO_4 , filtered and concentrated to yield a white solid. Purification was done using column chromatography over silica gel (50% EtOAc/Hexane) to obtain 6-(4-(trifluoromethoxy)phenyl)nicotinic acid (3.25 g, 77%) as white solid. ^1H NMR (400 MHz, CDCl_3) δ 9.34 (d, $J = 1.5$ Hz, 1H), 8.45 (dd, $J = 8.3, 2.1$ Hz, 1H), 8.13 (d, $J = 8.9$ Hz, 2H), 7.85 (d, $J = 8.3$ Hz, 1H), 7.37 (d, $J = 8.1$ Hz, 2H). ESI HRMS: m/z calculated for $\text{C}_{13}\text{H}_9\text{NO}_3\text{F}_3$ ($[\text{M}+\text{H}]^+$) 284.0535, found 284.0547.

Preparation of **N-(2-acetyl-5-methoxyphenyl)-6-(4-(trifluoromethoxy)phenyl)nicotinamide, 67**

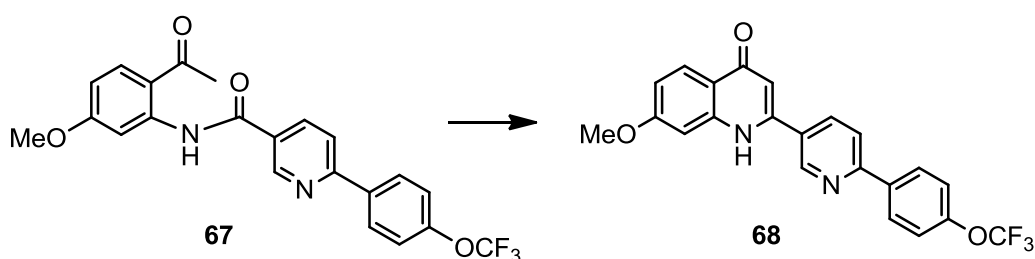


To a solution of 6-(4-(trifluoromethoxy)phenyl)nicotinic acid, **66** (1.7 g, 6 mmol) in anhydrous DCM (40 mL) was added thionyl chloride (0.7 mL, 1.14 g, 9 mmol) and a few drops of DMF. The reaction was left for 2 hours at room temperature. After the reaction was completed (TLC), all solvent was evaporated to obtain a crude product that was used in the next step without any further purification.

To a solution of the crude acyl chloride from previous step in THF (40 mL) was added 1-(2-amino-4-methoxyphenyl)ethanone, **67** (991 mg, 6 mmol) and triethylamine (0.9 mL, 668 mg, 6.6 mmol). The reaction was stirred overnight. After the reaction was completed, brine (40 mL) was added and the mixture was extracted with EtOAc (3 x 40 mL). The combined organic layer was washed with bicarb., brine, dried over MgSO_4 and evaporated to yield a crude which was purified by column chromatography (40% EtOAc/Hexane) to obtain the product as white solid (2.46 g, 95% over 2 steps).

^1H NMR (400 MHz, CDCl_3) δ 13.31 (s, 1H), 9.40 (d, $J = 2.2$ Hz, 1H), 8.63 (d, $J = 2.6$ Hz, 1H), 8.45 (dd, $J = 8.3, 2.3$ Hz, 1H), 8.19 – 8.11 (m, 2H), 7.94 – 7.86 (m, 2H), 7.37 (d, $J = 8.2$ Hz, 2H), 6.71 (dd, $J = 8.9, 2.6$ Hz, 1H), 3.96 (s, 3H), 2.68 (s, 3H). ^{13}C NMR (101 MHz, CDCl_3) δ 202.22, 165.51, 164.41, 158.61, 149.30, 144.12, 136.88, 136.47, 134.29, 129.45, 121.59, 120.72, 115.89, 110.76, 104.60, 56.16, 28.69. ESI HRMS: m/z calculated for $\text{C}_{22}\text{H}_{17}\text{N}_2\text{O}_4\text{F}_3\text{Na}$ ($[\text{M}+\text{Na}]^+$) 453.1038, found 453.1043.

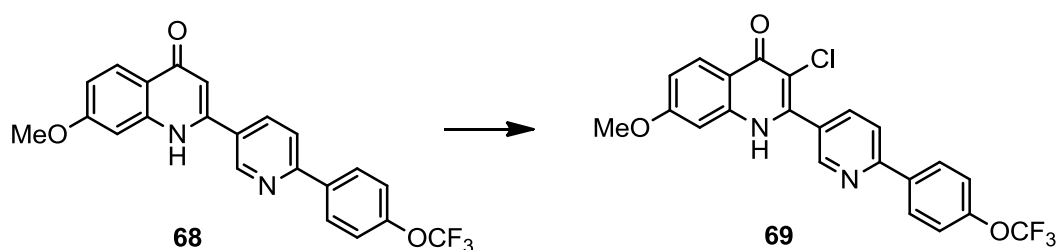
Preparation of **7-methoxy-2-(6-(4-(trifluoromethoxy)phenyl)pyridin-3-yl)quinolin-4(1H)-one**, PG226 or **68**.



67 (1.59 g, 3.7 mmol) was dissolved in *t*-butanol (25 mL) and allowed to stir. *t*-BuOK (1.45 g, 12.5 mmol) was added and the mixture was heated at 75°C overnight. The reaction mixture was allowed to cool before 2 M HCl was added until the solution turn acidic. The yellow precipitate crashed out and it was filtered to yield a solid which was washed with water to obtain **68**.

^1H NMR (400 MHz, DMSO) δ 11.74 (s, 1H), 9.15 (s, 1H), 8.40 – 8.32 (m, 3H), 8.25 (d, $J = 8.4$ Hz, 1H), 8.02 (d, $J = 9.0$ Hz, 1H), 7.55 (d, $J = 8.3$ Hz, 2H), 7.18 (d, $J = 1.8$ Hz, 1H), 6.97 (dd, $J = 8.8, 1.7$ Hz, 1H), 6.45 (s, 1H), 3.89 (s, 3H). ESI HRMS: m/z calculated for $\text{C}_{22}\text{H}_{16}\text{N}_2\text{O}_3\text{F}_3$ ($[\text{M}+\text{H}]^+$) 413.1113, found 413.1127.

Preparation of **3-chloro-7-methoxy-2-(6-(4-(trifluoromethoxy)phenyl)pyridin-3-yl)quinolin-4(1H)-one**, PG227 or **69**.

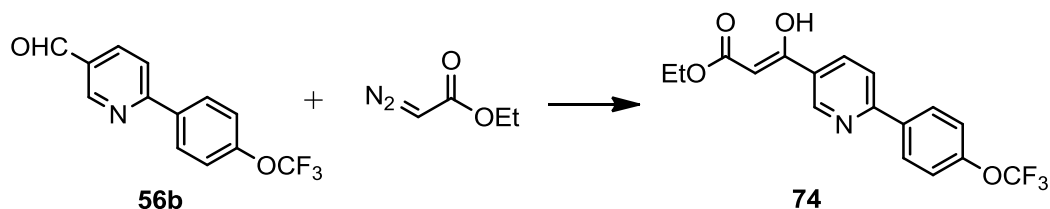


68 was dissolved in MeOH (60 mL) and 1 M NaOH (40 mL) was added. Sodium dichloroisocyanurate was added to yield a yellow solution after heating with a heat gun to aid the dissolving of the starting material. The mixture was allowed to stir at room temperature overnight. After this time, MeOH was removed *in vacuo* to yield a yellow solid which was then dissolved in EtOAc and washed with water. The organic layer was dried over MgSO₄ and purified by column chromatography eluting with EtOAc to obtain the desired product **69**.

¹H NMR (400 MHz, DMSO) δ 12.25 (s, 1H), 8.97 (s, 1H), 8.34 (d, *J* = 8.9 Hz, 2H), 8.29 – 8.23 (m, 2H), 8.09 (d, *J* = 9.7 Hz, 1H), 7.56 (d, *J* = 8.0 Hz, 2H), 7.07 – 7.01 (m, 2H), 3.87 (s, 3H). ESI HRMS: *m/z* calculated for C₂₂H₁₄N₂O₃F₃³⁵ClNa ([M+Na]⁺) 469.0543, found 469.0538. Elemental Analysis calculated for C₂₂H₁₄N₂O₃F₃Cl: C, 59.14; H, 3.16; N, 6.27. Found: C, 58.85; H, 3.09; N, 5.78.

Route B: Synthesis of PG227 via β -keto ester and the Conrad-Limpach cyclisation (see Scheme 4.13)

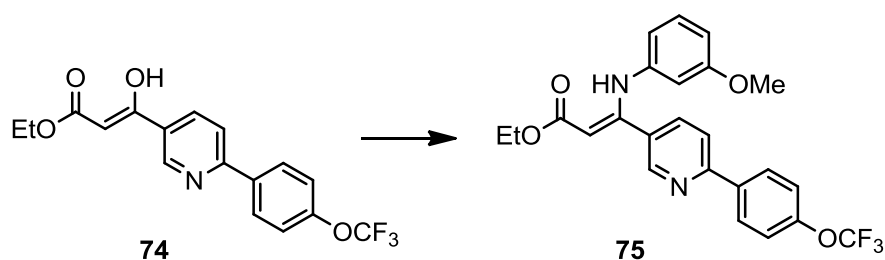
Preparation of **ethyl 3-hydroxy-3-(6-(4-(trifluoromethoxy)phenyl)pyridin-3-yl)acrylate, 74**



Aldehyde **56b** (5.78 g, 21.6 mmol) and NbCl₅ (238 mg, 1.08 mmol) were dissolved in dry DCM (150 mL) under N₂. Ethyl diazoacetate (2.7 mL, 2.95 g, 25.9 mmol) was added dropwise and the reaction allowed to stir at room temperature for 3 days. Water (150 mL) was added and the layers separated. The aqueous layer was extracted with DCM (3 x 150 mL) and the combined organic layer was dried over MgSO₄, filtered, and the solvent was evaporated. The crude was purified by column chromatography (10% EtOAc/Hexane) to give ethyl 3-hydroxy-3-(6-(4-(trifluoromethoxy)phenyl)pyridin-3-yl)acrylate as white solid (3.34 g, 43%).

¹H NMR (400 MHz, CDCl₃) δ 12.61 (s, 1H, enol OH), 9.06 (dd, J = 2.2, 0.6 Hz, 1H), 8.14 (dd, J = 8.4, 2.3 Hz, 1H), 8.09 (d, J = 8.9 Hz, 2H), 7.78 (dd, J = 8.4, 0.7 Hz, 1H), 7.34 (d, J = 8.0 Hz, 2H), 5.75 (s, 1H, CO-CH=CO), 4.30 (q, J = 7.1 Hz, 2H), 1.36 (t, J = 7.1 Hz, 3H). ESI HRMS: m/z calculated for C₁₇H₁₄NO₄F₃Na ([M+Na]⁺) 376.0773, found 376.0774.

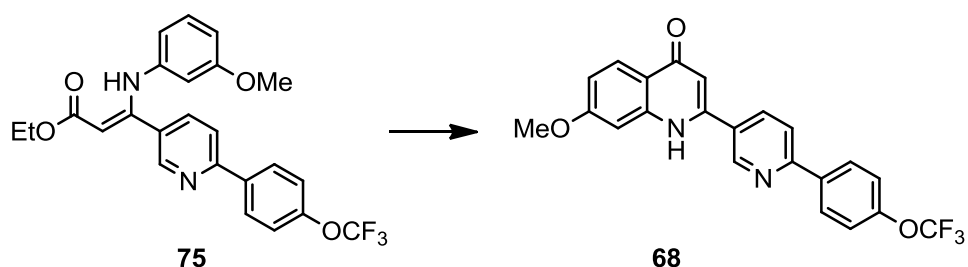
Preparation of ethyl 3-((3-methoxyphenyl)amino)-3-(6-(4-(trifluoromethoxy)phenyl)pyridin-3-yl)acrylate, **75**



β -keto ester **74**, ethyl 3-oxo-3-(6-(4-(trifluoromethoxy)phenyl)pyridin-3-yl)propanoate (3.34 g, 9.45 mmol), and *m*-anisidine (5.3 mL, 5.8 g, 47 mmol) were heated in a solution of acetic acid (2.7 mL, 2.82 g, 47 mmol) and ethanol (10 mL) at reflux for 2 hours. The reaction was cooled down to r.t. and the solvent evaporated. The resulting residue was dissolved in DCM (30 mL) and washed with 2 M HCl and water. The organic layer was dried over MgSO_4 , filtered, and concentrated under vacuum. The crude was chromatographed (20% EtOAc/Hexane) to yield the desired product as light yellow oil (2.16 g, 50%).

^1H NMR (400 MHz, CDCl_3) δ 10.23 (s, 1H), 8.74 (s, 1H), 8.06 (d, $J = 8.7$ Hz, 2H), 7.75 (d, $J = 8.6$ Hz, 1H), 7.67 (d, $J = 8.3$ Hz, 1H), 7.33 (d, $J = 8.5$ Hz, 2H), 7.01 (t, $J = 8.1$ Hz, 1H), 6.52 (dd, $J = 8.3, 2.4$ Hz, 1H), 6.31 (t, $J = 2.0$ Hz, 1H), 6.28 (dd, $J = 8.1, 1.7$ Hz, 1H), 5.09 (s, 1H), 4.24 (q, $J = 7.1$ Hz, 2H), 3.63 (s, 3H), 1.34 (t, $J = 7.1$ Hz, 3H). ESI HRMS: m/z calculated for $\text{C}_{24}\text{H}_{21}\text{N}_2\text{O}_4\text{F}_3\text{Na}$ ($[\text{M}+\text{Na}]^+$) 481.1351, found 481.1361.

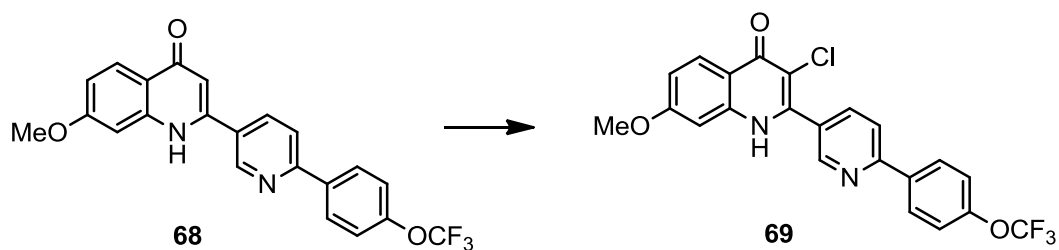
Preparation of 7-methoxy-2-(6-(4-(trifluoromethoxy)phenyl)pyridin-3-yl)quinolin-4(1H)-one, PG226 or **68**.



75 (2.42 g, 5.28 mmol) was dissolved in Dowtherm A (10 mL) and heated to 240 °C for an hour. The reaction was cooled, and diluted with hexane. The resulting

precipitate was collected and washed with hexane and ethyl acetate to give the product (1.4 g, 64%) as off-white solid without any further purification. Spectroscopic data were consistent with previously reported data.

Preparation of **3-chloro-7-methoxy-2-(6-(4-(trifluoromethoxy)phenyl)pyridin-3-yl)quinolin-4(1H)-one**, PG227 or **69**.



68 (1.4 g, 3.4 mmol) in acetic acid (7 mL) was sonicated and allowed to warm until all had dissolved, then NCS (498 mg, 3.73 mmol) was added and the mixture was allowed to warm to 35°C for 18 hours. After cooling down, the solid was filtered off. The filtrate was concentrated and purified by column chromatography (80% EtOAc/Hexane) to give **69** (910 mg, 60%). Spectroscopic data were consistent with previously reported data.

4.5 References

1. Leung, S. C.; Gibbons, P.; Amewu, R.; Nixon, G. L.; Pidathala, C.; Hong, W. D.; Pacorel, B.; Berry, N. G.; Sharma, R.; Stocks, P. A.; Srivastava, A.; Shone, A. E.; Charoensutthivarakul, S.; Taylor, L.; Berger, O.; Mbekeani, A.; Hill, A.; Fisher, N. E.; Warman, A. J.; Biagini, G. A.; Ward, S. A.; O'Neill, P. M., Identification, design and biological evaluation of heterocyclic quinolones targeting Plasmodium falciparum type II NADH:quinone oxidoreductase (PfNDH2). *Journal of medicinal chemistry* **2012**, *55* (5), 1844-57.
2. Yeates, C. L.; Batchelor, J. F.; Capon, E. C.; Cheesman, N. J.; Fry, M.; Hudson, A. T.; Pudney, M.; Trimming, H.; Woolven, J.; Bueno, J. M.; Chicharro, J.; Fernandez, E.; Fiandor, J. M.; Gargallo-Viola, D.; de las Heras, F. G.; Herreros, E.; Leon, M. L., Synthesis and structure-activity relationships of 4-pyridones as potential antimalarials. *Journal of medicinal chemistry* **2008**, *51* (9), 2845-2852.
3. Cross, R. M.; Monastyrskyi, A.; Mutka, T. S.; Burrows, J. N.; Kyle, D. E.; Manetsch, R., Endochin optimization: structure-activity and structure-property relationship studies of 3-substituted 2-methyl-4(1H)-quinolones with antimalarial activity. *Journal of medicinal chemistry* **2010**, *53* (19), 7076-94.
4. Pidathala, C.; Amewu, R.; Pacorel, B.; Nixon, G. L.; Gibbons, P.; Hong, W. D.; Leung, S. C.; Berry, N. G.; Sharma, R.; Stocks, P. A.; Srivastava, A.; Shone, A. E.; Charoensutthivarakul, S.; Taylor, L.; Berger, O.; Mbekeani, A.; Hill, A.; Fisher, N. E.; Warman, A. J.; Biagini, G. A.; Ward, S. A.; O'Neill, P. M., Identification, Design and Biological Evaluation of Bisaryl Quinolones Targeting Plasmodium falciparum Type II NADH:Quinone Oxidoreductase (PfNDH2). *Journal of medicinal chemistry* **2012**, *55* (5), 1831-1843.
5. Peters, W.; Robinson, B. L., The chemotherapy of rodent malaria. LVI. Studies on the development of resistance to natural and synthetic endoperoxides. *Ann Trop Med Parasit* **1999**, *93* (4), 325-339.
6. Osborn, A. R.; Schofield, K., Cinnolines .34. 5-Hydroxy-Cinnolines,6-Hydroxy-Cinnolines and 7-Hydroxy-Cinnolines and 5-Amino-Cinnolines,6-Amino-Cinnolines and 7-Amino-Cinnolines. *J Chem Soc* **1955**, 2100-2103.
7. Brzascz, M.; Kloc, K.; Maposah, M.; Mlochowski, J., Selenium(IV) oxide catalyzed oxidation of aldehydes to carboxylic acids with hydrogen peroxide. *Synthetic Commun* **2000**, *30* (24), 4425-4434.
8. Brouet, J. C.; Gu, S.; Peet, N. P.; Williams, J. D., A Survey of Solvents for the Conrad-Limpach Synthesis of 4-Hydroxyquinolones. *Synth Commun* **2009**, *39* (9), 5193-5196.
9. Kuo, S. C.; Lee, H. Z.; Juang, J. P.; Lin, Y. T.; Wu, T. S.; Chang, J. J.; Lednicer, D.; Paull, K. D.; Lin, C. M.; Hamel, E.; et al., Synthesis and cytotoxicity of 1,6,7,8-substituted 2-(4'-substituted phenyl)-4-quinolones and related compounds: identification as antimetabolic agents interacting with tubulin. *Journal of medicinal chemistry* **1993**, *36* (9), 1146-56.
10. Yadav, J. S.; Reddy, B. V. S.; Eeshwaraiah, B.; Reddy, P. N., Niobium(V) chloride-catalyzed C-H insertion reactions of alpha-diazoesters: synthesis of beta-keto esters. *Tetrahedron* **2005**, *61* (4), 875-878.
11. GlaxoGroupLtd ANTIBACTERIAL AGENTS. US2007287701 (A1) 2006.

Chapter V: Design, synthesis and *in vitro*
evaluation of activity-based protein profiling
probes in *Plasmodium falciparum*

Chapter V: Design, synthesis and *in vitro* evaluation of activity-based protein profiling probes in *Plasmodium falciparum*

	page
5.1 Introduction to artemisinin	167
5.2 Proposed mechanism of action	169
5.2.1 Activation of artemisinin	169
5.2.2 Potential molecular targets of the artemisinins	172
5.2.2.1 Heme	172
5.2.2.2 <i>Pf</i> ATP6ase	173
5.2.2.3 Parasite's proteins and other macromolecules	174
5.3 Activity-based proteomics or activity-based protein profiling (ABPP)	175
5.4 Aim	176
5.5 Results and discussion	178
5.5.1 The synthesis of artemisinin-based ABPP chemical probes	178
5.5.2 Biological experiments	187
5.5.2.1 Antimalarial activity	187
5.5.2.2 Protein profiling	189
5.6 Conclusion	191
5.7 Experimental	192
5.7.1 Synthesis	193
5.7.2 Protein tagging and identification	206
5.8 References	209

Design, synthesis and *in vitro* evaluation of activity-based protein profiling probes to investigate the targets of artemisinin

5.1 Introduction to artemisinin

Artemisinin (ART), a sesquiterpene lactone natural product from the leaves of sweet woodworm - *Artemisia annua*, has been used in Chinese folk medicine for thousand years to treat fever and illness. Its structure was first determined in 1979 by x-ray analysis showing a unique peroxide bridge in its molecule¹, and it is well documented that this functional group is critical to its antimalarial activity².

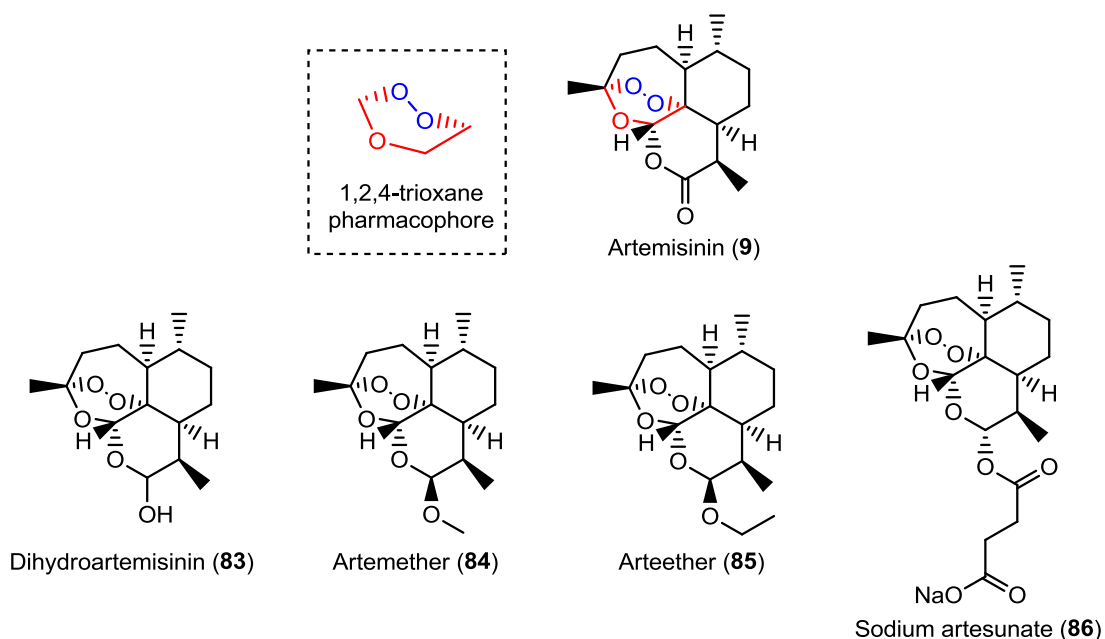


Figure 5.1 Artemisinin and its first generation derivatives.

Although ART is toxic to malaria parasites at low nanomolar concentrations and is relatively safe in humans, its poor physicochemical property limits its effectiveness. This led to the development of semi-synthetic first generation artemisinin derivatives including dihydroartemisinin (DHA) (**83**), artemether (**84**), arteether (**85**), and carboxyl-containing artesunate(**86**). The main drawback of early ART derivatives is the short half-life of the active metabolite dihydroartemisinin (DHA) (**83**) which is rapidly eliminated by metabolic transformation leading to a half-life of less than 1 hour³. Several fully synthetic follow-up agents to ART are summarised in the Chapter I.

Use of ART derivatives alone as monotherapies is discouraged by WHO as there has been a sign that parasites are developing resistance to the drug. As a result, ART derivatives are used in a combination with a longer half-life drug such as amodiaquine (**12**), mefloquine (**4**), lumefantrine, sulfadoxine/pyrimethamine or piperazine. Artemisinin-based combination therapy (ACT) features several improvements over monotherapy administration. The slow-acting partner drug not only possesses a longer half-life, but it generally operates through a different mechanism of action. Therefore, when ACT is taken, the endoperoxide rapidly kills most of the parasites before it is metabolised and excreted, and the non-peroxidic drug slowly clears the rest⁴. ACT is still used as the first line treatment in most of the malarial endemic areas⁵ and is recommended by the WHO for uncomplicated *falciparum* malaria⁶. To ensure that both active ingredients in ACTs are taken, combining an artemisinin derivative with a slower-acting partner drug in one tablet is preferred (a fixed-dose combination). Unfortunately, a single-dose cure is not possible with current ACTs.

Combination	Description
Artesunate and amodiaquine (Coarsucam or ASAQ)	A potential disadvantage is a suggested link with neutropenia.
Artesunate and mefloquine (Artequin or ASMQ)	This has been used as a first-line treatment in areas of Thailand for many years. Mefloquine is known to cause some side effects; interestingly these adverse reactions seem to be reduced when the drug is combined with artesunate.
Artemether and lumefantrine (Coartem Riamet, Faverid, Amatem, Lonart or AL)	This combination has been extensively tested proving effective in children under 5 and has been shown to be better tolerated than artesunate-mefloquine combinations. There are no serious side effects. This is the most viable option for widespread use.

Combination	Description
Artesunate and sulfadoxine/pyrimethamine (Ariplus or Amalar plus)	This is a well-tolerated combination but the overall level of efficacy still depends on the level of resistance to sulfadoxine and pyrimethamine thus limiting its usage.
Dihydroartemisinin and piperaquine (Duo-Cotecxin, or Artekin)	Has been studied mainly in China, Vietnam and other countries in Southeast Asia. The drug has been shown to be highly efficacious (greater than 90%).

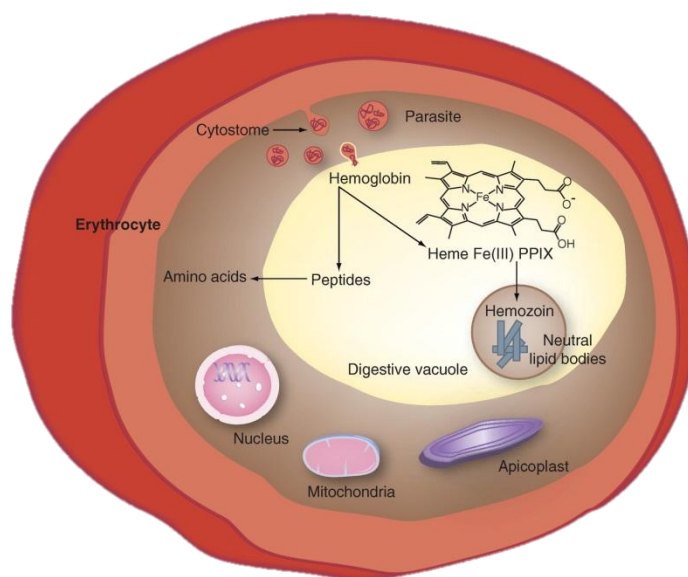
Table 5.1 Table of available ACTs⁶

5.2 Proposed mechanism of action⁷

In terms of the mechanism of action of the artemisinins, several proposals have been published over years, but the exact mechanism has yet to be clarified. Understanding the mechanism will allow us to predict any potential resistance mechanisms and aid the design of future antimalarial agents within this class. It is now well known that the peroxide bridge is essential for activity of these antimalarials. Reduction of the endoperoxide bridge of artemisinin gives an analogue, deoxyartemisinin (**87**), which lacks pharmacological activity.

5.2.1 Activation of artemisinin

During the trophozoite stage of *Plasmodium* parasite, host haemoglobin is digested by parasite's protease enzymes to release small peptides and amino acids which are necessary as nutrients for the parasite. Free heme is also produced and is highly toxic to the parasite. To circumvent this toxicity, the parasite has developed a detoxifying mechanism where heme undergoes biocrystallisation to form an insoluble non-toxic hemozoin⁸.



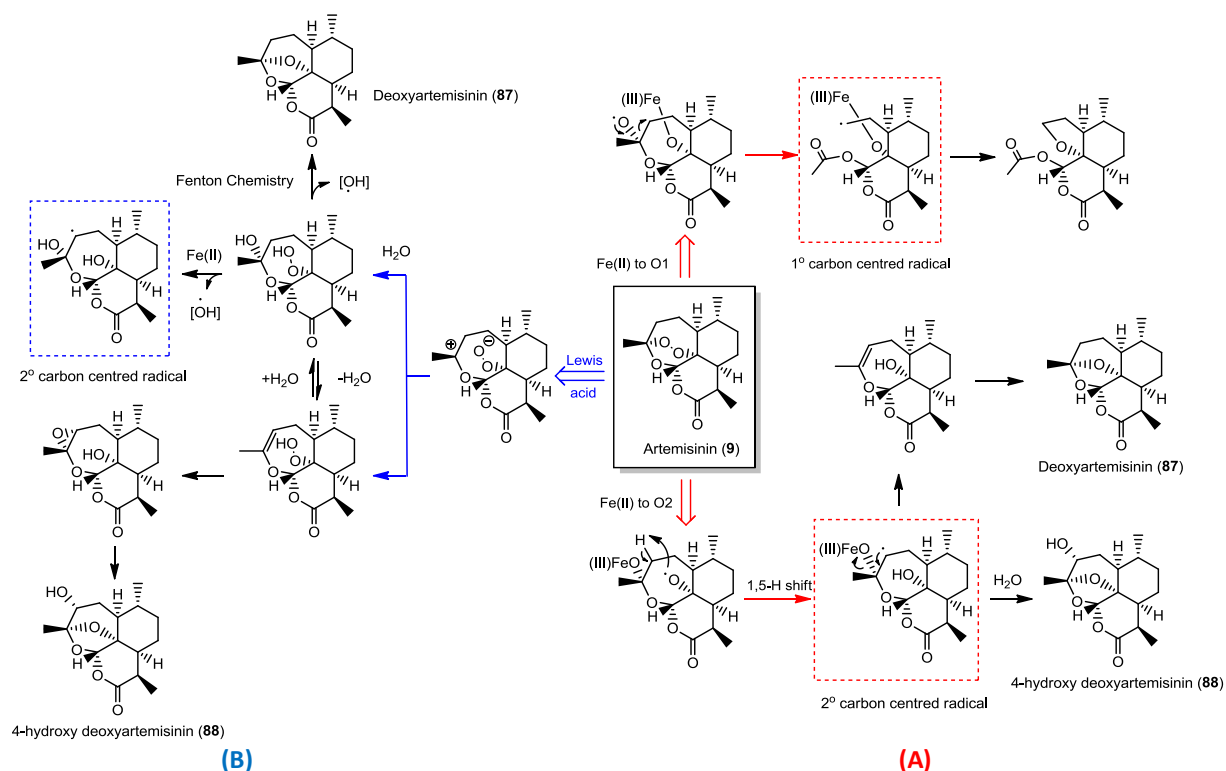
Scheme 5.1 Representation of hemozoin formation within a host red blood cell⁹.

One of the first studies completed by the Meshnick group¹⁰ showed that the activation of 1,2,4-trioxanes is triggered by iron (II) produced during haemoglobin degradation and it generates toxic activated oxygen products. Early works done by Posner¹¹ and Jefford¹² also proposed that these oxygen centred radicals subsequently rearrange to form carbon centred radicals. Since these findings, it has been suggested that the interaction between artemisinin and iron plays a role in the activation of artemisinin.

There are two different type of reductive activation of artemisinin depending on the role of iron in the activation of artemisinin and its capability to interact with artemisinin to produce a range of reactive intermediates.

Reductive scission model suggests that low valent irons (ferrous or Fe^{2+} ion) were found to bind to artemisinin and, after a single-electron transfer (SET), the reductive cleavage of peroxide bridge was induced to produce oxygen centred radicals where rearrangement occurs to give carbon radicals (**Scheme 5.2A**). Due to the unsymmetrical structure of artemisinin, iron was found to react with the endoperoxide in different ways to form either a primary or secondary carbon

centred radical¹³. Both of them have been characterised by EPR trapping techniques¹⁴.



Scheme 5.2 Reductive bioactivation of artemisinin. (A) Reductive scission model shows the homolytic activation in red. (B) Open peroxide model shows heterolytic bioactivation in blue⁷.

Alternatively, Haynes has proposed the open peroxide model that the ring opening can be facilitated by protonation of the peroxide or by complexation with Fe²⁺ which, in this case, acts as a Lewis acid initiating the ionic-type heterolytic cleavage of artemisinin endoperoxide¹⁵ (**Scheme 5.2B**). It has also been suggested that non-peroxidic oxygen plays a role in the ring opening to generate the open hydroperoxide¹⁶. The oxygen atom can stabilise the positive charge, and lower the activating energy required for the ring opening. The cleavage of endoperoxide bridge and subsequent reactions lead to the formation of an unsaturated hydroperoxide which can directly oxidise protein residues. This mechanism has the potential to produce reactive oxygen species that may infer the antimalarial activity of these compounds.

5.2.2 Potential molecular targets of the artemisinins

5.2.2.1 Heme

The identification of heme-drug adducts by mass spectrometry first reported by Meshnick is a solid evidence of heme alkylation^{10, 17}. The further experiments on artemisinin and heme show that artemisinin can alkylate a heme model at different positions¹⁸. Studies with synthetic peroxides also support this mechanism as elucidated by LC-MS¹⁹.

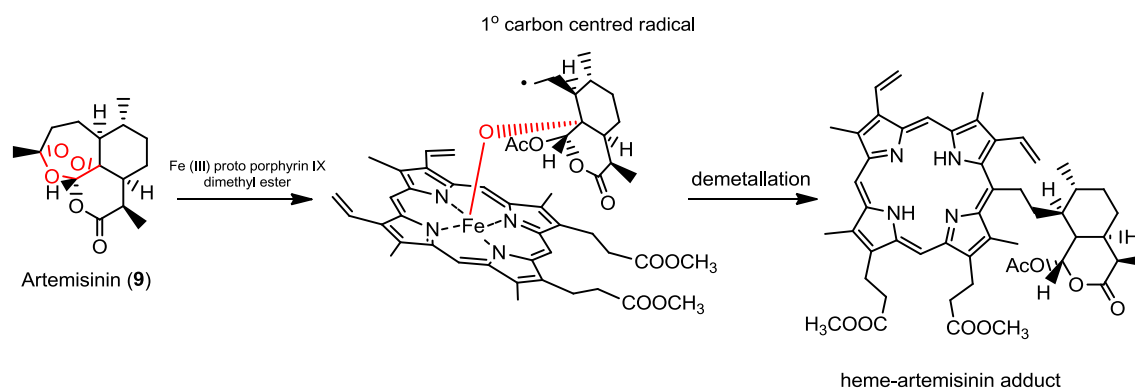
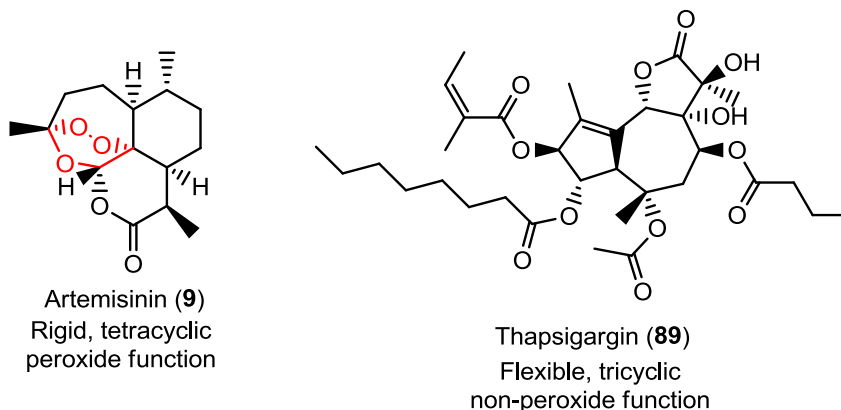


Figure 5.2 Alkylation of a heme model by a carbon-centred radical derived from artemisinin¹⁸.

The heme-artemisinin adducts were also found in the urine of mice infected with malaria and treated with artemisinin²⁰. While these results suggest that the interference with hemozoin formation is a possible mechanism, it has also been attested since the *in vivo* result can be doubted. In the studies with infected mice model, it was found that the heme-drug adducts possibly came from *ex vivo* process occurring in liver and spleen of infected mice²¹.

5.2.2.2 PfATP6ase

SERCA or sarco/endoplasmic reticulum membrane calcium ATPase is a Ca^{2+} transporting enzyme. SERCA and its homologues are critical for calcium homeostasis in eukaryotic cells and their dysregulation has important consequences for cell signalling and functions. *P. falciparum* has only one enzyme homologous to SERCA - PfATP6ase²².



Thapsigargin, a sesquiterpene lactone, is a selective inhibitor of a mammalian SERCA. Because artemisinin is structurally similar to thapsigargin, it was hypothesised that artemisinins specifically inhibit PfATP6²³. Devoid of endoperoxide moiety and antimalarial activity, it is well documented that thapsigargin can inhibit PfATP6 enzyme irreversibly in a similar manner as artemisinin while deoxyartemisinin, quinine and chloroquine provided no activities²³. Desferrioxamine (DFO), an iron chelator, in combination with either thapsigargin or artemisinin was added to infected red blood cells to examine the effect on PfATP6. DFO demolishes the inhibitory effects of artemisinin on PfATP6 but doesn't alter the inhibition by thapsigargin suggesting that artemisinins act by inhibiting PfATP6 after activation by iron²³. Several following studies and debates from this hypothesis were published²⁴. Interestingly, one docking studies of antimalarials on the PfATP6 model shows no correlation between affinity of the compounds for PfATP6 and *in vitro* antimalarial activity²⁵. More detailed studies with accuracy are required to resolve the point at which PfATP6 plays a role.

5.2.2.3 Parasite's proteins and other macromolecules

A number of studies show that radiolabeled artemisinin can react covalently with several parasitic proteins²⁶. Autoradiograms of SDS-PAGE showed six malarial proteins radiolabelled by three different endoperoxides; arteether, dihydroartemisinin (DHA) and arteflene. The labelling occurred at physiological concentration of the drug and was not stage or strain specific²⁷.

In a different study, artemisinin also alkylated various proteins *in vitro*. Between 5–18% of added drug bound to hemoproteins such as catalase, cytochrome *c* and hemoglobin, however the drug did not react with heme-free globin. In addition, the *in vitro* alkylation of human albumin by artemisinin is well documented and is shown to react on both the thiol and amino moieties *via* iron dependent and independent reactions^{26a}. Further work in this area has identified cysteine adducts of artemisinin-derived radicals suggesting that general alkylation of cysteine residues may be involved in the mechanism of action by interfering with protein function²⁸. Artemisinins have also been shown to inhibit the falcipains, a papain-family cysteine protease that aid hemoglobin degradation. This mechanism of protease inhibition was shown to increase in the presence of heme²⁹. Recently artemisinin was shown to accumulate with neutral lipids and cause parasite membrane damage. This effect was due to the endoperoxide moiety since analogues lacking the O-O bridge failed to cause oxidative membrane damage³⁰.

5.3 Activity-based proteomics or activity-based protein profiling (ABPP)

Activity-based protein profiling (ABPP) was first reported in 1990s and is a functional proteomic technique that uses chemical probes reacting with related classes of enzymes³¹. The technique was summarised in several reviews³². The Cravatt laboratory is a recognised pioneer having demonstrated profiling across a remarkably broad range of enzymes³¹. The most important part of ABPP is the chemical probe, which typically comprises two elements - a reactive group (sometimes called a "warhead") and a tag. The reactive group usually contains a specifically designed electrophile that can covalently bind to a nucleophilic residue within the active site of a target enzyme. To allow the identification of the complex sample, the probe should contain a tag which can be either a reporter tag such as a fluorophore or an affinity label such as biotin or an alkyne-azide coupling pair for use with the 1,3-dipolar cycloaddition (also known as click chemistry).

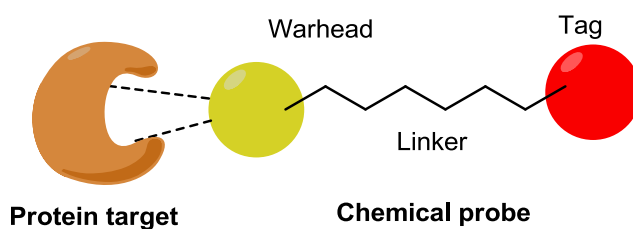


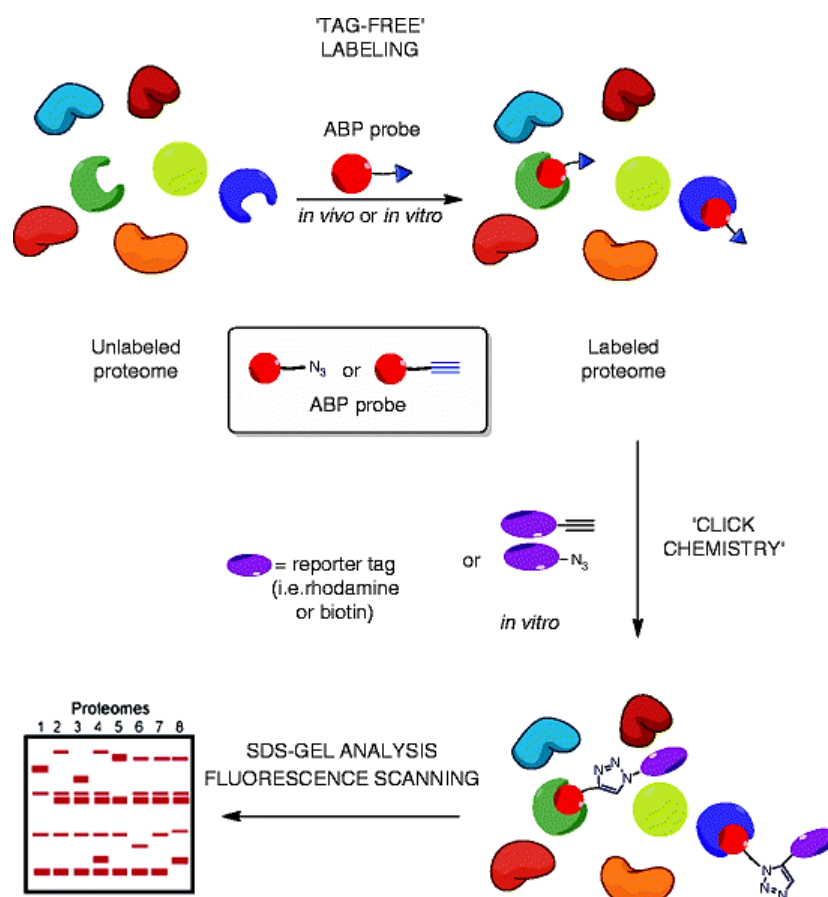
Figure 5.4 ABPP chemical probe

A major advantage of ABPP is the ability to monitor the availability of the enzyme active site directly, rather than being limited to protein or mRNA abundance. Classes of enzymes such as the serine proteases and metalloproteases often interact with endogenous inhibitors or that exist as inactive zymogens, this technique offers a valuable advantage over traditional techniques that rely on abundance rather than activity^{32a}.

Finally, in recent years ABPP has been combined with tandem mass spectrometry enabling the identification of hundreds of active enzymes from a single sample. This technique is very useful especially for selectivity profiling as the potency of an inhibitor can be tested against multiple targets at the same time^{32a}.

5.4 Aim

Although it is widely accepted that the reductive bioactivation of artemisinin with ferrous ion leads to the generation of toxic carbon-centred free radicals, their interaction with target proteins is poorly understood. The formal identification of target proteins and their interacting partners is a key to probe and predict any potential in drug resistance development and aid the systematic drug design for this class of antimalarials. In this chapter, the objective is to identify, for the first time, the protein targets of the artemisinin class using a proteomic strategy. The research includes different components - synthesis of the probe molecules, protein tagging and identification.



Scheme 5.3 Tag-free ABPP method for proteomic analysis of drug target^{32b}

At the beginning of this research, several chemical probes based on artemisinin and endoperoxide derivatives as a warhead have already been prepared including biotin-tagged and fluorescent active probes. They demonstrate *in vitro*

antimalarial activity in nanomolar concentration³³. This is solid evidence that a tag can be introduced into the peroxide structure without a negative effect on activity. Unfortunately, the direct biotinylation tag method requires harsh condition and it is not suitable for further proteomic techniques making the protein identification extremely difficult³³. The novel “tag-free” strategy relies on the click chemistry of the azide-alkyne Huisgen cycloaddition (click chemistry) between a chemical probe and a reporter tag due to its high efficiency in terms of yield and regiochemistry. By using this method, proteins are labelled by small alkynes (or azides) attached to the drug. Addition of a reporter tag containing a fluorescent biotin group and an azide (or alkyne) arm using click chemistry leads to the formation of tagged-proteins. The protein identification and analysis can be done using streptavidin affinity pull down of covalently tagged proteins followed by the isolation of the protein through biotin-streptavidin binding and LC-MS analysis. Four chemical probes were designed including two control probes containing non-peroxidic moiety. The linker length between a warhead and a tag is required and, based on previous work a linkage of four carbon atoms was inserted between the warhead and the affinity tag (**Figure 5.5**).

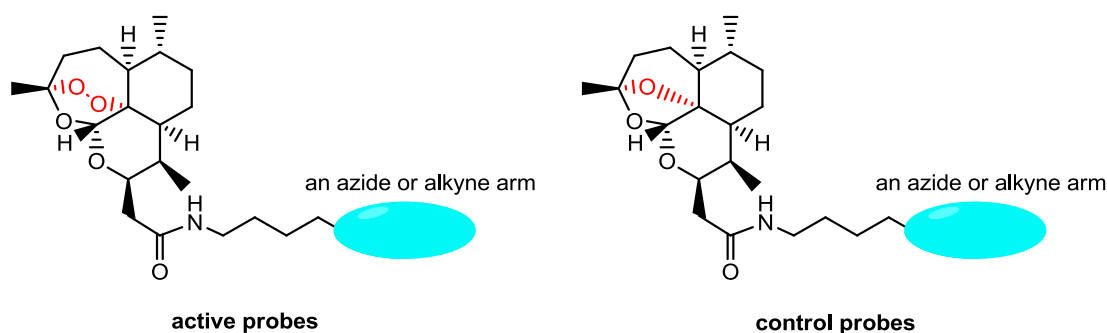


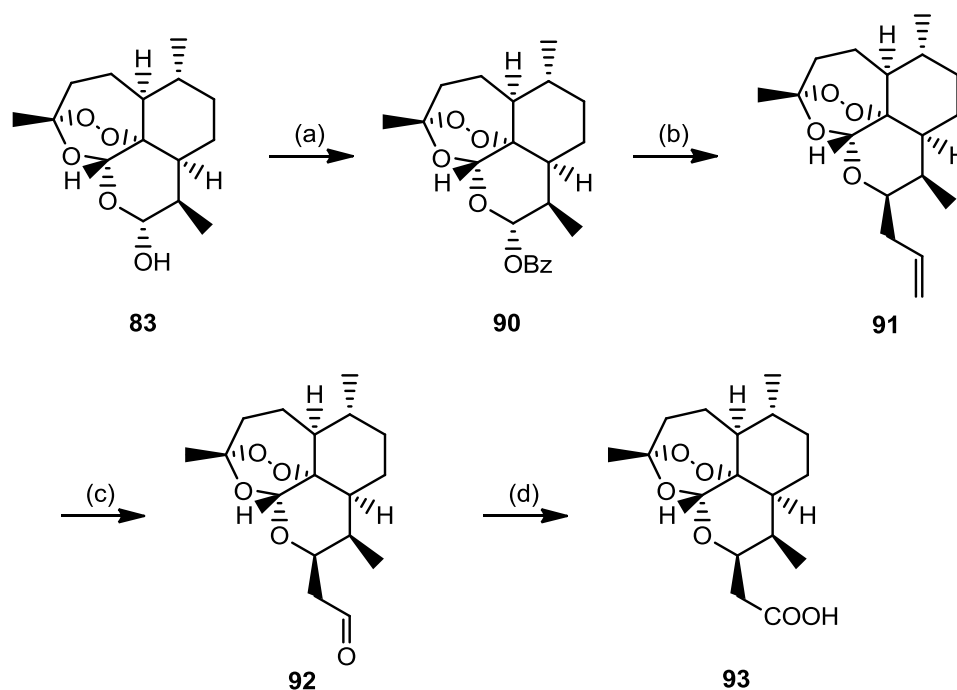
Figure 5.5 Rationale of chemical probes

As this work is now being progressed in collaboration with the Liverpool School of Tropical Medicine, the synthesis of chemical ABPP probes and related preliminary *in vitro* results will be summarised in this chapter. The complete proteomic analysis will be published elsewhere since at the time of writing it is still not complete.

5.5 Results and discussion

5.5.1 The synthesis of artemisinin-based ABPP chemical probes

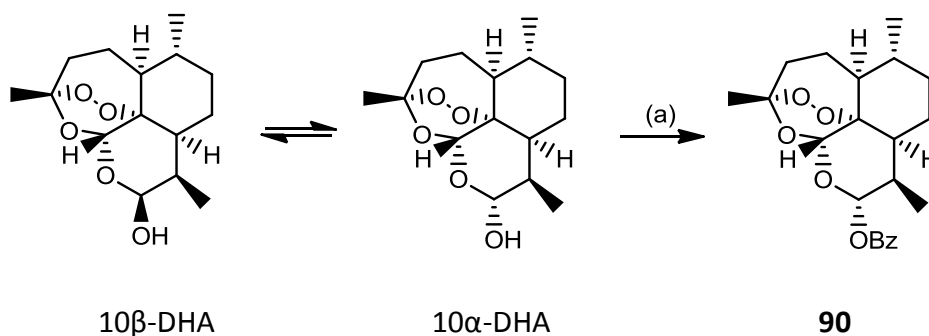
The synthetic route towards the 10 β -(2-carboxyethyl)deoxyartemisinin **93**, an important intermediate used in this studies, was well documented, though slight modifications have been made over time³³⁻³⁴.



Scheme 5.4 Synthesis of 10 β -(2-carboxyethyl)deoxyartemisinin **93** ;
Reagents: (a) PhCOCl, pyridine, DCM, 0 °C, overnight, 90%. (b) allyltrimethylsilane, ZnCl₂, DCE, 4 Å molecular sieve, under N₂, 4 h, 76%. (c) O₃, MeOH, -78 °C, 1 h then PPh₃, r.t., overnight, 53%. (d) NaClO₂, 2-methyl-2-butene, NaH₂PO₄, *t*-BuOH/water (5:1), r.t., 2 h, 89%.

The synthesis begins with a commercially available dihydroartemisinin (DHA) **83**. DHA normally appears as a mixture of two epimers according to the stereochemistry of 10-OH; α - and β -epimer. Any synthesis starting from DHA often suffers from a mixture of C10-epimer products. The Ziffer group reported a stereoselective preparation of 10 β -allyldeoxyartemisinin **91** from DHA using a Lewis acid-mediated reaction to provide a series of C10-alkyl derivatives³⁵. The additional

methodology studies developed in the O'Neill group showed the advantage of using dihydroartemisinin C10-benzoate **90** over DHA^{34a}.



Scheme 5.5 Synthesis of dihydroartemisinin 10α-benzoate **90**; Reagents: (a) PhCOCl, pyridine, DCM, 0 °C, overnight, 90%.

The acylation of DHA **83** with benzoyl chloride using pyridine as a nucleophilic catalyst stereoselectively provided dihydroartemisinin 10α-benzoate **90** in high yield. The stereochemistry at C10 can be determined by ¹H-NMR spectroscopy through the use of ³J coupling constant between H10 and H9. The doublet signal at 6.02 ppm represents the H10 with a ³J_{H9-H10} of 9.8 Hz. According to the Karplus curve, this value suggests the dihedral angle of 180° between H10 and H9 indicating the 10β-H (the *trans-trans* diaxial relationship). This stereoselective manner can be rationalised through the neighbouring methyl at C-9. The steric effect due to this methyl group allows only 10α-DHA to react with acyl pyridinium intermediate. Any 10β-DHA left can equilibrate to give the 10α-DHA ready to react with the acyl chloride.

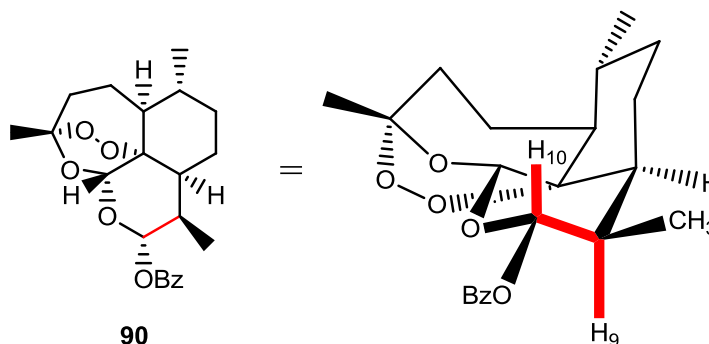
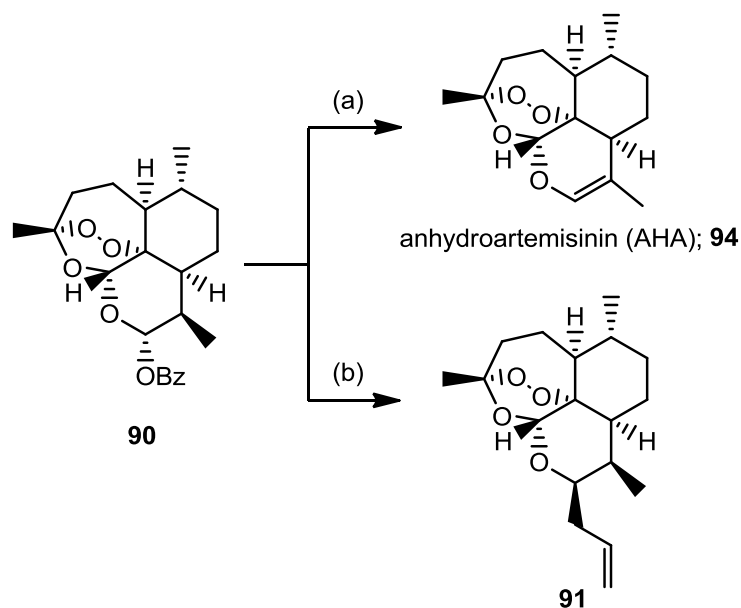


Figure 5.6 The dihedral angle of 180° between H10 and H9

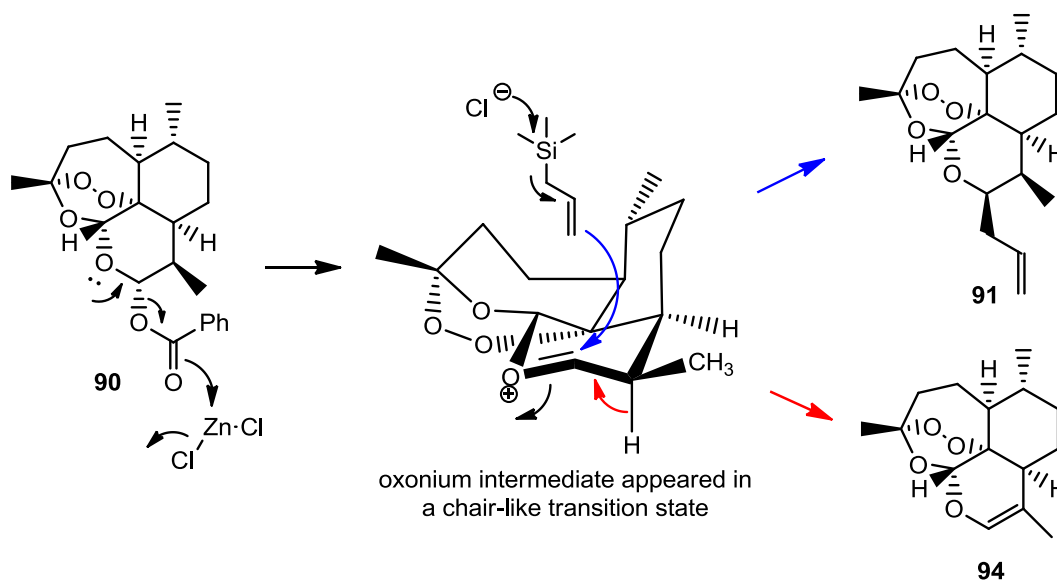
The synthesis towards 10 β -allyldeoxyartemisinin **91** was well documented. The drawback in the procedure is the harsh nature of the Lewis acid resulting in the generation of substantial amount of anhydroartemisinin (AHA) **94** *via* the proton loss from the oxonium intermediate^{34a}. This makes the purification extremely difficult as both 10 β -allyldeoxyartemisinin **91** and AHA **94** share very similar *R_f*s on TLC when eluted with 10% EtOAc in hexane. In considering the choice of Lewis acid, it is noted that hard Lewis acid such as BF₃.Et₂O, has the ability to rearrange the oxonium intermediate resulting in the formation of AHA. Trimethylsilyl trifluoromethanesulfonate (TMSOTf) was first explored as it was employed in a similar reaction. The reaction of 10 α -DHA benzoate with excess allyltrimethylsilane in the presence of TMSOTf provided unwanted AHA in good yield suggesting that TMSOTf is far too strong for this reaction. The spectroscopic data is consistent to the literature.



Scheme 5.6 Synthesis of 10 β -allyldeoxyartemisinin **91**; *Reagents*: (a) TMSOTf, ZnCl₂, DCE, 4 Å molecular sieve, under N₂, 4 h, 76%. (b) allyltrimethylsilane, ZnCl₂, DCE, 4 Å molecular sieve, under N₂, 4 h, 76%.

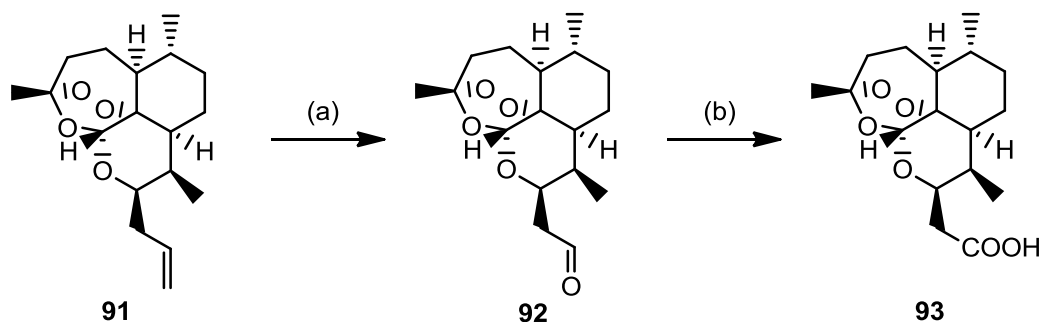
Considering the use of a milder Lewis acid, ZnCl₂ was chosen. The reaction of dihydroartemisinin 10 α -benzoate **90** with excess allyl trimethylsilane in the presence of ZnCl₂ as a Lewis-acid additive at 0 °C for 4 h under anhydrous condition gave desired 10 β -allyldeoxyartemisinin **91** in 76% yield. The reaction proceeds *via*

S_N1 mechanism with the inversion of configuration at C10 through the favourable axial attack of allyltrimethylsilane on the intermediate oxonium ion *via* a chair-like transition state. It is noteworthy that the reaction only gives minor quantities of AHA. The formation of AHA was minimised by using a weaker Lewis acid allowing the controlled formation of the oxonium ion and subsequent reaction with a large excess of allyltrimethylsilane^{34a}.



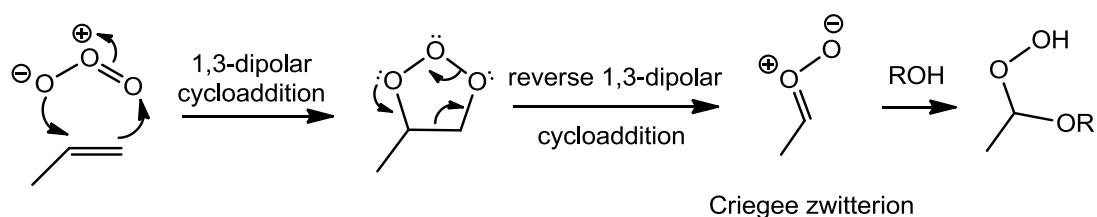
Scheme 5.7 The allylation mechanism of dihydroartemisinyll 10 α -benzoate

The required carboxylic acid **93** has been previously prepared directly from the allyl derivative **91** by oxidation of the terminal alkene with sodium periodate and potassium permanganate. However, the product obtained was shown to degrade rapidly. Therefore, the two-step synthesis of the carboxylic *via* the corresponding aldehyde was employed^{34c}.



Scheme 5.8 Two-step oxidation of 10β-allyldeoxoartemisinin **91**; *Reagents*: (a) O₃, MeOH, -78 °C, 1 h then PPh₃, r.t., overnight, 53%. (b) NaClO₂, 2-methyl-2-butene, NaH₂PO₄, *t*-BuOH/water (5:1), r.t., 2 h, 89%.

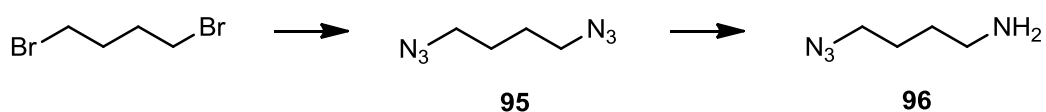
The aldehyde **92** can be made directly from the ozonolysis of alkenes followed by a reductive quenching. The reaction went successfully when methanol is used as a solvent. Described by Criegee in 1953, the alkene and ozone form an intermediate molozonide in a 1,3-dipolar cycloaddition. The molozonide then reverts to its corresponding carbonyl oxide (also called the Criegee zwitterion) and aldehyde or ketone in a retro-1,3-dipolar cycloaddition fashion³⁶. The resulting carbonyl oxide is trapped by the solvent giving peroxide ether which can be subsequently degraded by triphenyl phosphine. The ozonolysis of allyl **91** in methanol at -78 °C yielded the aldehyde **92** in 53% after a chromatographic purification. The oxidation of aldehyde **92** with sodium chlorite gave the acid **93** in near quantitative yield.



Scheme 5.9 Mechanism of ozonolysis and the Criegee zwitterion

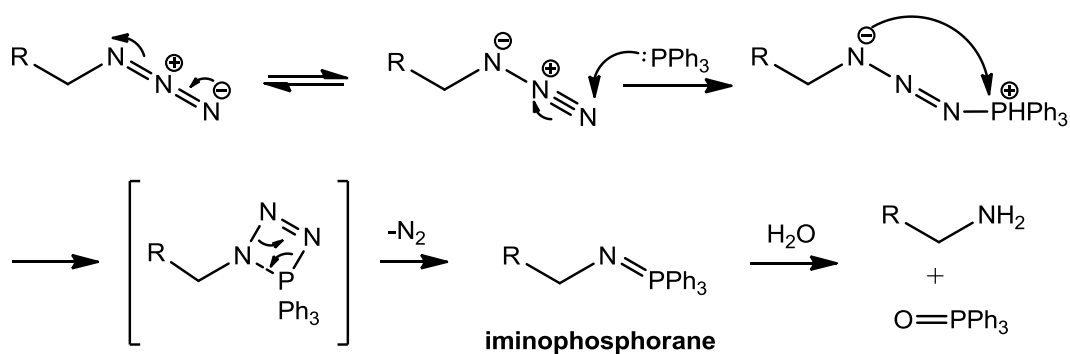
The 4-azidobutan-1-amine **96** was synthesised according to the procedure published in 2001³⁷. The group led by Kim has successfully prepared a series of α,ω-diaminoalkanes from the corresponding dibromo starting materials. 1,4-

Diazidobutane **95** is easily prepared from the 1,4-dibromobutane using sodium azide in a solution of DMF and water without any purification required.



Scheme 5.10 Synthesis of azidobutanamine **96**; *Reagents*: NaN_3 , DMF, 80°C , 20 h, 89%. (b) PPh_3 , 1 M HCl (9 mL), Et_2O , EtOAc, 0°C – r.t., overnight, 82%.

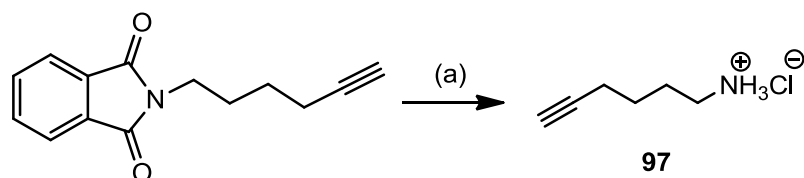
1,4-Diazidobutane **95** is reacted with triphenylphosphine in a mixture of ether/ethyl acetate in the presence of 5% HCl. Once the azidoamine is formed, it is protonated by the acid and migrates into the aqueous layer preventing the over-reduction to diamine. This azide reduction is also known as the Staudinger reaction discovered by and named after Hermann Staudinger³⁸. The reaction mechanism was shown below involving the formation of an iminophosphorane through nucleophilic addition of the phosphine at the terminal nitrogen atom of the azide followed by liberation of molecular nitrogen. This intermediate is then hydrolysed in later step to obtain the amine and triphenylphosphine oxide.



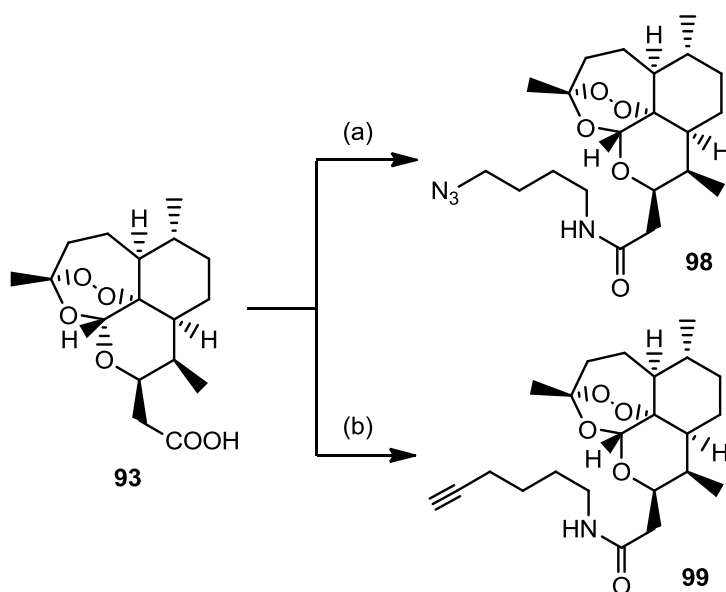
Scheme 5.11 Staudinger reaction mechanism

When the reduction completes, the organic layer is discarded and the aqueous layer is washed with DCM to get rid of the remaining triphenylphosphine oxide by-product and non-ionic components. Addition of a base to the aqueous layer followed by extraction with DCM gives azidoamine **96** in 82% yield without any further purification.

Hex-5-yn-1-aminium chloride salt **97** can be prepared from the corresponding phthalimide. *N*-protected phthalimide was treated in the ethereal solution of hydrazine which is normally used to release a free amino group. Due to the fact that a low-molecular-weight free amine is volatile, one mL of concentrated HCl was added upon the workup procedure allowing the formation of stable aminium chloride salt appeared as white solid³⁹.



Scheme 5.12 Synthesis of hex-5-yn-1-aminium chloride **97**; *Reagents*: (a) hydrazine hydrate, THF (20 mL), reflux, 6 h then conc. HCl, reflux, 2 h then cool overnight, 75%.



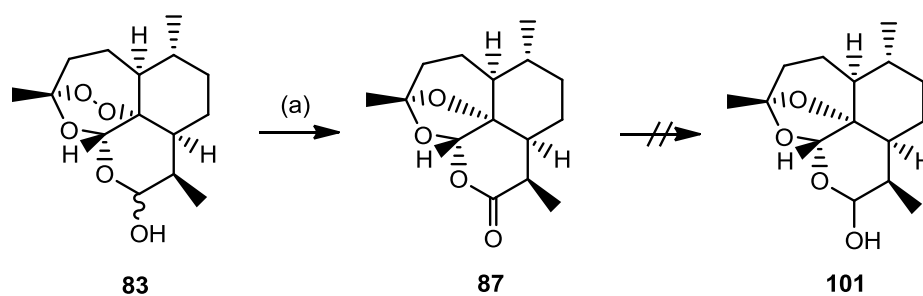
Scheme 5.13 Synthesis of the artemisinin-based ABPP active probes; *Reagents*: (a) EDCI, DCM, under nitrogen, 5 min then **96**, DMAP, r.t., overnight, 50%. (b) EDCI, DCM, under nitrogen, 5 min then **97**, DMAP, Et₃N, r.t., overnight, 40%.

Coupling reactions between the warhead and an azide/alkyne arm can be done by a usual condition using EDCI followed by DMAP and a choice of amine⁴⁰. In cases of an alkyne arm, triethylamine was also added to liberate a free amine from

its salt form. The coupling between **93** and either **96** or **97** was achieved in good yield.

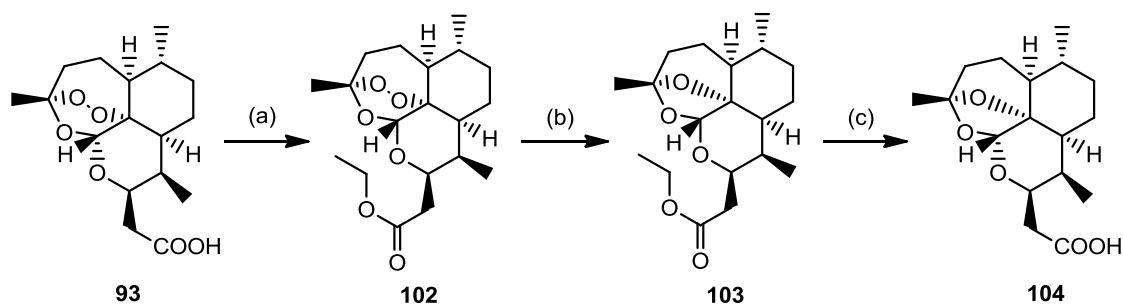
Since the pharmacophore for artemisinin is the endoperoxide moiety, the control probes were designed to include the framework of artemisinin without the peroxide part. This strategy allows us to investigate the possible off-target bindings which may bias the target identification.

The synthesis of analogous deoxyartemisinin **87** devoid of endoperoxide moiety was well documented and can be achieved in good yield from DHA using triethylamine in ethanol under a reflux condition. The plan was to reduce the six-membered-ring lactone into hemiacetal deoxydihydroartemisinin **101**. Several attempts had been invested including the use of NaBH_4 and it was not possible to get the deoxyDHA **101** in an isolatable yields.



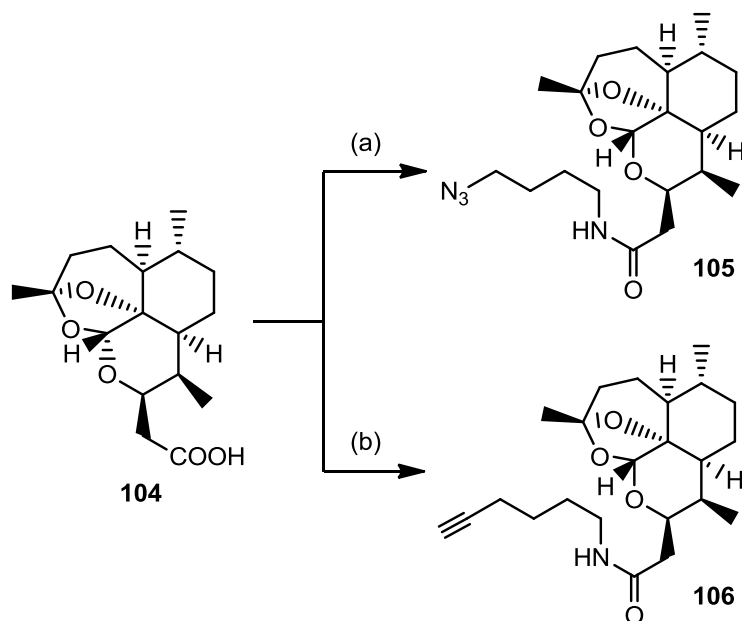
Scheme 5.14 Synthesis of deoxydihydroartemisinin **101**; *Reagents:* (a) triethylamine, EtOH, 90 °C, under nitrogen, 21 h, 60%.

The multi-step synthesis towards deoxyartemisinin probes was eventually made from the deoxyartemisinin carboxylic acid **104**. The protection of carboxylic group using ethyl ester was done using ethanol as a nucleophile in a presence of EDCI and DMAP.



Scheme 5.15 Synthesis of the deoxyartemisinin carboxylic acid **104**;
Reagents: (a) EDCI, DCM, under nitrogen, 5 min then ethanol, DMAP, r.t., overnight, 63%. (b) activated Zn dust, acetic acid, r.t., 72 h, 41%. (c) 15% NaOH (aq.), EtOH, 3 h, 93%

The reduction of the endoperoxide moiety of the ethyl ester **102** was achieved by activated zinc powder in acetic acid. ^{13}C -NMR was used to identify the change in chemical shift of C3 atom from 107.1 to 103.2 ppm suggesting a deshielded effect from losing one oxygen atom. The deoxyartemisinin acid **104** was then made by the saponification of ethyl ester **103** in an ethanolic solution of aqueous 15% NaOH in excellent yield. Coupling reactions between the deoxyartemisinin warhead and an azide/alkyne arm can be done in a similar manner using EDCI followed by DMAP and a choice of amine. The coupling between **104** and either **96** or **97** was achieved in good yield.



Scheme 5.16. Synthesis of the artemisinin-based ABPP control probes; *Reagents:* (a) EDCI, DCM, under nitrogen, 5 min then **96**, DMAP, r.t., overnight, 75%. (b) EDCI, DCM, under nitrogen, 5 min then **97**, DMAP, Et₃N, r.t., overnight, 50%.

5.5.2 Biological experiments

5.5.2.1 Antimalarial activity

Four synthetic ABPP artemisinin probes were deposited and submitted for antimalarial assessment against the 3D7 strain of *P. falciparum* at the Liverpool School of Tropical Medicine (**Table 5.2**). Drug IC₅₀'s were calculated from the logarithm of the dose/response relationship. It is clear that peroxide-containing probes **98** and **99** show an excellent activity against malaria parasite which is comparable to ART and DHA. The control probes **105** and **106** undoubtedly provide no activity in this assay due to the absence of endoperoxide moiety in their molecules. Further biological works including protein tagging and identification are currently ongoing. The preliminary result shows that **99** performs well in streptavidin pull down technique providing protein samples for LC-MS/MS analysis and this will briefly be described in the following section.

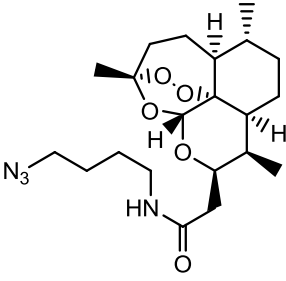
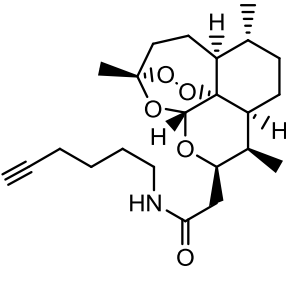
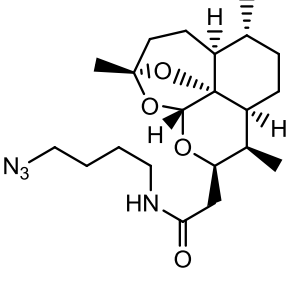
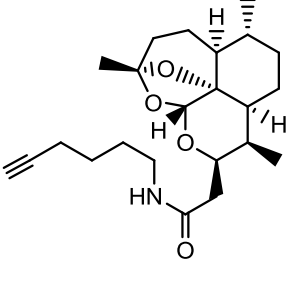
Compound	Chemical structure	IC ₅₀ (nM) ± SE
98		17.86 ± 0.14
99		14.26 ± 0.21
105		inactive
106		inactive

Table 5.2 *In vitro* antimalarial activity of synthetic ABPP chemical probes against *P. falciparum* 3D7 strain. ART and DHA were used as standard with an IC₅₀ of 20.9 ± 2 nM and 3.12 ± 0.03 nM, respectively.

5.5.2.2 Protein profiling

This part of work was carried out in collaboration with the Liverpool School of Tropical Medicine and as mentioned is still ongoing. More details of this work will be published elsewhere. Parasite proteins were tagged *in vitro* using ABPP artemisinin probe and click chemistry can be done following the method found in the experimental section at the end of this chapter. Instead of using traditional SDS-gel electrophoresis for protein analysis (**Scheme 5.3**), protein-probe-biotin complexes were pulled out using streptavidin-agarose beads and proteins were digested to peptide fragments ready for sequencing using mass spectrometry.

Peptide sequences obtained from the MS were subjected to database search for corresponding proteins. A fully automated protocol, Multidimensional Protein Identification Technology (MudPIT) using solely LC-MS/MS techniques was used to identify the protein targets of the artemisinin probes. MudPIT has many advantages over gel-based methodologies *i.e.* samples can be repeated and validated in quick succession to effectively analyze and identify not only abundant targets but also minor target proteins. Protein matrix were identified using the Mascot search algorithm and semi quantified by the exponentially modified protein abundance index (emPAI), based on protein coverage by the peptide matches in a database search, allowing approximate, label-free, relative quantitation of proteins in a mixture⁴¹.

Active endoperoxide probe **99** pulled out approximately 45 different proteins of which 23 proteins belong to *Plasmodium*. 24 proteins were pulled down using control probe **106** of which 2 proteins belong to the parasite. DMSO control treatments were acceptable. These proteins are involved in pathogenesis, membrane transport, pyrimidine biosynthetic pathway and catalytic processes.

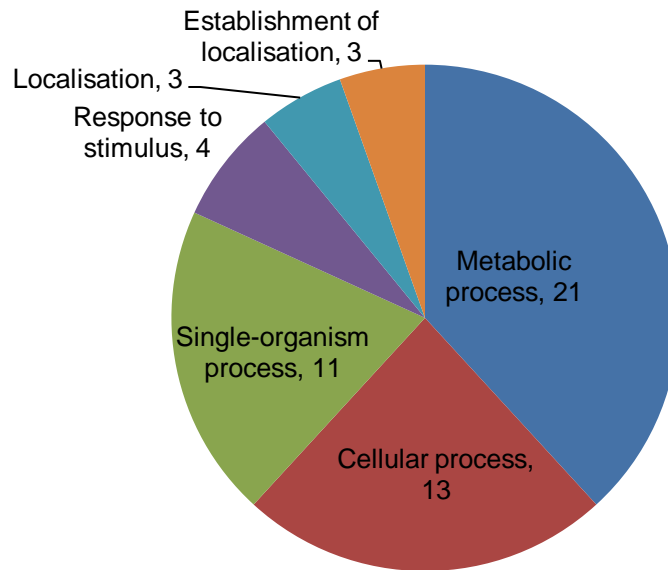


Figure 5.6 Pulled down proteins catagorised by their biological process
(Note: some proteins were involved in more than one biological process)

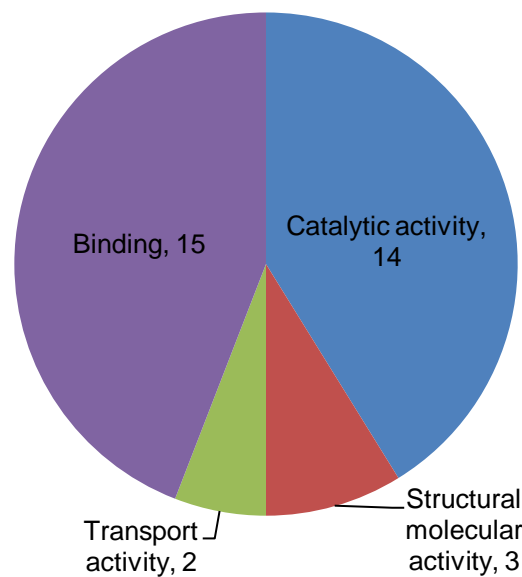


Figure 5.7 Pulled down proteins catagorised by their molecular function
(Note: some proteins have more than one molecular function)

A number of valuable proteins that are essential to parasite life are identified with artemisinin ABPP probe **99** including ornithine δ -aminotransferase (OAT), L-lactate dehydrogenase, enolase, V-type proton ATPase catalytic subunit,

which are redox-active proteins that play a crucial role in the maintenance and control of redox reactions. For example, Trx-mediated control of OAT activity for coordinating ornithine homeostasis, polyamine synthesis, proline synthesis, and mitotic cell division in rapidly growing cells, represents a new potential target for chemotherapeutic intervention⁴². Additionally OAT of *P. falciparum* catalyzes the reversible conversion of ornithine into glutamate-5-semialdehyde and glutamate and is in contrast to its human counterpart is activated by thioredoxin (Trx) by 10 fold⁴². Calcium-transporting ATPase was also found in the pulled down protein sample which corresponds to the early proposal described in the section 5.2.2.

Interestingly, the majority of the proteins identified with endoperoxide probe **99** were absent with control probe **106** devoid of peroxide moiety. This implies that proteins pulled down by **99** may well be essential to the survival of the parasite.

5.6 Conclusion

Artemisinin combination therapy (ACT) is still used as the first line treatment in most of the malarial endemic areas. The emergence of drug resistance requires greater understanding of drug action. Several ABPP probes including biotin-tagged and fluorescent probes have previously been prepared. The “tag-free” ABPP proteomic technique is introduced based on the click chemistry of the azide-alkyne Huisgen cycloaddition between a chemical probe and a reporter tag.

The synthesis of the artemisinin ABPP probes was fairly uncomplicated. The peroxide-containing probes demonstrate excellent *in vitro* activity against malaria parasite which is consistent to the previous work. The control deoxy probes provide no activity in the assay. The preliminary result reveals that active probe **99** can perform well in streptavidin pull down resulting in 45 proteins being identified. A number of key proteins that are essential to parasite life have been identified with artemisinin-based ABPP chemical probes and future work will complete this proteomic analysis to provide a unified mechanism of action for this most important class of antimalarial.

5.7 Experimental

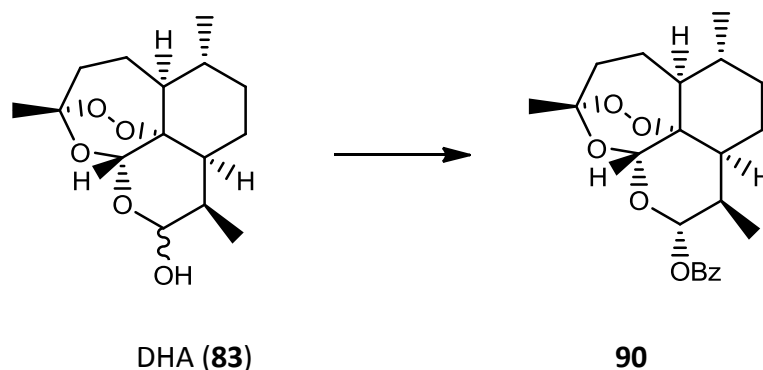
Anhydrous solvents were either purchased from reliable commercial sources or distilled from a still prior to use under inert gas atmosphere. THF was distilled from Na with benzophenone as an indicator. DCM was distilled from CaH₂. All reagents were purchased from reliable commercial sources and were used without any purification unless otherwise indicated. TLC analysis was performed to confirm the reagents purity.

TLC was performed on 0.25 mm thickness Merck silica gel 60 with fluorescent indicator at 254 nm and visualised under UV light. UV inactive compounds were stained and visualised using iodine, *p*-anisaldehyde, or potassium permanganate solution followed by gentle heating. Flash column chromatography was performed using normal phase silica gel purchased from Sigma-Aldrich.

NMR spectra were recorded in a solution of CDCl₃ or DMSO-*d*₆ on a Bruker AMX400 spectrometer (¹H 400 MHz, ¹³C 100 MHz). Chemical shifts (δ) were expressed in ppm relative to tetramethylsilane (TMS) used as an internal standard. *J* coupling constants are in hertz (Hz) and the multiplicities were designed as follows: s, singlet; d, doublet; t, triplet; q, quartet; dd, double of doublet; m, multiplet. Mass spectra were recorded on either a Micromass LCT Mass Spectrometer using electrospray ionisation (ESI) or Trio-1000 Mass Spectrometer using chemical ionisation (CI). Reported mass values are within error limits of ± 5 ppm. Elemental analysis (%C, %H, %N) was performed in the University of Liverpool microanalysis laboratory. All melting points were determined with Gallenkamp melting point apparatus and were uncorrected.

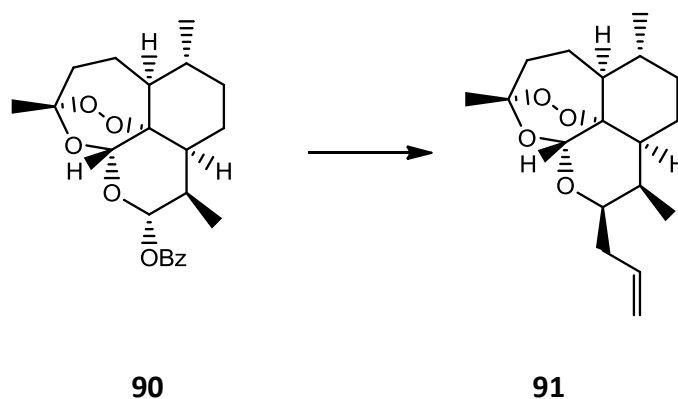
Biological experiments were performed in collaboration with the Liverpool School of Tropical Medicine by Matthew Panchana and Dr Hanafy M. Ismail under a supervision of Professor Stephen A. Ward.

5.7.1 Synthesis

Preparation of Dihydroartemisinin 10 α -benzoate, **90**^{34b}

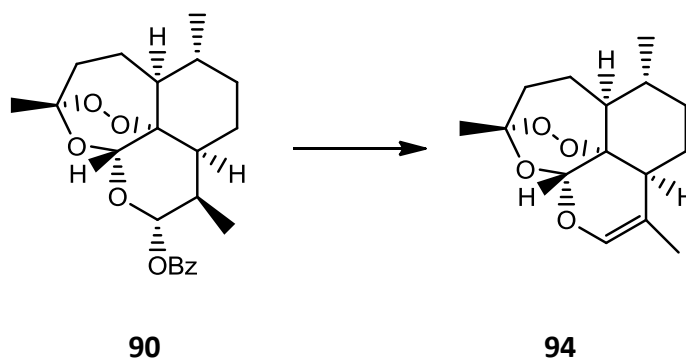
Benzoyl chloride (7.7 mL, 54.5 mmol) was added to a stirring solution of dihydroartemisinin (DHA) (10.0 g, 35.2 mmol) in anhydrous DCM (120 mL) and anhydrous pyridine (18 mL) at 0 °C. After being allowed to stir at room temperature overnight, 7% aq. citric acid solution (100 mL) was added. The organic layer was separated and the aqueous layer was extracted with EtOAc (3 x 100 mL). The combined organic layers were washed with 7% aq. citric acid solution, sat. NaHCO₃, and dried over MgSO₄. After filtration and evaporation, the obtained crude solid was recrystallised from a small amount of 50% Et₂O/Hexane mixture to give the product as a white crystalline solid (12.23 g, 90%). Alternatively, the crude mixture can be purified by column chromatography (10% EtOAc/Hexane)

¹H NMR (400 MHz, CDCl₃) δ 8.13 (dd, *J* = 8.4, 1.3 Hz, 2H), 7.57 (t, *J* = 7.4 Hz, 1H), 7.45 (t, *J* = 7.7 Hz, 2H), 6.02 (d, *J* = 9.8 Hz, 1H), 5.53 (s, 1H), 2.76 (dq, *J* = 14.2, 7.1, 4.6 Hz, 1H), 2.39 (ddd, *J* = 14.5, 13.4, 4.0 Hz, 1H), 2.05 (ddd, *J* = 14.6, 4.8, 3.0 Hz, 1H), 1.96 – 1.87 (m, 1H), 1.83 (ddd, *J* = 13.2, 7.6, 3.5 Hz, 1H), 1.75 (ddd, *J* = 13.4, 6.5, 3.3 Hz, 1H), 1.69 (dt, *J* = 13.7, 4.5 Hz, 1H), 1.58 – 1.44 (m, 2H), 1.43 (s, 3H), 1.41 – 1.26 (m, 2H), 1.05 (ddd, *J* = 11.7, 8.3, 2.8 Hz, 1H), 0.99 (d, *J* = 6.1 Hz, 3H), 0.93 (d, *J* = 7.2 Hz, 3H). ¹³C NMR (101 MHz, CDCl₃) δ 165.72, 133.71, 130.54, 130.04, 128.70, 104.85, 92.93, 92.01, 80.61, 52.07, 45.76, 37.70, 36.67, 34.54, 32.41, 26.38, 25.00, 22.48, 20.66, 12.65. ESI HRMS: *m/z* calculated for C₂₂H₂₈O₆Na ([M+Na]⁺) 411.1784, found 411.1776. Elemental Analysis calculated for C₂₂H₂₈O₆ : C, 68.02; H, 7.27; N, 0.0. Found: C, 67.55; H, 7.25; N, 0.0.

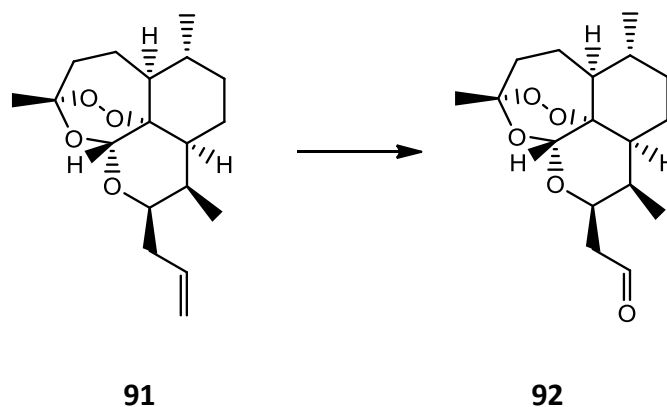
Preparation of **10 β -allyldeoxyartemisinin, 91**^{34b}

To a solution of allyltrimethylsilane (7.1 mL, 44.7 mmol, 4.8 eq.) in anhydrous DCE (40 mL) was added ZnCl₂ (1.53 g, 11.2 mmol, 1.2 eq.) and a spatula of 4 Å molecular sieve under N₂. The mixture was allowed to stir and cooled to 0 °C before slowly added a solution of dihydroartemisinin 10 α -benzoate (3.62 g, 9.32 mmol) in DCE (40 mL). After stirring at 0 °C for 4 hours, the solvent was removed *in vacuo*. The reaction mixture was diluted with EtOAc (50 mL), washed with 7% aq. citric acid solution, saturated aq. NaHCO₃ and brine. The organic extract was dried over MgSO₄, filtered, and concentrated to give a crude oil which was purified by column chromatography (10% EtOAc/Hexane) to obtain the product as a white solid (2.19 g, 76%)

¹H NMR (400 MHz, CDCl₃) δ 5.93 (ddt, J = 16.9, 10.2, 6.6 Hz, 1H), 5.33 (s, 1H), 5.12 (dd, J = 17.2, 1.7 Hz, 1H), 5.06 (dd, J = 10.2, 1.3 Hz, 1H), 4.30 (ddd, J = 10.0, 6.1, 3.7 Hz, 1H), 2.75 – 2.63 (m, 1H), 2.46 – 2.27 (m, 3H), 2.25 – 2.17 (m, 1H), 2.07 – 2.00 (m, 1H), 1.96 – 1.87 (m, 1H), 1.81 (ddd, J = 13.4, 7.5, 3.6 Hz, 1H), 1.71 – 1.56 (m, 4H), 1.42 (s, 3H), 1.36 (dd, J = 13.4, 3.4 Hz, 1H), 1.27 (dd, J = 11.2, 5.9 Hz, 1H), 0.97 (d, J = 5.9 Hz, 3H), 0.89 (d, J = 7.6 Hz, 3H). ¹³C NMR (101 MHz, CDCl₃) δ 136.88, 116.48, 103.54, 89.50, 81.48, 75.12, 52.75, 44.73, 37.88, 37.00, 34.89, 34.63, 30.60, 26.50, 25.30, 25.11, 20.60, 13.39. ESI HRMS: m/z calculated for C₁₈H₂₈O₄Na ([M+Na]⁺) 331.1885, found 331.1877. Elemental Analysis calculated for C₁₈H₂₈O₄: C, 70.10; H, 9.15. Found: C, 69.53; H, 9.23.

Preparation of **anhydroartemisinin, 94**

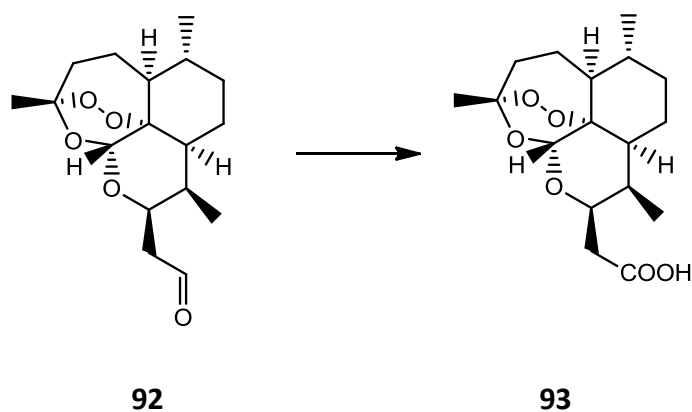
^1H NMR (400 MHz, CDCl_3) δ 6.19 (q, $J = 1.4$ Hz, 1H), 5.54 (s, 1H), 2.41 (ddd, $J = 14.6, 13.1, 4.0$ Hz, 1H), 2.10 – 2.00 (m, 2H), 1.92 (ddt, $J = 9.8, 9.0, 3.4$ Hz, 1H), 1.71 (dd, $J = 12.4, 4.5$ Hz, 1H), 1.66 (dd, $J = 12.9, 3.0$ Hz, 1H), 1.59 (d, $J = 1.3$ Hz, 3H), 1.58 – 1.40 (m, 3H), 1.43 (s, 3H), 1.29 – 1.03 (m, 2H), 0.98 (d, $J = 6.0$ Hz, 3H). CI-HRMS: m/z calculated for $\text{C}_{15}\text{H}_{23}\text{O}_4$ ($[\text{M}+\text{H}]^+$) 267.1596, found 267.1583. Elemental Analysis calculated for $\text{C}_{15}\text{H}_{22}\text{O}_4$: C, 67.64; H, 8.33. Found: C, 67.71; H, 8.42.

Preparation of **10 β -(2-oxoethyl)deoxoartemisinin, 92**^{34c}

10 β -Allyldeoxoartemisinin (5.55 g, 18 mmol) was dissolved in anhydrous MeOH (50 mL) under nitrogen at -78 °C. Ozone was bubbled through the solution for an hour until the solution became saturated with ozone and turned blue. The ozone was removed and replaced by nitrogen. The solution became clear. PPh_3 (9.44 g, 36 mmol) was added to the solution at -78 °C and stirred overnight. The reaction was concentrated under reduced pressure and purified by column chromatography (10% EtOAc/Hexane) to yield a white solid (2.94 g, 53%)

^1H NMR (400 MHz, CDCl_3) δ 9.79 (dd, $J = 3.2, 1.5$ Hz, 1H), 5.32 (s, 1H), 4.95 (ddd, $J = 10.2, 6.2, 3.6$ Hz, 1H), 2.77 – 2.64 (m, 2H), 2.45 (ddd, $J = 16.3, 3.5, 1.4$ Hz, 1H), 2.33 (ddd, $J = 14.5, 13.5, 4.0$ Hz, 1H), 2.04 (ddd, $J = 14.0, 4.7, 3.2$ Hz, 1H), 1.97 – 1.89 (m, 1H), 1.80 (ddd, $J = 13.3, 7.4, 3.5$ Hz, 1H), 1.73 – 1.64 (m, 3H), 1.41 (s, 3H), 1.35 – 1.22 (m, 4H), 0.97 (d, $J = 5.9$ Hz, 3H), 0.87 (d, $J = 7.5$ Hz, 3H). ^{13}C NMR (101 MHz, CDCl_3) δ 202.26, 103.59, 89.68, 81.28, 69.83, 52.50, 44.77, 44.35, 37.87, 36.85, 34.73, 30.13, 26.35, 25.11, 25.03, 20.51, 13.40. HRMS (ESI): m/z calculated for $\text{C}_{17}\text{H}_{26}\text{O}_5\text{Na}$ ($[\text{M}+\text{Na}]^+$) 333.1678, found 333.1674. Elemental Analysis calculated for $\text{C}_{17}\text{H}_{26}\text{O}_5$: C, 65.78; H, 8.44. Found: C, 65.68; H, 8.54.

Preparation of **10 β -(2-carboxyethyl)deoxoartemisinin, 93**^{34c}

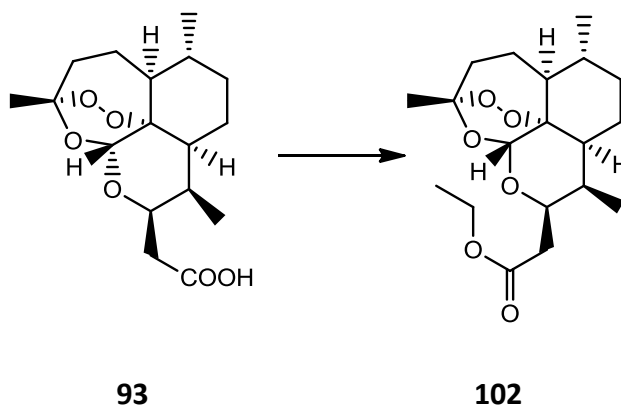


NaH_2PO_4 (2.2 g, 14.2 mmol) was added to a stirred solution of 10 β -(2-oxoethyl)deoxoartemisinin (2.94 g, 9.47 mmol) in *t*-BuOH (50 mL) and water (10 mL) followed by 2-methyl-2-butene (52 mL, 2.0 M in THF, 104 mmol) and NaClO_2 (2.5 g, 28.4 mmol). The resulting pale yellow solution was stirred at room temperature for 2 hours, and then concentrated under reduced pressure. 1 M NaOH (40 mL) was added and the resulting solution was washed with DCM (3 x 50 mL). The aqueous layer was acidified with 1 M HCl and extracted with DCM (3 x 50 mL). The combined organic layers were dried over MgSO_4 , filtered and concentrated to give the desired product as a colourless oil (2.77 g, 89%).

^1H NMR (400 MHz, CDCl_3) δ 5.39 (s, 1H), 4.89 (ddd, $J = 10.5, 6.2, 3.2$ Hz, 1H), 2.72 – 2.62 (m, 2H), 2.51 (dd, $J = 15.9, 3.2$ Hz, 1H), 2.33 (ddd, $J = 14.4, 13.4, 4.0$ Hz, 1H), 2.01 – 1.20 (m, 13H), 0.97 (d, $J = 5.8$ Hz, 3H), 0.88 (d, $J = 7.6$ Hz, 3H). ^{13}C NMR (101 MHz, CDCl_3) δ 176.97, 103.70, 89.53, 81.21, 71.72, 52.52, 44.38, 37.77, 36.82,

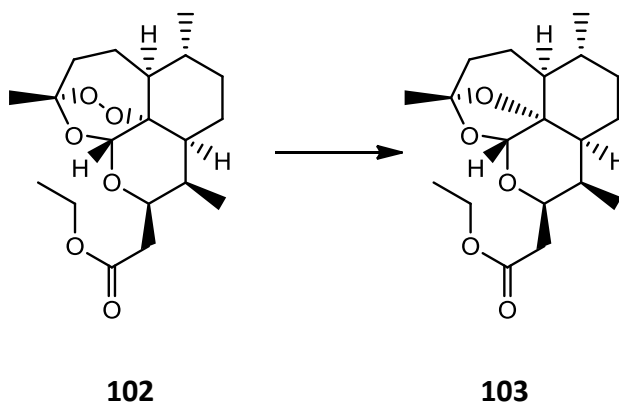
36.14, 34.74, 30.03, 26.20, 25.05, 25.00, 20.51, 13.28. ESI HRMS: m/z calculated for $C_{17}H_{26}O_6Na$ ($[M+Na]^+$) 349.1627, found 349.1628.

Preparation of ethyl 10 β -(2-carboxyethyl)deoxoartemisinin, **102**



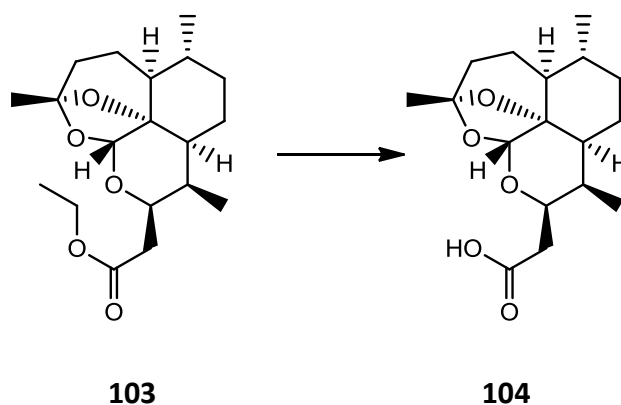
10 β -(2-carboxyethyl)deoxoartemisinin (2.1 g, 6.43 mmol) was dissolved in DCM (50 mL) under nitrogen. EDCI (1.50 g, 9.65 mmol) was added and the reaction was allowed to stir for 5 minutes. Ethanol (1.3 mL, 7.72 mmol) and DMAP (1.18 g, 9.65 mmol) was then added to the reaction and the mixture was left overnight at room temperature. When completed, the reaction was diluted with EtOAc and washed with sat. NH_4Cl (aq.), water, brine, and dried over $MgSO_4$. The organic portion was filtered and concentrated to give a crude product. Purification was performed using CC over silica gel (10% EtOAc/Hexane) to obtain a white solid product (1.44 g, 63%).

1H NMR (400 MHz, $CDCl_3$) δ 5.33 (s, 1H), 4.81 (ddd, $J = 10.1, 6.2, 4.1$ Hz, 1H), 4.26 – 4.09 (m, 3H), 2.82 – 2.71 (m, 1H), 2.65 (dd, $J = 15.2, 9.9$ Hz, 1H), 2.45 (dd, $J = 15.2, 4.0$ Hz, 1H), 2.38 – 2.28 (m, 1H), 2.03 (dt, $J = 14.6, 4.0$ Hz, 1H), 1.95 – 1.87 (m, 1H), 1.80 (ddd, $J = 13.3, 7.5, 3.5$ Hz, 1H), 1.71 – 1.59 (m, 3H), 1.42 (s, 3H), 1.31 – 1.23 (m, 6H), 0.98 – 0.95 (m, 3H), 0.87 (d, $J = 7.5$ Hz, 3H). ^{13}C NMR (101 MHz, $CDCl_3$) δ 171.65, 103.25, 89.08, 80.88, 71.63, 60.66, 52.26, 44.22, 37.46, 36.51, 36.05, 34.43, 29.72, 25.98, 24.71, 24.64, 20.17, 14.21, 13.04. ESI HRMS: m/z calculated for $C_{19}H_{30}O_6Na$ ($[M+Na]^+$) 377.1940, found 377.1928.

Preparation of ethyl 10 β -(2-carboxyethyl)deoxo-2-deoxyartemisinin, **103**

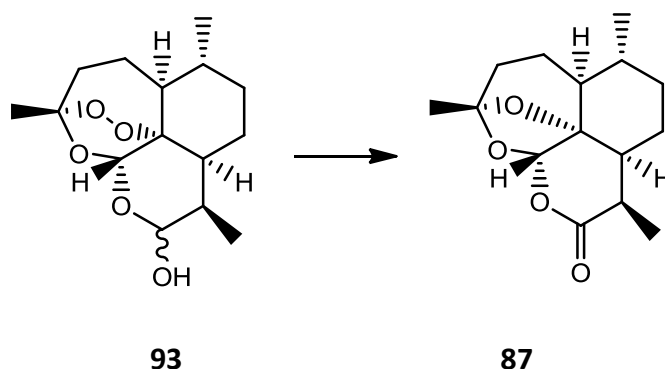
Activated Zn dust (300 mg) (prepared by washing Zn dust with 5% HCl (aq.), water, and Et₂O (3 x 15 mL each wash), then thoroughly dried *in vacuo*) was added to a stirring solution of ethyl 10 β -(2-carboxyethyl)deoxoartemisinin in glacial acetic acid (100 mL). The reaction mixture was allowed to stir at room temperature for 72 hours with the same amount of Zn added every 24 hours. After that period, DCM (80 mL) was added and the mixture was filtered through a sinter glass funnel and washed with DCM (3 x 15 mL). The organic portions were combined and neutralized with sat. NaHCO₃ (aq.). The organic layer separated and washed with sat. NaHCO₃(aq.), water, brine, and dried over MgSO₄, filtered and concentrated. Purification was performed using CC over silica gel (10% EtOAc/Hexane) to yield the desired product as colourless oil (560 mg, 41%).

¹H NMR (400 MHz, CDCl₃) δ 5.24 (s, 1H), 4.70 – 4.57 (m, 1H), 4.27 – 4.07 (m, 2H), 2.52 – 2.38 (m, 2H), 2.37 – 2.25 (m, 1H), 1.96 (ddd, *J* = 12.9, 8.5, 4.1 Hz, 1H), 1.89 – 1.82 (m, 1H), 1.77 (ddd, *J* = 13.2, 7.3, 3.5 Hz, 1H), 1.70 (dt, *J* = 9.1, 4.3 Hz, 2H), 1.64 – 1.58 (m, 1H), 1.56 (s, *J* = 4.9 Hz, 3H), 1.28 (d, *J* = 7.1 Hz, 3H), 1.33 – 1.15 (m, 4H), 1.01 – 0.91 (m, 1H), 0.89 (d, *J* = 5.8 Hz, 3H), 0.86 (d, *J* = 7.6 Hz, 3H). ¹³C NMR (101 MHz, CDCl₃) δ 171.69, 107.15, 96.99, 82.44, 65.86, 60.48, 45.30, 40.27, 37.57, 35.54, 34.52, 34.46, 29.00, 25.03, 23.63, 22.17, 18.78, 14.23, 12.41.

Preparation of **10 β -(2-carboxyethyl)deoxo-2-deoxyartemisinin, 104**

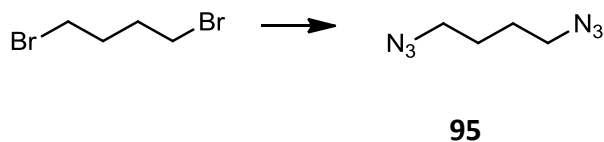
Ethyl 10 β -(2-carboxyethyl)deoxo-2-deoxyartemisinin (540 mg, 1.60 mmol) was dissolved in EtOH (50 mL) and 15% NaOH (aq.) (50 mL) was added to the reaction and left for 3 hours. The reaction was acidified with 1 M HCl (aq.) and ethanol was removed. The aqueous layer was washed with DCM (3 x 50 mL). The combined organic portion was dried over MgSO₄ and evaporated to dryness to yield a product as a colourless liquid (460 mg, 93%).

¹H NMR (400 MHz, CDCl₃) δ 5.27 (s, 1H), 4.62 (dd, J = 14.3, 7.3 Hz, 1H), 2.52 (d, J = 3.0 Hz, 1H), 2.50 (s, 1H), 2.40 – 2.28 (m, 1H), 1.97 (ddd, J = 12.9, 8.5, 4.1 Hz, 1H), 1.86 (dd, J = 9.8, 5.3 Hz, 1H), 1.78 (ddd, J = 13.2, 7.2, 3.5 Hz, 1H), 1.75 – 1.65 (m, 2H), 1.64 – 1.56 (m, 1H), 1.55 (s, 3H), 1.32 – 1.13 (m, 4H), 1.02 – 0.92 (m, 1H), 0.92 – 0.85 (m, 6H). ¹³C NMR (101 MHz, CDCl₃) δ 176.57, 107.42, 96.90, 82.51, 65.62, 45.23, 40.18, 37.19, 35.54, 34.47, 34.40, 28.94, 25.03, 23.57, 22.15, 18.76, 12.35. HRMS (ESI): m/z calculated for C₁₇H₂₆O₅Na ([M+Na]⁺) 333.1678, found 333.1679.

Preparation of **2-deoxyartemisinin, 87**

To a solution of DHA (5.0 g, 17.6 mmol) in EtOH (120 mL) was added triethylamine (6.2 mL, 44 mmol) and it was heated at gentle reflux 90 °C under nitrogen for 21 hours. After this period, the solution was treated with saturated aq. NH_4Cl and extracted with EtOAc (3 x 50mL). The combined organic layer was dried over MgSO_4 . Filtration and concentration under a reduced pressure gave a pale yellow residue which was chromatographed over a silica gel (30% EtOAc/Hexane) to obtain an off-white solid (2.8 g, 60%).

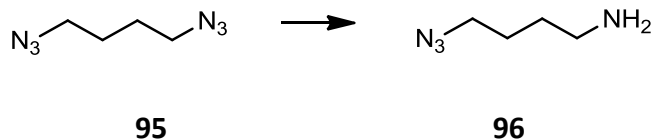
^1H NMR (400 MHz, CDCl_3) δ 5.70 (s, 1H), 3.19 (qd, $J = 7.2, 4.6$ Hz, 1H), 2.01 (dt, $J = 12.9, 4.4$ Hz, 1H), 1.96 – 1.87 (m, 2H), 1.84 – 1.74 (m, 2H), 1.67 – 1.57 (m, 1H), 1.53 (s, 3H), 1.32 – 1.23 (m, 3H), 1.20 (d, $J = 7.2$ Hz, 3H), 1.15 – 0.97 (m, 2H), 0.94 (d, $J = 5.8$ Hz, 3H). ^{13}C NMR (101 MHz, CDCl_3) δ 172.25, 109.61, 100.04, 82.81, 45.02, 42.82, 35.76, 34.37, 33.85, 33.16, 24.37, 23.92, 22.42, 18.98, 13.02. ESI HRMS: m/z calculated for $\text{C}_{15}\text{H}_{23}\text{O}_4$ ($[\text{M}+\text{H}]^+$) 267.1596, found 267.1589.

Preparation of **1,4-diazidobutane, 95**³⁷.

1,4-Dibromobutane (0.59 mL, 5 mmol) was dissolved in DMF (5 mL) and treated with a solution of NaN_3 (975 mg, 15 mmol) in 4 mL of water. The mixture was stirred and heated at 80°C for 20 hours. The reaction was washed with brine and extracted with hexane (3 x 15 mL). The combined organic layer was dried over MgSO_4 and concentrated to yield the product as a colourless liquid (621 mg, 89%).;

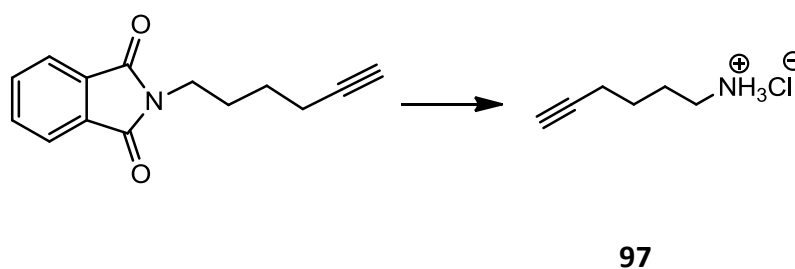
^1H NMR (400 MHz, CDCl_3) δ 3.39 – 3.27 (m, 2H), 1.74 – 1.63 (m, 2H). ^{13}C NMR (101 MHz, CDCl_3) δ 51.33, 26.58.

Preparation of **4-azidobutan-1-amine, 96**³⁷



To a solution of 1,4-diazidobutane (684 mg, 4.88 mmol) in 1 M HCl (9 mL), Et_2O (3 mL) and EtOAc (3 mL) cooled to 0°C was added PPh_3 (1.28 g, 4.88 mmol) in a small portion during 1 h. The mixture was warmed to room temperature and stirred overnight. The organic layer was separated and discarded. The aqueous layer was washed with Et_2O (2 x 30 mL) to remove triphenylphosphine oxide residue. The resulting aqueous layer was basified to pH 13 by 1 M aq. NaOH and extracted with DCM (3 x 30 mL). The combined extracts were dried with MgSO_4 and concentrated to yield the desired product as colourless liquid with a distinct smell (458 mg, 82%).; ^1H NMR (400 MHz, CDCl_3) δ 3.30 (t, $J = 6.8$ Hz, 2H), 2.74 (t, $J = 7.0$ Hz, 2H), 1.71 – 1.60 (m, 2H), 1.58 – 1.48 (m, 2H). ^{13}C NMR (101 MHz, CDCl_3) δ 51.75, 42.08, 31.19, 26.71.

Preparation of **hex-5-yn-1-aminium chloride, 97**³⁹

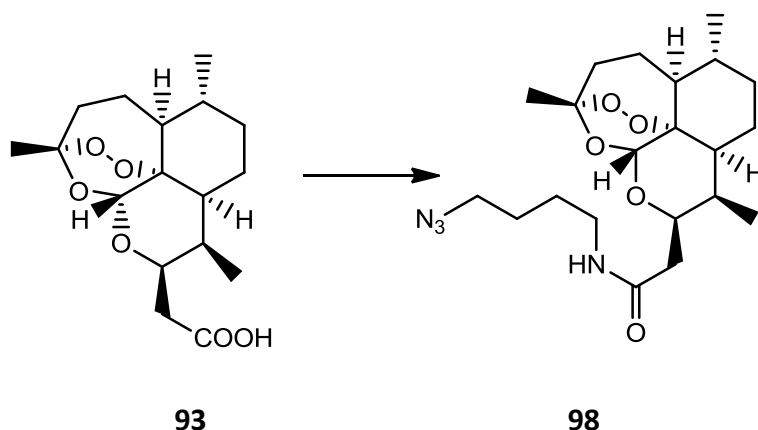


To a solution of *N*-(5-hexynyl)phthalimide (1.39 g, 6.11 mmol) in THF (20 mL), hydrazine hydrate (1 mL, 19.3 mmol) was added, and the resulting solution was heated at reflux for 6 hours. The solution was allowed to cool to room temperature, and concentrated HCl (1 mL) was added slowly. The solution was refluxed for another 2 hours then allowed to cool and stirred overnight. The white precipitate was removed by filtration, and the solvent was evaporated. The white residue was

then dissolved in water (25 mL) and washed with DCM (3 x 25 mL). The aqueous layer was concentrated to give a product as an off-white solid (612 mg, 75%).

^1H NMR (400 MHz, MeOD) δ 3.02 – 2.93 (m, 2H), 2.36 – 2.23 (m, 3H), 1.89 – 1.74 (m, 2H), 1.68 – 1.57 (m, 2H). ^{13}C NMR (101 MHz, MeOD) δ 82.61, 68.98, 38.95, 26.34, 24.99, 17.16. Elemental Analysis calculated for $\text{C}_6\text{H}_{12}\text{ClN}$: C, 53.93; H, 9.05; N, 10.48. Found: C, 53.18; H, 8.47; N, 11.52.

Preparation of **10 β -(N-(4-azidobutyl)acetamido)deoxoartemisinin, 98**

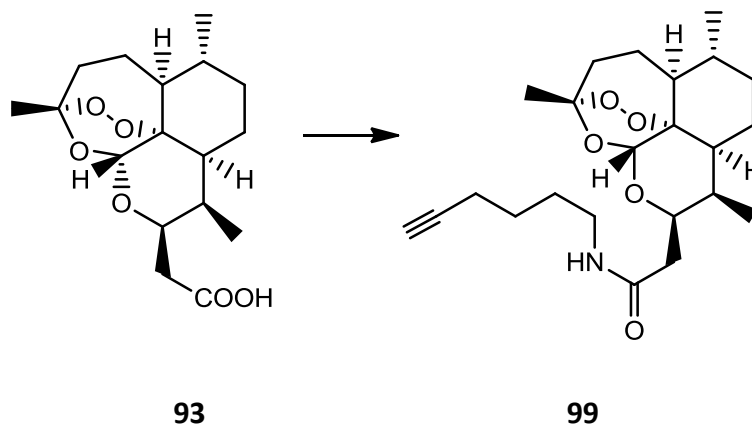


10 β -(2-Carboxyethyl)deoxoartemisinin (200 mg, 0.61 mmol) was dissolved in DCM (30 mL) under nitrogen. EDCI (143 mg, 0.92 mmol) was added and the reaction was allowed to stir for 5 minutes. 4-Azidobutylamine (84 mg, 0.74 mmol) and DMAP (112 mg, 0.92 mmol) were then added to the reaction and the mixture was left overnight at room temperature. When completed, the reaction was diluted with EtOAc and washed with sat. NH_4Cl (aq.), water, brine, and dried over MgSO_4 . The organic portion was filtered and concentrated to give a crude. Purification was performed using CC over silica gel (gradient from 40% EtOAc/Hexane to 100% EtOAc) to obtain a white solid product (130 mg, 50%).

^1H NMR (400 MHz, CDCl_3) δ 7.13 – 7.00 (m, 1H), 5.38 (s, 1H), 4.77 (ddd, J = 11.4, 6.2, 1.6 Hz, 1H), 3.41 (td, J = 13.3, 6.6 Hz, 1H), 3.34 – 3.26 (m, 3H), 3.21 – 3.10 (m, 1H), 2.60 – 2.47 (m, 2H), 2.38 – 2.27 (m, 2H), 2.10 – 1.94 (m, 2H), 1.83 – 1.54 (m, 6H), 1.40 (s, 3H), 1.33 – 1.18 (m, 4H), 0.98 (d, J = 5.8 Hz, 4H), 0.87 (d, J = 7.6 Hz, 3H). ^{13}C NMR (101 MHz, CDCl_3) δ 172.14, 103.31, 90.58, 81.24, 77.63, 70.05, 52.17, 51.49, 43.79, 39.13, 37.95, 37.75, 36.90, 34.59, 30.82, 27.16, 26.71, 26.20, 25.19,

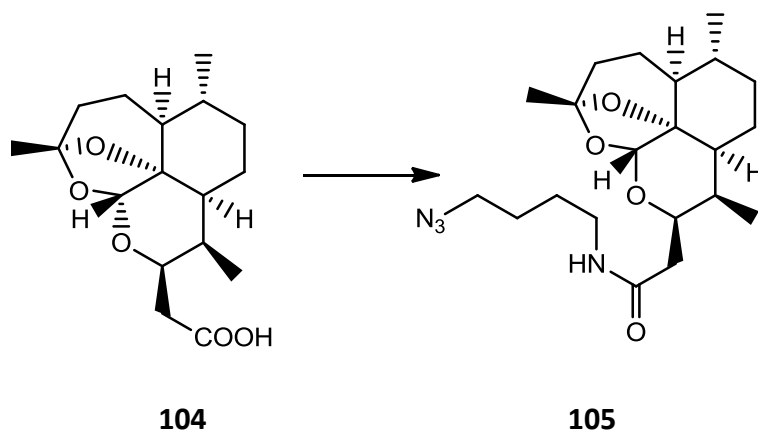
20.39, 12.45. HRMS (ESI): m/z calculated for $C_{21}H_{34}N_4O_5Na$ ($[M+Na]^+$) 445.2427, found 445.2430. Elemental Analysis calculated for $C_{21}H_{34}N_4O_5$: C, 59.70; H, 8.11; N, 13.26. Found: C, 58.97; H, 8.12; N, 13.19.

Preparation of **10 β -(N-(Hex-5-yn-1-yl)acetamido)deoxoartemisinin, 99**



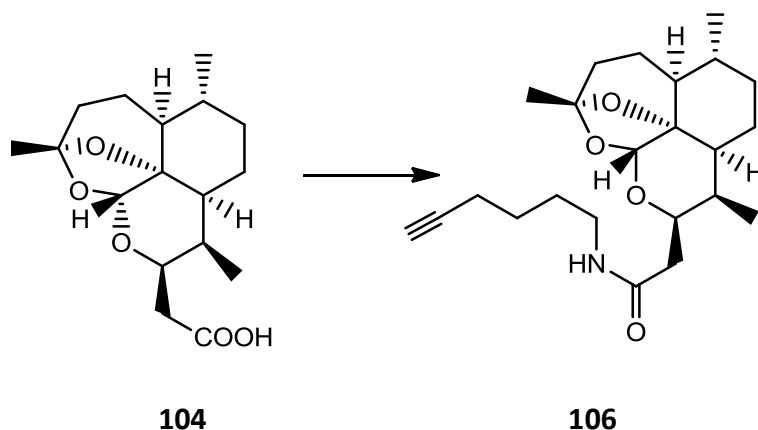
10 β -(2-Carboxyethyl)deoxoartemisinin (260 mg, 0.80 mmol) was dissolved in DCM (30 mL) under nitrogen. EDCI (186 mg, 1.2 mmol) was added and the reaction was allowed to stir for 5 minutes. Hex-5-yn-1-aminium chloride (128 mg, 0.96 mmol), triethylamine (0.13 mL, 0.96 mmol) and DMAP (146 mg, 1.2 mmol) were then added to the reaction and the mixture was left overnight at room temperature. When completed, the reaction was diluted with EtOAc and washed with sat. NH_4Cl (aq.), water, brine, and dried over $MgSO_4$. The organic portion was filtered and concentrated to give a crude. Purification was performed using CC over silica gel (60% EtOAc/Hexane) to obtain an off-white solid product (129 mg, 40%).

1H NMR (400 MHz, $CDCl_3$) δ 7.05 (s, $J = 18.9$ Hz, 1H), 5.38 (s, 1H), 4.76 (dd, $J = 10.1, 6.2$ Hz, 1H), 3.38 (td, $J = 13.3, 6.6$ Hz, 1H), 3.24 – 3.12 (m, 1H), 2.63 – 2.47 (m, 2H), 2.38 – 2.27 (m, 2H), 2.26 – 2.18 (m, 2H), 2.10 – 1.90 (m, 4H), 1.83 – 1.52 (m, 7H), 1.40 (s, 3H), 1.33 – 1.15 (m, 4H), 0.98 (d, $J = 5.5$ Hz, 3H), 0.87 (d, $J = 7.6$ Hz, 3H). ^{13}C NMR (101 MHz, $CDCl_3$) δ 171.68, 102.94, 90.09, 84.12, 80.84, 77.24, 69.79, 68.58, 51.79, 43.44, 38.87, 37.56, 37.29, 36.50, 34.21, 30.41, 28.57, 25.85, 25.77, 24.80, 20.01, 18.12, 12.11. HRMS (ESI): m/z calculated for $C_{23}H_{35}NO_5Na$ ($[M+Na]^+$) 428.2413, found 428.2406. Elemental Analysis calculated for $C_{23}H_{35}NO_5$: C, 68.12; H, 8.70; N, 3.45. Found: C, 67.88; H, 8.88; N, 3.34.

Preparation of **10 β -(2-(4-azidobutyl)acetamido)deoxo-2-deoxyartemisinin, 105**

10 β -(2-Carboxyethyl)deoxo-2-deoxyartemisinin (172 mg, 0.55 mmol) was dissolved in DCM (30 mL) under nitrogen. EDCI (129 mg, 0.83 mmol) was added and the reaction was allowed to stir for 5 minutes. 4-Azidobutylamine (76 mg, 0.66 mmol) and DMAP (102 mg, 0.83 mmol) were then added to the reaction and the mixture was left overnight at room temperature. When completed, the reaction was diluted with EtOAc and washed with sat. NH₄Cl (aq.), water, brine, and dried over MgSO₄. The organic portion was filtered and concentrated to give a crude. Purification was performed using CC over silica gel (gradient from 40% EtOAc/Hexane to 100% EtOAc) to obtain a white solid product (168 mg, 75%).

¹H NMR (400 MHz, CDCl₃) δ 6.80 (s, 1H), 5.31 (s, 1H), 4.57 – 4.42 (m, 1H), 3.41 – 3.26 (m, 3H), 3.26 – 3.16 (m, 1H), 2.45 – 2.29 (m, 2H), 2.29 – 2.18 (m, 1H), 1.98 (ddd, *J* = 13.0, 8.6, 4.0 Hz, 1H), 1.94 – 1.86 (m, 1H), 1.81 (dd, *J* = 13.5, 3.4 Hz, 1H), 1.76 – 1.56 (m, 8H), 1.52 (s, 3H), 1.24 – 1.10 (m, 4H), 0.91 (d, *J* = 5.3 Hz, 3H), 0.87 (d, *J* = 7.6 Hz, 3H). ¹³C NMR (101 MHz, CDCl₃) δ 171.82, 107.71, 97.17, 82.59, 65.38, 60.42, 51.12, 45.19, 39.78, 38.65, 38.17, 35.62, 34.42, 34.38, 29.64, 26.76, 26.28, 25.26, 23.61, 22.14, 21.09, 18.76, 14.21, 11.84. HRMS (ESI): *m/z* calculated for C₂₁H₃₄N₄O₄Na ([M+Na]⁺) 429.2478, found 429.2489. Elemental Analysis calculated for C₂₁H₃₄N₄O₄: C, 62.04; H, 8.43; N, 13.78. Found: C, 60.79; H, 8.47; N, 13.45.

Preparation of **10 β -(N-(Hex-5-yn-1-yl)acetamido)deoxo-2-deoxyartemisinin, 106**

10 β -(2-Carboxyethyl)deoxo-2-deoxyartemisinin (207 mg, 0.67 mmol) was dissolved in DCM (30 mL) under nitrogen. EDCI (155 mg, 1.0 mmol) was added and the reaction was allowed to stir for 5 minutes. Hex-5-yn-1-aminium chloride (107 mg, 0.80 mmol), triethylamine (0.11 mL, 0.80 mmol) and DMAP (122 mg, 1.0 mmol) were then added to the reaction and the mixture was left overnight at room temperature. When completed, the reaction was diluted with EtOAc and washed with sat. NH₄Cl (aq.), water, brine, and dried over MgSO₄. The organic portion was filtered and concentrated to give a crude. Purification was performed using CC over silica gel (60% EtOAc/Hexane) to obtain a pale yellow oil product (130 mg, 50%).

¹H NMR (250 MHz, CDCl₃) δ 6.78 (s, 1H), 4.50 (ddd, J = 10.0, 6.9, 3.2 Hz, 1H), 3.43 – 3.27 (m, 1H), 3.27 – 3.10 (m, 1H), 2.50 – 2.15 (m, 5H), 2.07 – 1.96 (m, 2H), 1.91 – 1.57 (m, 10H), 1.53 (s, 3H), 1.32 – 1.10 (m, 5H), 0.91 (d, J = 5.6 Hz, 3H), 0.87 (d, J = 7.6 Hz, 3H). ¹³C NMR (101 MHz, CDCl₃) δ 171.70, 107.68, 97.15, 84.16, 82.56, 68.49, 65.36, 45.20, 39.79, 38.75, 38.18, 35.62, 34.42, 34.40, 29.64, 28.61, 25.72, 25.25, 23.62, 22.16, 18.76, 18.12, 11.84. HRMS (ESI): m/z calculated for C₂₃H₃₅NO₄Na ([M+Na]⁺) 412.2461, found 412.2475.

5.7.2 Protein tagging and identification

Biological experiments were performed by Matthew Panchana and Dr Hanafy M. Ismail at the Liverpool School of Tropical Medicine. The following is a standard protocol adapted from Speers and Cravatt work published in 2004⁴³ with slight modifications.

Protein labelling

Parasites were treated *in vitro* with 1 μ M probes for 6 hours under the culture condition. Each experiment consists of 10 flasks of 50 mL culture. After 6-hour incubation, parasites were harvested by centrifugation and released from RBC using 0.15% saponin solution and stored at -80°C until further process.

Bradford protein quantitation assay

Protein concentration in samples was quantified by Bradford protein assay which were performed in micro-well plates. Standard calibration curve was prepared from bovine serum albumin (BSA) ranging from 1 mg/mL to 0.1 mg/mL. Samples were 10-fold diluted by adding Dulbecco's phosphate buffered saline (D-PBS, Invitrogen, Mg and Ca-free) prior to quantitation. Each well contains 5 μ L protein sample, 45 μ L D-PBS, and 250 μ L Bradford reagent (Sigma). Protein quantitation was performed by absorbance measurement at 595 nm. Protein concentration in sample was estimated from calibration curve. Samples analysed in same batch were adjusted to same concentration using D-PBS prior to further process.

Biotin-azide conjugation via click chemistry (tagged protein)

The alkyne-labelled proteome was reacted with azide-biotin conjugate (Invitrogen) in the presence of copper catalyst. To a 500 μ L solution of 2 mg/mL labeled protein sample, 5.65 μ L solution of 5 mM azide-biotin conjugate, 11.3 μ L of 50 mM TCEP (tris(2-carboxyethyl)phosphine) solution, , 34 μ L of 1.7 mM TBTA (Tris[(1-benzyl-1H-1,2,3-triazol-4-yl)methyl]amine) solution, and 11.3 μ L 50 mM CuSO₄ were added in order. The reaction was mixed using vortex mixer after each

component added. The mixture was then incubated for 1 h at room temperature under a dark condition with a gentle mix every 15 min.

After 1 h, the majority of proteins precipitated and the excess reagents were removed as follow. The reaction mixture was combined and centrifuged at 6,500 G for 4 min at 4°C to pellet protein. 750 µL of cold methanol was added to the pellet and it was sonicated for 3 to 4 seconds. The methanol wash was repeated two times. 650 µL of 2.5% SDS in D-PBS was added to the protein sample and it was sonicated for 3 to 4 seconds to dissolve all remaining pellet. The sample was then heated at 95°C for 5 min in a heating block and sonicated twice for 3 to 4 seconds afterwards to dissolve pellet. The sample was centrifuged and its supernatant was collected and adjusted to 3.5 mL with D-PBS. The sample was frozen at -20°C until further process.

Protein processing for mass spectrometry analysis

This part describes the pull down procedure of tagged protein using streptavidin-agarose beads and the protein digestion. Tagged proteins were processed as follow; to the 3.5 mL sample was added D-PBS to adjust the volume to 8.3 mL. 150 µL of streptavidin-agarose beads solution containing 50 µL streptavidin-agarose bead (pre-washed 3 times with 1 mL D-PBS) was added to the sample and the mixture was rotated on an end-over rotator for 1.5 hours. The sample was then centrifuged at 1,400G for 2 min at room temperature to pellet the beads. Most supernatant was removed. The beads were transferred to Micro Bio-Spin column (Bio-Rad) and washed (3 times each) with 1 mL of 1% SDS, 1 mL of 6 M urea, and 1 mL of D-PBS. The washed beads were then transferred to a low-adhesion screw cap tube with 200 µL D-PBS and centrifuged for 2 min at 1,400g to pellet the beads and removed supernatant.

On-bead reduction, alkylation and digestion were performed as follow. Beads were re-suspended in 500 µL of 6 M urea. 25 µL of 200 mM DL-dithiothreitol (DTT) was then added to the beads and the mixture was incubated at 65°C in a heating block for 15 min. 25 µL of 500 mM 3-indoleacetic acid (IAA) was added to the mixture and it was rotated for 30 min at r.t. under dark condition. The mixture

was centrifuged at 1,400g for 2 min to pellet beads and its supernatant was removed. The collected beads were washed with 1 mL D-PBS and they were re-suspended in 200 μ L of 2 M urea in D-PBS. 2 μ L of 100 mM CaCl_2 , and 4 μ L of 0.5 mg/ml sequencing grade modified trypsin were added to the solution and the mixture was incubated overnight at 37°C in an orbital shaker incubator to allow agitation. After the incubation, the sample was centrifuged at 1,400g for 2 min. The beads and supernatant were transferred to Micro Bio-Spin column. 100 μ L of D-PBS was added to the column to assist an elution giving a total volume of 300 μ L. 17 μ L of 90% formic acid was then added to the eluents.

Mass Spectrometry

Peptide sequencing was performed on ultra-high-performance liquid chromatography coupled with tandem mass spectrometry system (UHPLC-MS/MS). The UHPLC used in the study was the Thermo Scientific UltiMate 3000LC chromatography system. Mass spectrometry was run using Thermo Scientific LTQ Orbitrap Velos equipped with the Xcalibur software v2.1 (Thermo Scientific). The peptide sample was injected to the analytical column (Dionex Acclaim PepMap RSLC C18, 2 μ m, 100 Å, 75 μ m i.d. x 15 cm, nanoViper.), which was maintained at 35°C and at a flow rate of 0.3 μ L/min. Peptides were separated over linear chromatographic gradients using buffer A (2.5 % ACN: 0.1% formic acid) and buffer B (90% ACN: 0.1 % formic acid). Two gradients, 60 minutes (3-50 % buffer B in 40 min) and 120 minutes (3-60 % buffer B in 90 min), were employed for analysis. Full scan MS spectra were acquired over the m/z in a range of 350-2000 in positive mode by the Orbitrap at a resolution of 30,000. A data-dependent Top20 collision induced dissociation (CID) data acquisition method was used. The ion-trap operated with CID MS/MS on the 20 most intense ions (above the minimum MS signal threshold of 500 counts).

Protein Identification

Protein identification was performed on MASCOT search engine via Thermo Scientific Proteome Discoverer v1.2. Spectrum files from mass spectrometer were imported to the software and processed with following MASCOT parameters:

precursor mass tolerance of 10 ppm, fragment ion tolerance 0.8 Da with one tryptic missed cleavage permitted. Carbamidomethyl (C) was set as a static modification with oxidation of methionine (M) and deamidation (N,Q) set as dynamic modifications. A decoy database was searched and relaxed peptide confidence filters applied to the dataset (ion scores $p < 0.05$ / FDR 5%).

5.8 References

1. Antimalaria studies on Qinghaosu. *Chinese medical journal* **1979**, *92* (12), 811-6.
2. Dhingra, V.; Rao, K. V.; Narasu, M. L., Artemisinin: present status and perspectives. *Biochem Educ* **1999**, *27* (2), 105-109.
3. Binh, T. Q.; Ilett, K. F.; Batty, K. T.; Davis, T. M.; Hung, N. C.; Powell, S. M.; Thu, L. T.; Thien, H. V.; Phuong, H. L.; Phuong, V. D., Oral bioavailability of dihydroartemisinin in Vietnamese volunteers and in patients with falciparum malaria. *British journal of clinical pharmacology* **2001**, *51* (6), 541-6.
4. (a) Ashley, E. A.; White, N. J., Artemisinin-based combinations. *Current opinion in infectious diseases* **2005**, *18* (6), 531-6; (b) Adjuik, M.; Babiker, A.; Garner, P.; Olliaro, P.; Taylor, W.; White, N.; International Artemisinin Study, G., Artesunate combinations for treatment of malaria: meta-analysis. *Lancet* **2004**, *363* (9402), 9-17.
5. WHO World Malaria Report 2013. http://www.who.int/malaria/publications/world_malaria_report_2013/en/ (accessed 27 March 2014).
6. Organization, W. H., *Guidelines for the treatment of malaria*. 2 ed.; 2010; p 194.
7. O'Neill, P. M.; Barton, V. E.; Ward, S. A., The Molecular Mechanism of Action of Artemisinin-The Debate Continues. *Molecules* **2010**, *15* (3), 1705-1721.
8. Pagola, S.; Stephens, P. W.; Bohle, D. S.; Kosar, A. D.; Madsen, S. K., The structure of malaria pigment beta-haematin. *Nature* **2000**, *404* (6775), 307-10.
9. Fong, K. Y.; Wright, D. W., Hemozoin and antimalarial drug discovery. *Future medicinal chemistry* **2013**, *5* (12), 1437-50.
10. Meshnick, S. R.; Thomas, A.; Ranz, A.; Xu, C. M.; Pan, H. Z., Artemisinin (qinghaosu): the role of intracellular hemozoin in its mechanism of antimalarial action. *Molecular and biochemical parasitology* **1991**, *49* (2), 181-9.
11. (a) Posner, G. H.; Wang, D.; Cumming, J. N.; Oh, C. H.; French, A. N.; Bodley, A. L.; Shapiro, T. A., Further evidence supporting the importance of and the restrictions on a carbon-centered radical for high antimalarial activity of 1,2,4-trioxanes like artemisinin. *Journal of medicinal chemistry* **1995**, *38* (13), 2273-5; (b) Posner, G. H.; Oh, C. H.; Wang, D.; Gerena, L.; Milhous, W. K.; Meshnick, S. R.; Asawamahasadka, W., Mechanism-based design, synthesis, and *in vitro* antimalarial testing of new 4-methylated trioxanes structurally related to artemisinin: the importance of a carbon-centered radical for antimalarial activity. *Journal of medicinal chemistry* **1994**, *37* (9), 1256-8.
12. (a) Jefford, C. W.; Favarger, F.; Vicente, M. D. G. H.; Jacquier, Y., The Decomposition of Cis-Fused Cyclopenteno-1,2,4-Trioxanes Induced by Ferrous Salts and Some Oxophilic Reagents. *Helvetica chimica acta* **1995**, *78* (2), 452-458; (b) Jefford, C. W.; Vicente, M. G. H.; Jacquier, Y.; Favarger, F.; Mareda, J.; MillassonSchmidt, P.; Brunner, G.; Burger, U., The deoxygenation and isomerization of artemisinin and artemether and their relevance to antimalarial action. *Helvetica chimica acta* **1996**, *79* (5), 1475-1487.

13. O'Neill, P. M.; Bishop, L. P. D.; Searle, N. L.; Maggs, J. L.; Storr, R. C.; Ward, S. A.; Park, B. K.; Mabbs, F., Biomimetic Fe(II)-mediated degradation of arteflene (Ro-42-1611). The first EPR spin-trapping evidence for the previously postulated secondary carbon-centered cyclohexyl radical. *Journal of Organic Chemistry* **2000**, *65* (5), 1578-1582.
14. Wu, W. M.; Wu, Y. K.; Wu, Y. L.; Yao, Z. J.; Zhou, C. M.; Li, Y.; Shan, F., Unified mechanistic framework for the Fe(II)-induced cleavage of Qinghaosu and derivatives/analogues. The first spin-trapping evidence for the previously postulated secondary C-4 radical (vol 120, pg 3316, 1998). *Journal of the American Chemical Society* **1998**, *120* (49), 13002-13002.
15. Haynes, R. K.; Chan, W. C.; Lung, C. M.; Uhlemann, A. C.; Eckstein, U.; Taramelli, D.; Parapini, S.; Monti, D.; Krishna, S., The Fe²⁺-mediated decomposition, PfATP6 binding, and antimalarial activities of artemisone and other artemisinins: The unlikelihood of C-centered radicals as bioactive intermediates. *ChemMedChem* **2007**, *2* (10), 1480-1497.
16. (a) Haynes, R. K.; Vonwiller, S. C., The behaviour of qinghaosu (artemisinin) in the presence of non-heme Iron(II) and (III). *Tetrahedron Lett* **1996**, *37* (2), 257-260; (b) Haynes, R. K.; Vonwiller, S. C., The behaviour of qinghaosu (artemisinin) in the presence of heme Iron(II) and (III). *Tetrahedron Lett* **1996**, *37* (2), 253-256; (c) Haynes, R. K.; Pai, H. H. O.; Voerste, A., Ring opening of artemisinin (qinghaosu) and dihydroartemisinin and interception of the open hydroperoxides with formation of N-oxides - A chemical model for antimalarial mode of action. *Tetrahedron Lett* **1999**, *40* (25), 4715-4718.
17. Yang, Y. Z.; Little, B.; Meshnick, S. R., Alkylation of Proteins by Artemisinin - Effects of Heme, Ph, and Drug Structure. *Biochemical pharmacology* **1994**, *48* (3), 569-573.
18. Cazelles, J.; Robert, A.; Meunier, B., Alkylation of heme by artemisinin, an antimalarial drug. *Cr Acad Sci li C* **2001**, *4* (2), 85-89.
19. Creek, D. J.; Charman, W. N.; Chiu, F. C. K.; Prankerd, R. J.; Dong, Y.; Vennerstrom, J. L.; Charman, S. A., Relationship between antimalarial activity and heme alkylation for spiro- and dispiro-1,2,4-trioxolane antimalarials. *Antimicrobial agents and chemotherapy* **2008**, *52* (4), 1291-1296.
20. Robert, A.; Benoit-Vical, F.; Claparols, C.; Meunier, B., The antimalarial drug artemisinin alkylates heme in infected mice. *Proceedings of the National Academy of Sciences of the United States of America* **2005**, *102* (38), 13676-13680.
21. Bousejra-El Garah, F.; Claparols, C.; Benoit-Vical, F.; Meunier, B.; Robert, A., The antimalarial trioxaquine DU1301 alkylates heme in malaria-infected mice. *Antimicrobial agents and chemotherapy* **2008**, *52* (8), 2966-9.
22. Krishna, S.; Pulcini, S.; Moore, C. M.; Teo, B. H.; Staines, H. M., Pumped up: reflections on PfATP6 as the target for artemisinins. *Trends in pharmacological sciences* **2014**, *35* (1), 4-11.
23. Eckstein-Ludwig, U.; Webb, R. J.; Van Goethem, I. D.; East, J. M.; Lee, A. G.; Kimura, M.; O'Neill, P. M.; Bray, P. G.; Ward, S. A.; Krishna, S., Artemisinins target the SERCA of *Plasmodium falciparum*. *Nature* **2003**, *424* (6951), 957-61.
24. del Pilar Crespo, M.; Avery, T. D.; Hanssen, E.; Fox, E.; Robinson, T. V.; Valente, P.; Taylor, D. K.; Tilley, L., Artemisinin and a series of novel endoperoxide antimalarials exert early effects on digestive vacuole morphology. *Antimicrobial agents and chemotherapy* **2008**, *52* (1), 98-109.
25. Garah, F. B.; Stigliani, J. L.; Cosledan, F.; Meunier, B.; Robert, A., Docking studies of structurally diverse antimalarial drugs targeting PfATP6: no correlation between in silico binding affinity and in vitro antimalarial activity. *ChemMedChem* **2009**, *4* (9), 1469-79.
26. (a) Yang, Y. Z.; Asawamahsakda, W.; Meshnick, S. R., Alkylation of human albumin by the antimalarial artemisinin. *Biochemical pharmacology* **1993**, *46* (2), 336-9; (b) Yang, Y. Z.; Little, B.; Meshnick, S. R., Alkylation of proteins by artemisinin. Effects of heme, pH, and drug structure. *Biochemical pharmacology* **1994**, *48* (3), 569-73.

27. Asawamahasakda, W.; Ittarat, I.; Pu, Y. M.; Ziffer, H.; Meshnick, S. R., Reaction of antimalarial endoperoxides with specific parasite proteins. *Antimicrobial agents and chemotherapy* **1994**, *38* (8), 1854-8.
28. Wu, W. M.; Chen, Y. L.; Zhai, Z.; Xiao, S. H.; Wu, Y. L., Study on the mechanism of action of artemether against schistosomes: the identification of cysteine adducts of both carbon-centred free radicals derived from artemether. *Bioorganic & medicinal chemistry letters* **2003**, *13* (10), 1645-7.
29. Pandey, A. V.; Tekwani, B. L.; Singh, R. L.; Chauhan, V. S., Artemisinin, an endoperoxide antimalarial, disrupts the hemoglobin catabolism and heme detoxification systems in malarial parasite. *The Journal of biological chemistry* **1999**, *274* (27), 19383-8.
30. Hartwig, C. L.; Rosenthal, A. S.; D'Angelo, J.; Griffin, C. E.; Posner, G. H.; Cooper, R. A., Accumulation of artemisinin trioxane derivatives within neutral lipids of *Plasmodium falciparum* malaria parasites is endoperoxide-dependent. *Biochemical pharmacology* **2009**, *77* (3), 322-36.
31. (a) Jessani, N.; Cravatt, B. F., The development and application of methods for activity-based protein profiling. *Current opinion in chemical biology* **2004**, *8* (1), 54-9; (b) Speers, A. E.; Adam, G. C.; Cravatt, B. F., Activity-based protein profiling *in vivo* using a copper(i)-catalyzed azide-alkyne [3 + 2] cycloaddition. *Journal of the American Chemical Society* **2003**, *125* (16), 4686-7; (c) Liu, Y.; Patricelli, M. P.; Cravatt, B. F., Activity-based protein profiling: the serine hydrolases. *Proceedings of the National Academy of Sciences of the United States of America* **1999**, *96* (26), 14694-9.
32. (a) Nodwell, M. B.; Sieber, S. A., ABPP methodology: introduction and overview. *Topics in current chemistry* **2012**, *324*, 1-41; (b) Krysiak, J.; Breinbauer, R., Activity-based protein profiling for natural product target discovery. *Topics in current chemistry* **2012**, *324*, 43-84.
33. Barton, V.; Ward, S. A.; Chadwick, J.; Hill, A.; O'Neill, P. M., Rationale design of biotinylated antimalarial endoperoxide carbon centered radical prodrugs for applications in proteomics. *Journal of medicinal chemistry* **2010**, *53* (11), 4555-9.
34. (a) O'Neill, P. M.; Pugh, M.; Stachulski, A. V.; Ward, S. A.; Davies, J.; Park, B. K., Optimisation of the allylsilane approach to C-10 deoxy carba analogues of dihydroartemisinin: synthesis and *in vitro* antimalarial activity of new, metabolically stable C-10 analogues. *J Chem Soc Perk T 1* **2001**, (20), 2682-2689; (b) Hindley, S.; Ward, S. A.; Storr, R. C.; Searle, N. L.; Bray, P. G.; Park, B. K.; Davies, J.; O'Neill, P. M., Mechanism-based design of parasite-targeted artemisinin derivatives: Synthesis and antimalarial activity of new diamine containing analogues. *Journal of medicinal chemistry* **2002**, *45* (5), 1052-1063; (c) Chadwick, J.; Jones, M.; Mercer, A. E.; Stocks, P. A.; Ward, S. A.; Park, B. K.; O'Neill, P. M., Design, synthesis and antimalarial/anticancer evaluation of spermidine linked artemisinin conjugates designed to exploit polyamine transporters in *Plasmodium falciparum* and HL-60 cancer cell lines. *Bioorganic & medicinal chemistry* **2010**, *18* (7), 2586-2597.
35. Pu, Y. M.; Ziffer, H., Synthesis and antimalarial activities of 12 beta-allyldeoxyartemisinin and its derivatives. *Journal of medicinal chemistry* **1995**, *38* (4), 613-6.
36. Criegee, R., Mechanism of Ozonolysis. *Angewandte Chemie-International Edition in English* **1975**, *14* (11), 745-752.
37. Lee, J. W.; Jun, S. I.; Kim, K., An efficient and practical method for the synthesis of mono-N-protected alpha,omega-diaminoalkanes (vol 42, pg 2709, 2001). *Tetrahedron Lett* **2001**, *42* (25), 4279-4279.
38. Staudinger, H.; Meyer, J., On new organic phosphorus bonding III Phosphine methylene derivatives and phosphinimine. *Helvetica chimica acta* **1919**, *2*, 635-646.
39. Altman, R. A.; Nilsson, B. L.; Overman, L. E.; de Alaniz, J. R.; Rohde, J. M.; Taupin, V., Total Synthesis of (+)-Nankakurines A and B and (+/-)-5-epi-Nankakurine A. *Journal of Organic Chemistry* **2010**, *75* (22), 7519-7534.

40. Liu, Y. G.; Wong, V. K. W.; Ko, B. C. B.; Wong, M. K.; Che, C. M., Synthesis and cytotoxicity studies of artemisinin derivatives containing lipophilic alkyl carbon chains. *Organic letters* **2005**, *7* (8), 1561-1564.
41. Ishihama, Y.; Oda, Y.; Tabata, T.; Sato, T.; Nagasu, T.; Rappsilber, J.; Mann, M., Exponentially modified protein abundance index (emPAI) for estimation of absolute protein amount in proteomics by the number of sequenced peptides per protein. *Molecular & Cellular Proteomics* **2005**, *4* (9), 1265-1272.
42. Jortzik, E.; Fritz-Wolf, K.; Sturm, N.; Hipp, M.; Rahlfs, S.; Becker, K., Redox Regulation of Plasmodium falciparum Ornithine δ -Aminotransferase. *Journal of Molecular Biology* **2010**, *402* (2), 445-459.
43. Speers, A. E.; Cravatt, B. F., Profiling enzyme activities in vivo using click chemistry methods. *Chem Biol* **2004**, *11* (4), 535-546.